

Norwegian University of Life Sciences
Faculty of Science and Technology

Philosophiae Doctor (PhD)
Thesis 2023:71

Soundscape analysis for biodiversity monitoring in tropical rainforest ecosystems

Lydanalyse for overvåking av biologisk
mangfold i tropisk regnskog

Thomas Luybaert

Soundscape analysis for biodiversity monitoring in tropical rainforest ecosystems

Lydanalyse for overvåking av biologisk mangfold i tropisk regnskog

Philosophiae Doctor (PhD) Thesis

Thomas Luybaert

Norwegian University of Life Sciences

The PhD programme in Ecology and Natural Resource Management
at the

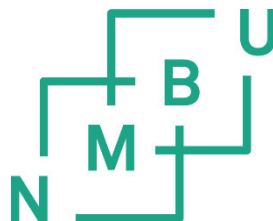
Faculty of Environmental Sciences and Natural Resource Management

Ås 2023

Thesis number 2023:71

ISSN 1894-6402

ISBN 978-82-575-2102-8



Supervisors and Evaluation Committee

Main supervisor: Professor Torbjørn Haugaasen
Norwegian University of Life Sciences (NMBU), Faculty of Environmental Sciences
and Natural Resource Management (MINA), Tropical Rainforest Ecology Lab
(TREcoL)

Co-supervisor: Professor Carlos Augusto Peres
University of East Anglia, School of Environmental Sciences (Norwich, U.K.) -
Instituto Juruá (Manaus, Brazil)

First opponent: Assistant Professor Zuzana Buřivalová

Second opponent: Dr. Oliver Metcalf

Committee coordinator: Associate Professor Erik Trond Aschehoug

"A great silence is spreading over the natural world even as the sound of man is becoming deafening"

- Bernie Krause -

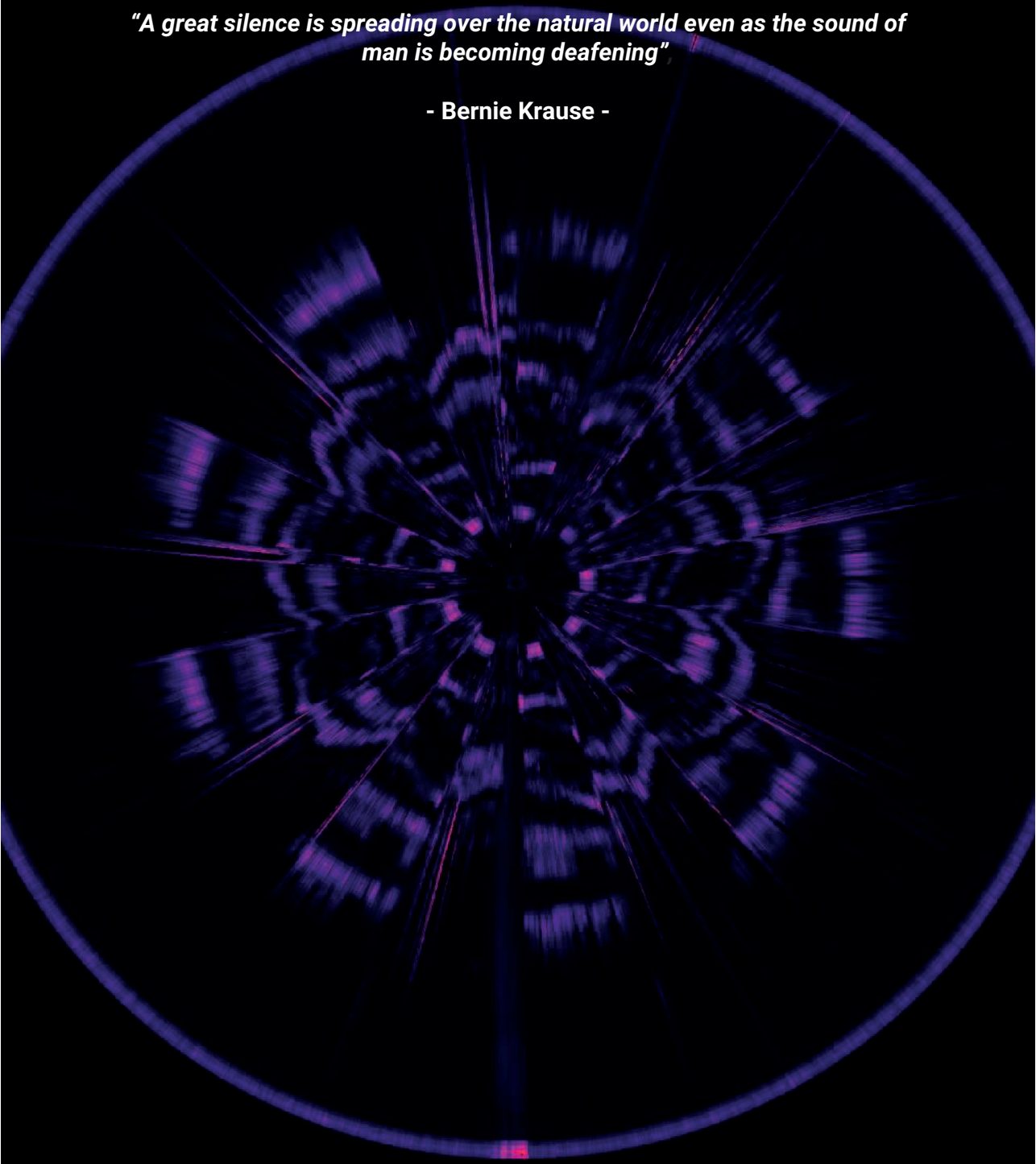


Image:

A 9-day soundscape showing circadian patterns in CVR-index values for Fuzaca Island in the Balbina Hydroelectric Reservoir, plotted in the polar coordinate system.

Acknowledgements

First and foremost, I would like to express my heartfelt gratitude to my first PhD supervisor, Torbjørn Haugaasen. Tor, thank you for recognizing my potential and allowing me to embark on this three-year deep dive into the world of sound and tropical rainforests. In the face of a global pandemic, your guidance was instrumental in redirecting the course of my PhD thesis and providing me with the freedom to choose my own research path and manage my time. Your mentorship style and team-player attitude have been invaluable. I deeply appreciate your expertise, critical feedback, and continuous challenge to push the boundaries of my work and strive for excellence.

I am also indebted to my second PhD supervisor, Carlos Peres, for his invaluable guidance and support. I am grateful for entrusting me with your acoustic dataset, which enabled a new direction for my PhD work when the limitations imposed by COVID-19 rendered previous plans impossible. Without this, the presented PhD project would not have been possible. Your extensive knowledge of Amazonian ecology, abundance of project ideas, and unending enthusiasm have been truly inspiring.

This thesis owes a great deal to one collaborator in particular, Anderson Bueno. Anderson, I am grateful for the countless hours we spent exchanging thoughts and refining my work through WhatsApp. Your patience in deciphering my complex ideas through "little drawings" and your constructive criticism and attention to detail in reviewing my manuscripts have been immensely helpful. It is a privilege to have you as a mentor, collaborator, and friend.

Many other collaborators played crucial roles in the successful completion of this PhD thesis, including Igor Luis Kaefer, Marconi Campos-Cerqueira, Gabriel Masseli, and Tom Bradfer-Lawrence. I extend my sincere thanks for their contributions and unwavering support. I would also like to express my gratitude to Joe Hawes for his guidance and mentorship during the three months of fieldwork in the Brazilian Amazon preceding this PhD project. Thank you for your invaluable help. Additionally, a big thank you to Yennie for her friendship and for translating my thesis abstract into Norwegian.

I am thankful to the Norwegian University of Life Sciences and the Faculty of Environmental Science and Natural Resource Management for providing the PhD funding and institutional support. I would like to extend my gratitude to Kari Thue, Iren Abrahamsen, Jan Vermaat, and Stein Moe for their administrative support throughout my PhD. I also want to acknowledge the valuable contributions of Douglas Sheil, Asunción Semper Pascual, and Simon Schowanek, who reviewed my seminars and provided constructive feedback that significantly improved the quality of the research presented in this thesis.

Several individuals at the University of Copenhagen have played integral roles in shaping my PhD experience over the past three years. I am deeply grateful to Morten Tange Olsen for graciously accepting me as an unofficial member of the Marine Mammal Group while I was working remotely from Copenhagen. Morten, thank you for providing me with a workspace in your office and for wholeheartedly involving me in the group's social activities. The supportive environment your team fostered was indispensable to my PhD journey. I would also like to express my profound appreciation to Kristine Bohmann, who generously hosted me in the Environmental DNA group for a three-month scientific exchange. Kristine, thank you for embracing me as part of your team, affording me the opportunity to refine my bioinformatic analysis skills, offering invaluable input on my research ideas, and positively encouraging my grant writing endeavours.

Beyond the professional connections I forged, a remarkable group of individuals transformed my PhD years into a period enriched with friendship and adventure. Magie and Ed, Bia and Isma, Dóra and Cica, Marc, Phen, and Lennart – I am grateful for your unwavering friendship and the countless memorable moments we shared, from delightful dinners to fiercely competitive board game sessions, from exploring Copenhagen by boat to embarking on adventures across the globe. To the extended, transient, and recent members of the marine mammal pod – Andreas, Annika, Sarah, Jakob, Éadin, Youri, Iben, and everyone else – thank you for your companionship during these past three years. I would also like to extend my gratitude to my friends back home in Belgium, who warmly embrace me with open arms during every visit, regardless of my prolonged stays abroad.

To my parents, Veerle and Michel, I am deeply thankful for your unwavering support and for encouraging me to pursue my dreams, even when they led me far away from home. I also extend my heartfelt appreciation to my three sisters, Eva,

Sofie, and Hanna, for being my steadfast pillars of support and for your unwavering belief in me. Finally, I want to express a heartfelt thank you to Morgan, my partner in life and love. Throughout the highs and lows of my PhD journey and the challenges posed by a global pandemic, you have stood by my side. Thank you for our countless conversations about science and life, and for the adventures we embarked on together along the way.

Table of Contents

Supervisors and Evaluation Committee	iii
Acknowledgements.....	vii
1 Abbreviations and definitions	1
2 List of papers.....	3
3 Abstract.....	4
4 Norsk sammendrag.....	6
5 Synopsis.....	8
5.1 Introduction.....	8
5.1.1 Biodiversity in the Anthropocene	8
5.1.2 The fate of tropical forests.....	9
5.1.3 Ecological monitoring in tropical rainforests.....	11
5.1.4 Acoustic sensors as an addition to the monitoring toolbox	13
5.1.5 Soundscape analysis.....	20
5.1.6 Thesis objectives.....	33
5.1.7 Thesis structure.....	35
5.2 Materials and Methods	36
5.2.1 Designing the workflow.....	36
5.2.2 Testing workflow characteristics using simulated soundscapes	40
5.2.3 Testing workflow performance in a tropical rainforest ecosystem.....	41

5.2.4	Guiding data collection and workflow parameter choices	44
5.2.5	Building software for workflow implementation	44
5.3	Results and discussion	45
5.3.1	Workflow novelty.....	45
5.3.2	Index characteristics.....	49
5.3.3	Indices as biodiversity proxies or ecological indicators	50
5.3.4	soundscapeR: a new addition to the ecoacoustics toolbox	60
5.4	Conclusion and future perspectives	62
5.4.1	Further framework development.....	62
6	References	66
7	Papers.....	90
I	A framework for quantifying soundscape diversity using Hill numbers	92
II	Extending species-area relationships to the realm of ecoacoustics: The Soundscape-Area Relationship	148
III	soundscapeR: An R-package for the exploration, visualisation, diversity quantification and comparison of soundscapes	210
8	Appendices	255

1 Abbreviations and definitions

Abbreviation	Meaning
ADI	Acoustic Diversity Index
AEI	Acoustic Evenness Index
AI	Artificial Intelligence
ASU	Acoustic Space Use
BHR	Balbina Hydroelectric Reservoir
BI	Bioacoustic Index
CE	Current Era
CVR	Acoustic Cover Index
dB	Decibel
ENS	Effective Number of Species
FFT	Fast Fourier Transformation
GPS	Global Positioning System
H	Acoustic Entropy
Hf	Spectral Entropy
HPC	High Performance Computer
Hz	Hertz
IBT	Island Biogeography Theory
IUCN	International Union for the Conservation of Nature
kHz	Kilohertz
LPR	Living Planet Report
MCH	Morphological Constraint Hypothesis
ML	Machine Learning
OSU	Operational Sound Unit
PCH	Phylogenetic Constraint Hypothesis
RFCx	Rainforest Connection
ROI	Region Of Interest
SAR	Species-Area Relationship

SIE	Small Island Effect
SIR	Species-Isolation Relationship
SNR	Signal-to-Noise Ratio
SSAR	SoundScape-Area Relationship
TB	Terrabyte

2 List of papers

Paper 1:

Thomas Luypaert, Anderson S Bueno, Gabriel S Masseli, Igor L Kaefer, Marconi Campos-Cerqueira, Carlos A Peres, Torbjørn Haugaasen. **A framework for quantifying soundscape diversity using Hill numbers.** *Methods in Ecology and Evolution* (2022). <https://doi.org/10.1111/2041-210X.13924>

Contribution:

Workflow conceptualisation, preliminary testing, data analysis, manuscript writing

Appearance in thesis: Chapter I

Paper 2:

Thomas Luypaert, Anderson S Bueno, Torbjørn Haugaasen, Carlos A Peres. **Extending the species-area relationship to the realm of ecoacoustics: the soundscape-area relationship.** *Manuscript submitted to Ecology Letters* (15/05/2023).

Contribution:

Project conception, data analysis, manuscript writing

Appearance in thesis: Chapter II

Paper 3:

Thomas Luypaert, Anderson S Bueno, Tom Bradfer-Lawrence, Carlos A Peres, Torbjørn Haugaasen. **soundscapeR: an R-package for the exploration, visualisation and quantification of soundscape diversity using Hill numbers.** *Manuscript in preparation for Methods in Ecology and Evolution.*

Contribution:

Project conception, coding R package, writing vignette, writing manuscript

Appearance in thesis: Chapter III

3 Abstract

Tropical rainforests harbour up to 66% of the world's terrestrial biodiversity but have been reduced in extent by up to 60% due to persistent deforestation and forest degradation, resulting in the population decline or loss of ecologically and socio-economically important wildlife species. In recognition of the biodiversity crisis as an actor of global change, several international initiatives, including the Convention of Biological Diversity and its 'Aichi Biodiversity Targets for 2020', have been implemented to curb biodiversity loss. Here, the collection of primary data that provide an objective record of community-level biodiversity is crucial to understanding fundamental ecological processes, the trends and drivers of change, and the progress made towards conservation targets. Yet, the rapid and global nature of the biodiversity crisis means that monitoring biodiversity at appropriate spatio-temporal scales is riddled with difficulties. Passive Acoustic Monitoring (PAM) yields promising perspectives, such as increased taxonomic breadth and the potential for automation. Still, deriving taxonomic information from acoustic data is complicated by the time-consuming nature of aural annotation and the lack of existing automated species identifiers and reference databases. Ecoacoustic is a new field of research that instead is aimed at inferring ecological information from the soundscape – or collection of sounds emanating from the landscape – without the need for species identification. Here, mathematical formulae called acoustic indices are used to summarise the diversity of acoustic signals in sound files and link values to diversity patterns. Although this discipline has made substantial progress towards becoming a useful monitoring tool, the ability of acoustic indices to reflect biodiversity trends or ecological patterns must be validated before this technology is implemented on a global scale. Several limitations and research opportunities remain to be addressed and will be the focus of this thesis.

This thesis presents a novel analytical workflow that combines ecoacoustic methods with the analytical framework of Hill numbers, resulting in a comprehensive set of intuitive acoustic indices for measuring soundscape diversity patterns at multiple scales. Chapter I introduces the analytical approach, confirming that the derived acoustic indices adhere to essential criteria for diversity indices, while also evaluating their effectiveness in capturing richness patterns of sound-producing species in tropical rainforests. In Chapter II, the investigation delves deeper into the

spatial variations of soundscape richness within a highly insularised rainforest system, revealing a positive correlation between island size and soundscape richness across multiple scales, and linking the observed patterns to underlying ecological mechanisms. Chapter III introduces soundscapeR, a user-friendly software tool implemented in the R coding language, facilitating the use of the workflow. Collectively, these chapters demonstrate the potential of this new approach, presenting a valuable addition to the ecoacoustic monitoring toolbox that can be used to shed light on ecological mechanisms and their drivers in acoustically complex rainforest settings.

4 Norsk sammendrag

Tropiske regnskoger huser opptil 66 % av verdens biologiske mangfold på land, men har blitt redusert i omfang med opptil 60 % på grunn av vedvarende avskoging og skogforringelse, noe som har resultert i en nedgang i antallet individer eller tap av økologisk og sosioøkonomisk viktige dyrearter. I anerkjennelse av naturkrisen som en bidragsyter til de globale endringene vi står overfor, har flere internasjonale initiativer, inkludert Konvensjonen om biologisk mangfold (Convention on Biological Diversity, forkortet CBD) og Aichi-målene (Aichi Biodiversity Targets for 2020), blitt iverksatt for å stanse tapet av biologisk mangfold. For å evaluere fremskritt mot bevaringsmålene, trender og drivere av endring, og forstå grunnleggende økologiske prosesser er innsamling av felldata, som gir en objektiv oversikt over biologisk mangfold på samfunnsnivå, avgjørende. Likevel betyr naturkrisens raske og globale karakter at det er vanskelig å overvåke biologisk mangfold i tilstrekkelig utstrekning i tid og rom. Passiv Akustisk Overvåking (Passive Acoustic Monitoring, forkortet PAM) er i denne sammenheng en lovende metode og bidrar med økt taksonomisk bredde og potensial for automatisering. Likevel er det krevende å utlede taksonomisk informasjon fra akustiske data. Mangel på eksisterende automatiserte metoder for å identifisere arter og mangel på referansedatabaser gjør det anstrengende og tidskrevende å klassifisere lydkomponenter i et maskinforståelig format utefra hvilket arter kan bestemmes. Økoakustikk (Ecoacoustic) er et nytt forskningsfelt som i stedet tar sikte på å utlede økologisk informasjon fra lydbildet – eller samlinger av lyder som kommer fra landskapet – uten behov for artsidentifikasjon. Her brukes matematiske formler kalt akustiske indekser for å oppsummere mangfoldet av akustiske signaler i lydfiler og knytte verdier til mangfoldsmønstre. Selv om betydelige fremskritt har blitt gjort på dette feltet mot å bli et nyttig overvåkingsverktøy, må akustiske indeksers evne til å reflektere biologisk mangfoldstrender eller økologiske mønstre valideres før denne teknologien kan brukes på global skala. Flere begrensninger og forskningsmuligheter gjenstår å adressere og disse har vært fokus for denne oppgaven.

Denne oppgaven presenterer en ny analytisk arbeidsflyt som kombinerer økoakustiske metoder med det analytiske rammeverket til Hill-tallene. Dette resulterer i et omfattende sett med intuitive akustiske indekser som kan brukes for

å måle lydlandskapsmangfoldsmønstre på flere skalaer. Kapittel I introduserer den analytiske tilnærmingen, viser at de akustiske indeksene overholder essensielle kriterier for mangfoldsindekser, og evaluerer indeksenes kapasitet til å reflektere mønstre i artsmangfold for lydproduserende arter i tropiske regnskoger. I kapittel II går undersøkelsen dypere inn i de romlige variasjonene av lydlandskapsmangfoldet i et svært isolert regnskogsystem, og avslører en positiv korrelasjon mellom øystørrelse og lydlandskapsmangfold på tvers av flere skalaer. Kapittel II kobler så de observerte mønstrene til underliggende økologiske mekanismer. Kapittel III introduserer soundscapeR, et brukervennlig programvareverktøy i R-kodespråk, som underletter arbeidsflyten. Samlet viser disse kapitlene potensialet til denne nye, økoakustiske tilnærmingen. De utgjør dermed et verdifullt bidrag til de akustiske overvåkingsmetodene som kan brukes for å kaste lys over økologiske mekanismer og deres drivere i akustisk komplekse regnskogsmiljøer.

5 Synopsis

5.1 Introduction

5.1.1 Biodiversity in the Anthropocene

The Anthropocene marks a newly proposed geological epoch in which human activities have fundamentally altered the Earth's systems, leading to profound changes in the atmosphere, biosphere, hydrosphere, and geosphere (Crutzen and Stoermer 2000; Steffen et al. 2011). Despite the debate on its onset (Smith and Zeder 2013), the impact of human activities on planetary processes is undeniable and many indicators suggest we're well outside the boundaries the planet can sustain (Steffen et al. 2015). Today, up to 75% of the Earth's terrestrial land surface has been altered by humans (Shukla et al. 2019) and every year, approximately 40% of the world's primary productivity is appropriated for human consumption (Imhoff et al. 2004; McGill et al. 2015). Following the industrialisation and globalisation of human production and trade, the planet's biogeochemical cycles have been thrown out of kilter, including a projected doubling of atmospheric CO₂ by 2050 (Hofmann et al. 2009), a doubling of biologically available nitrogen (Millennium Ecosystem Assessment 2005), and a 75% increase in phosphorous storage in terrestrial and freshwater ecosystems (Bennett et al. 2001). The compounding and synergistic effects of these anthropogenic pressures are rapidly destabilising the functioning of planetary processes.

The human impact on the Earth transcends biogeochemical cycles alone, also leading to a dramatic alteration of the biosphere (Schramski et al. 2015). For instance, the Earth's plant biomass has declined approximately twofold since the start of human civilisation, and while the present-day biomass of all mammals has increased four-fold in this period, the biomass of wild mammals has decreased seven-fold. This stark difference can be attributed to the expansion of the human population and associated livestock and the decrease in wild mammal populations. Yet, the impact of human activities on the biosphere is not just limited to changes in the biomass. Between 100,000 – 500 years before the present, our planet lost more than 10% of its mammal species, 23% of its turtle and tortoise species, and 10% of its bird species (Johnson et al. 2017), among other groups. This loss was especially

pervasive for large-bodied species (Dirzo et al. 2014), with 80% of megaherbivores and 60% of megacarnivores going extinct during this period (Malhi et al. 2016). Although this remains a topic of debate (Stewart et al. 2021), these extinction events largely track the movement of early humans across the planet and are thus believed to be the consequence of anthropogenic actions (Duncan et al. 2013; Bartlett et al. 2016; Malhi et al. 2016). In more recent times (500 CE – present), 711 vertebrate species, and almost 600 species of plants and invertebrates, have gone extinct (IUCN 2023; Johnson 2023). Considering many groups remain unassessed by the International Union for the Conservation of Nature (IUCN), the true number is likely much higher (Dirzo et al. 2014).

While species losses are important, they do not fully reflect humanity's impact on the biosphere. If we look beyond global species extinctions, it becomes clear that species population declines are widespread and accelerating. The Living Planet Report (LPR), a biennial report investigating population trends for approximately 32,000 populations, suggests that global species population abundance has declined by 69% on average since 1970 (Almond et al. 2022). While the populations included in the LPR report only represent a fraction of global populations, and the interpretation of the metric has been criticised for being misleading (Leung et al. 2020), the pervasive nature of human-induced population declines has been numerous shown at regional (Heikkinen et al. 2004; Seibold et al. 2019) and global (Newbold et al. 2015; Jung et al. 2019; Morton et al. 2021) scales for a broad range of taxonomic groups. The effects of these population declines translate into the extinction risk of species. According to the IUCN Red List of Threatened Species, currently, 27% of mammals, 13% of birds, 41% of amphibian species, and 21% of reptiles are threatened with extinction (IUCN 2023). Although much less is known about other taxonomic groups, such as insects, many reports highlight pervasive declines in formerly abundant species (Wagner et al. 2021).

5.1.2 The fate of tropical forests

The degradation of biotas and the subsequent loss of individuals, populations, and species exhibit non-random patterns, displaying nestedness within specific regions, ecosystems, and phylogenetic groups. Understanding the distribution of biodiversity and human threats is crucial for effective conservation efforts.

Tropical rainforests, which cover a mere 6.5% of the Earth's terrestrial surface area, are estimated to sustain up to two-thirds of the world's terrestrial biodiversity

(Malhi et al. 2014; Gardner 2011; Rainforest Foundation Norway 2020). Paradoxically, these ecosystems also face some of the highest degrees of human threat. The intensification of global agriculture, urbanization, forestry, and infrastructure development in the Anthropocene has resulted in extensive deforestation, leading to forest destruction, degradation, and fragmentation (Gardner et al. 2009). These primary threats are compounded by secondary factors, including increased wildfire prevalence (Aragão et al. 2018), overexploitation of natural resources through hunting and wildlife trade (Peres 2000; Morton et al. 2021), altered biogeochemical cycles (Leite-Filho et al. 2021), the introduction of invasive species and pathogens (Ghazoul and Sheil 2010; Lips 2016), and climate change (Brodie et al. 2012). Consequently, tropical rainforests have been reduced by one-third of their original extent, with only half of the remaining forests considered intact (Rainforest Foundation Norway 2020). This has led to a significant risk of extinction for the biological communities inhabiting these ecosystems. Notably, 28-34% of endemic tropical forest vertebrates and up to 42% of amphibians face the threat of extinction (Pillay et al. 2022).

The spatial relationship between high biodiversity and high anthropogenic threat in tropical rainforests is exemplified by the concept of "biodiversity hotspots" (Pimm and Raven 2000). Biodiversity hotspots are areas that support at least 1,500 endemic plant species and have experienced a reduction of 70% or more in their primary vegetation (Myers et al. 2000; Habel et al. 2019). Globally, only 2.5% of the Earth's land surface qualifies as a biodiversity hotspot (Myers et al. 2000). Remarkably, 60% of these hotspots are located within tropical rainforests, emphasizing the critical conservation concern for these ecosystems (Corlett and Primack 2008). The vulnerability of tropical rainforest species to human pressures varies across the tree of life, with the fossil record suggesting that animals are more susceptible to mass extinction events than plants (Stork et al. 2009). Extinction risk for animals is heightened among rare species with small populations, limited geographic ranges, high endemism, slow population growth, specialized ecological habits, poor dispersal, large size, and high trophic levels (McKinney 1997; McKinney and Lockwood 1999; Dirzo et al. 2014). Consequently, small and large vertebrate species face an elevated risk of extinction (Ripple et al. 2017).

The health of tropical rainforests and the biodiversity they support are crucial for the functioning of these ecosystems and the services they provide to humankind (Malhi et al. 2014). Tropical forests, for instance, store more living biomass than any

other ecosystem on the planet, making them vital for climate regulation (Rainforest Foundation Norway 2020). Moreover, the wildlife within rainforests constitutes a vital source of sustenance, timber, and medicine, supports the livelihoods of many communities, among others (Brandon 2014). To reverse negative biodiversity trends, it is vital that we understand the trends and drivers of change, the ecological consequences of anthropogenic disturbances, and the progress we make towards conservation targets (Gardner 2011; Proença et al. 2017). However, the global and rapid nature of the biodiversity crisis makes it exceedingly difficult to gather fine-scale data on biodiversity trends at the spatio-temporal scales relevant to conservation, especially for tropical rainforests, which cover vast areas.

5.1.3 Ecological monitoring in tropical rainforests

Various approaches to ecological monitoring in tropical rainforests exist, each with distinct advantages and limitations. Traditionally, biodiversity surveys in tropical rainforests have relied on human observers conducting fieldwork and using visual or acoustic cues to detect wildlife and their associated signs (Zwerts et al., 2021). In-field human observations have been successfully applied to monitor tropical rainforest biodiversity in a wide range of contexts and taxonomic groups (e.g., Opper 2006; Maas et al. 2009; Endo et al. 2010). This approach is particularly suitable for research projects with limited financial resources, as it requires minimal upfront investment and technological tools. More so, it allows for direct in-field species identification, reducing post-processing workloads (Zwerts et al., 2021). Nevertheless, the unique characteristics of tropical rainforest environments present challenges that can compromise the validity of observational data if not carefully considered. Tropical rainforests are characterized by limited visibility, high biological complexity, exceptional species richness, and numerous cryptic species living at low population densities (Zwerts et al., 2021). These factors contribute to a low detection probability for most tropical rainforest species, which means that biodiversity surveys require substantial effort (Witmer, 2005). Tropical rainforests often span vast expanses of remote and logistically challenging habitats, and the concentration and cognitive strain required for this type of work impose limits on the number of hours an expert can remain focused (Loffeld et al., 2022). Consequently, getting a comprehensive diversity profile using in-field observation can require thousands of person-hours, making multi-taxa studies at broad spatial scales a slow, laborious, and costly endeavour (Gardner et al., 2008).

The probability of detecting species can also vary significantly, thereby increasing the risk of introducing bias into diversity estimates. In-field human observations tend to favour easily detectable species, such as large, vocal, diurnal, and abundant mammals and birds (Zwerts et al. 2021). Conversely, rare, small, nocturnal, and cryptic species are often overlooked (Zwerts et al. 2021). An observer's ability to discriminate between individuals of different species also significantly impacts the outcome of ecological monitoring efforts but is subject to multiple sources of bias (Tuia et al., 2022). Observers may differ in their overall skill level, taxonomic specialization, or audio-visual acuity (Faanes and Bystrak, 1981). The cognitive demands of visual and acoustic surveys can also affect an observer's accuracy in detecting and identifying individuals to the species level, potentially varying with the time of day or duration of the field season (Lardner et al., 2019). Although it is possible to mitigate these biases to some extent (Fitzpatrick et al., 2009), data resulting from these surveys are inherently linked to the observer and cannot be validated at a later stage (Sethi, 2020b; Tuia et al., 2022). This lack of an objective record of community-level diversity introduces challenges regarding research reproducibility.

In summary, our ability to monitor biodiversity patterns in tropical forests using traditional observational methods is hindered by: (i) the required in-field effort; (ii) potential observer biases; (iii) the lack of an objective diversity record; and (iv) the required temporal and financial investment. If we are to understand how ecosystems respond to human disturbance or conservation actions, we require scalable and reliable field survey methods that can easily provide us with bias-free fine-scale biodiversity data at broad spatial and temporal scales at a reduced cost. In recent times, the information revolution has brought about major advances in computer and communications technologies, which have the potential to transform the way we monitor ecosystems by removing some of the aforementioned limitations (Hampton et al. 2013). Several technological breakthroughs, paired with the maturing of existing technologies, have reduced the cost and size of autonomous sensors, including camera traps (Glover-Kapfer et al. 2019), GPS tags (Beuchert et al. 2022), satellite-borne cameras (Yang et al. 2014), drone-borne multi-spectral sensors (Kays et al. 2019), and microphones (Hill et al. 2018). These devices now allow us to collect, analyse and store novel types of data at faster speeds, larger volumes, and broader spatial and temporal scales (Pimm et al. 2015). Additionally, this new generation of monitoring tools can increasingly operate semi- or fully

autonomously (Sethi et al. 2018), thus providing scalable solutions to complement the traditional ecological monitoring approaches mentioned before. When paired with wireless sensor networks and on-board machine learning capabilities, in the future, these sensors could be integrated into the Internet of Things, thus providing real-time data on a broad range of ecological phenomena (Gallacher et al. 2021) or human threats (ARBIMON RFCx 2022).

It is important to acknowledge, however, that most of these technologies are still in their infancy and will require substantial refinement, training, and validation before they can be deployed in a fully autonomous manner. More so, many of these technological breakthroughs present their own challenges, such as extensive post-processing, technology-specific biases, or substantial field effort for their deployment. For the remainder of this thesis, I will focus on one of these technological approaches in particular, passive acoustic monitoring, discussing its biodiversity monitoring opportunities, limitations, and areas requiring further development.

5.1.4 Acoustic sensors as an addition to the monitoring toolbox

5.1.4.1 The strength of passive acoustic monitoring

Many species use sound to convey ecologically important information to sympatric individuals (Darwin 1872), including contacting conspecifics (Bond and Diamond 2005), attracting a mate (Gerhardt et al. 2003), navigating and hunting (Madsen and Surlykke 2013), fighting (Versluis et al. 2000), or as a defence mechanism (Smith and Langley 1978) – be it through vocalisations, stridulations, or by interacting with their environment (Caldwell 2014). As such, the cumulative collection of sounds that emanate from a landscape, also known as the soundscape, carries ecologically relevant information, including information on species' presence, abundance, behaviour, and interactions (Gibb et al. 2019). In addition to biological sounds (i.e., biophony), soundscapes also contain information on non-biological phenomena, such as geophysical sounds (i.e., geophony - sounds produced by the natural processes of the Earth) and anthropogenic sounds (i.e., anthropophony - sounds produced by humans), which can shed light on broader ecosystem-level processes or anthropogenic threats (Krause 1987; Pijanowski et al. 2011b).

Recording environmental sound to infer ecological patterns, a field that we will henceforth refer to as ‘ecoacoustics’ (Sueur and Farina 2015), offers a multitude of advantages against other ecological monitoring tools. First, recent advances in the technology, size, and cost of semi- or fully autonomous passive acoustic recording devices mean that recordings can now be taken continuously, over long periods, and with reduced human effort, thus greatly increasing the temporal scope and spatial scalability of this tool (Hill et al. 2018; Gibb et al. 2019; Roe et al. 2021). Moreover, the resulting big acoustic datasets maintain a high resolution in the frequency and temporal domain, meaning ecological phenomena can be investigated on a broad range of timescales, ranging from seconds (Oñate-Casado et al. 2023) to years (Phillips et al. 2017). These unique properties of acoustic datasets open novel avenues of research that allow us to examine the interplay between fine-scale and large-scale ecological processes (Sugai et al. 2019b; Sethi 2020b). Additionally, when these acoustic sensors are applied to gather high-resolution data at large spatio-temporal scales, they have the potential to be more cost-effective relative to conventional methods, though this is dependent on the research question at hand (Gasc et al. 2013; Wood et al. 2019).

Second, as opposed to the narrow taxonomic focus of most other methods, passive acoustic sensors are distinct in the wealth of information they capture from a single data source (Ross et al. 2023). For instance, the acoustic fingerprint of the environment contains sounds of a wide range of taxonomic groups (e.g., insects, birds, mammals, amphibians, fish, reptiles, crustaceans), as well as human threats (e.g., hunting, illegal logging, forest fires), and geophysical events (e.g., rainstorms, treefalls, wind, wildfires; Sethi 2020b). Furthermore, since acoustic sensors can record sounds that are inaudible to the human ear (ultrasound), they allow us to monitor species that are otherwise hard to study, such as bats (Froidevaux et al. 2014) or katydids (Symes et al. 2022).

Third, acoustic recordings represent an objective and permanent record of the sound-producing community at a specific place and moment in time. These records can be cross-examined at any point, thus overcoming issues with research reproducibility that trouble in-field aural identification of species by a human observer. In addition to their current importance, these acoustic data may hold a key role in future research efforts. Recordings of environmental sound can be seen as a type of ‘bioacoustic time capsule’, providing baseline information on the state of sound-producing communities at some point in the past, and potentially containing

records on the activity of species that were previously unknown to science or have since gone extinct (Sugai and Llusia 2019).

In summary, passive acoustic sensors represent a valuable addition to the ecological monitoring toolbox, allowing us to scale up ecological monitoring studies at a reduced cost and with relative ease, while at the same time retaining a high resolution for a broad range of taxonomic groups. Yet, despite the promise of passive acoustic monitoring, several pertinent barriers remain before this tool can be implemented to monitor the state of ecosystems on a global scale.

5.1.4.2 Challenges in acoustic biodiversity monitoring

Ecoacoustics as a big data science

To illustrate the challenging nature of deriving ecological information from acoustic datasets, let's imagine a simple example. Say we would like to conduct a high-resolution study that investigates the acoustic community of a protected area spanning 100 km². The protected area has a certain degree of habitat heterogeneity, so as a trade-off between coverage and cost, we decide to deploy the acoustic sensors at a density of 1 sensor/km² (100 sensors) and record the audible part of the soundscape (sampling rate: 48 kHz) continuously for 1 month (31 days) using the AudioMoth (Hill et al. 2018) recording device. As we want to account for a potential temporal turnover in the acoustic community throughout the year, we repeat the data collection 4 times per year. Using this setup, our study would generate approximately 100 TB of data spanning 297,600 total recording hours, or 12,400 days of recording. Should we want to include the ultrasonic part of the frequency spectrum using AudioMoth's upper frequency limit (sampling rate: 384 kHz), we would produce 806 TB of data.

Admittedly, this hypothetical case study represents an optimal sampling scenario, and we could probably achieve robust results with fewer sensors or a lower temporal/frequency coverage, yet it illustrates this point nicely: even a study in a single area with reasonable sampling assumptions (Metcalf et al. 20203) produces vast amounts of data, especially when ultrasonic sounds are also of interest. Although big data has been a buzzword in science for the past few decades, and this wealth of information brings numerous opportunities to the table, a new set of challenges now presents itself: how do we manage and analyse these vast datasets?

Storing ecoacoustic data in perpetuity

The first obstacle in the big acoustic data workflow is presented by the deluge of data that is generated and how we should manage it (Truskinger et al. 2014; Gibb et al. 2019). After data collection, soundscape recordings need to be stored, and later, archived in perpetuity (Villanueva-Rivera and Pijanowski 2012; Darras et al. 2020). Ideally, this data should be freely available to the scientific community on a user-friendly platform (Deichmann et al. 2018), be accompanied by all relevant metadata (Roch et al. 2016), and if annotated, be checked for accuracy.

Although, for now, most acoustic datasets don't reach an equivalent size to those in the fields of genomics, astronomy, or particle physics (Stephens et al. 2015), the permanent storage of ecoacoustic data in global databases is complicated by several factors. Firstly, whereas fields such as astronomy or genomics are relatively mature, having dealt with the challenges of big data for several decades (Stephens et al. 2015), the big data aspect of ecoacoustic research is a relatively novel development (Towsey et al. 2014a). Secondly, in these other disciplines, much of the raw data can be processed to less storage-demanding forms before being archived (Stephens et al. 2015). For ecoacoustics, part of the value of the data lies in its ability to serve as a historical record of the structure and dynamics of ecosystems at a given moment in time (Sugai and Llusia 2019), acting as a type of 'acoustic fossil'. Therefore, the raw data must be stored in perpetuity, highlighting the need for a global ecoacoustic archiving system.

Presently, the required infrastructure for the permanent archival of ecoacoustic datasets is lagging. Several databases exist for the storage of acoustic data of species' calls (bioacoustics data), including the Macaulay Library (macaulaylibrary.org) and Xeno-Canto (xeno-canto.org), however, only the second hosts soundscape recordings (Deichmann et al. 2018). Existing databases dedicated to the storage of ecoacoustic data include Ecosounds (www.ecosounds.org), Biosounds (Darras et al. 2020), the Terrestrial Ecosystem Research Network EcoAcoustics Portal (bioacoustics.tern.org.au), the Sound of Norway (thesoundofnorway.com), the Remote Environmental Assessment Laboratory (remoteenvironmentalassessmentlaboratory.com), the Center for Global Soundscapes (centerforglobalsoundscapes.org) and its Record The Earth project (recordtheearth.org), and the ARBIMON platform (arbimon.rfcx.org). Yet, several of

these repositories are exclusive to data collected in specific countries or regions, and none of them allows users to upload or download large ecoacoustic datasets in bulk using a simple web-interface (Deichmann et al. 2018). More so, since these ecoacoustic datasets exist in many disparate archives, discovering what data is out there, and harmonising the different database architectures to extract and synthesise the ecological information held within, represents a sizeable challenge.

If we are to make the most out of existing datasets to address questions at larger spatial scales and over longer timeframes, and avoid redundancy in data collection efforts, we need to create a centralised ecoacoustic data archive that allows the scientific community to work collaboratively to collect, archive and share ecoacoustic data between locations, projects, and research groups (Hampton et al. 2013). Successful examples of global data repositories in other scientific disciplines include Wildlife Insights for camera trapping (<https://www.wildlifeinsights.org/>) and the Barcode of Life Database for genetic and genomic data ([boldsystems.org](https://www.boldsystems.org/)), among others.

Analysing large acoustic datasets

Even if we manage to store and archive all ecoacoustic data successfully, there is a mismatch between the ever-growing volume of raw audio recordings acquired for ecological studies, and our ability to distil ecologically meaningful information from these recordings rapidly and at large scale (Tuia et al. 2022).

The extraction of taxonomic information on the sound-producing species in ecoacoustic datasets generally consists of two data processing steps: (i) isolating the time-frequency coordinates of potential signals or regions of interest (ROIs) from the raw data files; and (ii) classifying those ROIs into species' detections or non-detections (Wood et al. 2019). Historically, these steps were performed by trained taxonomic experts by manually annotating sound files using aural and visual cues (Eldridge et al. 2018; Kahl et al. 2021a). Yet, as ecoacoustics emerges as a big data science, the time-consuming and knowledge-demanding nature of manual annotations renders this approach highly impractical in theory, and impossible in reality (Kahl et al. 2020). This is exemplified by the hypothetical case study: should a taxonomic expert be able to listen to the data non-stop for 8 hrs/day, it would take them 37,200 work days, or 102 years, to listen to the data just once. Even if this were a feasible approach, the resulting data would still be subject to the effects of

observer bias. Hence, we require automated methods to accurately convert ecoacoustic data into relevant information that can inform ecology and conservation biology.

Here, artificial intelligence (AI) can provide solutions. Machine learning (ML) algorithms, for instance, are skilled at learning patterns from the data they are presented with (Marvin et al. 2016; Farley et al. 2018). We can distinguish two general ML techniques: (i) supervised ML, where algorithms are trained with large amounts of raw data that are labelled with their expected classification outcomes (e.g. species identity), thus learning a mathematical function that uses some of the data's features to accurately classify previously unseen data into the correct categories; and (ii) unsupervised ML, where no training data is provided, but algorithms classify the input data based only on distinguishable patterns in the data's features (Sethi 2020). These computational models have the potential to massively speed up classification tasks such as species identification (Mac Aodha et al. 2018), while at the same time reducing the cost and error rates (Tuia et al. 2022). Nonetheless, even though ML algorithms have been widely developed in other ecological disciplines, including camera trapping (Ahumada et al. 2020) or remote sensing (Zhu et al. 2017), their application to big ecoacoustic datasets has been more limited (Tuia et al. 2022).

The broad uptake of ML in ecoacoustics is hindered by several factors. The vast size of ecoacoustic datasets means that applying ML models to identify species from sound files comes with high computational requirements, for which advanced computing infrastructure is needed (Tuia et al. 2022). Purchasing High-Performance Computing (HPC) platforms is prohibitively expensive for most research groups, a cost which is added onto by the continued price of running and maintaining these machines (Carlyle et al. 2010). The need for private HPC infrastructure can be overcome by using the computing resources of the institution (e.g., university), or by employing cloud-based computing services. However, these also bring about considerable costs (Carlyle et al. 2010; Tuia et al. 2022), and the use of the former is often slowed down by competition for computing resources (personal observation). Finally, as these platforms are energy-intensive, they also have a significant carbon footprint (Portegies Zwart 2020).

Aside from computational power, to build accurate supervised ML-algorithms for signal classification of sound files, we require large training datasets. Although several projects have started aggregating these data into robust and large-scale

libraries, including Xeno-Canto and the Macaulay Library for birds, there is a discrepancy between the quality of the acoustic signals of interest in these training datasets, and the quality of field recordings collected using passive acoustic sensors. The labelled sound files that are available in these online libraries generally boast high signal-to-noise ratios (SNR), mostly collected using high-quality handheld devices (Sethi 2020). Conversely, the non-targeted way passive acoustic sensors record sound using omnidirectional microphones means that the resulting ecoacoustic datasets tend to be quite noisy, and thus have low SNRs (Goëau et al. 2018). The task of ML-classifiers is further complicated by the complexity of natural soundscapes and acoustic competition between species (Tuia et al. 2022; Truskinger et al. 2014), leading to overlap in the vocalisations of sympatric species. Currently available training datasets usually only carry a label for the signal with the highest quality in the recording, leaving the quieter background signals unlabelled (Denton et al. 2022). Therefore, ML-algorithms that are trained on singularly annotated sound files from high-quality training datasets struggle to reach high classification accuracies when applied to raw soundscape data (Wimmer et al. 2013; Truskinger et al. 2014; Goëau et al. 2018; Denton et al. 2022). Furthermore, apart from birds, training datasets are missing for most other sound-producing taxa.

Building accurate ML classifiers is especially challenging in tropical rainforests. These ecosystems are particularly species-rich and contain many poorly known or elusive species for which few reference acoustic signals are available (Riede 2018). Moreover, rainforests represent one of the noisiest habitats on Earth, showcasing high call densities and considerable call overlap (Gasc et al. 2013), which further complicates the performance of ML algorithms. The problematic nature of automated acoustic species classification in tropical rainforests is exemplified by the BirdCLEF challenge, the largest bird sound recognition competition in terms of dataset size and species diversity. Across all entries in the 2020 edition, the ML algorithms consistently performed the worst for soundscape recordings from the Peruvian Amazon compared to other localities, reaching low overall classification scores (Kahl et al. 2020).

Ironically, ML algorithms tend to perform the worst for species of conservation concern, such as those naturally existing in low population densities, small home ranges, or species that are endangered by extinction. This is due to a lack of training data for these species, a situation which is exacerbated when ecosystems are species rich (Kahl et al. 2021a), such as in tropical rainforests. Generally, where training

datasets exist, they are often unbalanced in the diversity of geographic locations, sensor types, or the abundance of labelled signals for different species (LeBien et al. 2020; Tuia et al. 2022). This matters, as unbalanced training data can lead to bias in the ML-algorithm's classification performance (Tuia et al. 2022). For instance, species' vocalisations can vary regionally (i.e., regional dialects - Martins et al. 2018). Hence, if a training dataset has insufficient coverage of a species' acoustic signals across its distribution, the resulting ML-algorithm may bear the risk of working well locally, but not generalise to other regions (Sethi 2020).

Although signal processing and machine learning have taken considerable steps towards the automated classification of sounds, and several deep-learning algorithms now exist in Europe and North-America (Mac Aodha et al. 2018; Kahl et al. 2021b) and the tropics (LeBien et al. 2020), there is a lack of existing automated species identifiers and reference databases for the majority of taxa and regions (Gibb et al. 2019), rendering large-scale taxonomic diversity assessments in tropical rainforest using ecoacoustic datasets impossible.

5.1.5 Soundscape analysis

5.1.5.1 Selective pressures on acoustic trait diversity

In addition to their taxonomic information, species' sounds also carry functional significance, playing a crucial role in various social interactions, including courting, territorial defence, predator avoidance, and food sharing (Darwin 1872; Seyfarth and Cheney 2003). Therefore, sounds are subject to selective pressures at multiple scales, resulting in an immense diversity of acoustic traits in the landscape, expressed through the timing, frequency, and amplitude features of acoustic signals (Zsebők et al. 2021).

In any environment, sounds travelling through a medium experience attenuation, or the decrease in signal amplitude as a function of the distance to the sound source. In ideal conditions, sounds propagating through air experience an approximate 6 dB (decibel) reduction in signal amplitude every time the distance is doubled. However, in reality, sounds are further attenuated through the effects of reflection, absorption, reverberation, and scattering (Wiley and Richards 1978). Therefore, the physical structure of the surrounding environment influences the success of signal

transmission by sound-producing species. For instance, in areas with dense vegetation, sounds experience greater attenuation than in open environments (Morton 1975). This is especially true for high-frequency vocalisations, which attenuate more rapidly than low-frequency sounds (Morton 1975). Similarly, the temporal patterning of species vocalisations also affects sound attenuation, with short notes repeated at greater time intervals experiencing less sound reverberation in densely vegetated environments (Slabbekoorn et al. 2002). According to the Acoustic Adaptation Hypothesis (AAH), these physical habitat attributes put selective pressure on species' vocalisations, forcing the evolution of sound signals to minimise attenuation and maximise propagation in their habitat (Morton 1975). Conversely, the Acoustic Habitat Hypothesis (AHH) states that sound-dependent species actively select their habitats based on their acoustic characteristics, favouring those environments that suit a species' functional needs and maximise sound production and reception (Mullet et al. 2017). Regardless of which mechanism is at work, both hypotheses posit that the physical structure of the habitat shapes the acoustic properties of the soundscape, imposing an environmental filter that leads to the homogenisation of acoustic trait diversity at local scales and the diversification of acoustic traits across space (Dingle et al. 2008; Sueur and Farina 2015).

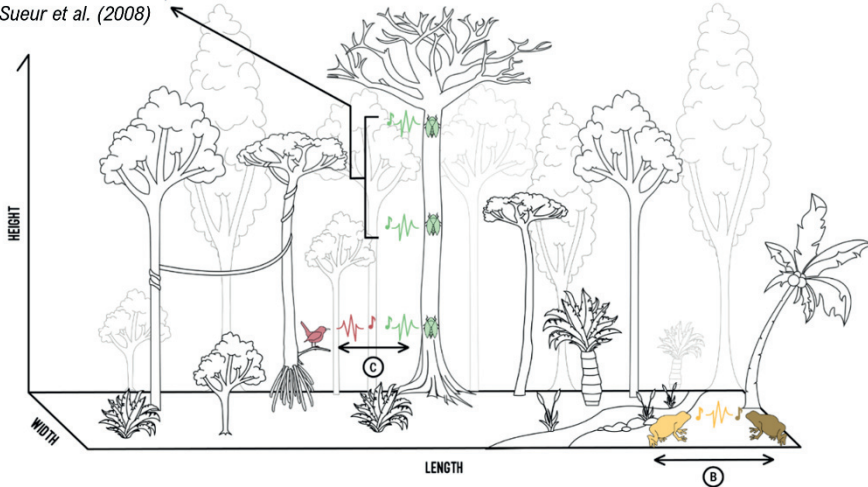
The Acoustic Niche Hypothesis (ANH), also known as the theory of acoustic niche partitioning, is a cornerstone theory of ecoacoustics that proposes acoustic space as a fundamental ecological resource for which sound-producing organisms compete (Krause 1987). Overlap in the time-frequency domain of acoustic signals produced by different species leads to inefficient signal transmission and reduced fitness (Magrath et al. 2015; Allen-Ankins and Schwarzkopf 2021), and consequently, sympatric species partition their acoustic niche to avoid overlap. Species may partition their acoustic niche in various ways (Fig. 1), such as shifting the location of vocalisation in 3-dimensional space (Sueur 2002), shifting the dominant frequency peak at which they produce sound (Villanueva-Rivera 2014), shifting the peak of temporal activity in the 24h circadian cycle (Hart et al. 2015), or shifting the peak of temporal activity seasonally (Boquimpani-Freitas et al. 2007). Following this reasoning, the ANH suggests that a more speciose community should experience increased competition, and thus, lead to increased partitioning of acoustic niche space, resulting in a greater diversity of acoustic traits at local scales (Pijanowski et al. 2011a; Sueur and Farina 2015). These hypotheses (ANH, AAH, AHH) are reflections of the same underlying mechanism: sensory systems (sound emission,

propagation, and reception) are under selective pressure to maximise signal transmission in the local environment, known as the sensory drive hypothesis (Endler 1992).

It is worth noting here that the AAH, AHH and ANH are not universally accepted in the scientific community, with both evidence for (e.g., Villanueva-Rivera 2014; Hart et al. 2015; Mullet et al. 2017; Goutte et al. 2018; Hart et al. 2021) and against (e.g., Boncoraglio and Saino 2007; Tobias et al. 2014; Mikula et al. 2021) their existence. Still, in evolutionary terms, the adaptation of acoustic signal production to the surrounding acoustic environment, be it biotic or abiotic, is entirely tenable (Eldridge et al. 2016).

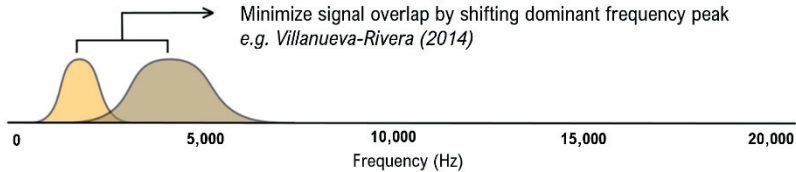
A. SPATIAL NICHE PARTITIONING

Minimize signal overlap by vocalising at a different location in 3D-space
e.g. Sueur et al. (2008)



B. SPECTRAL NICHE PARTITIONING

Minimize signal overlap by shifting dominant frequency peak
e.g. Villanueva-Rivera (2014)



C. TEMPORAL NICHE PARTITIONING

Minimize signal overlap by shifting time of peak vocal activity
e.g. Hart et al. (2015)

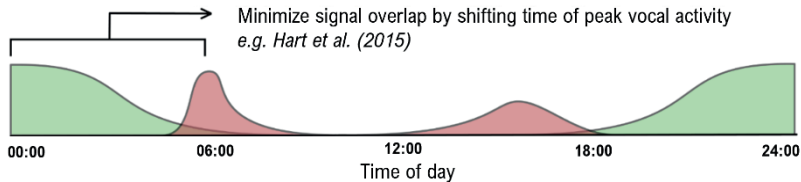


Figure 1: A graphical representation of the various ways in which species can partition their acoustic niche. **A.** Spatial niche partitioning: species minimise signal overlap by producing sound at a different location in 3D space; **B.** Spectral niche partitioning: species minimise signal overlap by shifting their dominant frequency peak; **C.** Temporal niche partitioning: species minimise signal overlap by shifting their peak of vocal activity. The seasonal shift in vocalisation timing is omitted here.

Aside from selection for optimal signal transmission, the diversity of acoustic traits in the landscape is also the result of the evolutionary legacy of the sound-producing

organisms (Hart et al. 2021). The Morphological Constraint Hypothesis (MCH) suggests that the acoustic repertoire of a species is constrained by its morphological parameters (Ryan and Brenowitz 1985; Pearse et al. 2018; Mikula et al. 2021). For example, in birds, the size of the sound-producing organ is correlated with body mass, and the larger the sound-producing organ, the lower the frequency it produces (Tietze et al. 2015). This is why body mass exhibits a strong negative relationship with the sound frequency a species can produce. Similarly, the Phylogenetic Constraint Hypothesis (PCH) proposes that the evolutionary ancestry of a species limits the range of sound frequencies it can produce (Pearse et al. 2018; Mikula et al. 2021). Deviations from the negative allometric relationship between body size and vocalisation frequency may occur due to variations in the morphology of the sound-producing organ resulting from evolutionary history. Finally, if the acoustic features of a signal reflect a species' size, dominance, fighting ability, or health, the species' sounds could be subject to sexual selection (the sexual selection hypothesis; Mikula et al. 2021).

It is likely that a combination of various selective pressures operate on the diversity of acoustic traits in the landscape simultaneously, and vary across space and time, thus generating a rich tapestry of unique soundscapes within and between habitats. This diversity of acoustic traits in the soundscape contains useful information regarding the ecological and evolutionary mechanisms at work.

5.1.5.2 Ecoacoustics beyond species

To bypass the need for species identification and support the analysis and interpretation of big acoustic datasets, a new sub-discipline of ecoacoustics has emerged in the last two decades: soundscape analysis (Pijanowski et al. 2011a; Metcalf et al. 2023). This field of research exploits the variation in acoustic traits in the landscape, and its link to the underlying selective pressures and ecological mechanisms, to infer information about the ecological processes shaping biological communities (Bradfer-Lawrence et al. 2019). Instead of focussing on the diversity or relationship between individual vocalisations in the soundscape, soundscape analytical methods focus on the signal diversity of all sounds emanating from a population, community, or landscape (Sueur et al. 2008; Pijanowski et al. 2011b).

The underlying premise is that animal sounds constitute a major source of variation in the acoustic trait diversity of the soundscape, and if ecological processes or human activities alter the composition of the sound-producing community, these changes will be reflected in the diversity of acoustic traits emanating from the landscape. Furthermore, if the ANH holds, a greater species diversity should lead to increased competition for acoustic niche space, resulting in a greater diversity of acoustic traits in the soundscape (Pijanowski et al. 2011a; Sueur and Farina 2015), thus establishing a theoretical link between acoustic trait diversity and the underlying diversity of sound-producing species.

Acoustic indices

To quantify the diversity of acoustic traits in the soundscape, soundscape analysis takes inspiration from the biodiversity indices that have long been used in ecology. The discipline summarises the acoustic trait diversity and complexity of the soundscape in space and time using acoustic diversity indices (Sueur et al. 2014). These acoustic indices are mathematical formulae that summarise the presence, distribution, and complexity of acoustic energy across the time-frequency dimensions of the soundscape (Eldridge et al. 2018; Sueur et al. 2014). Since the first acoustic index was proposed in 2007 (Boelman et al. 2007), the design, development, and application of acoustic indices have surged (Alcocer et al. 2022). A decade later, more than 65 unique acoustic indices had been described (Buxton et al. 2018), a figure that has undoubtedly increased since.

These indices can be categorised in several ways (Sueur et al. 2014; Alcocer et al. 2022). Firstly, a distinction can be made between within-group indices (e.g., alpha indices), which quantify the acoustic diversity within certain sound sample (e.g., a 1-minute sound files), and between-group indices (beta indices), which quantify the between-sample similarity or dissimilarity (Sueur et al. 2014; Burivalova et al. 2019). Within the alpha indices, metrics can be divided into: (i) intensity indices, which focus on the amplitude of the sound sample; (ii) complexity indices, which summarise the complexity of the amplitude variation across the time/frequency-domain of the soundscape; and (iii) soundscape indices, that quantify the contribution of different soundscape components (e.g., biophony, geophony, anthropophony) to the overall soundscape (Sueur et al. 2014). Another distinction can be made between indices that quantify the variation in the sound sample's signal amplitude across the temporal domain, frequency domain, or time-frequency

domain. Additionally, indices can be grouped into first-order indices, that use a single index to quantify the acoustic diversity, or second-order indices, that combine the properties of multiple indices into a new index (Towsey et al. 2014a). Finally, acoustic indices can be distinguished between those that quantify the acoustic diversity in a short-duration sample of the soundscape (often 1-minute sound files; Truskinger and Towsey 2019), or over longer durations (e.g., 24h period).

The vast majority of acoustic indices used in the literature are short-duration, first-order alpha indices that summarise the diversity or complexity of the amplitude variation in the temporal or frequency domain. These indices have been widely applied to find a link between the acoustic diversity in sound files, and landscape configuration (Tucker et al. 2014), ecosystem health (Fuller et al. 2015), diel patterns in different environments (Rodriguez et al. 2014; Farina et al. 2015), seasonal changes in soundscapes (Farina et al. 2011), habitat identity (Villanueva-Rivera et al. 2011; Depraetere et al. 2012), among others. Moreover, the performance of these indices as proxies for the underlying diversity (e.g., richness, abundance, diversity, evenness) of species or acoustic morphospecies (or sonotypes; Sueur et al. 2008b; Pieretti et al. 2011; Buxton et al. 2016; Papin et al. 2019; Farina et al. 2013; Sousa-Lima et al. 2018; Burivalova et al. 2019), and phylogenetic diversity or functional diversity (Gasc et al. 2013) is often investigated. Most recently, these indices have been used as acoustic features for convolutional neural networks to categorise soundscapes by their structure and dynamics and detect acoustic anomalies in big acoustic datasets (Sethi et al. 2020).

The advantage of these acoustic indices is that they offer a simple solution to describe the complexity of acoustic data using a single value (Sueur et al. 2014). In doing so, the information contained in sound recordings is greatly condensed, which allows researchers to efficiently process, inspect, and analyse acoustic datasets across larger spatial and temporal scales. This facilitates the exploration of complex ecological questions that were previously infeasible. Although this discipline has made substantial progress towards becoming a useful biomonitoring tool, its ability to reflect ecological patterns and biodiversity trends must be validated before this technology is implemented. While many acoustic indices have been developed, there is no consensus on the optimal set of indices to use for different ecological applications (Alcocer et al. 2022). The performance of acoustic indices can also be affected by factors such as the quality of the recordings, the presence of non-target sounds (e.g., anthropophony and geophony), and the environmental context. As a

result, we must carefully consider the choice of acoustic indices and the methods used to process the data.

Limitations and research opportunities

The last decade has shown that caution should be used when applying these indices as biological indicators (Alcocer et al. 2022), particularly when using them as proxies for biodiversity. A series of recent works have drawn attention to the fact that the performance of acoustic indices as biodiversity indicators is highly variable within and between communities (Bradfer-Lawrence et al. 2019; Metcalf et al. 2021; Alcocer et al. 2022), sometimes even showing contrasting results when using the same index (e.g., Mammides et al. 2017 versus Bradfer-Lawrence et al. 2020). Furthermore, studies investigating the relationship between acoustic indices and ground-truthed diversity show a decline in effect sizes over time since the start of this line of research (Alcocer et al. 2022). Several factors potentially contribute to these contradictory results. Below, I outline 10 points that I believe complicate the use and comparability of acoustic indices between studies and warrant attention in future efforts for the design and application of acoustic indices.

Point 1. In real-world environments, the acoustic trait diversity in soundscapes is influenced by factors beyond the diversity of the sound-producing community (Depraetere et al. 2012; Gasc et al. 2015). For instance, human-related noise, wind and rain, or broad-band choruses by stridulating insects (orthopterans and cicadas) may mask the acoustic signal of other sound-producing groups (Metcalf et al. 2021) and disconnect acoustic index values from the taxonomic group used for index validation (Hart et al. 2015; Fairbrass et al. 2017; Metcalf et al. 2021; Ross et al. 2021). Additionally, the values of certain acoustic indices are sensitive to the relative amplitude of songs in the recording, which in turn is influenced by the physical structure of the surrounding vegetation, meteorological conditions, the distance between the sound source (a vocalising individual) and the sensor, and inherent biological differences between species (Sueur et al. 2014). Finally, the observed acoustic trait diversity in the soundscape is subject to differences in the vocal repertoire size of the species in the community (Alcocer et al. 2022). Therefore, the efficacy of acoustic indices as biological indicators will depend on their ability to capture ecological processes while remaining insensitive to these potentially confounding factors.

Point 2. The novelty of ecoacoustics as a field brings about challenges in the standardisation of data collection and analytical procedures (Bradfer-Lawrence et al. 2019). Until recently, there was no agreement on the required data quantity, sampling intensity, data compression, noise reduction, acoustic index selection, and data processing (e.g., FFT window length), all of which may introduce variation in the data and contribute to inconsistent index behaviours in the literature (Bradfer-Lawrence et al. 2019; Sugai et al. 2020; Heath et al. 2021; Metcalf et al. 2021). To resolve this, recent studies have started to shed light on the variability introduced by these methodological differences, and proposed guidelines for the use of acoustic indices (Bradfer-Lawrence et al. 2019; Heath et al. 2021; Metcalf et al. 2023). Establishing the influence of methodological choices on index behaviours should become common practice for any newly proposed index, or the novel application of existing indices.

Point 3. Most studies to date have used individual acoustic indices to describe their acoustic environment (Buxton et al. 2018). These indices condense the information contained in acoustic recordings into a single value. Although this allows researchers to process big acoustic datasets more easily, this extreme information reduction likely leads to the loss of ecologically relevant data. When only considering a single index, which has a limited range of potential values, it seems unlikely we can properly capture the full complexity of a wide range of soundscapes (Towsey et al. 2014b; Buxton et al. 2018; Alcocer et al. 2022). Although many researchers have argued several acoustic indices should be used in concert to describe the soundscape accurately (Towsey et al. 2014b; Bradfer-Lawrence et al. 2019; Buxton et al. 2018; Alcocer et al. 2022), the design, development, and application of multi-index protocols have remained limited.

Point 4. Most acoustic indices to date either provide a statistical summary of the amplitude variation in the temporal domain (collapsed in the frequency domain) or the frequency domain (collapsed in the temporal domain; Eldridge et al. 2016). This means these indices are fundamentally limited in their ability to detect amplitude variations across the time-frequency domains simultaneously. Yet, the spectro-temporal partitioning of the acoustic niche (as described by the ANH) is a foundational premise of ecoacoustic research. As quoted from Eldridge et al. (2016): “If acoustic niches exist, they’re unlikely to lie along 1-dimensional vectors in the frequency and time domain, but dance dynamically across the time-frequency-amplitude domain”. Furthermore, this uni-dimensionality means indices are

constrained in the range of values they can take, and the type of acoustic features they can capture. As a result, many acoustic indices that operate along the same acoustic dimension tend to be highly correlated (e.g., ADI, AEve and H; Heath et al. 2021), limiting their use in multi-index studies or as acoustic features in ML-based soundscape classification (Sethi et al. 2020b).

Point 5. There are large differences between indices in terms of their conceptual background, computation, and interpretation, as well as variations in how the same index is calculated between studies (Alcocer et al. 2022). Acoustic indices can be presented in different forms, such as single values (e.g., summary indices) or vectors of values (e.g., spectral indices). They can be also computed as scalar quantities, ratios, averages, or normalised values (Alcocer et al. 2022), and measure a wide range of parameters, including energy intensity, energy variability, and the richness, evenness, diversity, or abundance of energy in the time or frequency domains (Sueur et al. 2014). Even within the acoustic indices that are derived from the same taxonomic diversity metric (e.g., the Shannon index), and operate along the same dimensions (e.g., the frequency domain), indices differ in their unit of diversity measurement, equations, and the duration of the sound recording on which they are calculated (e.g., Hf, H', ADI - Sueur et al. 2008b; Villanueva-Rivera et al. 2011; Pekin et al. 2012; Eldridge et al. 2016). Although there is value in capturing different aspects of the acoustic diversity using these various approaches, this lack of a unified unit of diversity measurement and mathematical framework for diversity quantification can lead to confusion and complicates the interpretation of index values between studies, potentially contributing to the reported contradictions.

Point 6. Many of the commonly used acoustic indices are derived from the Shannon index and associated functions and are thus measures of entropy (Sueur et al. 2008b; Sueur et al. 2014; Eldridge et al. 2016). Yet, there are some conceptual and statistical problems with applying these functions to acoustic analyses (outlined in section 5.2.1.1). Entropy metrics are often criticised in biodiversity research because they lack a fixed range, condense two unrelated biodiversity variables (richness and abundance) into a single value, are very sensitive to small samples, and penalise rare species (Jost 2006). Moreover, entropy indices are notorious for having ecologically counter-intuitive behaviours that can cause misleading interpretations of results (Jost 2006; Sandoval et al. 2019). For instance, Shannon index values do not scale linearly with the underlying diversity of the system (the replication principle or doubling property). This lack of a proportional diversity-

index value relationship complicates the interpretation of results and reduces the utility of these indices for comparative studies or meta-analyses (Sandoval et al. 2019). Finally, Shannon indices measure the uncertainty of the occurrence of a random variable (Pielou 1966). However, the vocalisations of sound-producing communities are non-random, showing predictable circadian and seasonal patterns, and non-random responses to biotic or abiotic events, thus violating the randomness assumption (Sandoval et al. 2019).

Point 7. Most acoustic indices are calculated from short-duration sound files, usually around 1 minute long (Truskinger and Towsey 2019; Alcocer et al. 2022). Yet, many species exhibit circadian patterns in their vocalisations that repeat every 24h (e.g., Agostino et al. 2020). Hence, natural soundscapes show daily acoustic regimes with clear temporal and spectral structures that are ecologically significant and result from underlying ecosystem processes (Sankupellay et al. 2015; Phillips et al. 2018; Wang et al. 2019). Sankupellay et al. (2015) suggested that this 24h cycle in acoustic activity is unique to a given habitat or location and can therefore be used as a type of acoustic fingerprint. Therefore, it is likely that the assembly processes structuring the presence and distribution of sound in acoustic trait space also operate at a broader temporal scale, such as the 24h period over which circadian patterns repeat. However, there are currently very few tools available to investigate soundscape diversity at this scale.

Various visualisation tools, such as false colour spectrograms and ribbon plots (Towsey et al. 2014c; Phillips et al. 2017), have been developed to examine the acoustic structure of sounds at broader temporal scales. However, quantitative protocols for comparing acoustic diversity between sites or periods have been scarce. Sankupellay et al. (2015) used vectors of acoustic indices derived from 24h sound recordings to cluster "acoustic states" in the daily cycle and compare them within the same site across multiple days, and between sites, to identify acoustic fingerprints. Building on this, Wang et al. (2019) used social network analysis on these clusters to identify differences in acoustic states over time. While these methods are a step in the right direction, they rely on visual inspection, are more complicated than the approach used by most acoustic indices, and are not fully quantitative, making them less popular in the ecoacoustic literature. An alternative approach, described by Aide et al. (2017), measured the saturation of the 24h acoustic trait space (known as the Acoustic Space Use; ASU), which strongly

correlated with the richness of acoustic morphospecies such as birds, anurans, and insects. Further development of this approach could be promising.

Point 8. Biodiversity indices, such as the commonly used entropy indices in ecoacoustics, generally measure two aspects of diversity: richness and abundance (Daly et al. 2018). In short-duration acoustic indices that use entropy-based methods, richness is measured by the number of frequency or temporal bins that have sound, and abundance is measured by the proportion of sound in each bin (Sueur et al. 2008b). At larger temporal scales, the ASU metric only quantifies the richness of sound in the acoustic trait space, without quantifying its abundance (Aide et al. 2017). As of yet, to my knowledge, no framework currently exists for the quantification of both the richness and evenness of sound at broad temporal scales. Many indices quantify abundance as the amplitude or amount of sound in a time or frequency bin. I argue that exploring different aspects of abundance could provide new insights into the use of the acoustic trait space. For instance, the temporal prevalence of sound in the same section of the acoustic trait space has not been explored but could shed light on potential patterns of dominance or rarity.

Point 9. Although the variation in the composition of ecological communities represents one of the most fundamental diversity aspects (Jost et al. 2010), and the demand for metrics that accurately compare the composition of acoustic communities is growing (Zhang et al. 2023), the development of beta indices in ecoacoustics has been limited compared to alpha indices (Sueur et al. 2014). The first beta acoustic indices were proposed by Sueur et al. (2008), who measured the temporal (Dt) and spectral (Df) dissimilarity between short-duration sound files in Tanzania, and showed a linear increase with the number of unshared species. Further developments of beta indices have included the Kolmogorov-Smirnov distance, the Symmetric Kullback-Leibler distance, and the Vectorial Correlation Coefficient (Gasc et al. 2013), which were shown to correlate with functional and phylogenetic components of avian diversity. Yet, despite promising initial results, further investigation in a broader range of settings revealed that these indices generate high dissimilarity values for highly similar samples due to slight time- or frequency-shifts (Depraetere et al. 2012; Sueur et al. 2014; Lellouch et al. 2014). The one-dimensional nature of these indices, combined with the pointwise comparison of time-steps/bins in amplitude envelopes/frequency profiles, means that perfect temporal homology is required between amplitude envelopes or frequency spectra, which is rarely attained (Sueur et al. 2014). Furthermore, these beta indices also

present issues with the sensitivity to song overlap, the distance of the sound source to the sensor, and background noise, meaning there is currently no universally accepted dissimilarity measure for sound (Burivalova et al. 2019).

Burivalova et al. (2019) proposed an alternative approach, using the pairwise mean dissimilarity calculated on a sub-section of the acoustic trait space (1 hour * 1,376 Hz) as a proxy for beta diversity to investigate differences in soundscapes between logging concessions. This approach successfully revealed a higher beta diversity in unlogged forests and the homogenisation of soundscapes in logging concessions. Still, this method does not operate at broader temporal scales (e.g., 24h) and does not provide a direct link to other diversity aspects, such as the overall system diversity (gamma) and its local diversity (alpha) components.

Point 10. Finally, ecoacoustic research suffers from taxonomic and geographic biases. For instance, to date, most research in ecoacoustics has focussed on northern temperate regions, whereas tropical regions have received considerably much less attention (Buxton et al. 2018; Sugai et al. 2019b). Tropical ecosystems like rainforests are extremely species-rich and constitute one of the noisiest environments on the planet, with highly saturated and complex soundscapes (Gasc et al. 2013; Pijanowski et al. 2011a; Alcocer et al. 2022), which likely affects the performance of acoustic indices in these places. Additionally, tropical rainforests contain many poorly known species, complicating the validation of acoustic index performance against the diversity of sound-producing species. Finally, most research investigating the performance of acoustic indices as biodiversity proxies has focussed on birds (e.g., Towsey et al. 2014a; Mammides et al. 2017; Eldridge et al. 2018; Bradfer-Lawrence et al. 2020), whereas validation against other taxonomic groups or whole soniferous communities has received far less attention (Alcocer et al. 2022).

To conclude, acoustic indices act as powerful tools for extracting ecologically meaningful information from large acoustic datasets. However, while this approach has already shown great promise in a variety of ecological applications, continued development and refinement of these indices and associated computational methods will be essential to realise the full potential of passive acoustic monitoring for ecological research.

5.1.6 Thesis objectives

This thesis seeks to address some of the limitations hindering the broad uptake of acoustic indices in tropical rainforest research and open new avenues of scientific inquiry. To achieve this objective, a novel analytical pipeline is developed to facilitate the rapid visual exploration and diversity quantification of large ecoacoustic datasets. Specifically, the overarching aims are to:

1. Develop a conceptual workflow to facilitate the visual exploration and diversity quantification of large ecoacoustic datasets using Hill numbers as a unified framework (Chapter I).

This workflow:

- a. Addresses some of the limitations and research opportunities highlighted in 5.2.2.
- b. Provides a suite of acoustic indices that facilitate the measurement of various diversity aspects (e.g., richness, evenness, and diversity) at a range of spatial scales (e.g., gamma, alpha and beta diversities), and spectro-temporal subsets using a single unit of diversity measurement (or species equivalents).
- c. Generates acoustic indices that are ecologically intuitive and abide by several fundamental properties for biodiversity indices.
- d. Provides clear methodological guidelines regarding data collection and workflow parameter choices.
- e. Accurately captures patterns in the taxonomic richness of sound-producing species in the complex acoustic environment characteristic of tropical rainforests.

2. Assess whether the newly proposed acoustic indices succeed in capturing ecological patterns in complex ecosystems at various spatial scales and provide insights into the mechanisms structuring acoustic trait diversity in space (Chapter II).
 - a. Test whether the acoustic indices can capture one of the most fundamental ecological patterns: the species-area relationship.
 - b. If so, assess whether the acoustic indices display a breakdown in the diversity-area relationship at the smallest spatial scales, known as the small-island effect.
 - c. Partition the acoustic indices into multiple diversity components (gamma, alpha, and beta) and link observed patterns to the mechanisms driving diversity in fragmented landscapes.
3. Create an open-source and user-friendly tool for implementing the analytical workflow (Chapter III).
 - a. Create a new suite of visualization tools for the exploration of big ecoacoustic data.
 - b. Create functions for the implementation of the workflow described in point one.
 - c. Provide a user guide for the tool.

5.1.7 Thesis structure

This thesis comprises three chapters, one of which has been published (Chapter I), another submitted for publication (Chapter II), and a third to be submitted soon (Chapter III).

Chapter I presents a new analytical framework based on Hill numbers for the analysis of big ecoacoustic datasets. Three newly proposed acoustic indices are evaluated for their desirable properties and ability to act as proxies for the taxonomic richness of sound-producing species in the tropical rainforests of Brazilian Amazonia.

Chapter II assesses whether one of the newly proposed acoustic indices, the soundscape richness index, can capture one of the most fundamental ecological patterns: the spatial scaling of diversity with patch size (species-area relationship). The results demonstrate that the spatial scaling of diversity extends to the realm of ecoacoustics, showing a strong positive relationship between the soundscape richness and the island size, which is termed the ‘SoundScape-Area Relationship’ (SSAR). The findings are interpreted in light of the ecological mechanisms structuring spatial diversity patterns in an insular landscape and shed light on potential drivers of acoustic diversity.

Chapter III introduces the soundscapeR R package, a user-friendly and open-source tool for implementing the workflow presented in Chapter I. The package includes a range of functions for quantifying soundscape diversity using Hill numbers, for various diversity facets, spatial scales, and spectro-temporal subsets. It also provides highly customisable visualisation tools for the rapid exploration of soundscape data.

5.2 Materials and Methods

As this thesis is primarily methodological in nature, I will not repeat the methodological details provided in the individual chapters here. Instead, I outline the thought process underlying the conceptualisation of the workflow and elucidate how the various chapters contribute to the overarching goals of the project.

5.2.1 Designing the workflow

In biodiversity research, the diversity of ecological communities is generally quantified by: (i) defining what constitutes a sample of the natural environment (e.g., a bucket of pond water); (ii) collecting samples; (iii) delineating individuals in a sample (e.g., individual invertebrates); (iv) classifying these individuals into groups with shared characteristics (e.g., species); (v) attributing an importance value to each group (e.g., raw counts per species), and finally; (vi) applying some type of mathematical equation to quantify and compare different aspects of biodiversity between samples (e.g., water from other ponds).

For the workflow in this thesis, the same procedure is followed to quantify the diversity of sounds emanating from the landscape, asking the following questions to guide workflow design:

1. What constitutes a meaningful sample of the soundscape?
2. When renouncing the identification of individual vocalisations from sound files, how should the soundscape equivalent of individuals be delineated and grouped into units of diversity measurement?
3. What constitutes a meaningful measure of importance (or abundance) in the context of the workflow?
4. What mathematical framework provides the most intuitive way to compute biodiversity metrics?

Following this structure, for each step, the choices and associated reasoning are outlined in Chapter I: 'A framework for quantifying soundscape diversity using Hill numbers'. In the next section, I provide additional detail with regard to point 4: mathematical frameworks for diversity quantification.

5.2.1.1 A note on diversity indices

Any study exploring the diversity of a system requires a quantitative measure to explore and compare patterns across space, over time periods, and more. Over the past century, a multitude of mathematical equations, known as ‘diversity indices’, have been put forth to quantify diversity patterns. However, the plethora of available indices, combined with the lack of a unified set of mathematical behaviours and ecological interpretations, have led to widespread confusion among ecologists, leading some to question the validity of diversity as a concept at large (Hurlbert 1979; Daly et al. 2018). The source of this confusion, however, should not be attributed to the notion of diversity, but rather to the indices that are used to measure it (Jost 2006).

The most used diversity index in ecology is the Shannon-Wiener index, also known as the Shannon index (Jost 2006). This is a measure of entropy that quantifies the uncertainty associated with predicting the identity of an individual (e.g., species or equivalent) in a sample (Jost 2006; Daly et al. 2018). The Shannon index works as a diversity index because, in more diverse systems, the uncertainty of predicting the identity of an individual becomes higher. Therefore, the Shannon index increases with the diversity of the system. Similarly, other classical diversity indices such as Pielou’s evenness index or the Gini-Simpson diversity index are also measures of entropy (Daly et al. 2018).

Although these entropy-based metrics scale positively with the uncertainty of the sampling process, they do not track the underlying diversity of the system in a linear manner. If we merged two equally diverse but completely distinct samples (no shared species), intuitively, we expect the diversity value to double (known as the replication principle; Hill 1973; Jost 2006). However, this is not true for entropy-based diversity indices (Jost 2006). For instance, the relationship between the Shannon index and the species richness is non-linear. At low levels of species richness, adding a single species will have a large effect on the Shannon index value, whereas at elevated levels of richness, the Shannon index value will only increase marginally (Daly et al. 2018). This non-linear behaviour means that, although we can evaluate whether two communities are statistically different in terms of their diversity index values, comparing the magnitude of these differences reliably is not possible. Additionally, when calculating diversity ratios such as the beta diversity ($\beta = \gamma / \alpha$), the non-linear scaling of entropy metrics introduces mathematical artefacts

in the diversity values (Jost 2007). Indeed, for the Shannon diversity index, this ratio always approaches 1 (suggesting highly similar systems) when the mean within-group diversity (alpha) is high, even when the systems being compared are distinct (Jost 2007; Tuomisto 2010; Chao et al. 2010).

To resolve the issues with the non-linear scaling of entropy metrics, commonly-used entropy-based diversity metrics can be converted to their number of ‘species equivalents’ or ‘effective number of species’ (ENS)– that is, the number of species (or species equivalents) in a perfectly even community (identical abundance values) that would yield the same diversity index value (Hill 1973; Jost 2006; Daly et al. 2018). To do so, simple algebraic conversions can be used (see Table 1). Interestingly, no matter what entropy metric we start with, all the associated ENS equations (Table 1 – column 4) can be reformulated to a single overarching equation:

$${}^qD = \left(\sum_{i=1}^S p_i^q \right)^{\frac{1}{1-q}}$$

This is the equation to calculate Hill numbers, with S being the number of species (or species equivalents), p_i the relative abundance of species i , and q the order of diversity. Using this equation, the sensitivity to the relative abundance of species can be modulated using the parameter q without changing the interpretation of qD . For instance, when $q=0$, the relative abundance is disregarded and the equation yields ${}^qD = S$, *i.e.*, the richness of species. The higher the q -value, the more importance is given to abundant species. When $q=1$, 1D equals the exponential of the Shannon entropy, or the number of common species.

By expressing the diversity as the ENS, Hill numbers represent ‘*true diversities*’: they capture the diversity of the underlying system in a linear manner (Jost 2006). For instance, if one community has an ENS value of 10, and a second community has an ENS of 30, we can say truly that the latter is three times more diverse than the former, which is not the case for entropy indices. Therefore, by using Hill numbers

as a mathematical framework of diversity measurement, no matter the importance given to common or rare species, all diversity values will have a common unit of measurement (ENS) and can be measured and compared easily. This avoids misinterpretation stemming from the non-linearity of indices. For these reasons, the unified mathematical framework provided by Hill numbers was selected to develop the workflow presented in this thesis.

Table 1: Algebraic conversion of commonly-used entropy indices to their effective number of species. Modified from www.loujost.com

Index name	Original equation	Algebraic conversion	Converted equation
Species richness	$x \equiv \sum_{i=1}^S p_i^0$	x	$\sum_{i=1}^S p_i^0$
Shannon entropy	$-\sum_{i=1}^S p_i \ln p_i$	exp(x)	$\exp(-\sum_{i=1}^S p_i \ln p_i)$
Simpson concentration	$x \equiv \sum_{i=1}^S p_i^2$	1/x	$1/\sum_{i=1}^S p_i^2$
Gini-Simpson index	$x \equiv 1 - \sum_{i=1}^S p_i^2$	1/(1-x)	$1/\sum_{i=1}^S p_i^2$
Renyi entropy	$x \equiv (-\ln \sum_{i=1}^S p_i^q)/(q-1)$	exp(x)	$(\sum_{i=1}^S p_i^q)^{1/(1-q)}$

5.2.2 Testing workflow characteristics using simulated soundscapes

Prior to adopting the newly proposed acoustic diversity indices generated by the workflow, it is imperative to assess whether these metrics abide by a set of desirable properties for biodiversity indices and behave in an ecologically intuitive manner.

As such, following the criteria for trait-based diversity indices outlined in Ricotta (2005), Villéger et al. (2008) and Mouchet et al. (2010), and supplemented by behaviours deemed important for these metrics, this thesis tested the acoustic indices for the following properties:

1. Indices can only have positive values
2. Indices can be strictly contained between 0-1
3. Indices are conceptually independent of the species richness
4. Indices are independent of one another
5. Indices for a subset of the community should have lower values than the whole community (set monotonicity principle)
6. Index values change proportionally with the underlying diversity of the system (replication principle)
7. Indices can be decomposed into their alpha, beta, and gamma components

For points 1-3, these behaviours arise implicitly from how the workflow is designed and should therefore not be tested. To test points 4-7, in Chapter I - Supplementary material 5, a series of simulated soundscapes is generated to assess these behaviours under a series of hypothetical scenarios. As highlighted in Villéger et al. (2008), here, each index does not have to abide by each criterion, but rather that the ensemble of indices does.

5.2.3 Testing workflow performance in a tropical rainforest ecosystem

To assess the utility of the workflow as an addition to the ecological monitoring toolbox, the acoustic indices were tested for their ability to: (i) act as a proxy for the species richness of the sound-producing community in an acoustically complex tropical rainforest ecosystem (Chapter I); and (ii) capture ecological patterns at multiple spatial scales, as well as shed light on the underlying mechanisms driving the diversity of acoustic traits across space (Chapter II).

5.2.3.1 Hydroelectric reservoirs as an experimental system

Hydroelectric reservoirs represent an ideal study system for this purpose. On the one hand, they constitute a rapidly emerging threat to Neotropical rainforest ecosystems. As developing nations are trying to keep up with the increasing demand for energy, the Neotropics is becoming a new frontier for the construction of hydroelectric dams (Finer and Jenkins 2012; Emer et al. 2013; Fearnside 2006). In areas with low elevational gradients, such as the Brazilian Amazon, hydroelectricity projects require large and shallow reservoirs, causing the inundation of vast areas of rainforest, and the creation of heavily fragmented archipelagos of land bridge islands. This results in high methane emissions and dire consequences for local diversity (Tundisi et al. 2014). Yet, the impact of this threat on natural soundscapes remains largely unknown (but see Han et al. 2022).

On the other hand, hydroelectric reservoirs represent an ideal experimental system against which to test the performance of the newly proposed acoustic indices for both ecological monitoring applications. They deal with several potentially confounding factors when investigating spatial diversity patterns (Whittaker and Fernández-Palacios 2007). For instance, all patches were formed simultaneously due to a single disturbance event. Moreover, these reservoirs have a uniform and largely untraversable matrix, a spatial scale comparable to terrestrial patches and were formed recently enough so that evolution and species adaptations have yet to take effect.

5.2.3.2 Mechanisms driving species richness in fragmented landscapes

In fragmented ecosystems, the diversity of species is influenced by two key landscape-scale variables: island size and isolation (MacArthur and Wilson 1967). According to the principles of Island Biogeography Theory (MacArthur and Wilson 1967), these variables play a crucial role in shaping colonisation and extinction dynamics, which give rise to two fundamental observations: (i) larger islands exhibit higher species richness compared to smaller islands, as described by the Species-Area Relationship (SAR); and (ii) more connected islands demonstrate greater species richness than more isolated islands, as represented by the Species-Isolation Relationship (SIR).

The SAR is arguably the most universally accepted law in ecology, having been documented numerous times across a wide range of taxonomic groups, biogeographic regions, spatial scales, and ecological disciplines (Arrhenius 1921; Rosenzweig 2010). Several mechanisms are believed to shape, regulate, and maintain SARs. Firstly, SARs may arise merely through sampling effects (Hill et al. 1994). For instance, larger islands require more intense sampling to characterise the diversity of biological communities, which leads to more individuals being sampled, and by probability, leads to more species being detected (sampling artefacts; Schoereder et al. 2004). Secondly, the theory of disproportionate effects suggests that SARs arise because island size affects the biological processes of species richness regulation, whereby larger islands experience reduced rates of extinction and increased rates of colonisation (target effects), among others (Chase et al. 2019). Disproportionate effects lead to an increase in both the local (plot-scale or alpha) and regional (island-wide or gamma) species richness with island size (Chase et al. 2019). Thirdly, the theory of heterogeneity effects postulates that larger islands contain a wider variety of habitats, each of which contains a set of uniquely specialised species, which increases the island-wide species richness (Kadmon and Allouche 2007). In this case, an increase in the gamma species richness, as well as the between-plot beta diversity, would be expected with increasing island size (Chase et al. 2019).

Compared to SARs, the mechanisms proposed to explain SIRs in patchy systems are simpler: increased geographic distance between islands and the source species pool (mainland or nearby islands) reduces the colonisation probability of isolated

islands, leading to reduced rescue effects, increased extinctions, and consequently, a reduced species richness (Giladi et al. 2014).

These ecological mechanisms underlying spatial diversity patterns in fragmented systems have been the subject of scientific inquiry at a range of spatial scales for over a century, and thus, provide an essential context against which to compare observed soundscape diversity patterns. Additionally, they could potentially help shed light on the mechanisms driving the diversity of acoustic traits across space, which is discussed in section 5.3.3.2.

5.2.3.3 Study system & data collection

In this thesis, long-duration acoustic recordings collected at the Balbina Hydroelectric Reservoir (BHR) in central Brazilian Amazonia (1° 40' S, 59° 40' W) were used. The BHR is a highly insularised system created when the area was flooded by the damming of the Uatamà River in 1987, turning over 3,500 former hilltops into islands of variable size (Fearnside 2006). Strong SARs have previously been demonstrated at the BHR for several taxonomic groups (Benchimol and Peres 2015a; Palmeirim et al. 2017; Storck-Tonon and Peres 2017), including several sound-producing groups (Benchimol and Peres 2015b; Bueno and Peres 2019; Bueno et al. 2020), providing a strong gradient in species richness against which to assess the performance of the acoustic indices described in this thesis as biodiversity proxies (Chapter I).

Acoustic surveys were carried out at the BHR for a previous study, collecting sound recordings between July-December 2015 for 151 plots situated on 74 islands and 4 continuous forest sites in 17 riparian and 134 non-riparian habitats. At each plot, an acoustic recorder was deployed at 1.5 m height with the microphone pointing downward. The device was set to record the soundscape for 1-min/5-min for 5 consecutive days at a sampling rate of 44.1 kHz using the ARBIMON Touch application. This total dataset was subsetted based on the availability of species richness data for birds, anurans, and large vertebrates (Chapter I), the quality of the sound recordings (e.g., faulty recorders, persistent rain or wind; Chapter I and 2), and a proportional relationship between the number of recorders per island and island size (Chapter II). For a full overview of data collection and site selection, consult Chapter I - Supplementary materials 6 and Chapter II - Supplementary materials 1.

5.2.4 Guiding data collection and workflow parameter choices

In addition to outlining the step-by-step procedure of the workflow and associated acoustic indices, it is important to quantify the variability in index performance in relation to methodological variations such as data collection and workflow parameters choices, and to provide guidelines for how these choices should be made (Bradfer-Lawrence et al. 2019).

As such, Chapter I - Supplementary materials 1 assessed the influence of the sampling duration and sampling regime on: (i) the relative relationship between sites in terms of the soundscape richness index; and (ii) the correlation between the soundscape richness index and the richness of sound-producing species. In Chapter I - Supplementary materials 2, the influence of the window length used in the Fast Fourier Transformation on the relationship between the soundscape richness index and soniferous species richness was tested. Finally, Chapter I - Supplementary materials 3 investigated the impact of threshold choice (a workflow parameter) on the observed soundscape richness-species richness relationship. Based on the results of these analyses, best-practice recommendations for using the workflow are provided.

5.2.5 Building software for workflow implementation

The growing complexity of tools to analyse big datasets means researchers require sophisticated statistical skills and software (Rocchini and Neteler 2012). However, oftentimes, such software tools are difficult to use, require advanced programming skills, or could be locked behind a paywall (Paradis 2020). Therefore, the development of easy-to-use and open-source software tools is imperative.

In Chapter III, the soundscapeR package is outlined, a user-friendly and open-source analytical pipeline implemented in the R coding language. The R coding language is an ideal platform for developing new software tools for ecology, due to its robust statistical capabilities, its widespread adoption and support within the scientific community, and its vast collection of libraries and packages, including several packages dedicated to acoustic analysis (e.g., seewave - Sueur et al. 2008a; soundecology - Villanueva-Rivera et al. 2018). Additionally, R also has an active community of developers who contribute to its packages and libraries or provide online support when problems arise. To ensure optimal uptake by potential users, a

comprehensive online vignette is provided, outlining the functionality of the package in detail (see Chapter III - Appendix).

5.3 Results and discussion

The workflow presented in this thesis expands on previous work in the field of ecoacoustics, building on the principles of acoustic niche theory to establish new insights into the diversity of acoustic signals in the soundscape and their relationship with landscape-scale ecosystem processes. The workflow presents several innovations that could open new avenues of scientific inquiry, and addresses limitations currently hindering the existing suite of acoustic indices.

5.3.1 Workflow novelty

Extending the temporal scale of a soundscape sample to 24h

As previously mentioned, the acoustic diversity of short-duration samples (e.g., 1-minute sound files) of the soundscape has been well explored in the literature. Conversely, analytical procedures to investigate the relationships between sounds at broader temporal scales, and quantify their diversity, have received comparatively less attention. The workflow presented in this thesis followed Sankupellay et al. (2015) and Aide et al. (2017), considering the relationship between sounds over a 24h sample period. Sampling the acoustic trait space over 24h could open new insights into the relationships between soundscapes and their sounds. For instance, many species' vocalisations display circadian rhythms, repeating their acoustic signalling activities at intervals of 24h in response to photic, temperature, humidity, or acoustic cues (Jianguo et al. 2011; Wang et al. 2012; da Silva et al. 2014; Agostino et al. 2020). Therefore, landscapes with stable sound-producing communities should display a predictable spectro-temporal acoustic structure at this scale, a concept which was termed an 'acoustic fingerprint' by Sankupellay et al. (2015). If these acoustic fingerprints are unique to a specific site, these can be used to classify soundscapes, determine the change in the use of the acoustic trait space over time, gauge the response of acoustic trait diversity to disturbances, and more. As species have previously been shown to shift their daily peak of vocal activity to avoid spectro-temporal overlap with other species (e.g., Hart et al. 2015), it is highly likely that some of the temporal partitioning of the

acoustic niche space occurs at these broader 24h scales. Therefore, quantifying soundscape diversity patterns at this scale may shed new light on the mechanisms underlying acoustic niche partitioning.

Aide et al. (2017) previously quantified the diversity of acoustic traits over a 24h period using the ASU metric, which correlated with the diversity of unique sound types (i.e., acoustic morphospecies) for birds, frogs, and insects. This index was also successfully applied to investigate the influence of elevation (Campos-Cerqueira and Aide 2017), natural gas exploration (Deichmann et al. 2017), gold mining (Alvarez-Berrios et al. 2016), forest certification (Campos-Cerqueira et al. 2020), protected area establishment (Herrera-Montes 2018), and habitat restoration (Ramesh et al. 2023) on natural soundscapes. The workflow in this thesis expands on these diversity quantification efforts in several ways, and these are outlined below.

Formalising a unit of soundscape diversity measurement

The unit of diversity measurement adopted here is defined as: the ‘Operational Sound Unit’ (OSU). These OSUs are obtained by dividing the acoustic trait space (00:00-23:59h; 0-20,000 Hz) into many discrete spectro-temporal bins, which are the soundscape equivalent of time-frequency bins in a spectrogram. By doing so, OSUs group sounds with shared spectro-temporal properties (having similar coordinates in the acoustic trait space) into units that can be used to measure diversity, and that can be compared between soundscapes. Although these OSUs are conceptually alike to the time-frequency bins used for diversity quantification in Aide et al. (2017), there is value in explicitly formalising what is being measured. By doing so, the attempt is to alleviate some of the confusion troubling studies on acoustic indices regarding what constitutes the unit on which diversity indices are computed (i.e., the soundscape equivalent of species; Alcocer et al. 2022), and ease the interpretation, transferability, and comparison of diversity measures between studies. These OSUs differ from the time-frequency bins in Aide et al. (2017) in the amplitude features that are used to determine the presence and prevalence of sound in the acoustic trait space, and the resolution of bins along the temporal axis.

Including a measure of temporal sound incidence

The workflow presented here goes beyond measuring the richness of acoustic traits in the soundscape (e.g., ASU) by including a measure of importance (e.g., relative

abundance) in the soundscape diversity quantification. To do so, an incidence-based framework was used, determining the detection (1) / non-detection (0) of OSUs in each 24h sample of the soundscape using a detection threshold, and calculating the incidence frequency (or relative abundance) of each OSU across the recording period (all 24h soundscape samples). To my knowledge, no acoustic index has explored the temporal incidence of sound in the same section of the acoustic trait space over multiple days. Yet, using the occurrence of sound at the same time-frequency coordinates over multiple days as a measure of relative abundance could provide new insights into the use of the acoustic trait space. By quantifying the evenness, the temporal dominance or rarity of sound in different sections of the acoustic trait space could be explored and compared between soundscapes and over time. This approach could reveal how effectively the acoustic trait space is used as a resource over time and shed new light on the competition for the acoustic niche within the ANH framework (Krause 1987).

Integrating soundscape diversity quantification with the framework of Hill numbers

The current study moves away from the entropy-based diversity indices that are commonly used in ecoacoustics (Sandoval et al. 2019). Instead, the diversity quantification is integrated with the framework of Hill numbers (Jost 2006). Although this statistical framework was suggested to be suitable for ecoacoustics almost a decade ago (Sueur et al. 2014), to my knowledge, the current workflow represents the first example of the application of Hill numbers for ecoacoustics. Hill numbers provide several advantages. Firstly, Hill numbers provide a unified statistical framework that is sufficiently robust and flexible to accommodate the quantification of different dimensions of diversity. For instance, Hill numbers can be used to quantify not only the soundscape diversity, but also taxonomic, functional, and phylogenetic diversity (Chao et al. 2014a). Using a unified framework for the measurement of different diversity dimensions gives the metrics a common behaviour and ensures that the observed relationships between diversity dimensions (e.g., soundscape diversity \sim taxonomic diversity) result from true ecological patterns, and not just from differences in the mathematical formulae used to calculate diversity (Chao et al. 2014b).

Secondly, unlike entropy-based metrics, Hill numbers scale linearly with the underlying diversity of the system (the replication principle or doubling property;

see 9.2 and Hill 1973; Jost 2006). This gives the resulting acoustic indices more intuitive behaviours and allows direct comparison of the magnitude of soundscape diversity values between studies. Additionally, using Hill numbers, the soundscape diversity can be partitioned into its different diversity components (e.g., richness, evenness, diversity), orders of diversity (e.g., $q=0$, $q=1$, $q=2$, ...), or spectro-temporal subsets (e.g., day, night, dawn, dusk). By doing so, the workflow can shed light on various aspects of acoustic diversity while maintaining the same analytical framework, unit of measurement (OSUs), and index behaviours, which facilitates the interpretation of values between indices and studies.

Thirdly, Hill numbers can also be used to reliably partition the regional diversity (γ) into its within- (α) and between-group (β) components using a simple multiplicative relationship (Jost 2007). Indeed, in ecology, the ratio of the mean within-group diversity (α) to the total pooled diversity (γ) is often used as a measure of compositional similarity or dissimilarity (β) between groups (Jost et al. 2010). Yet, for entropy-based indices, using this ratio as a measure of compositional differentiation can lead to serious misinterpretation of results due to the non-linear scaling of the index-diversity relationship (Jost 2006). Since Hill numbers scale linearly with the underlying diversity of the system, this issue is resolved (Daly et al. 2018). This is further discussed in section 5.3.2.

Hence, the current workflow provides a metric of compositional similarity between soundscapes (β) at a 24h scale with intuitive behaviours, a link to the other diversity components (α and γ), and a common unit of diversity measurement (OSUs). Although the β soundscape turnover can range from $1 - N$ (the number of soundscapes being compared), this metric can easily be transformed into a measure of similarity or dissimilarity (ranging from 0 – 1) by using equations such as the Jaccard dissimilarity or the Sørensen–Dice dissimilarity (Jost et al. 2010). Because this index of compositional differentiation operates on soundscapes at a more coarse resolution (OSUs collapse the features of sounds across 1-minute files), at broader temporal scales, and uses incidence data rather than raw amplitude values, I argue that the β soundscape turnover will be less sensitive to the time- or frequency-shifts that trouble many of the existing β acoustic indices.

5.3.2 Index characteristics

In Chapter I - Supplementary materials 5, it was tested whether the newly proposed acoustic indices abided by some essential properties for diversity indices, as well as some additional behaviours that were deemed important.

Firstly, the principle of 'set monotonicity' was tested, which states that any subset of the community under investigation should yield a lower richness and diversity value than the total community (Ricotta 2005; Villéger et al. 2008). The evenness, however, is not expected to follow this principle, as a subset of the community can have a more even relative abundance distribution than the community as a whole. These expectations are confirmed by our results: the monotonicity criterion held for the soundscape richness and the soundscape diversity, but not for the soundscape evenness (Chapter I – Fig. S8). The same observation was made by Villéger et al. (2008), who found that their index of functional richness abided by the monotonicity principle, but the functional evenness did not. The simulations further demonstrated that the soundscape richness and soundscape evenness indices are independent of one another (Chapter I – Fig. S9). Conversely, the soundscape diversity index was not independent, which follows expectations since it incorporates both measures of richness and evenness into the same value.

Next, the newly proposed acoustic indices were tested on their compliance to the replication principle (or doubling property; Hill 1973; Jost 2006). Unlike many entropy-based indices, which do not scale linearly with the underlying diversity of the system and therefore violate the replication principle, the acoustic indices presented in this thesis were shown to follow this intuitive notion of diversity (Chapter I – Fig. S10). This resolves the issues with the non-linear behaviour of diversity metrics, reduces the chances of index misinterpretations, and increases the comparability of index values between studies. Furthermore, this allows the beta diversity, calculated as the ratio of alpha to gamma diversity, to accurately reflect the compositional similarity of assemblages (Jost 2007; Daly et al. 2018). The metric of beta soundscape turnover described here (at $q=0$) followed this notion of compositional similarity (Chapter I – Fig. S12).

By confirming that these indices abided by these criteria, one can be confident that the proposed acoustic indices will represent true patterns, and not stem from unintuitive index behaviours or differences in mathematical formulae.

5.3.3 Indices as biodiversity proxies or ecological indicators

5.3.3.1 Indices as biodiversity proxies

Since their inception, a common aim for acoustic indices has been to provide a tool that can act as a proxy for biological diversity, mostly species richness or abundance, without the need for species identification from sound files (Boelman et al. 2007; Sueur et al. 2008; Farina et al. 2011). Subsequent studies have focussed on using acoustic indices in a variety of different ways, including as indicators of ecosystem health (e.g., Tucker et al. 2014) or landscape configuration (e.g., Fuller et al. 2015). However, the overall ambition to use these indices as biodiversity proxies has persisted as the field has matured (Alcocer et al. 2022).

Most of the work attempting to validate the performance of acoustic indices as biodiversity proxies has focussed on their relationship with the richness or abundance of birds in recordings (e.g., Depraetere et al. 2012; Mammides et al. 2017; Buxton et al. 2016; Eldridge et al. 2018; Bradfer-Lawrence et al. 2020), while studies investigating their relationship with the diversity of anurans, insects, mammals, or the soniferous community at large, remain scarce (but see Sousa-Lima et al. 2018; Aide et al. 2017). A recent meta-analysis by Alcocer et al. (2022) on the performance of acoustic indices as biodiversity proxies revealed mixed results, demonstrating substantial variability in index performance across target groups, study systems, and methodological approaches, and diminishing effect sizes over time. These observations are casting doubt on the use of these indices as direct biodiversity proxies and challenge the validity of the underlying theoretical and empirical assumptions. Concerningly, there is an increasing number of studies employing acoustic indices as direct biodiversity proxies without validating their performance against ground-truthed biodiversity, leading to an unsustainable situation that jeopardises the credibility of the field.

Consequently, it is essential to conduct index validation before utilising any new acoustic index or applying a previously described index in a new study system. Additionally, to avoid introducing additional uncertainty in the index-biodiversity relationships reported in the literature, it is critical to evaluate the impact of methodological variations on index performance and provide best-practice recommendations for data collection and index parameterisation. Therefore, one of the objectives of this thesis was to assess the performance of two recently proposed

acoustic indices (soundscape richness and evenness) as proxies for the richness of sound-producing organisms in the study system investigated here. To achieve this, a compound species richness index was constructed by aggregating the richness of three major sound-producing groups in tropical rainforests: birds, anurans, and primates. Although taxonomic richness data was missing for insects, a dominant sound-producing group, the combined activity of these three groups was deemed to be sufficient to influence rainforest soundscape and the proposed acoustic indices. Through simple linear regressions, the association between the compound richness metric and soundscape richness and evenness was examined across 35 sites spanning a species richness gradient in the BHR. Furthermore, the influence of the sampling regime, sampling duration, and Fast Fourier Transformation window length on the observed relationship between the index and species richness was investigated.

The soundscape richness

The soundscape richness exhibited a strong positive correlation with the richness of sound-producing species at the BHR ($r = 0.85$; $R^2 = 0.72$; $p < 0.001$). The soundscape richness index performed well compared to other conceptually similar acoustic indices that also measure the richness or saturation of the acoustic trait space and compare them with the overall diversity of the soniferous community. For instance, Aide et al. (2017) found a strong positive correlation (Spearman's $\rho = 0.85$) between the ASU metric and the richness of unique acoustic calls (or acoustic morphospecies) for birds, anurans, and insects, albeit with a relatively small sample size (8 sites). Similarly, the soundscape saturation metric (which measures the saturation of the acoustic trait space at a 1-minute scale) in Burivalova et al. (2019) showed a moderate correlation ($r = 0.56$ and $R^2 = 0.31$) with the richness of unique vertebrate calls in the same sound files. Importantly, both studies compared index values with the richness of unique acoustic morphospecies, whereas Chapter I compared this metric against the richness of soniferous species without specific knowledge of the diversity of their acoustic signals. The former approach is expected to have a more direct influence on the diversity of acoustic traits in the landscape since different calls in a species' acoustic repertoire tend to be spectro-temporally distinct (Alcocer et al. 2022), leading to improved correlations between the acoustic indices and measured biodiversity variables. Despite this discrepancy, the soundscape richness metric demonstrates equal or improved correlations, attesting to its robustness.

The performance of the soundscape richness index as a proxy for species richness was also found to be relatively insensitive to methodological variations. The soundscape richness - species richness relationship remained consistently high ($r > 0.8$) across all tested sampling regimes, even when only 1 minute per hour was sampled. Additionally, the performance of the soundscape richness as a biodiversity proxy was virtually unaffected by the window length used in the Fast Fourier Transformation. The relative relationship between sites in terms of soundscape richness was found to stabilise after a minimum of 24h of continuous recording, spread over 5 days. This suggests that the acoustic indices described in this thesis require less intensive sampling compared to previous studies (e.g., Bradfer-Lawrence et al., 2019, who recorded for 120 hours). However, it is important to note that the results at longer sampling durations in Chapter I are based on extrapolation rather than actual sampled data due to the nature of our testing data (i.e., 1-minute or 5-minute sampling regime, < 10 days of recording). This may compromise the comparability of the results. Therefore, to remain conservative, and considering that ecosystems may have different rates of acoustic turnover compared to our system, I recommend that users record their soundscapes for a minimum of 5 days and, if possible, for longer durations or more intensively.

These findings suggest that the soundscape richness metric holds promise as a biodiversity proxy. However, several limitations must be addressed before it can be widely accepted in this capacity. First, the metric's performance as a biodiversity proxy was only evaluated based on the richness of the sound-producing community. Soundscape analyses operate on the assumption that alterations in the diversity of the soniferous community reflect broader changes at the community level, resulting from shared ecosystem dynamics or disturbances (Bradfer-Lawrence et al. 2019; Alcocer et al. 2022). Yet, this assumption has seldom been rigorously tested. If the diversity trends observed in vocal groups do not align with those of non-vocal groups, or if non-vocal/quiet taxonomic groups are disproportionately affected by negative anthropogenic activities, employing acoustic indices as proxies for overall community biodiversity could lead to a misleading assessment of the biological community's health. Still, all biodiversity monitoring tools for tropical rainforest wildlife are taxonomically biased (Zwerts et al. 2021), and compared to other automated sensing methods, acoustic sensors capture a comparatively broad range of taxonomic groups (Sethi 2020).

Second, although a strong positive correlation between the species richness of sound-producing organisms and the richness of OSUs (soundscape richness) was demonstrated, it is important to note that these two units of diversity measurement are unlikely to be directly proportional. In other words, the addition of one species does not correspond to the addition of one OSU (Aide et al. 2017; Burivalova et al. 2018). This disparity arises from the fact that different species or taxonomic groups exhibit distinct spectro-temporal call structures and vocal repertoires (Aide et al. 2017), which directly influences their likelihood of a species' vocal activity triggering the detection of OSUs using the analytical framework I propose, as well as their potential impact on the acoustic trait space occupancy. For example, a loud, continuous, broadband cicada chorus is more likely to trigger the detection of OSUs using our workflow than sporadic short-duration calls, such as the alarm calls of brocket deer. Furthermore, insects and anurans primarily employ a single repeated call over time whereas birds can possess incredibly diverse vocal repertoires (Riede 1996), with each vocalisation exhibiting unique spectro-temporal characteristics within the acoustic trait space. These inherent differences significantly impact the contribution of vocalisations from different taxonomic groups to the soundscape richness metric. A study by Aide et al. (2017) previously explored the variable influence of different groups on the acoustic trait space, revealing that insects exert a greater influence than birds and anurans on the ASU metric. The case study presented in Chapter I lacked information on the richness or signal diversity of insects, which represents a significant gap in our understanding, given their substantial vocal presence within tropical rainforests. Thus, it is strongly recommended that future investigations employing the acoustic indices described here assess the relative influence of various species or taxonomic groups on the resulting metric values.

Third, the performance of the acoustic indices has only been tested in a single environment. Previous meta-analyses have revealed that the efficacy of indices as biodiversity proxies tends to decrease as they are applied to a broader range of ecological settings or taxonomic groups (Alcocer et al. 2022). Therefore, it will be crucial for future efforts to assess whether the indices that are described in this thesis will hold up in a wider variety of systems. Finally, although the proposed workflow incorporated several steps aimed at reducing the influence of non-target sounds on the acoustic index values, the performance of these new indices under a range of background noise conditions has yet to be assessed. Previous work has

shown that few indices can capture biodiversity patterns in a broad range of sonic conditions (Ross et al. 2021), highlighting the need for future work in this area.

In summary, the soundscape richness shows great potential to act as a proxy for the richness of sound-producing species in tropical rainforests, especially when the diversity of the resident soniferous community is poorly known, but further validation is required before it is broadly adopted in this capacity.

The soundscape evenness

The correlation analysis between the soundscape evenness metric and the richness of sound-producing species revealed a weak positive relationship ($r = 0.40$; $R^2 = 0.16$; $p < 0.05$). Based on theoretical expectations, a link between the richness of soniferous species and the evenness of the soundscape was not anticipated. However, it is possible that the mechanisms influencing species richness in the BHR also impact the temporal dominance or rarity of sounds during the recording period.

The soundscape evenness measures the distribution of relative abundances of Operational Sound Units within the acoustic trait space over time. The positive correlation observed between soundscape evenness and species richness suggests that acoustic communities with a higher number of species tend to utilise the available acoustic trait space more evenly over time. In contrast, communities with fewer species exhibit a greater discrepancy between common and rare sounds over time. This observation potentially aligns with the ANH, which proposes that disturbed species-poor sites may have an imbalanced equilibrium within their acoustic communities. It is plausible that such disturbances lead to a scenario where only a few acoustically dominant species coexist with numerous rare or transient sound-producing species, leading to the observed pattern. However, it is crucial to note that, to my knowledge, the temporal prevalence of sound in the acoustic trait space has not yet been investigated in soundscape research. Therefore, any proposed mechanisms explaining the observed patterns are purely speculative at this stage and require empirical testing before definitive conclusions can be drawn.

Nevertheless, I suggest that investigating not only the diversity of acoustic traits in a soundscape, but also the consistency of acoustic trait space occupancy over time,

could yield valuable and novel insights into the mechanisms that structure acoustic communities. Further exploration in this direction is warranted.

5.3.3.2 Indices as a tool to capture ecological patterns and drivers of acoustic trait diversity

Spatial patterns in acoustic diversity

In Chapter II, the spatial variation of the soundscape richness index was assessed in the BHR, linking acoustic diversity values to two core variables driving diversity patterns in insularised systems: the island size and isolation (MacArthur and Wilson 1967). Although studies have previously used soundscape analysis tools to investigate biogeographic patterns in acoustic diversity across space (Tucker et al. 2014; Fuller et al. 2015; Müller et al. 2020), the mechanisms governing the diversity of acoustic traits in fragmented systems have received surprisingly little attention (but see Han et al. 2022).

Unfortunately, due to the inherent negative correlation between the island size and isolation that exists in many hydroelectric reservoirs, including the BHR, the effect of island isolation on soundscape richness could not be reliably assessed. When omitting the isolation variable from the analysis, a strong positive relationship ($R^2_{\text{adj}} = 0.45$; $z\text{-value} = 0.14$; $\log_{10}c = 1.28$) between the island-wide (gamma) soundscape richness and island size was demonstrated, which was termed a ‘SoundScape-Area Relationship’ (SSAR). This SSAR displayed a breakdown at the smallest spatial scales (< 9.4 ha), indicative of a small island effect (SIE), whereby the effect of island size on the richness is obscured by stochastic effects (Lomolino and Weiser 2001). When excluding the islands below this threshold from subsequent analyses, the observed correlation improved considerably ($R^2_{\text{adj}} = 0.71$; $z\text{-value} = 0.28$; $\log_{10}c = 1.03$).

These results suggest that the soundscape richness index is sensitive to one of the most ubiquitous ecological patterns, the species-area relationship. Indeed, the strength and slope values of the observed SSAR correspond well with those described in previous studies investigating SARs for soniferous species at the BHR (see Chapter II – Table 2). Moreover, the observed SIE threshold aligns with those previously reported at the BHR. For instance, for large vertebrates, Benchimol and Peres (2015b) reported a breakdown of SARs below 10 ha. Similarly, for anurans,

SARs were weak below 100 ha, and non-significant below 4 ha (Bueno et al. 2020). These observations imply that the soundscape richness metric captures the same mechanisms that drive SARs at the BHR.

Several studies have previously investigated the role of habitat fragmentation or insularisation on the integrity and diversity of soundscapes. For instance, Tucker et al. (2014) investigated the impact of forest fragmentation on soundscapes across urban and rural landscapes in Australia, demonstrating an increase in low-frequency sound (1-2 kHz) and a decrease in mid- to high-frequency sound (3-11 kHz) with decreasing habitat patch size and connectivity. Similarly, Fuller et al. (2015) found that a habitat's decreasing biocondition (linked to decreasing patch size and connectedness) lead to an increase in human noise and a decrease in biophony, as well as an increase in acoustic entropy. Finally, Müller et al. (2020) found that smaller habitat patches in agricultural landscapes had a lower value for the Acoustic Diversity Index. These studies suggest that small and isolated habitat fragments experience an increase in the anthropophony and a decrease in acoustic diversity, which can potentially be linked to a reduced biophony.

Yet, positive diversity-area relationships can emerge through a range of mechanisms, including sampling effects (sampling artefacts and passive sampling), disproportionate effects, and heterogeneity effects. Furthermore, the observed correlation between the soundscape richness and island size (SSAR) could be the result of a direct effect of the richness of sound-producing species on the acoustic diversity but could equally arise through other underlying ecological or evolutionary mechanisms driving the diversity of acoustic traits in the landscape, which may have implications on the interpretation of the soundscape richness as a biodiversity proxy.

Drivers of acoustic trait diversity in a landscape

In the field of ecoacoustics, researchers generally consider two predominant mechanisms as drivers of acoustic trait diversity in a landscape: (i) the Acoustic Niche Hypothesis (ANH); and (ii) the Acoustic Adaptation Hypothesis (AAH) / Acoustic Habitat Hypothesis (AHH). The former hypothesis posits that the acoustic trait space itself represents a crucial ecological resource that is partitioned within the time-frequency domain to prevent signal overlap with sympatric species (Krause 1987), leading to the diversification of acoustic traits at local scales. The

later hypotheses suggest that the surrounding environment functions as an environmental filter, actively selecting for specific traits acoustic traits that optimise sound transmission and minimise attenuation in the habitat (Morton 1975; Mullet et al. 2017), either through evolutionary mechanisms (AAH) or through the ecological phenomenon of habitat selection (AHH). Ultimately, this filtering process leads to the homogenisation of acoustic traits at local scales. These two conceptual frameworks are not mutually exclusive; rather, they represent complementary perspectives that together contribute to our understanding of the complex dynamics underlying the diversity of acoustic traits in the landscape.

For this reason, the positive relationship between the island-wide (γ) soundscape richness and the island size may be explained in multiple ways. First, it is possible that neither of the aforementioned mechanisms is driving the diversity of acoustic traits at the BHR, and the observed SSAR is simply the result of sampling effects. For instance, larger islands need a higher sampling effort to accurately characterise the biological community, which leads to more acoustic signals being sampled, and by probability, increases the chance of detecting more OSUs (sampling artefacts; Hill et al. 1994). If this is true, the relationship between the γ soundscape richness and island size should disappear after equalising the sampling effort among islands using rarefaction (Chase et al. 2019).

Second, the correlation could indicate that the ANH holds, and disproportionate effects are causing a greater species richness in large islands, leading to more competition for acoustic niche space and the diversification of acoustic traits. In this way, species richness has a direct effect on the richness of acoustic traits in the landscape. If this is the only acting mechanism driving acoustic trait diversity, a positive relationship between the island size and the plot-scale (α) soundscape richness and island-wide (γ) richness, but not the between-plot (β) soundscape turnover, is expected.

Third, the observed pattern could also arise if larger islands have a greater habitat diversity than small ones, as predicted by the theory of heterogeneity effects. This could lead to both an increase in the γ species richness (unique species in each habitat) and the γ richness of acoustic traits (unique acoustic adaptations to each habitat), as described by the AAH or the AHH. This would suggest an indirect link between the species richness and acoustic trait richness, through the effects of habitat diversity. If this was the only acting mechanism, a

positive relationship between the island size and the gamma soundscape richness, as well as the between-plot (beta) soundscape turnover, but not the alpha soundscape richness, is expected.

By decomposing the soundscape richness values into components of island-wide and plot-scale soundscape richness, as well as a between-plot soundscape turnover component, and linking them to theoretical expectations based on the theory of island biogeography, the mechanisms structuring the diversity of acoustic traits in our study system may be elucidated. The second part of Chapter II dove deeper into these mechanisms. Although slightly weakened, the gamma SSAR persisted after equalising the sampling effort between islands (temporal-effort-based rarefaction: $R^2_{\text{adj}} = 0.54$, $z\text{-value} = 0.17$, $\log_{10} c = 1.15$; plot-based rarefaction: $R^2_{\text{adj}} = 0.40$, $z\text{-value} = 0.13$, $\log_{10} c = 1.20$), confirming that the observed pattern is caused by mechanisms beyond sampling artefacts. Additionally, the plot-scale alpha soundscape richness ($R^2_{\text{adj}} = 0.39$; $z\text{-value} = 0.13$; $\log_{10} c = 1.20$), but not the between-plot beta soundscape turnover ($R^2_{\text{adj}} = 0.00$; $z\text{-value} = 0.00$; $\log_{10} c = 0.14$), was found to scale positively with island size. This indicates that heterogeneity effects, paired with the AAH or AHH, are unlikely to be the dominant mechanism structuring acoustic trait diversity in the BHR. Instead, the perceived patterns line up well with the theoretical expectations under the ANH. In addition to the increased competition for the acoustic trait space within more speciose communities, the ANH posits that stable ecosystems achieve an evolutionary equilibrium in the spectro-temporal structure of sounds within their landscapes (Krause 1987). However, when these ecosystems undergo disturbances, detectable gaps in the utilisation of the acoustic trait space emerge, resulting in reduced acoustic diversity. Considering that the islands in the BHR were formed after a disturbance event, and severe edge effects have previously been shown at the BHR (Benchimol and Peres 2015a), it is plausible that the small islands have experienced losses of species occupying unique acoustic niches. This loss would lead to both diminished species richness and a reduction in acoustic trait diversity, as indicated by the soundscape richness metric.

Yet, correlation does not establish causation, and therefore, conclusive evidence for the ANH as a driving mechanism at the BHR cannot be provided. As highlighted in Sugai et al. (2021), there are other hypotheses potentially influencing the diversity of acoustic traits in the landscape, which have received comparatively less attention in the field of ecoacoustics. For instance, species sorting in the landscape may be

subject to a non-sensory environmental filter, promoting certain morphological or phylogenetic traits which exert an indirect influence on the diversity of acoustic traits. For instance, body size is an important trait involved in community assembly (Farjalla et al. 2012), but also exhibits a strong correlation with the potential frequency range species can produce (Tietze et al. 2015). As such, a selective pressure on body size would most likely also alter the distribution of trait values in the landscape. Similarly, phylogenetically close species often have similar acoustic traits (Gingras et al. 2013), so if an environmental filter selects for traits associated with a specific taxonomic group, this likely also filters the range of acoustic traits in the landscape. Finally, the observed patterns in Chapter II may match the expectations under the ANH, but could actually result from past evolutionary legacies, where traits evolved in an ecological context that is unrelated to the patterns that are observed today (Sugai et al. 2021). To fully elucidate the relative contribution of sexual selection, non-sensory morphological or phylogenetic selection, and sensory-driven selection on the acoustic trait diversity in the landscape, acoustic diversity patterns need to be studied in relation to phylogenetic, morphological, and the past and present ecological characteristics of communities (Sugai et al. 2021).

Only one other study has investigated the mechanisms driving the relationship between acoustic diversity indices and island biogeographic patterns in insular systems. Han et al. (2022) investigated the relationship between three acoustic indices (Acoustic Complexity Index - ACI, Bioacoustic Index - BI, Acoustic Evenness Index - AEI, Acoustic Entropy Index - H) and the island size and isolation at Thousand Island Lake in China. They reported a significant positive relationship between the island size and the Acoustic Complexity Index, Bioacoustic Index and Acoustic Evenness Index, but not the Acoustic Entropy Index. The Acoustic Evenness Index was also found to decrease with an increasing degree of island isolation. These findings suggest that, for indices calculated on short-duration sound files (1-minute) collected at dawn, larger islands exhibited a greater acoustic diversity and lower evenness. Furthermore, using structural equation models, these authors showed that the increase in the soundscape diversity values with island size could likely be attributed to the lack of vocal species on small islands. Contrary to the findings in Chapter II, this study also demonstrated an effect of habitat diversity on the relationship between island size and the acoustic complexity index, attributing the greater acoustic complexity to a rising diversity of background noise with

increasing habitat diversity, and the effect of acoustic adaptation to local habitats (Han et al. 2022).

The results of Chapter II demonstrate that measuring the soundscape richness index at multiple spatial scales, and linking observed patterns to ecological theory, can be used to unravel complex ecological mechanisms and shed light on potential drivers of soundscape diversity. This expands the potential of the acoustic indices described in the thesis beyond proxies for species richness, highlighting their use as non-invasive and efficient tools to study the biogeography and spatial dynamics in complex rainforest systems. Finally, this work shows that habitat destruction and insularisation have severe effects on the acoustic complexity of ecological communities, leading to the depletion of natural soundscapes, which may have adverse consequences for the functioning of rainforest ecosystems.

5.3.4 soundscapeR: a new addition to the ecoacoustics toolbox

Recent advancements in technology have led to the miniaturization of acoustic sensors and the increased capacity of data storage devices at a reduced cost. As a result, there has been a significant increase in the collection of large ecoacoustic datasets (Sugai et al. 2019b). However, the development of robust analytical methods to extract ecologically relevant information from these datasets has lagged behind (Gibb et al. 2019; Vella et al. 2022).

In Chapter III, we introduced soundscapeR, a user-friendly software tool designed to facilitate the workflow described in Chapter I. Implemented in the R coding language, soundscapeR enables efficient exploration, visualization, diversity quantification, and comparison of environmental sound using Hill numbers. The tool guides users through a series of easy-to-use functions, categorized into four workflow steps: (i) file management; (ii) soundscape preparation; (iii) exploration and diversity quantification of single soundscapes; and (iv) diversity quantification and comparison of multiple soundscapes. To enhance the usability of the workflow, we present a novel S4 data object called the 'soundscape' object. This data object is created during the 'soundscape preparation' phase and saves the resulting data, metadata, and parameter choices in predetermined slots as users progress through the analytical pipeline. By standardizing the expected data input for each slot, the soundscape object minimizes the risk of accidental errors during the soundscape

preparation phase. Furthermore, this data object serves as the foundation upon which all subsequent functions operate, allowing for easy saving and sharing of data between studies.

To demonstrate the efficacy of the soundscapeR workflow, we conducted a comparative analysis of the soundscapes of two islands with differing sizes in the BHR (Andre Island: 2.08 ha; Mascote Island: 668.03 ha) using the functions available in the package. Using soundscape heatmaps (`ss_heatmap`), we visually explored the soundscapes of Andre Island, revealing a distinct dawn chorus and a less diverse soundscape during the daytime. Further analysis using four types of soundscape diversity plots (`ss_diversity_plot`) unveiled patterns in the spectro-temporal usage of the acoustic trait space, confirming the presence of the dawn chorus and day-night patterns while also highlighting a significant absence of sound above 15,000 Hz. By utilizing differential heatmaps (`ss_compare`) to compare the soundscapes of Andre Island and Mascote Island, we discovered clear differences in the usage of the acoustic trait space. Mascote Island exhibited a considerably higher amount of sound during the daytime and featured two distinct bands of nocturnal sound above 15,000 Hz. These differences in acoustic trait space occupancy were also evident in the quantification of soundscape diversity (`ss_diversity`), with Mascote Island demonstrating a much higher richness value than Andre Island. Furthermore, Principal Coordinate Analysis (`ss_pcoa`) and dissimilarity quantification (`ss_pairdis`) revealed that the plot on Andre Island was the most dissimilar from all the plots on Mascote Island. Additionally, this analysis revealed a slight within-island variability in the usage of the acoustic trait space for Mascote Island, albeit to a lesser extent. To assist in the implementation of the workflow and further investigate patterns in soundscape diversity for the islands in the case study, we provided a comprehensive vignette (Chapter III – Appendix).

In summary, Chapter III solidifies soundscapeR as a valuable addition to the ecoacoustics toolbox, simplifying the exploration and analysis of large-scale acoustic data.

5.4 Conclusion and future perspectives

In this thesis, a novel framework for quantifying soundscape diversity patterns at broader temporal scales was outlined. This framework incorporates the temporal incidence of sound in the diversity quantification process and integrates the diversity measurement with the framework of Hill numbers. This allows one to quantify distinct aspects of diversity (richness, evenness, and diversity), partition diversity values into its sub-components (gamma, alpha, beta), calculate dissimilarity metrics and investigate soundscape diversity patterns for different spectro-temporal subsets using a single statistical framework. The acoustic indices presented in this thesis have a common unit of measurement which was termed the 'Operational Sound Unit', a common set of behaviours, and an ecologically intuitive interpretation. The utility of the soundscape richness and evenness indices as a proxy for the species richness of the soniferous community was assessed, demonstrating the potential of the soundscape richness index for this purpose. Moreover, this thesis showcased how decomposing the soundscape richness into its local (alpha), regional (gamma) and turnover (beta) components, and linking spatial patterns to ecological theory, may shed light on the mechanisms driving acoustic diversity in a landscape. Furthermore, this work also provided evidence for a strong simplification of the soundscape diversity with increasing habitat fragmentation, which potentially has severe consequences for the functioning of acoustic communities. Finally, soundscapeR was presented, a user-friendly and open-source software for the implementation of our workflow, as well as the visual exploration of big acoustic datasets.

Based on the foundations laid out in this thesis, I envision future developments in several areas, which are discussed below.

5.4.1 Further framework development

The soundscape dispersion

As previously discussed, most biodiversity indices consider only two aspects of diversity: the richness of diversity units (e.g., species richness), and the equitability in the abundances of these diversity units (e.g., species evenness). This view on diversity is known as the 'species-neutral diversity' (Chao et al. 2010; Daly et al.

2018) and assumes that all species (or other diversity units) are equally similar. However, this does not fully capture the intuitive notion of diversity. For instance, a community consisting of 10 vastly different species is expected to be more diverse than a community consisting of 10 very closely related species. Yet, these differences are not captured by the richness or evenness of the community. The same is true for the workflow presented in this thesis. The acoustic diversity indices treat OSUs as being equally similar. In reality, however, these OSUs are correlated in the acoustic trait space. OSUs with similar time-frequency coordinates should be perceived as being more similar, whereas OSUs on opposite sides of the acoustic trait space should be perceived as more different. These differences are not captured by the acoustic indices presented in this work. This third aspect of diversity, which includes the similarity between diversity units, is known as 'dispersion' or 'disparity' (Scheiner et al. 2017). Indices that include the dispersion aspect are known as 'similarity-sensitive' indices and are comparatively much rarer than 'species-neutral' indices (Leinster and Cobbold 2012). To account for the dispersion between diversity units, a measure of similarity or distance needs to be incorporated, based on an attribute that is considered important in the diversity quantification process. For the proposed acoustic indices, at first glance, an obvious measure of similarity would be the pairwise distance between OSUs in the acoustic trait space. However, upon further reflection, designing such a measure is more complicated.

Firstly, the acoustic trait space that was defined in this thesis does not exist on a plane. This is because the temporal dimension that was measured is not linear. To illustrate what is meant by this, let us think of an example. Imagine two OSUs, one existing five minutes before midnight, and one five minutes after midnight. Functionally, these two OSUs are similar – they are only 10 minutes apart. This should be reflected in their distance in the acoustic trait space. Yet, if their distance is quantified on a plane, they would be on exact opposite sides of the acoustic trait space, and therefore be perceived as distant. Hence, the temporal dimension of the acoustic trait space is circular, and therefore, the acoustic trait space can better be envisioned as a closed cylinder. Consequently, any pairwise distance measurement between OSUs should be measured as the shortest distance between points on the surface of a cylinder, which complicates the process.

Second, as discussed previously, any measure of diversity should be independent of other diversity aspects (e.g., soundscape richness and evenness), and be scalable

between 0-1. Theoretically, something like this could be achieved for the soundscape dispersion by calculating the sum of all pairwise distances between OSUs on the cylinder and dividing this number by the maximum possible sum of pairwise distances for the same number of OSUs, but maximally spread apart on the surface of the cylinder. This would yield a metric that is scalable, independent from other diversity aspects, and captures the degree of dispersion of OSUs in the acoustic trait space compared to the maximal possible dispersion. Yet, considering the number of OSUs involved, there is an impractically large number of configurations in which OSUs can exist, which makes deriving the maximal attainable dispersion mathematically infeasible.

In conclusion, although there may be value in adding soundscape dispersion to our framework, potentially opening up a new dimension of soundscape diversity that is currently unexplored, at the moment, progress in this respect is restricted by mathematical complications. I am open to exploring this subject further with anyone who may have suggestions or solutions to tackle the issues highlighted above

Second-order indices

Currently, the proposed framework makes use of the Acoustic Cover (CVR) spectral index to capture the acoustic features of sound in each frequency bin. However, previous work has suggested that, because these first-order indices capture a single 'type' acoustic feature and tend to have a limited range of potential values, it is unlikely they can capture the full complexity of a wide range of soundscapes using a single value (Towsey et al. 2014a; Heath et al. 2021; Alcocer et al. 2022). Instead, it has been suggested that using the properties of several indices in concert by constructing weighted combinations of 'raw' first-order indices might improve the sensitivity towards certain acoustic features of taxonomic groups of interest (Towsey et al. 2014a). Indeed, false colour spectrograms already exploit this concept (Towsey et al. 2014b), combining the properties of multiple spectral indices to provide a unique visual perspective on the usage of the acoustic trait space, and even revealing the vocalisations of individual species.

I see potential for future development of our workflow in this respect. Instead of using the CVR index to capture the acoustic features of interest, I envision that using a combination of multiple spectral indices could be useful to target specific sounds. For instance, previous work has suggested that a combination of three spectral

indices can be used to target the acoustic features of cicada chorusing (Brown et al. 2019; Ferroudj et al. 2014; Towsey et al. 2014a). This approach can be extended to our workflow, combining the properties of these indices to capture the acoustic features of cicadas, and following the workflow to provide a range of cicada-specific soundscape diversity indices.

6 References

- Agostino, P.V.;** Lusk, N.A.; Meck, W.H.; Golombek, D.A.; Peryer, G. (2020). Daily and seasonal fluctuation in Tawny Owl vocalization timing. *PloS one*, 15(4), p.e0231591.
- Ahumada, J.A.;** Fegraus, E.; Birch, T.; Flores, N.; Kays, R.; O'Brien, T.G.; Palmer, J.; Schuttler, S.; Zhao, J.Y.; Jetz, W.; Kinnaird, M. (2020). Wildlife insights: A platform to maximize the potential of camera trap and other passive sensor wildlife data for the planet. *Environmental Conservation*, 47(1), pp.1-6
- Aide, T.M.;** Hernández-Serna, A.; Campos-Cerqueira, M.; Acevedo-Charry, O.; Deichmann, J.L. (2017). Species richness (of insects) drives the use of acoustic space in the tropics. *Remote Sensing*, 9(11).
- Alcocer, I.;** Lima, H.; Sugai, L.S.M.; Llusia, D. (2022). Acoustic indices as proxies for biodiversity: a meta-analysis. *Biological Reviews*, 97(6), pp.2209-2236.
- Allen-Ankins, S.;** Schwarzkopf, L. (2021). Spectral overlap and temporal avoidance in a tropical savannah frog community. *Animal Behaviour*, 180, pp.1-11.
- Alvarez-Berrios, N.;** Campos-Cerqueira, M.; Hernández-Serna, A.; Amanda Delgado, C.J.; Román-Dañobeytia, F.; Aide, T.M. (2016). Impacts of small-scale gold mining on birds and anurans near the Tambopata Natural Reserve, Peru, assessed using passive acoustic monitoring. *Tropical Conservation Science*, 9(2), pp.832-851.
- Aragão, L.E.;** Anderson, L.O.; Fonseca, M.G.; Rosan, T.M.; Vedovato, L.B.; Wagner, F.H.; Silva, C.V.; Silva Junior, C.H.; Arai, E.; Aguiar, A.P.; Barlow, J. (2018). 21st Century drought-related fires counteract the decline of Amazon deforestation carbon emissions. *Nature communications*, 9(1).
- ARBIMON RFCx** (2022): The Guardian Platform. ARBIMON Rainforest Connection. Available online at <https://rfcx.org/guardian>, checked on 1/3/2023.
- Arrhenius, O.** (1921). Species and area. *Journal of Ecology*, 9(1), pp.95-99.
- Bartlett, L.J.;** Williams, D.R.; Prescott, G.W.; Balmford, A.; Green, R.E.; Eriksson, A.; Valdes, P.J.; Singarayer, J.S.; Manica, A. (2016). Robustness despite uncertainty: regional climate data reveal the dominant role of humans in explaining global extinctions of Late Quaternary megafauna. *Ecography*, 39(2), pp.152-161.

- Benchimol, M.; Peres, C.A. (2015a).** Edge-mediated compositional and functional decay of tree assemblages in Amazonian forest islands after 26 years of isolation. *Journal of Ecology*, 103(2), pp.408-420.
- Benchimol, M.; Peres, C.A. (2015b).** Widespread forest vertebrate extinctions induced by a mega hydroelectric dam in lowland Amazonia. *PloS one*, 10(7), p.e0129818.
- Bennett, E.M.; Carpenter, S.R.; Caraco, N.F. (2001).** Human impact on erodible phosphorus and eutrophication: a global perspective: increasing accumulation of phosphorus in soil threatens rivers, lakes, and coastal oceans with eutrophication. *BioScience*, 51(3), pp.227-234.
- Beuchert, J.; Matthes, A.; Rogers, A. (2023).** S NAPPER GPS: Open Hardware for Energy-Efficient, Low-Cost Wildlife Location Tracking with Snapshot GNSS. *Journal of Open Hardware*, 7(1).
- Boelman, N.T.; Asner, G.P.; Hart, P.J.; Martin, R.E. (2007).** Multi-trophic invasion resistance in Hawaii: bioacoustics, field surveys, and airborne remote sensing. *Ecological Applications*, 17(8), pp.2137-2144.
- Boncoraglio, G.; Saino, N. (2007).** Habitat structure and the evolution of bird song: a meta-analysis of the evidence for the acoustic adaptation hypothesis. *Functional Ecology*, pp.134-142.
- Bond, A.B.; Diamond, J. (2005).** Geographic and ontogenetic variation in the contact calls of the kea (*Nestor notabilis*). *Behaviour*, 142(1), pp.1-20.
- Boquimpani-Freitas, L.; Marra, R.V.; Van Sluys, M.; Rocha, C.F.D. (2007).** Temporal niche of acoustic activity in anurans: interspecific and seasonal variation in a neotropical assemblage from south-eastern Brazil. *Amphibia-Reptilia*, 28(2), pp.269-276.
- Bradfer-Lawrence, T.; Gardner, N.; Bunnefeld, L.; Bunnefeld, N.; Willis, S.G.; Dent, D.H. (2019).** Guidelines for the use of acoustic indices in environmental research. *Methods in Ecology and Evolution*, 10(10), pp.1796-1807.
- Bradfer-Lawrence, T.; Bunnefeld, N.; Gardner, N.; Willis, S.G.; Dent, D.H. (2020).** Rapid assessment of avian species richness and abundance using acoustic indices. *Ecological Indicators*, 115, p.106400.

- Brandon, K.** (2014). Ecosystem services from tropical forests: review of current science. Center for Global Development Working Paper.
- Brodie, J.;** Post, E.; Laurance, W.F. (2012). Climate change and tropical biodiversity: a new focus. *Trends in ecology & evolution*, 27(3), pp.145-150.
- Brown, A.;** Garg, S.; Montgomery, J. (2019). Automatic rain and cicada chorus filtering of bird acoustic data. *Applied Soft Computing*, 81, p.105501.
- Bueno, A.S.;** Peres, C.A. (2019). Patch-scale biodiversity retention in fragmented landscapes: Reconciling the habitat amount hypothesis with the island biogeography theory. *Journal of Biogeography*, 46(3), pp.621-632.
- Bueno, A.S.;** Masseli, G.S.; Kaefer, I.L.; Peres, C.A. (2020). Sampling design may obscure species–area relationships in landscape-scale field studies. *Ecography*, 43(1), pp.107-118.
- Burivalova, Z.;** Towsey, M.; Boucher, T.; Truskinger, A.; Apelis, C.; Roe, P.; Game, E.T. (2018). Using soundscapes to detect variable degrees of human influence on tropical forests in Papua New Guinea. *Conservation Biology*, 32(1), pp.205-215.
- Burivalova, Z.;** Purnomo; Wahyudi, B.; Boucher, T.M.; Ellis, P.; Truskinger, A.; Towsey, M.; Roe, P.; Marthinus, D.; Griscom, B.; Game, E.T. (2019). Using soundscapes to investigate homogenization of tropical forest diversity in selectively logged forests. *Journal of Applied Ecology*, 56(11), pp.2493-2504.
- Buxton, R.T.;** Brown, E.; Sharman, L.; Gabriele, C.M.; McKenna, M.F. (2016). Using bioacoustics to examine shifts in songbird phenology. *Ecology and Evolution*, 6(14), pp.4697-4710.
- Buxton, R.T.;** McKenna, M.F.; Clapp, M.; Meyer, E.; Stabenau, E.; Angeloni, L.M.; Crooks, K.; Wittemyer, G. (2018). Efficacy of extracting indices from large-scale acoustic recordings to monitor biodiversity. *Conservation Biology*, 32(5), pp.1174-1184.
- Caldwell, M.S.** (2014). Interactions between airborne sound and substrate vibration in animal communication, pp. 65–92. In: Cocroft, R.B.; Gogala, M.; Hill, P.S.M.; Wessel, A. (Eds): *Studying Vibrational Communication*, vol. 3. Berlin, Springer.
- Campos-Cerqueira, M.;** Aide, T.M. (2017). Changes in the acoustic structure and composition along a tropical elevational gradient. *Journal of Ecoacoustics*, 1(1).

- Campos-Cerqueira, M.;** Mena, J.L.; Tejada-Gómez, V.; Aguilar-Amuchastegui, N.; Gutierrez, N.; Aide, T.M. (2020). How does FSC forest certification affect the acoustically active fauna in Madre de Dios, Peru?. *Remote Sensing in Ecology and Conservation*, 6(3), pp.274-285.
- Carlyle, A.G.;** Harrell, S.L.; Smith, P.M. (2010). Cost-effective HPC: The community or the cloud? IEEE Second International Conference on Cloud Computing Technology and Science, Indianapolis, IN, pp. 169-176
- Chao, A.;** Chiu, C.H.; Jost, L. (2010). Phylogenetic diversity measures based on Hill numbers. *Philosophical Transactions of the Royal Society B: Biological Sciences*, 365(1558), pp.3599-3609.
- Chao, A.;** Chiu, C.H.; Jost, L. (2014a). Unifying species diversity, phylogenetic diversity, functional diversity, and related similarity and differentiation measures through Hill numbers. *Annual review of ecology, evolution, and systematics*, 45, pp.297-324.
- Chao, A.;** Gotelli, N.J.; Hsieh, T.C.; Sander, E.L.; Ma, K.H.; Colwell, R.K.; Ellison, A.M. (2014b). Rarefaction and extrapolation with Hill numbers: a framework for sampling and estimation in species diversity studies. *Ecological monographs*, 84(1), pp.45-67.
- Chase, J.M.;** Gooriah, L.; May, F.; Ryberg, W.A.; Schuler, M.S.; Craven, D.; Knight, T.M. (2019). A framework for disentangling ecological mechanisms underlying the island species–area relationship. *Frontiers of Biogeography*, 11(1). e40844
- Collen, B.;** Ram, M.; Zamin, T.; McRae, L. (2008). The tropical biodiversity data gap: addressing disparity in global monitoring. *Tropical Conservation Science*, 1(2), pp.75-88.
- Corlett, R.T.;** Primack, R.B. (2008). Tropical rainforest conservation: a global perspective. In Carson, W.; Schnitzer, S. (Eds.): *Tropical forest community ecology*, pp.442-457. Wiley-Blackwell.
- Crutzen, P.J.;** Stoermer, E.F. (2000). The ‘Anthropocene’. Springer International Publishing, pp. 19-21.
- Cui, J.G.;** Song, X.Y.; Fang, G.Z.; Xu, F.; Brauth, S.E.; Tang, Y.Z. (2011). Circadian rhythm of calling behavior in the Emei music frog (*Babina daunchina*) is

- associated with habitat temperature and relative humidity. *Asian Herpetological Research*, 2(3), pp.149-154.
- da Silva**, C.A.D.; Pontes, A.L.B.D.; Cavalcante, J.D.S.; Azevedo, C.V.M.D. (2014). Conspecific vocalisations modulate the circadian activity rhythm of marmosets. *Biological Rhythm Research*, 45(6), pp.941-954.
- Daly**, A.J.; Baetens, J.M.; De Baets, B. (2018). Ecological diversity: measuring the unmeasurable. *Mathematics*, 6(7), p.119.
- Darras**, K.; Pérez, N.; Hanf-Dressler, T. (2020). BioSounds: an open-source, online platform for ecoacoustics. *F1000Research*, 9(1224), p.1224.
- Darwin**, Charles (1872). *The Expression of the Emotions in Man and Animals*. First edition. London, United Kingdom: John Murray.
- Deichmann**, J.L.; Hernández-Serna, A.; Campos-Cerqueira, M.; Aide, T.M. (2017). Soundscape analysis and acoustic monitoring document impacts of natural gas exploration on biodiversity in a tropical forest. *Ecological Indicators*, 74, pp.39-48.
- Deichmann**, J.L.; Acevedo-Charry, O.; Barclay, L.; Burivalova, Z.; Campos-Cerqueira, M.; d'Horta, F.; Game, E.T.; Gottesman, B.L.; Hart, P.J.; Kalan, A.K.; Linke, S. (2018). It's time to listen: there is much to be learned from the sounds of tropical ecosystems. *Biotropica*, 50(5), pp.713-718.
- Denton**, T.; Wisdom, S.; Hershey, J.R. (2022). Improving bird classification with unsupervised sound separation. In *ICASSP 2022-2022 IEEE International Conference on Acoustics, Speech and Signal Processing (ICASSP)*, pp. 636-640.
- Depraetere**, M.; Pavoine, S.; Jiguet, F.; Gasc, A.; Duvail, S.; Sueur, J. (2012). Monitoring animal diversity using acoustic indices: implementation in a temperate woodland. *Ecological Indicators*, 13(1), pp.46-54.
- Dingle**, C.; Halfwerk, W.; Slabbekoorn, H. (2008). Habitat-dependent song divergence at subspecies level in the grey-breasted wood-wren. *Journal of Evolutionary Biology*, 21(4), pp.1079-1089.
- Dirzo**, R.; Young, H.S.; Galetti, M.; Ceballos, G.; Isaac, N.J.; Collen, B. (2014). Defaunation in the Anthropocene. *Science*, 345(6195), pp.401-406.

- Duncan**, R.P.; Boyer, A.G.; Blackburn, T.M. (2013). Magnitude and variation of prehistoric bird extinctions in the Pacific. *Proceedings of the National Academy of Sciences*, 110(16), pp.6436-6441.
- Eldridge**, Alice; Casey, Michael; Moscoso, Paola; Peck, Mika (2016): A new method for ecoacoustics? Toward the extraction and evaluation of ecologically-meaningful soundscape components using sparse coding methods. *PeerJ*, e2108.
- Eldridge**, A.; Guyot, P.; Moscoso, P.; Johnston, A.; Eyre-Walker, Y.; Peck, M. (2018). Sounding out ecoacoustic metrics: Avian species richness is predicted by acoustic indices in temperate but not tropical habitats. *Ecological Indicators*, 95, pp.939-952.
- Emer**, C.; Venticinque, E.M.; Fonseca, C.R. (2013). Effects of dam-induced landscape fragmentation on Amazonian ant-plant mutualistic networks. *Conservation Biology*, 27(4), pp.763-773.
- Endler**, J.A. (1992). Signals, signal conditions, and the direction of evolution. *The American Naturalist*, 139, pp.125-153.
- Endo**, W.; Peres, C.A.; Salas, E.; Mori, S.; Sanchez-Vega, J.L.; Shepard, G.H.; Pacheco, V.; Yu, D.W. (2010). Game vertebrate densities in hunted and nonhunted forest sites in Manu National Park, Peru. *Biotropica*, 42(2), pp.251-261.
- Faanes**, C.A.; Bystrak, D. (1981). The role of observer bias in the North American Breeding Bird Survey. *Studies in Avian Biology*, 6, pp.353-359.
- Fairbrass**, A.J.; Rennert, P.; Williams, C.; Titheridge, H.; Jones, K.E. (2017). Biases of acoustic indices measuring biodiversity in urban areas. *Ecological Indicators*, 83, pp.169-177.
- Farina**, A.; Pieretti, N.; Piccioli, L. (2011). The soundscape methodology for long-term bird monitoring: A Mediterranean Europe case-study. *Ecological Informatics*, 6(6), pp.354-363.
- Farina**, A.; Pieretti, N.; Morganti, N. (2013). Acoustic patterns of an invasive species: the Red-billed Leiothrix (*Leiothrix lutea* Scopoli 1786) in a Mediterranean shrubland. *Bioacoustics*, 22(3), pp.175-194.
- Farina**, A.; Ceraulo, M.; Bobryk, C.; Pieretti, N.; Quinci, E.; Lattanzi, E. (2015). Spatial and temporal variation of bird dawn chorus and successive acoustic morning activity in a Mediterranean landscape. *Bioacoustics*, 24(3), pp.269-288.

- Farjalla**, V.F.; Srivastava, D.S.; Marino, N.A.; Azevedo, F.D.; Dib, V.; Lopes, P.M.; Rosado, A.S.; Bozelli, R.L.; Esteves, F.A. (2012). Ecological determinism increases with organism size. *Ecology*, 93(7), pp.1752-1759.
- Farley**, S.S.; Dawson, A.; Goring, S.J.; Williams, J.W. (2018). Situating ecology as a big-data science: Current advances, challenges, and solutions. *BioScience*, 68(8), pp.563-576.
- Fearnside**, P.M. (2006). Dams in the Amazon: Belo Monte and Brazil's hydroelectric development of the Xingu River Basin. *Environmental management*, 38, pp.16-27.
- Ferroudj**, M.; Truskinger, A.; Towsey, M.; Zhang, L.; Zhang, J.; Roe, P. (2014). Detection of rain in acoustic recordings of the environment. In *PRICAI 2014: Trends in Artificial Intelligence: 13th Pacific Rim International Conference on Artificial Intelligence. Proceedings 13*, pp. 104-116. Springer International Publishing.
- Finer**, M.; Jenkins, C.N. (2012). Proliferation of hydroelectric dams in the Andean Amazon and implications for Andes-Amazon connectivity. *Plos One*, 7(4), p.e35126.
- Fitzpatrick**, M.C.; Preisser, E.L.; Ellison, A.M.; Elkinton, J.S. (2009). Observer bias and the detection of low-density populations. *Ecological applications*, 19(7), pp.1673-1679.
- Froidevaux**, J.S.; Zellweger, F.; Bollmann, K.; Obrist, M.K. (2014). Optimising passive acoustic sampling of bats in forests. *Ecology and Evolution*, 4(24), pp.4690-4700.
- Fuller**, S.; Axel, A.C.; Tucker, D.; Gage, S.H. (2015). Connecting soundscape to landscape: Which acoustic index best describes landscape configuration?. *Ecological indicators*, 58, pp.207-215.
- Gallacher**, S.; Wilson, D.; Fairbrass, A.; Turmukhambetov, D.; Firman, M.; Kreitmayer, S.; Mac Aodha, O.; Brostow, G.; Jones, K. (2021). Shazam for bats: Internet of Things for continuous real-time biodiversity monitoring. *IET Smart Cities*, 3(3), pp.171-183.
- Gardner**, T.A.; Barlow, J.; Araujo, I.S.; Ávila-Pires, T.C.; Bonaldo, A.B.; Costa, J.E.; Esposito, M.C.; Ferreira, L.V.; Hawes, J.; Hernandez, M.I.; Hoogmoed, M.S. (2008).

- The cost-effectiveness of biodiversity surveys in tropical forests. *Ecology letters*, 11(2), pp.139-150.
- Gardner**, T.A.; Barlow, J.; Chazdon, R.; Ewers, R.M.; Harvey, C.A.; Peres, C.A.; Sodhi, N.S. (2009). Prospects for tropical forest biodiversity in a human-modified world. *Ecology letters*, 12(6), pp.561-582.
- Gardner**, T. (2010). *Monitoring forest biodiversity: improving conservation through ecologically-responsible management*. Earthscan Publications.
- Gasc**, A.; Sueur, J.; Jiguet, F.; Devictor, V.; Grandcolas, P.; Burrow, C.; Depraetere, M.; Pavoine, S. (2013). Assessing biodiversity with sound: Do acoustic diversity indices reflect phylogenetic and functional diversities of bird communities?. *Ecological Indicators*, 25, pp.279-287.
- Gasc**, A.; Pavoine, S.; Lellouch, L.; Grandcolas, P.; Sueur, J. (2015). Acoustic indices for biodiversity assessments: Analyses of bias based on simulated bird assemblages and recommendations for field surveys. *Biological Conservation*, 191, pp.306-312.
- Gerhardt**, H.C.; Huber, F.; Simmons, A.M. (2003). Acoustic communication in insects and anurans: common problems and diverse solutions. *The Journal of the Acoustical Society of America*, 114(2), pp.559-559.
- Ghazoul**, J.; Sheil, D. (2010). *Tropical rain forest ecology, diversity, and conservation*. Oxford University Press.
- Gibb**, R.; Browning, E.; Glover-Kapfer, P.; Jones, K. (2019). Emerging opportunities and challenges for passive acoustics in ecological assessment and monitoring. *Methods in Ecology and Evolution*, 10(2), pp.169-185.
- Giese**, M. (1996). Effects of human activity on Adelie penguin *Pygoscelis adeliae* breeding success. *Biological Conservation*, 75(2), pp.157-164.
- Giladi**, I.; May, F.; Ristow, M.; Jeltsch, F.; Ziv, Y. (2014). Scale-dependent species-area and species-isolation relationships: a review and a test study from a fragmented semi-arid agro-ecosystem. *Journal of Biogeography* 41(6), pp.1055-1069.
- Gingras**, B.; Mohandesan, E.; Boko, D; Fitch, W. (2013). Phylogenetic signal in the acoustic parameters of the advertisement calls of four clades of anurans. *BMC evolutionary biology*, 13(1), pp.1-12.

- Glover-Kapfer**, P.; Soto-Navarro, C.A.; Wearn, O.R. (2019). Camera-trapping version 3.0: current constraints and future priorities for development. *Remote Sensing in Ecology and Conservation*, 5(3), pp.209-223.
- Goëau**, H.; Kahl, S.; Glotin, H.; Planqué, R.; Vellinga, W.P.; Joly, A. (2018). Overview of BirdCLEF 2018: monospecies vs. soundscape bird identification. *CLEF 2018-Conference and Labs of the Evaluation Forum*, 2125(9).
- Goutte**, S.; Dubois, A.; Howard, S.D.; Márquez, R.; Rowley, J.J.L.; Dehling, J.M.; Grandcolas, P.; Xiong, R.C.; Legendre, F. (2018). How the environment shapes animal signals: a test of the acoustic adaptation hypothesis in frogs. *Journal of Evolutionary Biology*, 31(1), pp.148-158.
- Habel**, J.C.; Rasche, L.; Schneider, U.A.; Engler, J.O.; Schmid, E.; Rödder, D.; Meyer, S.T.; Trapp, N.; Sos del Diego, R.; Eggermont, H.; Lens, L. (2019). Final countdown for biodiversity hotspots. *Conservation Letters*, 12(6), p.e12668.
- Hampton**, S.E.; Strasser, C.A.; Tewksbury, J.J.; Gram, W.K.; Budden, A.E.; Batcheller, A.L.; Duke, C.S.; Porter, J.H. (2013). Big data and the future of ecology. *Frontiers in Ecology and the Environment*, 11(3), pp.156-162.
- Han**, P.; Zhao, Y.; Kang, Y.; Ding, P.; Si, X. (2022). Island biogeography of soundscapes: Island area shapes spatial patterns of avian acoustic diversity. *Journal of Biogeography*, 0, pp.1-11.
- Hart**, P.J.; Hall, R.; Ray, W.; Beck, A.; Zook, J. (2015). Cicadas impact bird communication in a noisy tropical rainforest. *Behavioral Ecology*, 26(3), pp.839-842.
- Hart**, P.J.; Ibanez, T.; Paxton, K.; Tredinnick, G.; Sebastián-González, E.; Tanimoto-Johnson, A. (2021). Timing is everything: acoustic niche partitioning in two tropical wet forest bird communities. *Frontiers in Ecology and Evolution*, p.687.
- Heath**, B.E.; Sethi, S.S.; Orme, C.D.L.; Ewers, R.M.; Picinali, L. (2021). How index selection, compression, and recording schedule impact the description of ecological soundscapes. *Ecology and Evolution*, 11(19), pp.13206-13217.
- Heikkinen**, R.K.; Luoto, M.; Virkkala, R.; Rainio, K. (2004). Effects of habitat cover, landscape structure and spatial variables on the abundance of birds in an agricultural-forest mosaic. *Journal of Applied Ecology*, 41(5), pp.824-835.

- Herrera-Montes, M.I.** (2018). Protected area zoning as a strategy to preserve natural soundscapes, reduce anthropogenic noise intrusion, and conserve biodiversity. *Tropical Conservation Science*, 11.
- Hill, M.O.** (1973). Diversity and evenness: a unifying notation and its consequences. *Ecology*, 54(2), pp.427-432.
- Hill, J.L.; Curran, P.J; Foody, G.M.** (1994). The effect of sampling on the species-area curve. *Global Ecology and Biogeography Letters*, pp.97-106.
- Hill, A.P.; Prince, P.; Piña Covarrubias, E.; Doncaster, C.P.; Snaddon, J.L; Rogers, A.** (2018). AudioMoth: Evaluation of a smart open acoustic device for monitoring biodiversity and the environment. *Methods in Ecology and Evolution*, 9(5), pp.1199-1211.
- Hofmann, D.J.; Butler, J.H; Tans, P.P.** (2009). A new look at atmospheric carbon dioxide. *Atmospheric Environment*, 43(12), pp.2084-2086.
- Hurlbert, S.H.** (1971). The nonconcept of species diversity: a critique and alternative parameters. *Ecology*, 52(4), pp.577-586.
- Imhoff, M.L.; Bounoua, L.; Ricketts, T.; Loucks, C.; Harriss, R; Lawrence, W.T.** (2004). Global patterns in human consumption of net primary production. *Nature*, 429(6994), pp.870-873.
- IUCN** (2023). Red List of Threatened Species. Available online at <https://www.iucnredlist.org/>, updated on 4/24/2023, checked on 4/24/2023.
- Johnson, C.N.; Balmford, A.; Brook, B.W.; Buettel, J.C.; Galetti, M.; Guangchun, L; Wilmshurst, J.M.** (2017). Biodiversity losses and conservation responses in the Anthropocene. *Science*, 356(6335), pp.270-275.
- Johnson, C.N.** (2023). Past and future decline and extinction of species. The Royal Society. Available online at <https://royalsociety.org/topics-policy/projects/biodiversity/decline-and-extinction/>, updated on 4/24/2023, checked on 4/24/2023.
- Jost, L.** (2006). Entropy and diversity. *Oikos*, 113(2), pp.363-375.
- Jost, L.** (2007). Partitioning diversity into independent alpha and beta components. *Ecology*, 88(10), pp.2427-2439.

- Jost**, Lou; Chao, Anne; Chazdon, R. L. (2010). Compositional similarity and beta diversity. In Magurran, A.E.; McGill, B.J. (Eds.): *Biological Diversity: Frontiers in Measurement and Assessment*: Oxford University Press, pp. 66–84.
- Jung**, M.; Rowhani, P.; Scharlemann, J.P. (2019). Impacts of past abrupt land change on local biodiversity globally. *Nature Communications*, 10(1), p.5474.
- Kadmon**, R.; Allouche, O. (2007). Integrating the effects of area, isolation, and habitat heterogeneity on species diversity: a unification of island biogeography and niche theory. *The American Naturalist*, 170(3), pp.443-454.
- Kahl**, S.; Clapp, M.; Hopping, W.A.; Goëau, H.; Glotin, H.; Planqué, R.; Vellinga, W.P.; Joly, A. (2020). Overview of birdclef 2020: Bird sound recognition in complex acoustic environments. CLEF 2020 -Conference and Labs of the Evaluation Forum, 2696(262).
- Kahl**, S.; Denton, T.; Klinck, H.; Glotin, H.; Goëau, H.; Vellinga, W.P.; Planqué, R.; Joly, A. (2021a). Overview of BirdCLEF 2021: Bird call identification in soundscape recordings. CLEF - Working Notes, pp.1437-1450.
- Kahl**, S.; Wood, C.M.; Eibl, M.; Klinck, H. (2021). BirdNET: A deep learning solution for avian diversity monitoring. *Ecological Informatics*, 61, p.101236.
- Kays**, R.; Sheppard, J.; Mclean, K.; Welch, C.; Paunescu, C.; Wang, V.; Kravit, G; Crofoot, M. (2019). Hot monkey, cold reality: surveying rainforest canopy mammals using drone-mounted thermal infrared sensors. *International journal of remote sensing*, 40(2), pp.407-419.
- Köndgen**, S.; Kühl, H.; N'Goran, P.K.; Walsh, P.D.; Schenk, S.; Ernst, N.; Biek, R.; Formenty, P.; Mätz-Rensing, K.; Schweiger, B; Junglen, S. (2008). Pandemic human viruses cause decline of endangered great apes. *Current Biology*, 18(4), pp.260-264.
- Krause**, B. (1987). Bioacoustics, habitat ambience in ecological balance. *Whole Earth Review*, 57(472), pp.14-18.
- Lardner**, B.; Adams, A.A.Y.; Knox, A.J.; Savidge, J.A; Reed, R.N. (2019). Do observer fatigue and taxon bias compromise visual encounter surveys for small vertebrates?. *Wildlife Research*, 46(2), pp.127-135.
- LeBien**, J.; Zhong, M.; Campos-Cerqueira, M.; Velez, J.P.; Dodhia, R.; Ferres, J.L; Aide, T.M. (2020). A pipeline for identification of bird and frog species in tropical

- soundscape recordings using a convolutional neural network. *Ecological Informatics*, 59, p.101113.
- Leinster, T;** Cobbold, C.A. (2012). Measuring diversity: the importance of species similarity. *Ecology*, 93(3), pp.477-489.
- Leite-Filho, A.T.;** Soares-Filho, B.S.; Davis, J.L.; Abrahão, G.M; Börner, J. (2021). Deforestation reduces rainfall and agricultural revenues in the Brazilian Amazon. *Nature Communications*, 12(1), p.2591.
- Lellouch, L.;** Pavoine, S.; Jiguet, F.; Glotin, H; Sueur, J. (2014). Monitoring temporal change of bird communities with dissimilarity acoustic indices. *Methods in Ecology and Evolution*, 5(6), pp.495-505.
- Leung, B.;** Hargreaves, A.L.; Greenberg, D.A.; McGill, B.; Dornelas, M; Freeman, R. (2020). Clustered versus catastrophic global vertebrate declines. *Nature*, 588(7837), pp.267-271.
- Lewis, S.L.;** Edwards, D.P; Galbraith, D. (2015). Increasing human dominance of tropical forests. *Science*, 349(6250), pp.827-832.
- Lips, K.R.** (2016). Overview of chytrid emergence and impacts on amphibians. *Philosophical Transactions of the Royal Society B: Biological Sciences*, 371(1709), p.20150465.
- Loffeld, T.A.;** Black, S.A.; Carter, M.; Sterling, E; Humle, T. (2022). What makes conservationists persevere? Resilience strategies at work. *Oryx*, 56(5), pp.681-690.
- Lomolino, M.V.;** Weiser, M.D. (2001). Towards a more general species-area relationship: diversity on all islands, great and small. *Journal of biogeography*, pp.431-445.
- Maas, B.;** Putra, D.D.; Waltert, M.; Clough, Y.; Tschardtke, T.; Schulze, C.H. (2009). Six years of habitat modification in a tropical rainforest margin of Indonesia do not affect bird diversity but endemic forest species. *Biological Conservation*, 142(11), pp.2665-2671.
- Mac Aodha, O.;** Gibb, R.; Barlow, K.E.; Browning, E.; Firman, M.; Freeman, R.; Harder, B.; Kinsey, L.; Mead, G.R.; Newson, S.E; Pandourski, I. (2018). Bat detective—Deep learning tools for bat acoustic signal detection. *PLoS computational biology*, 14(3), p.e1005995.

- MacArthur**, R.H; Wilson, E.O. (1967). The theory of island biogeography. Princeton university press.
- Madsen**, P.T; Surlykke, A. (2013). Functional convergence in bat and toothed whale biosonar. *Physiology*, 28(5), pp.276-283.
- Magrath**, R.D.; Haff, T.M.; Fallow, P.M; Radford, A.N. (2015). Eavesdropping on heterospecific alarm calls: from mechanisms to consequences. *Biological Reviews*, 90(2), pp.560-586.
- Malhi**, Y.; Gardner, T.A.; Goldsmith, G.R.; Silman, M.R; Zelazowski, P. (2014). Tropical forests in the Anthropocene. *Annual Review of Environment and Resources*, 39, pp.125-159.
- Malhi**, Y.; Doughty, C.E.; Galetti, M.; Smith, F.A.; Svenning, J.C; Terborgh, J.W. (2016). Megafauna and ecosystem function from the Pleistocene to the Anthropocene. *Proceedings of the National Academy of Sciences*, 113(4), pp.838-846.
- Mammides**, C.; Goodale, E.; Dayananda, S.K.; Kang, L; Chen, J. (2017). Do acoustic indices correlate with bird diversity? Insights from two biodiverse regions in Yunnan Province, south China. *Ecological Indicators*, 82, pp.470-477.
- Martins**, B.A.; Rodrigues, G.S.R; de Araújo, C.B. (2018). Vocal dialects and their implications for bird reintroductions. *Perspectives in ecology and conservation*, 16(2), pp.83-89.
- Marvin**, D.C.; Koh, L.P.; Lynam, A.J.; Wich, S.; Davies, A.B.; Krishnamurthy, R.; Stokes, E.; Starkey, R; Asner, G.P. (2016). Integrating technologies for scalable ecology and conservation. *Global Ecology and Conservation*, 7, pp.262-275.
- McGill**, B.J.; Dornelas, M.; Gotelli, N.J; Magurran, A.E. (2015). Fifteen forms of biodiversity trend in the Anthropocene. *Trends in ecology & evolution*, 30(2), pp.104-113.
- McKinney**, M.L; Lockwood, J.L. (1999). Biotic homogenization: a few winners replacing many losers in the next mass extinction. *Trends in ecology & evolution*, 14(11), pp.450-453.
- McKinney**, M.L. (1997). Extinction vulnerability and selectivity: combining ecological and paleontological views. *Annual review of ecology and systematics*, 28(1), pp.495-516.

- Metcalf**, O.C.; Abrahams, C.; Ashington, B.; Baker, E.; Bradfer-Lawrence, T.; Browning, E.; Carruthers-Jones, J.; Darby, J.; Dick, J.; Eldridge, A.; Elliott, D. (2023). Good practice guidelines for long-term ecoacoustic monitoring in the UK. UK Acoustics Network.
- Metcalf**, O.C.; Barlow, J.; Devenish, C.; Marsden, S.; Berenguer, E; Lees, A.C. (2021). Acoustic indices perform better when applied at ecologically meaningful time and frequency scales. *Methods in Ecology and Evolution*, 12(3), pp.421-431.
- Mikula**, P.; Valcu, M.; Brumm, H.; Bulla, M.; Forstmeier, W.; Petrusková, T.; Kempenaers, B; Albrecht, T. (2021). A global analysis of song frequency in passerines provides no support for the acoustic adaptation hypothesis but suggests a role for sexual selection. *Ecology Letters*, 24(3), pp.477-486.
- Millennium Ecosystem Assessment** (2005): Ecosystems and human well-being: Island press Washington, DC (5).
- Morton**, E.S. (1975). Ecological sources of selection on avian sounds. *The American Naturalist*, 109(965), pp.17-34.
- Morton**, O.; Scheffers, B.R.; Haugaasen, T; Edwards, D.P. (2021). Impacts of wildlife trade on terrestrial biodiversity. *Nature Ecology & Evolution*, 5(4), pp.540-548.
- Mouchet**, M.A.; Villéger, S.; Mason, N.W; Mouillot, D. (2010). Functional diversity measures: an overview of their redundancy and their ability to discriminate community assembly rules. *Functional Ecology*, 24(4), pp.867-876.
- Müller**, S.; Shaw, T.; Güntert, D.; Helmbold, L.; Schütz, N.; Thomas, L.; Scherer-Lorenzen, M. (2020). Ecoacoustics of small forest patches in agricultural landscapes: acoustic diversity and bird richness increase with patch size. *Biodiversity*, 21(1), pp.48-60.
- Mullet**, T.C.; Farina, A; Gage, S.H. (2017). The acoustic habitat hypothesis: An ecoacoustics perspective on species habitat selection. *Biosemiotics*, 10, pp.319-336.
- Myers**, N.; Mittermeier, R.A.; Mittermeier, C.G.; Da Fonseca, G.A; Kent, J. (2000). Biodiversity hotspots for conservation priorities. *Nature*, 403(6772), pp.853-858.

- Newbold, T.;** Hudson, L.N.; Hill, S.L.; Contu, S.; Lysenko, I.; Senior, R.A.; Börger, L.; Bennett, D.J.; Choimes, A.; Collen, B; Day, J. (2015). Global effects of land use on local terrestrial biodiversity. *Nature*, 520(7545), pp.45-50.
- Oñate-Casado, J.;** Porteš, M.; Beran, V.; Petrusek, A; Petrusková, T. (2023). Guess who? Evaluating individual acoustic monitoring for males and females of the Tawny Pipit, a migratory passerine bird with a simple song. *Journal of Ornithology*, pp.1-14.
- Oppel, S.** (2006). Using distance sampling to quantify Odonata density in tropical rainforests. *International Journal of Odonatology*, 9(1), pp.81-88.
- Palmeirim, A.F.;** Vieira, M.V; Peres, C.A. (2017). Non-random lizard extinctions in land-bridge Amazonian forest islands after 28 years of isolation. *Biological Conservation*, 214, pp.55-65.
- Papin, M.;** Aznar, M.; Germain, E.; Guérol, F; Pichenot, J. (2019). Using acoustic indices to estimate wolf pack size. *Ecological Indicators*, 103, pp.202-211.
- Paradis, E.** (2020). A review of computer tools for prediction of ecosystems and populations: We need more open-source software. *Environmental Modelling & Software*, 134, p.104872.
- Pearse, W.D.;** Morales-Castilla, I.; James, L.S.; Farrell, M.; Boivin, F; Davies, T.J. (2018). Global macroevolution and macroecology of passerine song. *Evolution*, 72(4), pp.944-960.
- Pekin, B.K.;** Jung, J.; Villanueva-Rivera, L.J.; Pijanowski, B.C; Ahumada, J.A. (2012). Modeling acoustic diversity using soundscape recordings and LIDAR-derived metrics of vertical forest structure in a neotropical rainforest. *Landscape ecology*, 27, pp.1513-1522.
- Peres, C.A.** (2000). Effects of subsistence hunting on vertebrate community structure in Amazonian forests. *Conservation biology*, 14(1), pp.240-253.
- Phillips, Y.F.;** Towsey, M; Roe, P. (2017). Visualisation of environmental audio using ribbon plots and acoustic state sequences. *International Symposium on Big Data Visual Analytics (BDVA)*, pp.1-8.
- Phillips, Y.F.;** Towsey, M; Roe, P. (2018). Revealing the ecological content of long-duration audio-recordings of the environment through clustering and visualisation. *PloS One*, 13(3), p.e0193345.

- Pielou, E.C.** (1966). The measurement of diversity in different types of biological collections. *Journal of theoretical biology*, 13, pp.131-144.
- Pieretti, N.; Farina, A; Morri, D.** (2011). A new methodology to infer the singing activity of an avian community: The Acoustic Complexity Index (ACI). *Ecological indicators*, 11(3), pp.868-873.
- Pijanowski, B.C.; Farina, A.; Gage, S.H.; Dumyahn, S.L; Krause, B.L.** (2011a). What is soundscape ecology? An introduction and overview of an emerging new science. *Landscape ecology*, 26, pp.1213-1232.
- Pijanowski, B.C.; Villanueva-Rivera, L.J.; Dumyahn, S.L.; Farina, A.; Krause, B.L.; Napolitano, B.M.; Gage, S.H; Pieretti, N.** (2011b). Soundscape ecology: the science of sound in the landscape. *BioScience*, 61(3), pp.203-216.
- Pillay, R.; Venter, M.; Aragon-Osejo, J.; González-del-Pliego, P.; Hansen, A.J.; Watson, J.E.; Venter, O.** (2022). Tropical forests are home to over half of the world's vertebrate species. *Frontiers in Ecology and the Environment*, 20(1), pp.10-15.
- Pimm, S.L; Raven, P.** (2000). Extinction by numbers. *Nature*, 403(6772), pp.843-845.
- Pimm, S.L.; Alibhai, S.; Bergl, R.; Dehgan, A.; Giri, C.; Jewell, Z.; Joppa, L.; Kays, R; Loarie, S.** (2015). Emerging technologies to conserve biodiversity. *Trends in ecology & evolution*, 30(11), pp.685-696.
- Portegies Zwart, S.** (2020). The ecological impact of high-performance computing in astrophysics. *Nature Astronomy*, 4(9), pp.819-822.
- Proença, V.; Martin, L.J.; Pereira, H.M.; Fernandez, M.; McRae, L.; Belnap, J.; Böhm, M.; Brummitt, N.; García-Moreno, J.; Gregory, R.D; Honrado, J.P.** (2017). Global biodiversity monitoring: from data sources to essential biodiversity variables. *Biological Conservation*, 213, pp.256-263.
- Rainforest Foundation Norway** (2020): State of the tropical rainforests. The complete overview of the tropical rainforest, past and present. Eds: Anders Krogh. Rainforest Foundation Norway. Oslo, Norway.
- Ramesh, V.; Hariharan, P.; Akshay, V.A.; Choksi, P.; Khanwilkar, S.; DeFries, R; Robin, V.V.** (2023). Using passive acoustic monitoring to examine the impacts of ecological restoration on faunal biodiversity in the Western Ghats. *Biological Conservation*, 282, p.110071.

- Ricotta, C.** (2005). A note on functional diversity measures. *Basic and applied Ecology*, 6(5), pp.479-486.
- Riede, K.** (1996). Diversity of sound-producing insects in a Bornean lowland rain forest. In *Tropical Rainforest Research—Current Issues: Proceedings of the Conference held in Bandar Seri Begawan*, pp. 77-84. Springer Netherlands.
- Riede, K.** (2018). Acoustic profiling of Orthoptera. *Journal of Orthoptera Research*, 27(2), pp.203-215.
- Ripple, W.J.; Wolf, C.; Newsome, T.M.; Hoffmann, M.; Wirsing, A.J.; McCauley, D.J.** (2017). Extinction risk is most acute for the world's largest and smallest vertebrates. *Proceedings of the National Academy of Sciences*, 114(40), pp.10678-10683.
- Rocchini, D; Neteler, M.** (2012). Let the four freedoms paradigm apply to ecology. *Trends in Ecology & Evolution*, 27(6), pp.310-311.
- Roch, M.A.; Batchelor, H.; Baumann-Pickering, S.; Berchok, C.L.; Cholewiak, D.; Fujioka, E.; Garland, E.C.; Herbert, S.; Hildebrand, J.A.; Oleson, E.M; Van Parijs, S.** (2016). Management of acoustic metadata for bioacoustics. *Ecological informatics*, 31, pp.122-136.
- Rodriguez, A; Gasc, A.; Pavoine, S.; Grandcolas, P.; Gaucher, P; Sueur, J.** (2014). Temporal and spatial variability of animal sound within a neotropical forest. *Ecological Informatics*, 21, pp.133-143.
- Roe, P.; Eichinski, P.; Fuller, R.A.; McDonald, P.G.; Schwarzkopf, L.; Towsey, M.; Truskinger, A.; Tucker, D; Watson, D.M.** (2021). The Australian acoustic observatory. *Methods in Ecology and Evolution*, 12(10), pp.1802-1808.
- Rosenzweig, M.L.** (1995). *Species Diversity in Space and Time*. Cambridge University Press.
- Ross, S.R.J.; Friedman, N.R.; Yoshimura, M.; Yoshida, T.; Donohue, I; Economo, E.P.** (2021). Utility of acoustic indices for ecological monitoring in complex sonic environments. *Ecological Indicators*, 121, p.107114.
- Ross, S.R.J.; O'Connell, D.P.; Deichmann, J.L.; Desjonquères, C.; Gasc, A.; Phillips, J.N.; Sethi, S.S.; Wood, C.M; Burivalova, Z.** (2023). Passive acoustic monitoring provides a fresh perspective on fundamental ecological questions. *Functional Ecology*, 37, pp.959–975.

- Ryan, M.J;** Brenowitz, E.A. (1985). The role of body size, phylogeny, and ambient noise in the evolution of bird song. *The American Naturalist*, 126(1), pp.87-100.
- Sandoval, L.;** Barrantes, G; Wilson, D.R. (2019). Conceptual and statistical problems with the use of the Shannon-Weiner entropy index in bioacoustic analyses. *Bioacoustics*, 28(4), pp.297-311.
- Sankupellay, M.;** Towsey, M.; Truskinger, A; Roe, P. (2015). Visual fingerprints of the acoustic environment: The use of acoustic indices to characterise natural habitats. *IEEE - Big Data Visual Analytics*, pp.1-8.
- Sasse, D.B.** (2003). Job-related mortality of wildlife workers in the United States, 1937-2000. *Wildlife society bulletin*, pp.1015-1020.
- Scheiner, S.M.;** Kosman, E.; Presley, S.J; Willig, M.R. (2017). Decomposing functional diversity. *Methods in Ecology and Evolution*, 8(7), pp.809-820.
- Schoereder, J.H.;** Galbiati, C.; Ribas, C.R.; Sobrinho, T.G.; Sperber, C.F.; DeSouza, O; Lopes-Andrade, C. (2004). Should we use proportional sampling for species-area studies?. *Journal of Biogeography*, 31(8), pp.1219-1226.
- Schramski, J.R.;** Gattie, D.K; Brown, J.H. (2015). Human domination of the biosphere: Rapid discharge of the earth-space battery foretells the future of humankind. *Proceedings of the National Academy of Sciences*, 112(31), pp.9511-9517.
- Seibold, S.;** Gossner, M.M.; Simons, N.K.; Blüthgen, N.; Müller, J.; Ambarli, D.; Ammer, C.; Bauhus, J.; Fischer, M.; Habel, J.C; Linsenmair, K.E. (2019). Arthropod decline in grasslands and forests is associated with landscape-level drivers. *Nature*, 574(7780), pp.671-674.
- Sethi, S.S.;** Ewers, R.M.; Jones, N.S.; Orme, C.D.L; Picinali, L. (2018). Robust, real-time and autonomous monitoring of ecosystems with an open, low-cost, networked device. *Methods in Ecology and Evolution*, 9(12), pp.2383-2387.
- Sethi, S.S.;** Jones, N.S.; Fulcher, B.D.; Picinali, L.; Clink, D.J.; Klinck, H.; Orme, C.D.L.; Wrege, P.H; Ewers, R.M. (2020a). Characterising soundscapes across diverse ecosystems using a universal acoustic feature set. *Proceedings of the National Academy of Sciences*, 117(29), pp.17049-17055.

- Sethi, S.S.** (2020b): Automated acoustic monitoring of ecosystems. PhD dissertation. Imperial College London, London, United Kingdom. Department of Mathematics.
- Seyfarth, R.M;** Cheney, D.L. (2003). Signalers and receivers in animal communication. *Annual review of psychology*, 54(1), pp.145-173.
- Sheil, D;** Lawrence, A. (2004). Tropical biologists, local people and conservation: new opportunities for collaboration. *Trends in Ecology & Evolution*, 19(12), pp.634-638.
- Shukla, P.R.;** Skea, J.; Calvo Buendia, E.; Masson-Delmotte, V.; Pörtner, H.O.; Roberts, D.C.; Zhai, P.; Slade, R.; Connors, S.; Van Diemen, R; Ferrat, M. (2019). IPCC, 2019: Climate Change and Land: an IPCC special report on climate change, desertification, land degradation, sustainable land management, food security, and greenhouse gas fluxes in terrestrial ecosystems.
- Slabbekoorn, H.;** Eilers, J; Smith, T.B. (2002). Birdsong and sound transmission: the benefits of reverberations. *The Condor*, 104(3), pp.564-573.
- Smith, R.L;** Langley, W.M. (1978). Cicada stress sound: an assay of its effectiveness as a predator defense mechanism. *The Southwestern Naturalist*, pp.187-195.
- Smith, B.D;** Zeder, M.A. (2013). The onset of the Anthropocene. *Anthropocene*, 4, pp.8-13.
- Sousa-Lima, Renata S.;** Ferreira, Luane M.; Oliveira, Eliziane G.; Lopes, Lara C.; Brito, Marcos R.; Baumgarten, Júlio; Rodrigues, Flávio H. (2018). What do insects, anurans, birds, and mammals have to say about soundscape indices in a tropical savanna. *Journal of Ecoacoustics* 2(1).
- Steffen, W.;** Grinevald, J.; Crutzen, P; McNeill, J. (2011). The Anthropocene: conceptual and historical perspectives. *Philosophical Transactions of the Royal Society A: Mathematical, Physical and Engineering Sciences*, 369(1938), pp.842-867.
- Steffen, W.;** Richardson, K.; Rockström, J.; Cornell, S.E.; Fetzer, I.; Bennett, E.M.; Biggs, R.; Carpenter, S.R.; De Vries, W.; De Wit, C.A; Folke, C. (2015). Planetary boundaries: Guiding human development on a changing planet. *Science*, 347(6223), p.1259855.

- Stephens, Z.D.;** Lee, S.Y.; Faghri, F.; Campbell, R.H.; Zhai, C.; Efron, M.J.; Iyer, R.; Schatz, M.C.; Sinha, S; Robinson, G.E. (2015). Big data: astronomical or genetical?. *PLoS biology*, 13(7), p.e1002195.
- Stewart, M.;** Carleton, W.C; Groucutt, H.S. (2021). Climate change, not human population growth, correlates with Late Quaternary megafauna declines in North America. *Nature Communications*, 12(1), p.965.
- Storck-Tonon, D;** Peres, C.A. (2017). Forest patch isolation drives local extinctions of Amazonian orchid bees in a 26 years old archipelago. *Biological Conservation*, 214, pp.270-277.
- Stork, N.E.;** Coddington, J.A.; Colwell, R.K.; Chazdon, R.L.; Dick, C.W.; Peres, C.A.; Sloan, S; Willis, K. (2009). Vulnerability and resilience of tropical forest species to land-use change. *Conservation Biology*, 23(6), pp.1438-1447.
- Sueur, J.** (2002). Cicada acoustic communication: potential sound partitioning in a multispecies community from Mexico (Hemiptera: Cicadomorpha: Cicadidae). *Biological Journal of the Linnean Society*, 75(3), pp.379-394.
- Sueur, J.;** Aubin, T; Simonis, C. (2008a). Seewave, a free modular tool for sound analysis and synthesis. *Bioacoustics*, 18(2), pp.213-226.
- Sueur, J.;** Pavoine, S.; Hamerlynck, O; Duvail, S. (2008b). Rapid acoustic survey for biodiversity appraisal. *PloS one*, 3(12), p.e4065.
- Sueur, J.;** Farina, A.; Gasc, A.; Pieretti, N; Pavoine, S. (2014). Acoustic indices for biodiversity assessment and landscape investigation. *Acta Acustica united with Acustica*, 100(4), pp.772-781.
- Sueur, J;** Farina, A. (2015). Ecoacoustics: the ecological investigation and interpretation of environmental sound. *Biosemiotics*, 8, pp.493-502.
- Sugai, L.S.M;** Llusia, D. (2019a). Bioacoustic time capsules: Using acoustic monitoring to document biodiversity. *Ecological Indicators*, 99, pp.149-152.
- Sugai, L.S.M.;** Silva, T.S.F.; Ribeiro Jr, J.W; Llusia, D. (2019b). Terrestrial passive acoustic monitoring: review and perspectives. *BioScience*, 69(1), pp.15-25.
- Sugai, L.S.M.;** Desjonqueres, C.; Silva, T.S.F; Llusia, D. (2020). A roadmap for survey designs in terrestrial acoustic monitoring. *Remote Sensing in Ecology and Conservation*, 6(3), pp.220-235.

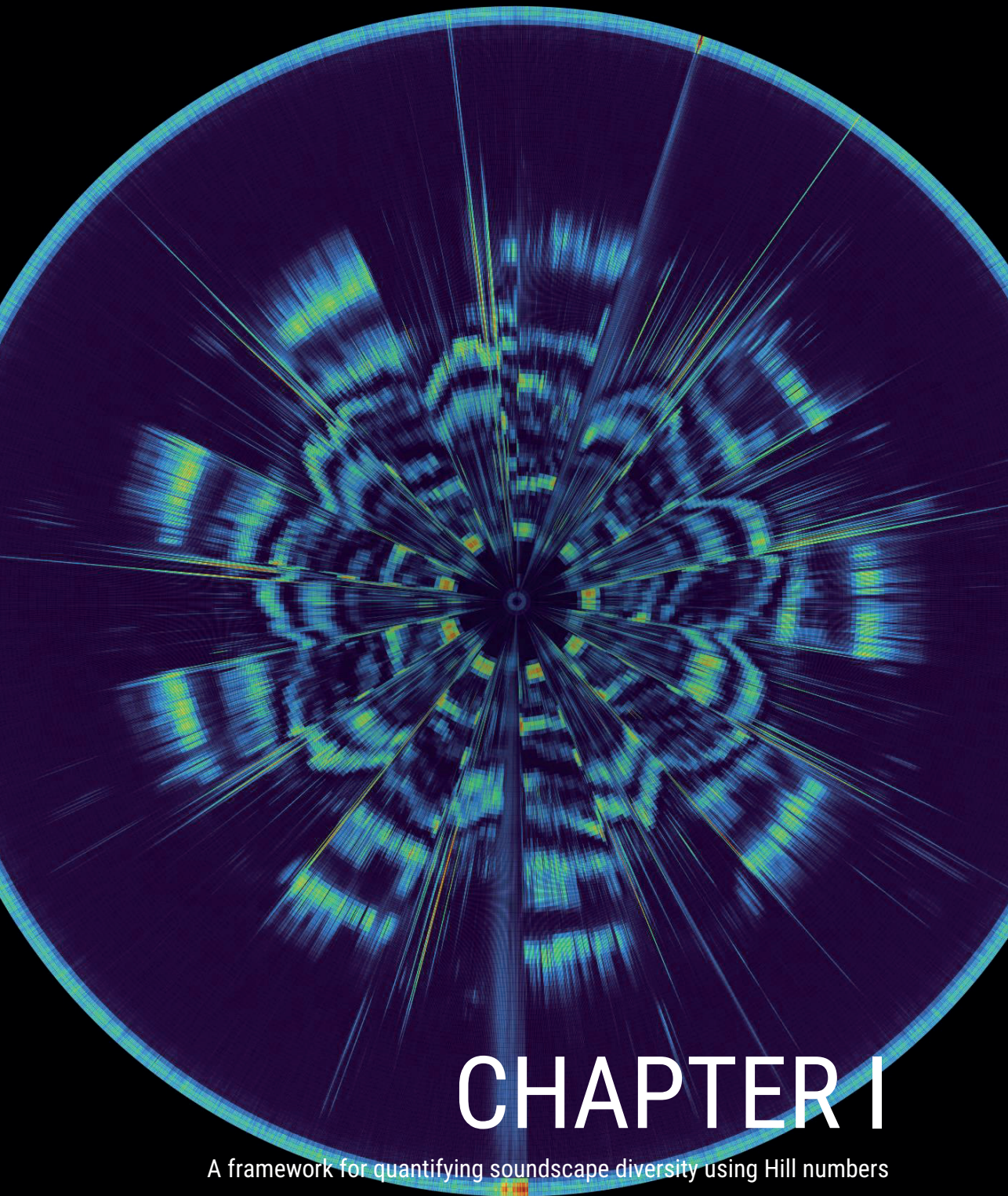
- Sugai, L.S.M.; Llusia, D.; Siqueira, T; Silva, T.S. (2021).** Revisiting the drivers of acoustic similarities in tropical anuran assemblages. *Ecology*, 102(7), p.e03380.
- Symes, L.; ter Hofstede, H.M.; Martinson, S.J.; Geipel, I.; Kernan, C.E; Madhusudhana, S. (2022).** Using passive acoustic monitoring and machine learning analysis to investigate katydid ecology and behavior. *The Journal of the Acoustical Society of America*, 151(4), pp.A29-A29.
- Tietze, D.T.; Martens, J.; Fischer, B.S.; Sun, Y.H.; Klusmann-Kolb, A; Päckert, M. (2015).** Evolution of leaf warbler songs (Aves: Phylloscopidae). *Ecology and Evolution*, 5(3), pp.781-798.
- Tobias, J.A.; Planqué, R.; Cram, D.L; Seddon, N. (2014).** Species interactions and the structure of complex communication networks. *Proceedings of the National Academy of Sciences*, 111(3), pp.1020-1025.
- Towsey, M.; Parsons, S; Sueur, J. (2014a).** Ecology and acoustics at a large scale. *Ecological Informatics*, 21, pp.1-3.
- Towsey, M.; Wimmer, J.; Williamson, I; Roe, P. (2014b).** The use of acoustic indices to determine avian species richness in audio-recordings of the environment. *Ecological Informatics*, 21, pp.110-119.
- Towsey, M.; Zhang, L.; Cottman-Fields, M.; Wimmer, J.; Zhang, J; Roe, P. (2014c).** Visualisation of long-duration acoustic recordings of the environment. *Procedia Computer Science*, 29, pp.703-712.
- Truskinger, A.; Cottman-Fields, M.; Eichinski, P.; Towsey, M; Roe, P. (2014).** Practical analysis of big acoustic sensor data for environmental monitoring. *IEEE - Fourth International Conference on Big Data and Cloud Computing*, pp.91-98.
- Truskinger, Anthony; Towsey, Michael (2019).** Why do we analyze data in 1-minute chunks? Available online at <https://research.ecosounds.org/2019/08/09/analyzing-data-in-one-minute-chunks.html>, updated on 5/4/2023, checked on 5/4/2023.
- Tucker, D.; Gage, S.H.; Williamson, I; Fuller, S. (2014).** Linking ecological condition and the soundscape in fragmented Australian forests. *Landscape Ecology*, 29, pp.745-758.

- Tuia, D.;** Kellenberger, B.; Beery, S.; Costelloe, B.R.; Zuffi, S.; Risse, B.; Mathis, A.; Mathis, M.W.; van Langevelde, F.; Burghardt, T; Kays, R. (2022). Perspectives in machine learning for wildlife conservation. *Nature communications*, 13(1), p.792.
- Tundisi, J.G.;** Goldemberg, J.; Matsumura-Tundisi, T; Saraiva, A.C. (2014). How many more dams in the Amazon?. *Energy Policy*, 74, pp.703-708.
- Tuomisto, H.** (2010). A diversity of beta diversities: straightening up a concept gone awry. Part 1. Defining beta diversity as a function of alpha and gamma diversity. *Ecography*, 33(1), pp.2-22.
- Turvey, S.T;** Crees, J.J. (2019). Extinction in the Anthropocene. *Current Biology*, 29(19), pp.982-986.
- Versluis, M.;** Schmitz, B.; Von der Heydt, A; Lohse, D. (2000). How snapping shrimp snap: through cavitating bubbles. *Science*, 289(5487), pp.2114-2117.
- Villanueva-Rivera, L.J.;** Pijanowski, B.C.; Doucette, J; Pekin, B. (2011). A primer of acoustic analysis for landscape ecologists. *Landscape ecology*, 26, pp.1233-1246.
- Villanueva-Rivera, L.J.;** Pijanowski, B.C. (2012). Pumilio: a web-based management system for ecological recordings. *Bulletin of the Ecological Society of America*, 93(1), pp.71-81.
- Villanueva-Rivera, L.J.** (2014). Eleutherodactylus frogs show frequency but no temporal partitioning: implications for the acoustic niche hypothesis. *PeerJ*, 2, p.e496.
- Villanueva-Rivera, L.J.;** Pijanowski, B.C; Villanueva-Rivera, M.L.J. (2018). Package 'soundecology'. R package version, 1(3), p.3.
- Villéger, S.;** Mason, N.W; Mouillot, D. (2008). New multidimensional functional diversity indices for a multifaceted framework in functional ecology. *Ecology*, 89(8), pp.2290-2301.
- Wagner, D.L.;** Grames, E.M.; Forister, M.L.; Berenbaum, M.R; Stopak, D. (2021). Insect decline in the Anthropocene: Death by a thousand cuts. *Proceedings of the National Academy of Sciences*, 118(2), p.e2023989118.
- Wang, G.;** Harpole, C.E.; Trivedi, A.K; Cassone, V.M. (2012). Circadian regulation of bird song, call, and locomotor behavior by pineal melatonin in the zebra finch. *Journal of Biological Rhythms*, 27(2), pp.145-155.

- Wang, J.;** Sankupellay, M.; Konovalov, D.; Towsey, M; Roe, P. (2019). Social network analysis of an acoustic environment: the use of visualised data to characterise natural habitats. *IEEE - Digital Image Computing: Techniques and Applications*, pp.1-7.
- Weissensteiner, M.H.;** Poelstra, J.W; Wolf, J.B. (2015). Low-budget ready-to-fly unmanned aerial vehicles: An effective tool for evaluating the nesting status of canopy-breeding bird species. *Journal of avian biology*, 46(4), pp.425-430.
- Whittaker, R.J.;** Fernández-Palacios, J.M. (2007). *Island biogeography: ecology, evolution, and conservation*. Oxford University Press.
- Wiley, R.H.;** Richards, D.G. (1978). Physical constraints on acoustic communication in the atmosphere: implications for the evolution of animal vocalizations. *Behavioral ecology and sociobiology*, 3, pp.69-94.
- Wimmer, J.;** Towsey, M.; Planitz, B.; Williamson, I; Roe, P. (2013). Analysing environmental acoustic data through collaboration and automation. *Future Generation Computer Systems*, 29(2), pp.560-568.
- Witmer, G.W.** (2005). Wildlife population monitoring: some practical considerations. *Wildlife Research*, 32(3), pp.259-263.
- Wood, C.M.;** Popescu, V.D.; Klinck, H.; Keane, J.J.; Gutiérrez, R.J.; Sawyer, S.C; Peery, M.Z. (2019). Detecting small changes in populations at landscape scales: a bioacoustic site-occupancy framework. *Ecological Indicators*, 98, pp.492-507.
- Almond, R.E.A.;** Grooten, M.; Juffe Bignoli, D; Petersen, T. (2022). *Living Planet Report 2022–Building a nature-positive society*. World Wildlife Fund.
- Yang, Z.;** Wang, T.; Skidmore, A.K.; De Leeuw, J.; Said, M.Y; Freer, J. (2014). Spotting East African mammals in open savannah from space. *PloS one*, 9(12), p.e115989.
- Zhang, Yimei;** Wang, Yanyi; He, Yan; Zhou, Bing; Tian, Miao; Xia, Canwei (2023). Characteristics and applications of beta acoustic indices. *Biodiversity Science* 31 (1), p.22513.
- Zhu, X.X.;** Tuia, D.; Mou, L.; Xia, G.S.; Zhang, L.; Xu, F; Fraundorfer, F. (2017). Deep learning in remote sensing: A comprehensive review and list of resources. *IEEE - Geoscience and remote sensing magazine*, 5(4), pp.8-36.

- Zsebők, S.; Schmera, D.; Laczi, M.; Nagy, G.; Vaskuti, É.; Török, J; Zsolt Garamszegi, L.** (2021). A practical approach to measuring the acoustic diversity by community ecology methods. *Methods in Ecology and Evolution*, 12(5), pp.874-884.
- Zwerts, J.A.; Stephenson, P.J.; Maisels, F.; Rowcliffe, M.; Astaras, C.; Jansen, P.A.; van Der Waarde, J.; Sterck, L.E.; Verweij, P.A.; Bruce, T; Brittain, S.** (2021). Methods for wildlife monitoring in tropical forests: Comparing human observations, camera traps, and passive acoustic sensors. *Conservation Science and Practice*, 3(12), p.e568.

7 Papers



CHAPTER I

A framework for quantifying soundscape diversity using Hill numbers

I **A framework for quantifying soundscape diversity using Hill numbers**

Authors

Thomas Luypaert^{1*}, Anderson S. Bueno², Gabriel S. Masseli³, Igor L. Kaefer⁴, Marconi Campos-Cerqueira⁵, Carlos A. Peres^{6,7}, Torbjørn Haugaasen¹

Affiliations

¹ Faculty of Environmental Sciences and Natural Resource Management, Norwegian University of Life Sciences, Ås, Norway

² Instituto Federal de Educação, Ciência e Tecnologia Farroupilha, Júlio de Castilhos, RS, Brazil

³ Programa de Pós-Graduação em Ecologia, Instituto Nacional de Pesquisas da Amazônia, Manaus, AM, Brazil

⁴ Instituto de Ciências Biológicas, Universidade Federal do Amazonas, Manaus, AM, Brazil

⁵ Science Department, Rainforest Connection, Katy, Texas, USA

⁶ School of Environmental Sciences, University of East Anglia, Norwich, United Kingdom

⁷ Instituto Juruá, Manaus, AM, Brazil

***Corresponding authors**

Thomas Luypaert (thomas.luypaert@nmbu.no / thomas.luypaert@outlook.com)

Keywords:

Acoustic indices, acoustic niche usage, ecoacoustics, Hill numbers, Operational Sound Units (OSUs), passive acoustic monitoring (PAM), soundscape diversity, trait-based ecology

A framework for quantifying soundscape diversity using Hill numbers

Thomas Luypaert¹  | Anderson S. Bueno²  | Gabriel S. Masseli³  | Igor L. Kaefer⁴  |
Marconi Campos-Cerqueira⁵  | Carlos A. Peres^{6,7}  | Torbjørn Haugaasen¹ 

¹Faculty of Environmental Sciences and Natural Resource Management (MINA), Norwegian University of Life Sciences, Ås, Norway; ²Instituto Federal de Educação, Ciência e Tecnologia Farroupilha, Júlio de Castilhos, RS, Brazil; ³Programa de Pós-Graduação em Ecologia, Instituto Nacional de Pesquisas da Amazônia, Manaus, AM, Brazil; ⁴Instituto de Ciências Biológicas, Universidade Federal do Amazonas, Manaus, AM, Brazil; ⁵Science Department, Rainforest Connection, Katy, Texas, USA; ⁶School of Environmental Sciences, University of East Anglia, Norwich, Norfolk, UK and ⁷Instituto Juruá, Manaus, AM, Brazil

Correspondence

Thomas Luypaert

Email: thomas.luypaert@outlook.com;
thomas.luypaert@nmbu.no

Funding information

Conselho Nacional de Desenvolvimento Científico e Tecnológico, Grant/Award Number: 200463/2014-4 and 309473/2019-5; Natural Environment Research Council, Grant/Award Number: NE/J01401X/1; Norges Miljø- og Biotivenskapelige Universitet; Reserva Biológica do Uatumã; Rufford Foundation, Grant/Award Number: 17715-1; University of East Anglia

Handling Editor: Sarab Sethi

Abstract

1. Soundscape studies are increasingly used to capture landscape-scale ecological patterns. Yet, several aspects of soundscape diversity remain unexplored. Although some processes influencing acoustic niche usage may operate in the 24-hr temporal domain, most acoustic indices only capture the diversity of sounds co-occurring in sound files at a specific time of day. Moreover, many indices do not consider the relationship between the spectral and temporal traits of sounds simultaneously. To provide novel insights into landscape-scale patterns of acoustic niche usage at broader temporal scales, we present a workflow to quantify soundscape diversity through the lens of trait-based ecology.
2. Our workflow quantifies the diversity of sound in the 24-hr acoustic trait space. We introduce the Operational Sound Unit (OSU), a unit of diversity measurement that groups sounds by their shared acoustic properties. Using OSUs and building on the framework of Hill numbers, we propose three metrics that capture different aspects of acoustic trait space usage: (i) soundscape richness, (ii) soundscape diversity and (iii) soundscape evenness. We demonstrate the use of these metrics by (a) simulating soundscapes to assess whether the indices possess a set of desirable behaviours and (b) quantifying soundscape richness and evenness along a gradient in species richness.
3. We demonstrate that (a) the indices outlined herein have desirable behaviours and (b) the soundscape richness and evenness are positively correlated with the richness of sound-producing species. This suggests that more acoustic niche space is occupied when the species richness is higher. Additionally, species-poor acoustic communities have a higher proportion of rare sounds and use the acoustic space less evenly.

This is an open access article under the terms of the [Creative Commons Attribution License](https://creativecommons.org/licenses/by/4.0/), which permits use, distribution and reproduction in any medium, provided the original work is properly cited.

© 2022 The Authors. *Methods in Ecology and Evolution* published by John Wiley & Sons Ltd on behalf of British Ecological Society.

4. Our workflow generates novel insights into acoustic niche usage at a landscape scale and provides a useful tool for biodiversity monitoring. Moreover, Hill numbers can also be used to measure the taxonomic, functional and phylogenetic diversity. Using a common framework for diversity measurement gives metrics a common behaviour, interpretation and standardised unit, thus ensuring comparisons between soundscape diversity and other metrics represent real-world ecological patterns rather than mathematical artefacts stemming from different formulae.

KEYWORDS

acoustic indices, acoustic niche usage, ecoacoustics, Hill numbers, Operational Sound Units (OSUs), passive acoustic monitoring (PAM), soundscape diversity, trait-based ecology

1 | INTRODUCTION

Passive acoustic monitoring (PAM) offers promising opportunities for ecological monitoring. Automated acoustic sensors can record environmental sound at broad spatiotemporal scales with reduced cost and human effort compared to equivalent active acoustic sampling by an in-situ observer (Gibb et al., 2019). Using acoustic data, the taxonomic diversity of a biological community can be derived by isolating and identifying species' calls, thus providing an objective and permanent record of the resident soniferous (sound producing) biological community (Gibb et al., 2019; Sugai et al., 2019). Yet, obtaining species-level information for broad spatiotemporal scales or taxonomic breadth presents numerous analytical difficulties, such as the time-consuming and knowledge-demanding nature of aural annotation, and the paucity of reliable automated species identifiers and reference databases for most taxa and regions (Gibb et al., 2019; Kahl et al., 2021; Sugai et al., 2019; Toledo et al., 2015).

In addition to taxonomic information, species' sounds carry functional significance. Acoustic signals are crucial for a broad range of social interactions including courting behaviour, territorial defence, predator avoidance and food sharing (Darwin, 1872; Seyfarth & Cheney, 2003). As such, species' sounds are subject to selective pressures at multiple scales (Zsebök et al., 2021), resulting in a wide variety of acoustic traits that are expressed in the timing, frequency and amplitude features of acoustic signals. The field of soundscape ecology exploits this variation in acoustic traits, attempting to infer ecological information from the soundscape—that is, the collection of biological (biophony), geophysical (geophony) and human-produced (anthrophony) sounds emanating from a landscape—without the need for species identification (Krause, 1987; Pijanowski, Farina, et al., 2011; Pijanowski, Villanueva-Rivera, et al., 2011). This approach assumes that the diversity of acoustic traits in the landscape can be used to understand ecological processes across spatial and temporal scales (Pijanowski, Villanueva-Rivera, et al., 2011). Consequently, more than 60 acoustic indices have been developed (Buxton et al., 2018), each of which reflects some aspect of the diversity of acoustic traits in a sound file.

The diversity of acoustic signals in trait space can illuminate underlying ecological and evolutionary mechanisms (Gasc et al., 2013).

For instance, one of the cornerstone theories of soundscape ecology is the Acoustic Niche Hypothesis, which views acoustic space as a core ecological resource for which soniferous sympatric species compete, leading to partitioning of the soundscape in the time–frequency domain to avoid spectro-temporal overlap in sound production (Krause, 1993). Therefore, a more speciose community should lead to increased competition and partitioning of acoustic niche space, which is reflected in the diversity of acoustic traits. Indeed, acoustic indices have been successfully applied as proxies for the diversity of species (Depaetere et al., 2012; Towsey et al., 2014) or sound types (Pijanowski, Villanueva-Rivera, et al., 2011).

Despite recent advances, several aspects of soundscape diversity quantification remain unexplored. For instance, most indices capture acoustic patterns using either time-averaged spectrograms (collapsed in the temporal domain) or measures of variation in amplitude over time (collapsed in the frequency domain). Hence, indices are fundamentally limited in their ability to detect diversity patterns across both the spectral and temporal dimensions simultaneously (Eldridge et al., 2016). Since spectro-temporal partitioning might be one of the mechanisms dictating acoustic community assembly, considering both the spectral and temporal dimensions of the acoustic trait space simultaneously may be key to evaluating how acoustic niches are structured. Moreover, most existing acoustic indices are calculated over relatively short-duration time-scales (e.g. 1-min sound files). We suggest that assembly processes structuring the presence and distribution of sound in acoustic trait space should also be considered at broader temporal scales. As many species' sound emissions follow circadian patterns (Agostino et al., 2020), some of the temporal partitioning of acoustic niches likely occurs in the 24-hr time domain. Yet, to date, explicit quantification of the relationship among sounds in the 24-hr acoustic trait space at a landscape scale has been scarce (but see Aide et al., 2017). To do so, we require a robust framework that produces informative metrics that capture within- and between-soundscape differences in spectro-temporal trait space usage.

Here, we describe a workflow to decompose the diversity of sound in acoustic trait space, hereafter referred to as soundscape diversity. This workflow is grounded in the principles of acoustic niche theory and leans heavily on trait-based ecological research. However, rather than focussing on fine-scale temporal patterns (i.e. bioacoustics studies) or

assessing the soundscape diversity of an acoustic assemblage at a particular time of day (i.e. many soundscape studies), we propose a framework to investigate the relationship among all sounds produced in a broader 24-hr acoustic trait space at a given geographical location. We develop a novel unit of diversity measurement, the Operational Sound Unit (OSU), which groups sounds by their shared properties in acoustic trait space (i.e. sounds occupy the same temporal and frequency space). Using OSUs and building on the framework of Hill numbers (a mathematically unified family of diversity indices), we introduce three metrics that capture different aspects of the acoustic trait diversity of the soundscape: (i) soundscape richness, (ii) soundscape diversity and (iii) soundscape evenness.

Our workflow offers unique insights that complement existing soundscape diversity metrics. Dissecting the soundscape diversity into its facets can provide insights into various aspects of 24-hr acoustic trait space usage, including patterns of acoustic niche saturation, evenness, dominance or rarity. Moreover, using Hill numbers, we can quantify soundscape diversity at various scales, decomposing the regional metacommunity diversity (γ -diversity) into its local diversities (α -diversity) and a community turnover component (β -diversity) using a simple multiplicative relationship. Additionally, Hill numbers can also be used to quantify taxonomic, functional and phylogenetic diversity, which ensures that observed relationships between soundscape diversity and other facets of biodiversity represent real-world ecological patterns. If the Acoustic Niche Hypothesis holds, this means these various soundscape diversity components could shed light on the species richness or diversity of soniferous communities using a common framework of reference.

To illustrate our approach, we show that the proposed soundscape diversity metrics follow a set of fundamental criteria for trait-based diversity metrics and act in an ecologically intuitive way. Moreover, in our case study, we use an acoustic dataset from Brazilian Amazonia to investigate how the soundscape diversity metrics behave along a gradient of species richness. We find positive correlations for both soundscape richness and evenness with the richness of soniferous species.

2 | METHODS

The implementation of this workflow is facilitated by the `SOUNDSCAPER` package, written in the R-programming language (R Core Team, 2020) and found on GitHub (<https://github.com/ThomasLuypaert/soundscapeR>).

2.1 | Defining acoustic trait space

The timing, frequency and amplitude of sounds are important acoustic traits that are subject to evolutionary processes and influence community assembly. As such, we use the timing and frequency of sounds as the variables that delineate a two-dimensional acoustic trait space and employ an amplitude-based threshold value to quantify the detection/non-detection of sounds within this acoustic space.

Although soniferous species produce sounds ranging from infrasound to ultrasound, we recommend constraining the upper-frequency limit to 22,050 Hz, which is approximately the maximal frequency audible to humans (Farina, 2013). Most wildlife sounds can be found in this frequency range (Farina & James, 2016), so the evolutionary mechanisms structuring acoustic assemblages are likely strongest in this range. Moreover, in downstream analyses, we use a spectral acoustic index to capture soundscape structure, and the effects of ultrasonic frequencies on such indices are not well studied. In the temporal domain, we follow Aide et al. (2017) and consider acoustic trait space over 24 hr. The reasoning here is twofold. First, we are interested in investigating the presence of all sounds produced at a given site for a particular time of year, not just sounds at a particular time of day. Second, almost all living organisms have 24-hr circadian rhythms in sound emission (Agostino et al., 2020; Cui et al., 2011; da Silva et al., 2014; Wang et al., 2012), making 24 hr an ecologically relevant sample duration.

2.2 | Defining a unit of soundscape diversity measurement

In trait-based ecology, diversity metrics are usually based on the traits of taxonomic species and their abundance (Shaner et al., 2021). Yet, taxonomic information is not always available. In some fields of research where the taxonomic identity of individuals is unknown, Operational Taxonomic Units (OTUs)—or groups of related individuals which share a set of observed properties (Sokal & Sneath, 1963)—are used to infer system diversity. Here, we attempt to measure and compare the acoustic properties of entities (sounds) in a system (acoustic trait space) without a taxonomic link to the source organisms. Hence, to quantify the soundscape diversity, we require a unit of measurement that groups sounds by their shared acoustic properties without the need for taxonomic information.

In analogy to OTUs, we propose a novel unit of diversity measurement, Operational Sound Units (OSUs), which group sounds by their shared spectro-temporal properties. OSUs are obtained by subdividing acoustic trait space into many discrete spectro-temporal bins which are the soundscape equivalent of the time-frequency bins in a spectrogram. Despite being conceptually analogous to the time-frequency bins used to calculate the 'Acoustic Space Use' (ASU) metric in Aide et al. (2017), the OSU differs in the amplitude features that are used to capture the presence and abundance of sound in acoustic trait space, and in the resolution along the temporal axis (see below).

2.2.1 | Assessing the presence of sound in acoustic trait space

Methodological choices made during acoustic data collection, such as the temporal sampling regime and sampling rate, will affect

subsequent analyses. We provide recommendations regarding these choices in the context of our workflow in S1 and S6.1. Here, we use a sampling regime of 1 min of recording every 5 min (henceforth 1 min/5 min) and a sampling rate of 44,100 Hz.

We are interested in all biological sounds produced at a given site, regardless of which source they emanate from. Therefore, we focus on the presence of sounds exceeding a 3-dB amplitude threshold for a certain duration of time in each 1-min recording. We pool sound files from the acoustic survey at a specific site into 24-hr samples of the acoustic trait space, each sample containing all 1-min sound files obtained in a single day (00:00–23:59 hr; [Figure 1a](#)). To determine where (frequency domain) and when (time domain) sound is present in the acoustic trait space, we use the Acoustic Cover (CVR) spectral acoustic index. For each 1-min sound file, the CVR index produces a vector of values, one value for each frequency bin of the spectrogram. Each value reflects the proportion of cells in a noise-reduced frequency bin that exceeds a 3-dB threshold and ranges between 0 and 1 (see [Towsey, 2017](#) for a detailed breakdown of index computation). We calculate the CVR index for all 1-min sound files in each 24-hr sample. Acoustic recordings are processed following [Towsey \(2017\)](#), computing indices using the QUT Ecoacoustics Analysis Programs software ([Towsey et al., 2018; Figure 1b](#)).

The CVR index vectors for all 1-min files in a sample are concatenated chronologically, creating a data frame with the time of recording as columns, the frequency bins as rows, and the value of the CVR index for each time–frequency bin as cells. This reveals the presence and distribution of sound in each sample of the 24-hr acoustic trait space ([Figure 1c](#)).

2.2.2 | The Operational Sound Unit (OSU)

By assessing the presence of sound in acoustic trait space as described in [Section 2.2.1.](#), we have divided the trait space into discrete time–frequency bins, grouping sounds by their acoustic properties (shared time and frequency values in trait space), thus capturing our concept of Operational Sound Units ([Figure 2](#)).

As with time–frequency bins in spectrograms, the resolution of OSUs in acoustic trait space, and thus the total number of OSUs, is variable. The temporal width of OSUs is dictated by the sound file length and the total number of OSUs in the temporal domain by the recording schedule. The 1-min duration employed for index calculation retains enough detail in the acoustic features for long-duration soundscape analysis, facilitates rapid computation, and has been used as the de facto standard in most soundscape studies ([Truskinger & Towsey, 2019](#)).

In the frequency domain, OSU resolution is determined by the width of the frequency bins of the CVR index vector. This is dictated by the sampling rate and window length, which are specified in the Fast Fourier Transformation (FFT). Choosing the appropriate window length depends on the soniferous community of interest. In [S.2](#), we provide guidance on window length choice and recommend using a 256-sample window length. With our recording settings (44,100 Hz

sampling rate, 1 min/5 min sampling regime and a window length of 256), the frequency domain consists of 128 frequency bins (number of bins = window length/2) of 172 Hz width (bin width = [sampling rate/2]/number of bins). The temporal domain consists of 288 bins (24 hr = 1440 min with 1 min/5 min recorded = 288 bins). As such, the total number of detectable OSUs in the trait space using these settings is 36,864 (128 frequency bins * 288 temporal bins).

2.3 | Assessing the prevalence of OSUs in acoustic trait space

Next, we need to attribute an importance value to each OSU. Instead of using the raw CVR values obtained in [Section 2.2.1](#), we use an incidence-based approach to derive an importance value for each OSU.

For every 24-hr sample of each site, we use a site-specific threshold to convert the OSU's raw CVR values to a binary variable. This binary variable captures the detection (CVR value \geq threshold = 1) or non-detection (CVR value < threshold = 0) of sound for the section of the acoustic trait space delineated by each OSU ([Figure 3a](#)). The choice of the threshold depends on the study system and is influenced by the sound transmission characteristics of the habitat and the amount of ambient noise in the surrounding environment ([Darras et al., 2016](#)). For a comparison of thresholding methods, consult [S.3](#).

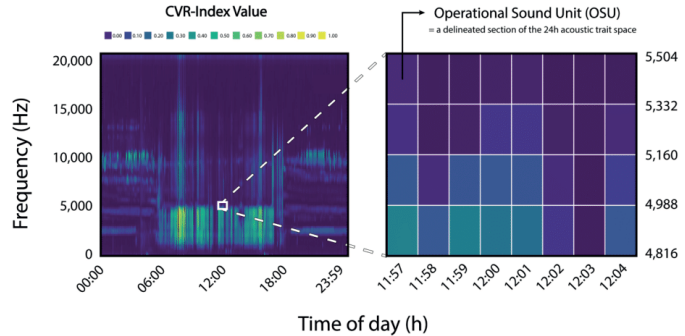
To ensure site-specific binarisation thresholds are objective, we use the 'IsoData' binarisation algorithm, available in the `auto-threshold` R-package ([Landini et al., 2017](#)). The IsoData algorithm is borrowed from image segmentation analysis and is designed to separate pixels in the foreground from those in the background ([Ridler & Calvard, 1978](#)). In the context of our workflow, the algorithm determines an initial threshold value based on the mean CVR index value of the site's soundscape. Based on this threshold, it divides the OSUs into two classes (foreground and background), calculates their mean CVR index values and updates the threshold to be the mean of these two mean values. This process is repeated iteratively until threshold convergence is achieved.

Finally, we compute the mean relative OSU abundance by averaging each OSU's binary values across all 24-hr samples of the acoustic trait space for a site ([Figures 3b,c](#)). To avoid confusion between sound frequency (Hz) and incidence frequency (relative number of OSU occurrences), we henceforth refer to the OSU importance value as the relative abundance.

2.4 | Quantifying soundscape diversity using Hill numbers

When quantifying the diversity of a system, diversity is typically broken down into two components: richness and evenness ([Hill, 1973](#)). Here, we add a third component, soundscape diversity, which incorporates aspects of the former two. Although a large number of indices have been proposed to measure diversity,

FIGURE 2 A conceptual visualisation of Operational Sound Units (OSUs) in the 24-hr acoustic trait space. Each 24-hr sample of the acoustic trait space can be divided into sections which we define as OSUs. These OSUs are delineated by the frequency-bin width of the spectral index vector (frequency domain) and the recording interval of the sampling regime (temporal domain), and group sounds by their shared functional properties in acoustic space.



Hill numbers are computed as follows:

$${}^qD = \left(\sum_{i=1}^S p_i^q \right)^{\frac{1}{1-q}} \tag{1}$$

With S being the number of OSUs, p_i the relative abundance of OSU i , and q the order of diversity. This equation expresses the diversity of the system as the 'effective number of entities' (OSUs)—the number of equally abundant OSUs that would yield the same value of diversity.

Here, we briefly describe the soundscape richness, diversity and evenness components and introduce the indices used for their measurement in the acoustic trait space.

2.4.1 | Soundscape richness and diversity

Sensitivity to the relative abundance of OSUs is modulated using the order of diversity (q) without changing the interpretation of qD . When $q = 0$, relative abundance is disregarded and Equation (1) yields ${}^0D = S$, that is, the richness of OSUs in acoustic trait space—or soundscape richness. In our workflow, soundscape richness measures the amount of acoustic trait space occupied by OSUs throughout the acoustic survey at a site without considering their relative abundance. Conceptually, our soundscape richness metric is analogous to the soundscape saturation metric in Burivalova et al. (2018); however, they measure the saturation of acoustic trait space at a 1-min scale. Similarly, our metric is related to the acoustic space use (ASU) metric described in Aide et al. (2017), which quantifies the saturation of acoustic trait space on a 24-hr scale, but uses a different methodology to detect sounds and aggregates those sounds at broader 1-hr intervals.

The higher the order of diversity q , the greater the weight given to highly abundant OSUs. For instance, when $q = 1$, soundscape diversity 1D equals the exponential of the Shannon entropy or the number of common OSUs in the soundscape. When $q = 2$, the soundscape diversity 2D equals the inverse of the Simpson index, or the number of dominant or highly abundant OSUs in the soundscape. These three Hill numbers represent simple transformations of the traditional and well-established diversity indices and calculate

mean species rarity using the arithmetic ($q = 0$), geometric ($q = 1$) and harmonic means ($q = 2$; Hill, 1973). Although the soundscape richness and diversity metrics are usually expressed in the total number of OSUs, soundscape metrics can still be compared between soundscapes with differing dimensions (a different number of detectable OSUs due to window length/sampling regime differences) by dividing the soundscape richness or diversity by the total number of detectable OSUs in the soundscape.

2.4.2 | Soundscape evenness

Evenness describes the equitability of abundances (Hill, 1973). Various measures of evenness can be calculated by taking the ratio between Hill numbers qD with $q = 1, 2, \dots$, and the richness 0D (Jost, 2010). Here, the choice of q -value determines the importance of OSU abundance on the evenness metric. For instance, since 1D roughly represents the number of common OSUs in the acoustic trait space, the evenness ratio ${}^1D/{}^0D$ represents the proportion of common OSUs in the community. Similarly, as 2D represents the number of dominant OSUs, the evenness ratio represents the proportion of dominant OSUs. Different q -values differ in the sharpness of the cut-off between rarity, commonness or dominance.

These patterns in evenness are best represented by constructing diversity profiles, a type of visualisation showing a series of Hill numbers derived using a continuous function of the order of diversity q (Chao et al., 2012; Jost, 2007; see Figure S11). Diversity profiles provide the most complete representation of the soundscape evenness, giving the relative abundance distribution of OSUs in the soundscape, and highlighting changes in diversity with changing importance of rarity. As soundscape diversity and evenness can both be calculated for an infinite number of q -values, for the remainder of this work we will follow Jost (2006) and define diversity as 2D and evenness as ${}^2D/{}^0D$. We make this choice because $q = 2$ corresponds to a common biodiversity metric used in literature (the Simpson index) and the q -value is large enough to incorporate patterns of rarity and dominance in the acoustic community.

In S.4, we outline the theoretical framework for decomposing the soundscape diversity into its alpha, beta and gamma components.

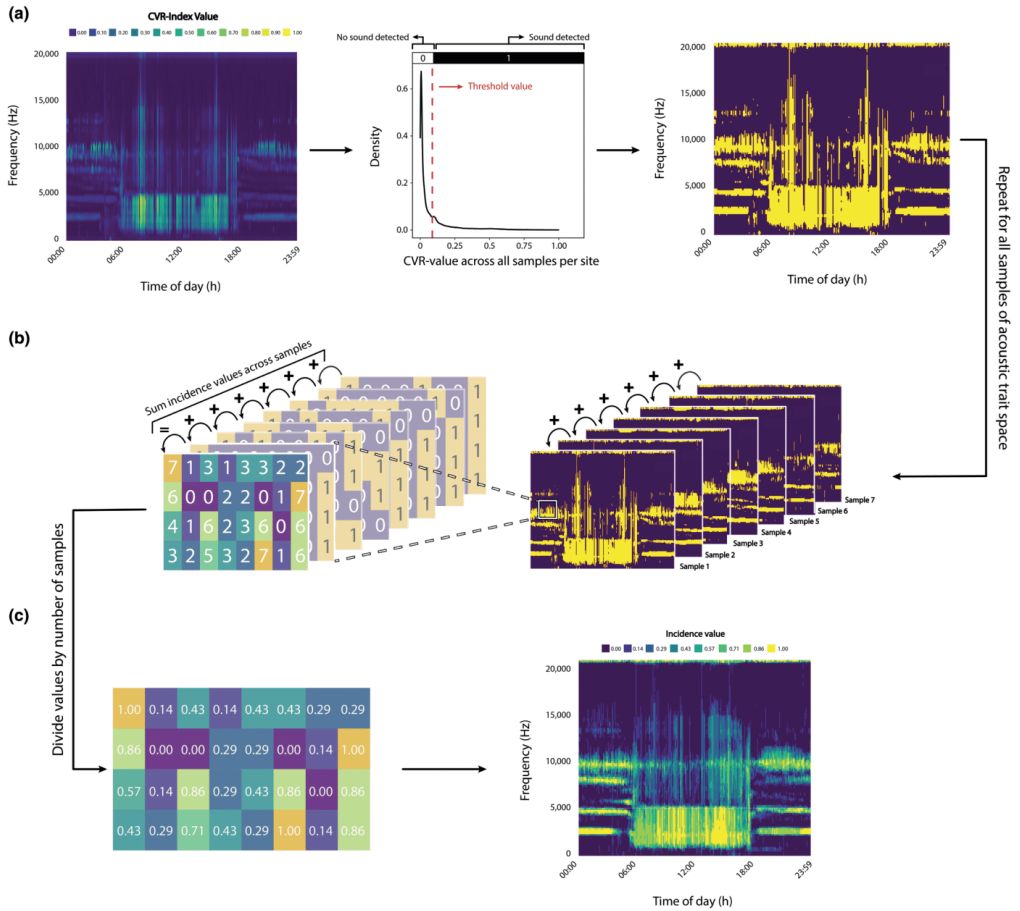


FIGURE 3 A conceptual representation of the methodology used to attribute an importance value to OSUs in acoustic trait space. (a) Per site, a binarisation algorithm is applied to each sample of acoustic trait space, resulting in a binary variable representing the detection/non-detection of OSUs across samples; (b) For each OSU, the detection (1) or non-detection (0) values are summed across all 24-hr samples of acoustic trait space for that site and divided by the number of samples to obtain the OSU's relative abundance (incidence frequency); (c) The presence, relative abundance and distribution of OSUs in acoustic trait space.

In S.5, we illustrate the behaviour and intuitive properties of the proposed soundscape diversity metrics by simulating artificial soundscapes. The simulated datasets serve to demonstrate the behaviour of the metrics with respect to some fundamental criteria for trait-based diversity metrics, as outlined in Ricotta (2005), Villéger et al. (2008), and Mouchet et al. (2010).

3 | CASE STUDY

To explore the behaviour of our metrics of soundscape diversity in a real-life ecological setting, we characterised the soundscape richness

and evenness along a gradient in soniferous species richness using an empirical dataset from Brazilian Amazonia (1°40'S, 59°40'W). Acoustic data were collected at 35 sites for 4–10 days in the Balbina Hydroelectric Reservoir (BHR) in Brazilian Amazonia (see Supporting Information S6.2 and Bueno et al., 2020 for further details). This work was conducted under the SISBIO 49068 research permit.

Under the Acoustic Niche Hypothesis, we expected soundscape richness to be positively related to soniferous species richness (Krause, 1993). For soundscape evenness, we did not expect a relationship with species richness unless changing species richness was associated with a shift in the relative abundance distribution of the acoustic community (Wilsey et al., 2005).

3.1 | Compound species richness of soniferous taxa

To assess the relationship between the soundscape diversity metrics and soniferous species richness, we generated a compound species richness index of three major tropical forest soniferous taxa: (i) anurans (Bueno et al., 2020), (ii) birds (this study) and (iii) primates (Benchimol & Peres, 2015). Species richness data for these three groups came from a manual and automated extraction from audio recordings and data from the literature (see Supporting Information S6.3). A total of 34 anuran species, 71 bird species and 7 primate species were detected across the 35 sites. We summed the richness values for these three taxa to obtain the compound richness index. Due to the absence of available taxonomic richness data, this compound richness did not include insects, a dominant acoustic group in tropical forests (Aide et al., 2017). However, we deem the combined acoustic activity of these three taxonomic groups to be sufficiently strong to influence the rainforest soundscape, and therefore be detectable with our soundscape diversity metrics.

3.2 | Soundscape diversity data

We calculated the soundscape richness and evenness for all sites using the workflow described above (see S.6.4). A priori knowledge of acoustic space usage can be used to subset the acoustic trait space to those time-frequency coordinates used by the soniferous groups of interest (Metcalf et al., 2020). This can reduce signal masking, and increase the sensitivity of soundscape metrics to species richness. We restricted the frequency domain below 11,025 Hz, where most anuran, bird and primate sounds are found, and excluded the part of the frequency spectrum dominated by insects. As the sampling duration was unequal between plots in the study, and we wished to retain the maximal amount of information, we used sample size-based rarefaction to equalise sampling effort among plots (see S.1). At most, we extrapolated to double the minimal sample size (Chao & Jost, 2012). We used the R-package 'iNEXT' (Hsieh et al., 2016) to calculate soundscape richness (0D) and evenness (${}^2D/{}^0D$) at a sampling effort of 8 days (twice the minimal sampling duration). Finally, we used a simple linear regression model to investigate the relationship between soundscape richness and evenness, and compound soniferous species richness. We provide additional analyses on the effect of sampling regime and window length on the relationship between soundscape richness and species richness in S.1.2.2 and S.2.

4 | RESULTS

4.1 | Properties of soundscape diversity metrics

Soundscape richness, evenness and diversity had strictly positive values constrained between 0 and 1, and are theoretically independent of the species richness (S.5.1). The monotonicity criterion held true for the soundscape richness and diversity metrics, but not

for soundscape evenness (S.5.2). Soundscape richness and evenness were independent of one another and described unique aspects of the soundscape diversity (S.5.3). Conversely, soundscape diversity at $q = 2$ displayed a positive relationship with both soundscape richness and evenness, and thus did not conform to the independence criterion. Unlike some commonly used biodiversity indices (i.e. Shannon–Wiener and Simpson biodiversity index), our metrics scaled linearly with the underlying diversity of the system—a theorem known as the replication principle (S.5.4). Finally, the same analytical workflow can be used to quantify the soundscape diversity at multiple scales or hierarchical levels, decomposing the regional metacommunity diversity (γ -diversity) into its local diversity (α -diversity) and community turnover (β -diversity) components using a simple multiplicative relationship (S.4; S.5.6).

4.2 | Relationship between soundscape metrics and species richness

The correlation between soundscape richness and soniferous species richness in our case study was strongly positive ($r = 0.85$; $R^2 = 0.72$; $p < 0.001$; Figure 4a-1; Table S4). This positive correlation was consistent, even for lower intensity sampling regimes (S.1.2.2), with r values staying high (>0.8) at all tested sampling intensities. We found that window length had a negligible impact on the correlation between both metrics ($r > 0.83$ for all window lengths; see S.2). Based on the visual inspection of acoustic trait space, sites containing a lower richness of soniferous species (Figure 4a-2) appeared to have more empty and less complex trait spaces than species-rich sites (Figure 4a-3). The trait space of low-richness sites had impoverished daytime soundscapes and lacked many of the sounds exceeding 5000 Hz that were present at taxonomically rich sites. For soundscape evenness, the correlation with soniferous species richness was weakly positive ($r = 0.40$; $R^2 = 0.16$; $p < 0.05$; Figure 4b-1). For low-evenness sites, low abundance sounds were more common compared to sites with a high soundscape evenness (Figure 4b-2 and 3).

5 | DISCUSSION

5.1 | Advantages of the workflow

Our soundscape metrics abided by a set of fundamental criteria for trait-based diversity indices (Mouchet et al., 2010; Ricotta, 2005; Villéger et al., 2008) and behaved in an ecologically intuitive manner. Furthermore, separating soundscape diversity into richness, evenness and diversity, and assessing how these behaved along a gradient of species richness, shed light on patterns of acoustic niche usage. Among the various theories that explain acoustic community assembly and niche usage, two hypotheses prevail in the soundscape literature: the Acoustic Adaptation Hypothesis and the Acoustic Niche Hypothesis (Pijanowski, Farina, et al., 2011; Pijanowski,

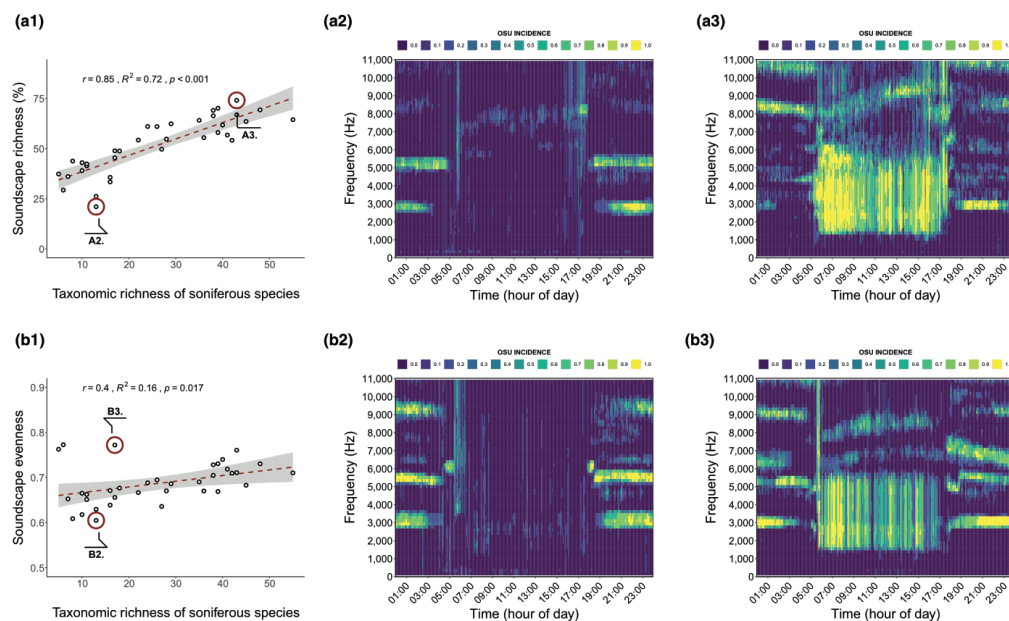


FIGURE 4 (a) The relationship between the soundscape richness and the richness of soniferous species (a1) with a visual representation of the 24-hr acoustic trait space for low-richness (a2) and high-richness (a3) soundscapes. The Pearson correlation coefficient and associated R^2 - and p -values indicate a strong positive relationship ($r = 0.85$) between the soundscape richness and species richness of sound-producing vertebrates. (b) The relationship between the soundscape evenness and the richness of soniferous species (b1) with a visual representation of low-evenness (b2) and high-evenness (b3) soundscapes. The Pearson correlation coefficient and associated R^2 - and p -values indicate a weak positive correlation ($r = 0.40$) between the soundscape evenness and species richness.

Villanueva-Rivera, et al., 2011). The former posits that species' acoustic traits (e.g. signal frequency, amplitude, timing and duration) are more similar than expected by chance as the environment filters for traits that maximise effective sound propagation and minimise attenuation (Mullet et al., 2017). The latter states that acoustic trait space is a core ecological resource and sonically sympatric species partition their acoustic niche so as to avoid spectro-temporal overlap in their vocalisations, which would lead to inefficient communication (Garcia-Rutledge & Narins, 2001; Krause, 1993). The Acoustic Niche Hypothesis implies that evolutionarily archaic and undisturbed ecosystems have acquired an evolutionary balance between all sounds in the landscape, resulting in soundscapes with high spectro-temporal complexity and signal diversity, and minimal overlap (Eldridge et al., 2016; Krause, 1993; Pijanowski, Farina, et al., 2011; Pijanowski, Villanueva-Rivera, et al., 2011). Conversely, disturbed systems in which 'acoustically optimised' species have been lost from the habitat are then characterised by an unbalanced equilibrium, showing readily detectable gaps in the soundscape.

Our soundscape richness metric quantifies the amount of acoustic niche space occupied by OSUs independent of how frequently OSUs were occupied over multiple days (the relative abundance). In our case study, we found a strong positive correlation

($r = 0.85$; $R^2 = 0.72$; $p < 0.001$) between soundscape richness and soniferous species richness. Soundscape richness is theoretically independent of species richness, so the observed relationship likely arose through processes of species assembly. Following the Acoustic Adaptation Hypothesis, we expected the richness of OSUs, driven by the richness of acoustic trait values, to be mostly insensitive to the richness of soniferous species. Given the strong positive relationship between soundscape richness and soniferous species richness, it is likely the acoustic community in the case study was structured by competition for acoustic niche space. As the species richness gradient in our study area originated from a disturbance event, it is plausible that the observed correlations between soundscape richness and species richness stemmed from the loss of species occupying unique acoustic niches in the acoustic trait space, resulting in a lower niche saturation at lower species richness.

The soundscape evenness metric captures the degree to which the relative abundances of OSUs are distributed in niche space. Hence, it quantifies how evenly the available acoustic resources are used at a landscape scale and sheds light on patterns of dominance and rarity. In the case study, soundscape evenness displayed a weak positive correlation ($r = 0.40$; $R^2 = 0.16$; $p < 0.05$)

with soniferous species richness. Changes in soniferous species richness were associated with changes in the distribution of the relative abundance of sounds in acoustic trait space. We posit that the correlation between soundscape evenness and soniferous species richness could reflect an unbalanced equilibrium, in which the acoustic community consists of a few acoustically dominant and many rare sound-producing species (Krause, 1993). As such, it appears that disturbed species-poor acoustic communities used acoustic niche resources less effectively (Mason et al., 2005). Indeed, the combination of both richness and evenness metrics provides unique insights into acoustic niche usage. Yet, many existing soundscape diversity metrics focus solely on the presence of sound in a short duration recording without accounting for the prevalence of sound in those same areas of acoustic trait space over the course of multiple days, thus overlooking the evenness component of soundscape diversity.

Our workflow potentially offers a robust and cost-effective method to track biodiversity changes at large spatial and temporal scales, or in systems where the knowledge of the resident biological community is incomplete. The strong positive correlation between soundscape richness and an independent estimate of soniferous species richness suggests this metric can be used as a proxy to infer taxonomic diversity patterns. Hence, it could be used as an early warning system, alerting researchers when declines in soundscape diversity exceed natural fluctuations (Krause & Farina, 2016; Pijanowski, Farina, et al., 2011; Pijanowski, Villanueva-Rivera, et al., 2011). The soundscape richness metric performed well as a biodiversity proxy compared to analogous metrics in the literature. For instance, in Burivalova et al. (2019), soundscape saturation (saturation of acoustic niche space for 1-min sound files), achieved a correlation of $r = 0.56$ and $R^2 = 0.31$ with the number of unique vertebrate calls (sonotypes) identified in the same sound file. The Acoustic Space Use metric in Aide et al. (2017) has a similarly strong relationship to our metric (Spearman's $\rho = 0.85$), but had a relatively small sample size (8 plots). Moreover, both studies investigated the correlation with the number of unique calls, whereas our study investigated the correlation with species richness. The former can be expected to attain higher correlations, as different calls tend to take up different parts of acoustic trait space and thus influence the soundscape saturation or acoustic space use more directly. Still, our workflow achieved high correlations, corroborating the robustness of the method.

Furthermore, even when a correlation is absent, our method allows us to measure where and when in acoustic trait space the occurrence and relative abundance of sound changes across space, time or hierarchical levels (e.g. local, regional or global) without requiring a link to the taxonomic identity of OSUs. In our case study, a visual comparison of acoustic trait space use between two extremes of the soundscape richness gradient showed that low-richness sites had an impoverished daytime soundscape and lacked sounds over 5000 Hz. Moreover, the low-evenness soundscape had a higher proportion of rare OSUs, suggesting the acoustic niche resource was used less effectively.

Finally, our workflow is robust, identifying an ecological gradient in an acoustically complex tropical rainforest setting. We used an amplitude threshold to remove transient and non-biological sounds. Although this step did not remove persistent non-focal high amplitude sounds, such as rain showers, thunder or wind, from the data, we still found strong positive correlations with species richness. Moreover, both the window length and sampling intensity had a minimal effect on the soundscape richness–soniferous species richness correlation. Additionally, the soundscape variability was captured with fewer hours of recording (a minimum of 24 hr) than previously suggested (i.e. 120 hr in Bradfer-Lawrence et al., 2019), although the minimum acoustic survey length needed to be the same (5 days). Yet, as ecosystems can differ in their sound turnover rate and therefore require different sampling efforts, we recommend sampling the soundscape for longer durations and/or higher sampling intensity if possible.

5.2 | Avenues of future research

The soundscape diversity metrics outlined herein treated all OSUs as equally similar. In reality, OSUs are not independent elements, but rather correlated units in acoustic trait space. As such, future work on our soundscape diversity metrics should incorporate the difference in acoustic trait values (time–frequency coordinates) of a particular OSU from all other OSUs in the acoustic space (Scheiner et al., 2017). Incorporating the distinctiveness of OSUs in acoustic trait space (soundscape dispersion) would allow us to further quantify the degree to which acoustic trait space is partitioned, providing further insights into acoustic niche differentiation and resource competition (Mason et al., 2005). For instance, if acoustic communities are structured by competition for acoustic space, we might expect overdispersion in acoustic trait space compared to the same number of OSUs drawn randomly from the regional OSU pool. Conversely, when the dispersion of OSUs in acoustic space is lower than expected compared to the randomly drawn OSU pool, environmental filtering is likely to be an acting process (Scheiner et al., 2017).

In this paper, we opted for an incidence-based approach to attribute an importance value to OSUs. Yet, the use of threshold values to convert continuous variables to detection/non-detection data has been critiqued in the literature (Lawson et al., 2014), as it results in information loss and complicates comparisons between different sites/studies for which different optimal threshold values may apply. Still, we posit this approach can be appropriate for soundscape data. Although acoustic indices are known to capture animal activity, there is an ongoing debate about their ability to capture patterns of abundance (Boelman et al., 2007; Bradfer-Lawrence et al., 2020). Moreover, acoustic indices can be sensitive to confounding environmental factors (Gasc et al., 2015). For instance, CVR index values may respond to abiotic sounds, such as geophony and anthrophony, which are considered confounding factors if the aim is to capture biophonic sounds. Additionally, the index values

can also be susceptible to the relative amplitude of songs in recordings, which, in turn, are shaped by the properties of the surrounding vegetation, the distance of the sound-emitting animal to the sensor, inherent biological differences between species and meteorological conditions (Bradfer-Lawrence et al., 2020). We argue that converting raw CVR index values to binary detection/non-detection data will reduce potential differences among sites and eliminate the non-focal transient and low amplitude sounds from the data. Even so, the influence of incidence-based versus continuous importance values on the observed patterns warrants further investigation.

Nonetheless, choosing a threshold value that is valid in all ecological contexts and accurately removes non-target sounds while retaining enough information to capture patterns in niche usage represents a challenge. Deriving a unique threshold value for each study system by validating the ability of the soundscape diversity metrics to capture a species richness gradient is not a feasible approach, as taxonomic data will not always be available. We found that the approach in Burivalova et al. (2018), for which the chosen threshold yields the most normal distribution of the obtained soundscape metric, did not yield the strongest correlation with species richness. Although a constant threshold value worked well for our specific case study, this threshold value will likely be different for other ecosystems, seasons or levels of non-target sound. We recommend that future studies derive incidence data using context-aware binarisation algorithms (see S.3). These algorithms produce a unique binarisation threshold per site by considering the distribution of CVR values in the acoustic trait space, which, in turn, is influenced by the soniferous community and sound transmission characteristics of the habitat. We found that the 'IsoData' binarisation algorithm worked best for our data, but further research in a wider variety of habitats is needed to confirm that this algorithm is consistently most appropriate.

Finally, we only used the CVR index to capture the amplitude features of our soundscapes. We posit that other spectral indices, alone or in combination, may better reflect sounds from specific taxonomic groups. For instance, cicada choruses are characterised by loud and long-duration stridulations, usually restricted to narrow frequency bands and often leaving wide frequency band footprints due to harmonics. Previous work suggests these features can be captured by a set of spectral indices: low spectral entropy, high background noise and high spectral density (Brown et al., 2019; Ferroudj et al., 2014; Towsey et al., 2014). Thus, these three indices could be combined into a compound soundscape diversity index, which could then be used to decompose the diversity of cicada choruses in 24-hr acoustic trait space.

6 | CONCLUSION

In this study, we present a novel workflow for the quantification of soundscape diversity that builds on trait-based ecology and uses Hill numbers to generate a robust set of soundscape diversity metrics.

By broadening the temporal scope of soundscape diversity quantification to cover 24 hr, and considering the spectral and temporal traits of sound simultaneously, these soundscape diversity metrics can yield novel insights into acoustic trait space usage at multiple spatiotemporal scales and act as a useful tool for biodiversity monitoring.

AUTHORS' CONTRIBUTIONS

T.L. designed the workflow, coded the accompanying package, analysed the case study and supplementary material data, and wrote the manuscript; A.S.B., T.H. and C.A.P. made significant contributions to the study conception, design and manuscript revision; A.S.B. and C.A.P. managed the design and collection of acoustic data; G.S.M. and I.L.K. performed identification of anuran species in sound files; M.C.-C. performed the aural identification of bird species in sound files. All authors contributed to the drafts and gave final approval for publication.

ACKNOWLEDGEMENTS

For their assistance in data collection, we are very grateful to Evanir Damasceno, Tatiane Abreu and Carla Fonseca. We are thankful to the staff at Reserva Biológica do Uatumã for logistical support. Data collection was funded by the Rufford Foundation (grant 17715-1), Reserva Biológica do Uatumã (ICMBio), the University of East Anglia and a NERC/UK grant (NE/J01401X/1) awarded to C.A.P. A.S.B. was funded by a PhD studentship (grant 200463/2014-4) from Conselho Nacional de Desenvolvimento Científico e Tecnológico (CNPq)—Brazil, which also awarded a productivity grant to I.L.K. (309473/2019-5). T.L. is supported by a PhD studentship from the Norwegian University of Life Sciences. We thank two anonymous reviewers for their constructive comments which considerably improved the manuscript quality.

CONFLICT OF INTEREST

We declare no conflict of interest.

DATA AVAILABILITY STATEMENT

The raw sound files used in the case study and supplementary materials are stored at <https://arbiton.rfcx.org/project/balbina/dashboard>. The processed data and code used in the case study and supplementary materials are available at <https://doi.org/10.5061/dryad.1vhhmgqtq> (Luypaert et al., 2022).

ORCID

Thomas Luypaert  <https://orcid.org/0000-0001-7491-7418>
 Anderson S. Bueno  <https://orcid.org/0000-0001-7416-6626>
 Gabriel S. Masseli  <https://orcid.org/0000-0002-5762-758X>
 Igor L. Kaefer  <https://orcid.org/0000-0001-6515-0278>
 Marconi Campos-Cerqueira  <https://orcid.org/0000-0001-6561-5864>
 Carlos A. Peres  <https://orcid.org/0000-0002-1588-8765>
 Torbjørn Haugaasen  <https://orcid.org/0000-0003-0901-5324>

REFERENCES

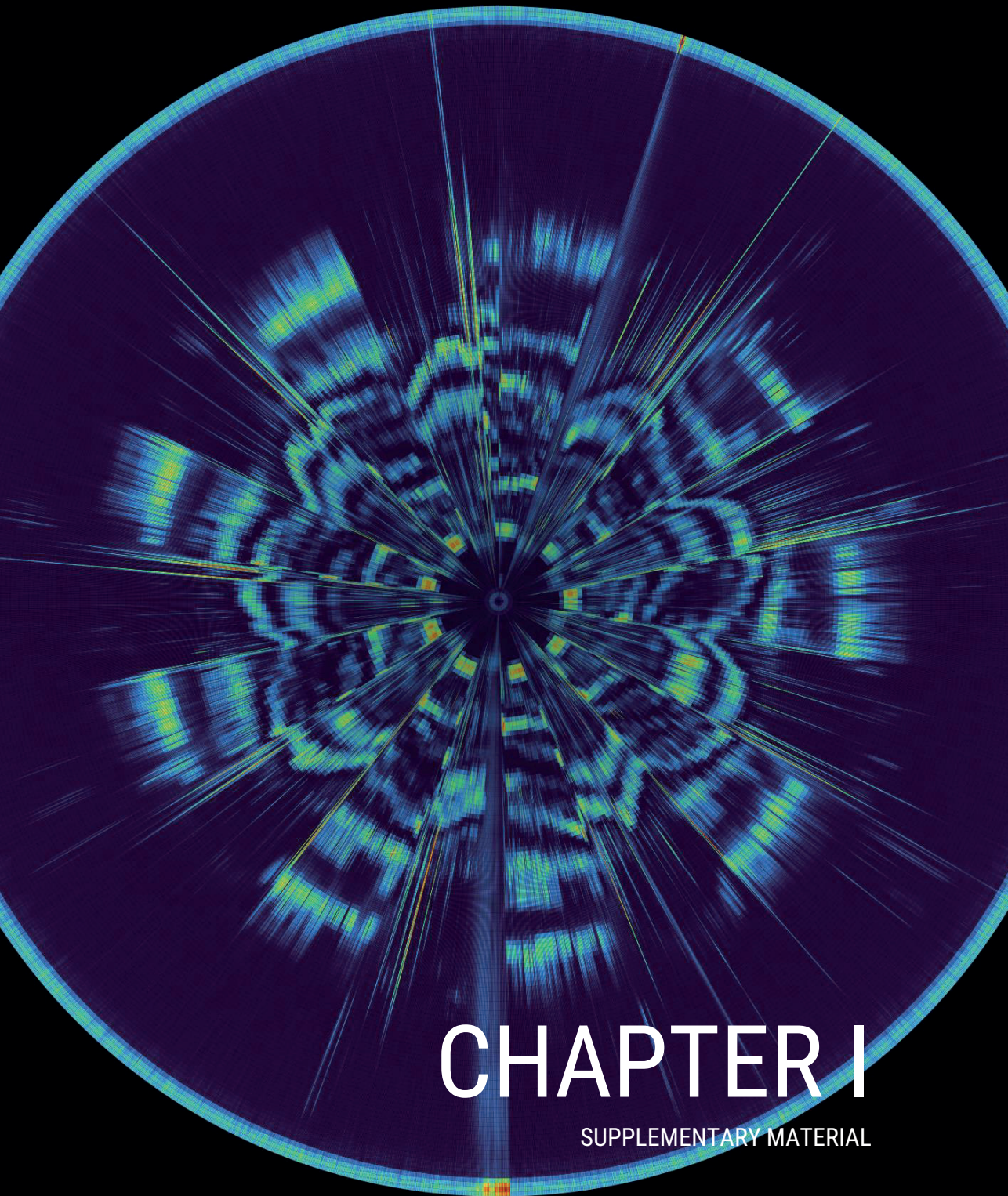
- Agostino, P. V., Lusk, N. A., Meck, W. H., Golombok, D. A., & Peryer, G. (2020). Daily and seasonal fluctuation in tawny owl vocalization timing. *PLoS ONE*, 15(4), e0231591. <https://doi.org/10.1371/journal.pone.0231591>
- Aide, T. M., Hernández-Serna, A., Campos-Cerqueira, M., Acevedo-Charry, O., & Deichmann, J. (2017). Species richness (of insects) drives the use of acoustic space in the tropics. *Remote Sensing*, 9(11), 1096–1108. <https://doi.org/10.3390/rs9111096>
- Benchimol, M., & Peres, C. A. (2015). Widespread Forest vertebrate extinctions induced by a mega hydroelectric dam in lowland Amazonia. *PLoS ONE*, 10(7), e0129818. <https://doi.org/10.1371/journal.pone.0129818>
- Boelman, N. T., Asner, G. P., Hart, P. J., & Martin, R. E. (2007). Multi-trophic invasion resistance in Hawaii: Bioacoustics, field surveys, and airborne remote sensing. *Ecological Applications*, 17(8), 2137–2144. <https://doi.org/10.1890/07-0004.1>
- Bradfer-Lawrence, T., Bunnefeld, N., Gardner, N., Willis, S. G., & Dent, D. H. (2020). Rapid assessment of avian species richness and abundance using acoustic indices. *Ecological Indicators*, 115, 106400. <https://doi.org/10.1016/j.ecolind.2020.106400>
- Bradfer-Lawrence, T., Gardner, N., Bunnefeld, L., Bunnefeld, N., Willis, S. G., & Dent, D. H. (2019). Guidelines for the use of acoustic indices in environmental research. *Methods in Ecology and Evolution*, 10(10), 1796–1807. <https://doi.org/10.1111/2041-210X.13254>
- Brown, A., Garg, S., & Montgomery, J. (2019). Automatic rain and cicada chorus filtering of bird acoustic data. *Applied Soft Computing*, 81, 10550. <https://doi.org/10.1016/j.asoc.2019.105501>
- Bueno, A. S., Masselli, G. S., Kaefer, I. L., & Peres, C. A. (2020). Sampling design may obscure species-area relationships in landscape-scale field studies. *Ecography*, 43(1), 107–118. <https://doi.org/10.1111/ecog.04568>
- Burivalova, Z., Purnomo, Wahyudi, B., Boucher, T. M., Ellis, P., Truskinger, A., Towsey, M., Roe, P., Marthinus, D., Griscom, B., & Game, E. T. (2019). Using soundscapes to investigate homogenization of tropical forest diversity in selectively logged forests. *Journal of Applied Ecology*, 56(11), 2493–2504. <https://doi.org/10.1111/1365-2664.13481>
- Burivalova, Z., Towsey, M., Boucher, T., Tssruskinger, A., Apelis, C., Roe, P., & Game, E. T. (2018). Using soundscapes to detect variable degrees of human influence on tropical forests in Papua New Guinea. *Conservation Biology*, 32(1), 205–215. <https://doi.org/10.1111/cobi.12968>
- Buxton, R. T., McKenna, M. F., Clapp, M., Meyer, E., Stabenau, E., Angeloni, L. M., Crooks, K., & Wittmeyer, G. (2018). Efficacy of extracting indices from large-scale acoustic recordings to monitor biodiversity. *Conservation Biology*, 32(5), 1174–1184. <https://doi.org/10.1111/cobi.13119>
- Chao, A., Chiu, C.-H., & Hsieh, T. C. (2012). Proposing a resolution to debates on diversity partitioning. *Ecology*, 93(9), 2037–2051. <https://doi.org/10.1890/11-1817.1>
- Chao, A., Chiu, C.-H., & Jost, L. (2014). Unifying species diversity, phylogenetic diversity, functional diversity, and related similarity and differentiation measures through Hill numbers. *Annual Review of Ecology, Evolution, and Systematics*, 45(1), 297–324. <https://doi.org/10.1146/annurev-ecolsys-120213-091540>
- Chao, A., & Jost, L. (2012). Coverage-based rarefaction and extrapolation: Standardizing samples by completeness rather than size. *Ecology*, 93(12), 2533–2547. <https://doi.org/10.1890/11-1952.1>
- Cui, J., Song, X., Fang, G., Xu, F., Brauth, S. E., & Tang, Y. (2011). Circadian rhythm of calling behavior in the Emei music frog (*Babina daunchina*) is associated with habitat temperature and relative humidity. *Asian Herpetological Research*, 2(3), 149–154. <https://doi.org/10.3724/SP.J.1245.2011.00149>
- da Silva, C. A., de Pontes, A. L. B., Cavalcante, J. D. S., & de Azevedo, C. V. M. (2014). Conspecific vocalisations modulate the circadian activity rhythm of marmosets. *Biological Rhythm Research*, 45(6), 941–954. <https://doi.org/10.1080/09291016.2014.939441>
- Darras, K., Pütz, P., Fahrurrozi, Rembold, K., & Tscharrtkte, T. (2016). Measuring sound detection spaces for acoustic animal sampling and monitoring. *Biological Conservation*, 201, 29–37. <https://doi.org/10.1016/j.biocon.2016.06.021>
- Darwin, C. (1872). *The expression of the emotions in man and animals*. John Murray.
- Depraetere, M., Pavoine, S., Jiguet, F., Gasc, A., Duvail, S., & Sueur, J. (2012). Monitoring animal diversity using acoustic indices: Implementation in a temperate woodland. *Ecological Indicators*, 13(1), 46–54. <https://doi.org/10.1016/j.ecolind.2011.05.006>
- Eldridge, A., Casey, M., Moscoso, P., & Peck, M. (2016). A new method for ecoacoustics? Toward the extraction and evaluation of ecologically-meaningful soundscape components using sparse coding methods. *PeerJ*, 4, e2108. <https://doi.org/10.7717/peerj.2108>
- Farina, A. (2013). *Soundscape ecology: Principles, patterns, methods and applications*. Springer Publishing.
- Farina, A., & James, P. (2016). The acoustic communities: Definition, description and ecological role. *Biosystems*, 147, 11–20. <https://doi.org/10.1016/j.biosystems.2016.05.011>
- Ferrouj, M., Truskinger, A., Towsey, M., Zhang, L., Zhang, J., & Roe, P. (2014). Detection of rain in acoustic recordings of the environment. In D.-N. Pham & S.-B. Park (Eds.), *Pacific rim international conference on artificial intelligence* (pp. 104–116). Springer Publishing.
- García-Rutledge, E. J., & Narins, P. M. (2001). Shared acoustic resources in an Old World frog community. *Herpetologica*, 57(1), 104–116. <https://www.jstor.org/stable/3893144>
- Gasc, A., Pavoine, S., Lellouch, L., Grandcolas, P., & Sueur, J. (2015). Acoustic indices for biodiversity assessments: Analyses of bias based on simulated bird assemblages and recommendations for field surveys. *Biological Conservation*, 191, 306–312. <https://doi.org/10.1016/j.biocon.2015.06.018>
- Gasc, A., Sueur, J., Jiguet, F., Devictor, V., Grandcolas, P., Burrow, C., Depraetere, M., & Pavoine, S. (2013). Assessing biodiversity with sound: Do acoustic diversity indices reflect phylogenetic and functional diversities of bird communities? *Ecological Indicators*, 25, 279–287. <https://doi.org/10.1016/j.ecolind.2012.10.009>
- Gibb, R., Browning, E., Glover-Kapfer, P., & Jones, K. E. (2019). Emerging opportunities and challenges for passive acoustics in ecological assessment and monitoring. *Methods in Ecology and Evolution*, 10(2), 169–185. <https://doi.org/10.1111/2041-210X.13101>
- Hill, M. O. (1973). Diversity and evenness: A unifying notation and its consequences. *Ecology*, 54(2), 427–432. <https://doi.org/10.2307/1934352>
- Hsieh, T. C., Ma, K. H., & Chao, A. (2016). iNEXT: An R package for rarefaction and extrapolation of species diversity (Hill numbers). *Methods in Ecology and Evolution*, 7(12), 1451–1456. <https://doi.org/10.1111/2041-210X.12613>
- Jost, L. (2006). Entropy and diversity. *Oikos*, 113(2), 363–375. <https://doi.org/10.1111/j.2006.0030-1299.14714.x>
- Jost, L. (2007). Partitioning diversity into independent alpha and beta components. *Ecology*, 88(10), 2427–2439. <https://doi.org/10.1890/06-1736.1>
- Jost, L. (2010). The relation between evenness and diversity. *Diversity*, 2(2), 207–232. <https://doi.org/10.3390/d2020207>
- Kahl, S., Wood, C. M., Eibl, M., & Klinck, H. (2021). BirdNET: A deep learning solution for avian diversity monitoring. *Ecological Informatics*, 61, 101236. <https://doi.org/10.1016/j.ecoinf.2021.101236>
- Krause, B. L. (1987). Bioacoustics, habitat ambience in ecological balance. *Whole Earth Review*, 57, 14–18.
- Krause, B. L. (1993). The niche hypothesis: A virtual symphony of animal sounds, the origins of musical expression and the health of habitats. *The Soundscape Newsletter*, 6, 6–10.

- Krause, B. L., & Farina, A. (2016). Using ecoacoustic methods to survey the impacts of climate change on biodiversity. *Biological Conservation*, 195, 245–254. <https://doi.org/10.1016/j.biocon.2016.01.013>
- Landini, G., Randell, D. A., Fouad, S., & Galton, A. (2017). Automatic thresholding from the gradients of region boundaries. *Journal of Microscopy*, 265(2), 185–195. <https://doi.org/10.1111/jmi.12474>
- Lawson, C. R., Hodgson, J. A., Wilson, R. J., & Richards, S. A. (2014). Prevalence, thresholds and the performance of presence-absence models. *Methods in Ecology and Evolution*, 5(1), 54–64. <https://doi.org/10.1111/2041-210X.12123>
- Luyppaert, T., Bueno, A. S., Masseli, G. S., Kaefer, I. L., Campos-Cerqueira, M., Peres, C. A., & Haugaasen, T. (2022). Data from: A framework for quantifying soundscape diversity using Hill numbers. *Methods in Ecology and Evolution*. <https://doi.org/10.5061/dryad.1vhmgqtq>
- Mason, N. W. H., Mouillot, D., Lee, W. G., & Wilson, J. B. (2005). Functional richness, functional evenness and functional divergence: The primary components of functional diversity. *Oikos*, 111(1), 112–118. <https://doi.org/10.1111/j.0030-1299.2005.13886.x>
- Metcalfe, O. C., Barlow, J., Devenish, C., Marsden, S., Berenguer, E., & Lees, A. C. (2020). Acoustic indices perform better when applied at ecologically meaningful time and frequency scales. *Methods in Ecology and Evolution*, 12(3), 421–431. <https://doi.org/10.1111/2041-210X.13521>
- Mouchet, M. A., Villéger, S., Mason, N. W. H., & Mouillot, D. (2010). Functional diversity measures: An overview of their redundancy and their ability to discriminate community assembly rules. *Functional Ecology*, 24(4), 867–876. <https://doi.org/10.1111/j.1365-2435.2010.01695.x>
- Mullet, T. C., Farina, A., & Gage, S. H. (2017). The acoustic habitat hypothesis: An Ecoacoustics perspective on species habitat selection. *Bioinformatics*, 10(3), 319–336. <https://doi.org/10.1007/s12304-017-9288-5>
- Pijanowski, B. C., Farina, A., Gage, S. H., Dumyahn, S. L., & Krause, B. L. (2011). What is soundscape ecology? An introduction and overview of an emerging new science. *Landscape Ecology*, 26(9), 1213–1232. <https://doi.org/10.1007/s10980-011-9600-8>
- Pijanowski, B. C., Villanueva-Rivera, L. J., Dumyahn, S. L., Farina, A., Krause, B. L., Napolitano, B. M., Gage, S. H., & Pieretti, N. (2011). Soundscape ecology: The science of sound in the landscape. *Bioscience*, 61(3), 203–216. <https://doi.org/10.1525/bio.2011.61.3.6>
- R Core Team. (2020). *R: A language and environment for statistical computing*. R Foundation for Statistical Computing. <https://www.r-project.org/>
- Ricotta, C. (2005). A note on functional diversity measures. *Basic and Applied Ecology*, 6(5), 479–486. <https://doi.org/10.1016/j.baae.2005.02.008>
- Ridler, T. W., & Calvard, S. (1978). Picture thresholding using an iterative selection method. *IEEE Transactions on Systems, Man, and Cybernetics*, 8(8), 630–632. <https://doi.org/10.1109/TSMC.1978.4310039>
- Scheiner, S. M., Kosman, E., Presley, S. J., & Willig, M. R. (2017). Decomposing functional diversity. *Methods in Ecology and Evolution*, 8(7), 809–820. <https://doi.org/10.1111/2041-210X.12696>
- Seyfarth, R. M., & Cheney, D. L. (2003). Meaning and emotion in animal vocalizations. *Annals of the New York Academy of Sciences*, 1000, 32–55. <https://doi.org/10.1196/annals.1280.004>
- Shaner, P.-J. L., Chen, Y.-K., & Hsu, Y.-C. (2021). Niche-trait relationships at individual and population level in three co-occurring passerine species. *Ecology and Evolution*, 11(12), 7378–7389. <https://doi.org/10.1002/ece3.7569>
- Sokal, R. R., & Sneath, P. H. A. (1963). *Principles of numerical taxonomy*. W. H. Freeman & Co.
- Sugai, L. S. M., Silva, T. S. F., Ribeiro, J. W., & Llusia, D. (2019). Terrestrial passive acoustic monitoring: Review and perspectives. *Bioscience*, 69(1), 15–25. <https://doi.org/10.1093/biosci/biy147>
- Toledo, L. P., Tipp, C., & Márquez, R. (2015). The value of audiovisual archives. *Science*, 347(6221), 484. <https://doi.org/10.1126/science.347.6221.484-b>
- Towsey, M. (2017). The calculation of acoustic indices derived from long-duration recordings of the natural environment. Available online at <https://eprints.qut.edu.au/110634/>
- Towsey, M., Wimmer, J., Williamson, I., & Roe, P. (2014). The use of acoustic indices to determine avian species richness in audio-recordings of the environment. *Ecological Informatics*, 21, 110–119. <https://doi.org/10.1016/j.ecoinf.2013.11.007>
- Towsey, N., Truskinger, A., Cottman-Fields, M., Roe, P. (2018). Ecoacoustics audio analysis software V18.03.041: Zenodo. <https://ap.qut.edu.ecoacoustics.info/tutorials/01-usingap/practical?tabs=windows>
- Truskinger, A., Towsey, M. (2019). Why do we analyse data in 1-min chunks?. <https://research.ecosounds.org/2019/08/09/analyzing-data-in-one-minute-chunks.html>
- Villéger, S., Mason, N. W. H., & Mouillot, D. (2008). New multidimensional functional diversity indices for a multifaceted framework in functional ecology. *Ecology*, 89(8), 2290–2301. <https://doi.org/10.1890/07-1206.1>
- Wang, G., Harpole, C. E., Trivedi, A. K., & Cassone, V. M. (2012). Circadian regulation of bird song, call, and locomotor behavior by pineal melatonin in the zebra finch. *Journal of Biological Rhythms*, 27(2), 145–155. <https://doi.org/10.1177/0748730411435965>
- Wilsey, B. J., Chalcraft, D. R., Bowles, C. M., & Willig, M. R. (2005). Relationships among indices suggest that richness is an incomplete surrogate for grassland biodiversity. *Ecology*, 86(5), 1178–1184. <https://doi.org/10.1890/04-0394>
- Zsebök, S., Schmera, D., Laczi, M., Nagy, G., Vaskuti, E., Török, J., & Garamszegi, L. S. (2021). A practical approach to measuring the acoustic diversity by community ecology methods. *Methods in Ecology and Evolution*, 12(5), 874–884. <https://doi.org/10.1111/2041-210X.13558>

SUPPORTING INFORMATION

Additional supporting information can be found online in the Supporting Information section at the end of this article.

How to cite this article: Luyppaert, T., Bueno, A. S., Masseli, G. S., Kaefer, I. L., Campos-Cerqueira, M., Peres, C. A., & Haugaasen, T. (2022). A framework for quantifying soundscape diversity using Hill numbers. *Methods in Ecology and Evolution*, 13, 2262–2274. <https://doi.org/10.1111/2041-210X.13924>



CHAPTER I

SUPPLEMENTARY MATERIAL

Supplementary Information

A framework for quantifying soundscape diversity using Hill numbers

Thomas Luypaert, Anderson S. Bueno, Gabriel S. Masseli, Igor L. Kaefer, Marconi Campos-Cerqueira, Carlos A. Peres and Torbjørn Haugaasen

S.1: Assessing the effect of sampling duration and sampling regime on soundscape diversity metrics and their observed relationship with richness of soniferous species

In this section, we assessed the effect of sampling duration (i.e., the number of full sampling days (24 hours) in the acoustic survey) and sampling regime (i.e., the temporal schedule that is used to record the soundscape throughout the acoustic survey) on the soundscape diversity metrics described in the main text. Additionally, we were interested in how these two factors influenced the observed relationship between the soundscape richness and the richness of soniferous species. Our aim here was to offer recommendations regarding sampling design using the soundscape diversity workflow described in this work and provide a framework for rarefaction/extrapolation in case of unequal sampling size between sites.

To address these questions, we used the same set of plots as described in the empirical case study (main text – section 3), for which 4-9 full days of soundscape recordings were acquired using a 1 min/5 min sampling regime at a 44.1 kHz sampling rate in Brazilian Amazonia. For a detailed overview of the data collection and processing, consult supplementary material S6. To assess the effect of the sampling regime, we subsetted the obtained OSU-by-sample matrix for each plot using the following recording schedules: 1 min/10 min; 1 min/15 min; 1 min/20 min; 1 min/30 min; 1 min/60 min. For sampling sites containing multiple plots, the obtained OSU-by-sample incidence matrices were grouped across plots.

1.1. A protocol for sampling effort equalization using iNEXT

To simulate the soundscape diversity metrics for a range of sampling durations, we used the obtained OSU-by-sample incidence matrices to compute sample-size-based rarefaction/extrapolation curves for each site at multiple orders of diversity using the R-package iNEXT (Hsieh et al. 2016). This package provides a range of functions for the computation of Hill numbers from raw incidence data and rarefaction and extrapolation with 95% confidence intervals. If the goal of the study is to simply rank the soundscape diversity of multiple communities,

the sample extrapolation size can be extended several times the observed sample size (Chao & Jost, 2012). Yet, if the goal is to estimate exact relationships between communities, Chao and Jost (2012) recommend extrapolation to double the observed reference sample size at most. In the empirical case study described in the main text, we wanted to quantify the exact relationships in the soundscape diversity metrics for a set of sites along a gradient in the richness of soniferous species (anurans, birds and primates). As the minimal sample size is four full days, we interpolated/extrapolated the soundscape diversity metrics to eight days of sampling (twice the minimal observed reference sample size) for each site and sampling regime. This way, we accounted for unequal sampling effort among sites while retaining the maximum amount of information in the datasets.

1.2. Providing recommendations regarding the sampling duration

1.2.1. The impact of sampling duration and regime on the relative soundscape richness ranking between sites

Using our workflow, we were interested in providing accurate quantification and comparison of soundscape diversity values for sites in a landscape. As such, we hoped to provide recommendations regarding what constitutes an ideal in-field sampling effort to reliably quantify relationships between sites. Yet, the sampling duration can only be reliably extrapolated to double the minimal sampling effort to quantify the exact relationships among sites. Given the constraints of our dataset, as the minimal sampling duration is 4 days, we could not reliably assess how longer sampling durations (e.g., >20 days) influence these exact relationships. Instead, we focussed on the relative soundscape richness ranking among sites, which can be extrapolated to multiple times the minimal sampling effort in a reliable manner (Chao & Jost, 2012).

To do so, we investigated the change in the soundscape richness ranking among sites along a sampling effort gradient for a set of sampling regimes. Specifically, we computed the soundscape richness of each site and sampling regime for a set of sampling effort values ranging from 1-28 days. Next, we calculated the richness ranking among sites at each sample effort value (i.e. the number of 24-hour sampling days). To quantify at which sampling effort the richness ranking stabilises among sites, thus providing the most accurate picture of the relationship among sites in the landscape, we computed the Mean Rank Shift (MRS) value using the 'codyn' R-package (v2.0.5; Hallet et al., 2016). This metric quantifies the average change in a ranked list between two consecutive periods. Finally, to elucidate at which sampling duration the Mean Rank Shift approaches a zero asymptote, we fitted negative exponential models ($y \sim a * \exp(-b * x)$), using the 'SSasymp' function for self-

starting models from the 'stats' R-package (R Core Team, 2020) to obtain starting values, and the 'nls' package (v1.0-2; Baty et al., 2015) to fit the models (Fig. S1; Table S1).

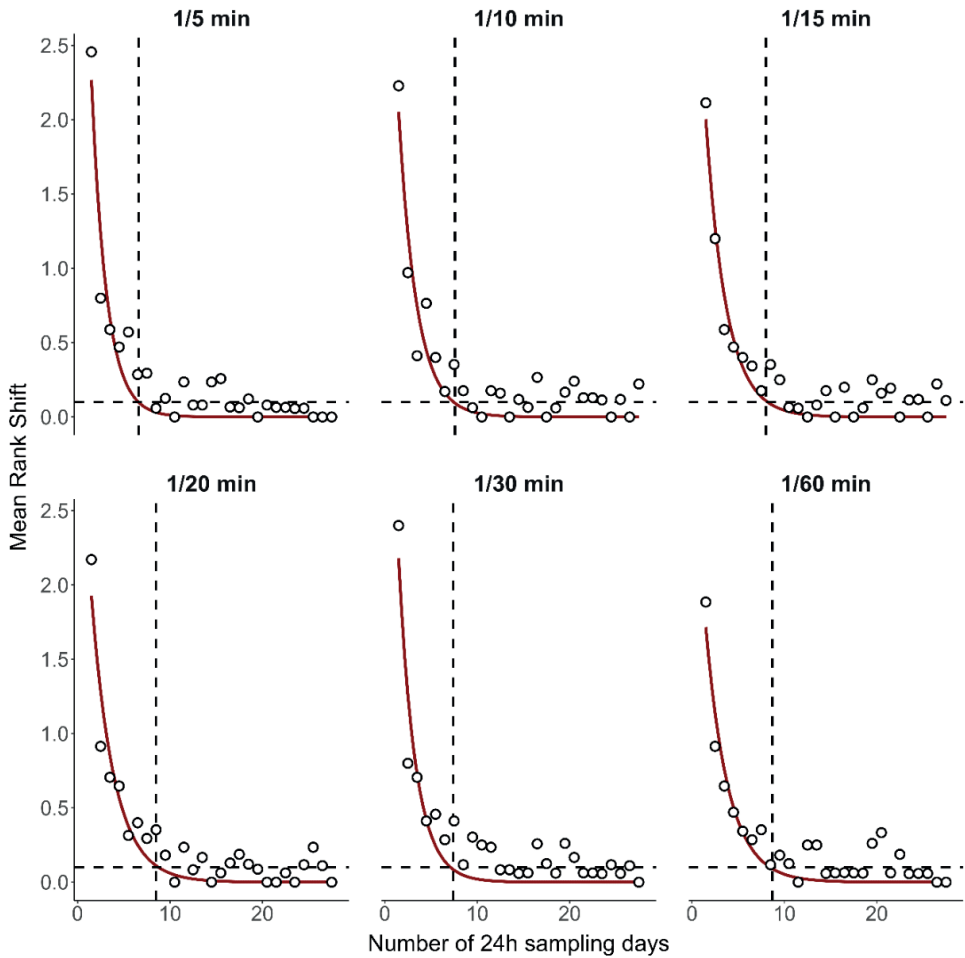


Figure S1: A set of scatterplots displaying the relationship between the sampling effort (number of 24-hour sampling days) and the Mean Rank Shift in the soundscape richness values for 35 sites and six sampling regimes in an Amazonian rain forest landscape. The maroon line represents a negative exponential model approaching an asymptote zero ($y \sim a * \exp(-b * x)$). The horizontal dashed lines represent the point at which the function start approaching the zero asymptote (Mean Rank Shift = 0.1).

Table S1: Summary of the negative exponential models ($y \sim a * \exp(-b * x)$) fitted for different sampling regimes, in which y represents the Mean Rank Shift and x represents the number of full sampling days ($p < 0.001$ for all fitted models).

Sampling regime	parameters	value	SE
1 min / 5 min	a	5.6950	0.9582
	b	0.6136	0.0816

1 min / 10 min	a	4.3993	0.7114
	b	0.5078	0.0711
1 min / 15 min	a	3.9223	0.4809
	b	0.4481	0.0502
1 min / 20 min	a	3.5522	0.4487
	b	0.4078	0.0489
1 min / 30 min	a	4.9609	0.8691
	b	0.5484	0.0803
1 min / 60 min	a	3.1705	0.4295
	b	0.4089	0.0525

We found that the negative exponential models with a zero-asymptote fit the data well (Fig. S1). Moreover, the parameter values were all significantly different from zero and have low standard errors. Based on these models, the Mean Rank Shift among sites seemed to approach an asymptote for MRS ~ 0.1 at approximately 7-9 sampling days for all sampling regimes. As such, knowing that the sampling effort can be reliably extrapolated to double the minimum reference sample size, we recommend future studies looking for the exact relationship in the soundscape diversity between sites attempt to record the soundscape for a minimum of 5 days per site.

Given that the sampling regime employed in this study (1 min / 5 min) did not correspond with regimes used in other studies assessing the required sampling effort (e.g. continuous sampling), we could not directly compare the number of required sampling days to capture the soundscape reliably. Instead, we used the total number of sampling hours per site as an indicator of the required effort. We deem this a good proxy for sampling effort for two reasons: (i) the total number of hours that can be recorded per site is directly influenced by the storage space available on the acoustic sensor's memory card, a factor which is often limiting the sampling effort in field studies; and (ii) the total number of hours can be directly compared for studies with differing sampling regimes. Considering the recommended minimum sampling effort of 5 days and knowing that our most intense sampling regime was 1 min / 5 min, this corresponds to 24 hours of recording per site. This recording duration associated with the optimal sampling duration is considerably lower than other minimal sampling durations previously reported in the literature (e.g. 120 hours in Bradfer-Lawrence et al., 2019).

1.2.2. *The impact of sampling regime on the observed soundscape richness – species richness relationship*

In addition to the soundscape richness rank change in function of sampling effort and regime, we investigated how the sampling regime influences the soundscape richness – species richness relationship among sites for a fixed sampling effort (number of 24-hour recording days). As we were now interested in the exact relationship between sites, and since we wanted to account for unequal sampling effort between sites, we interpolated/extrapolated the sampling effort to 8 days (twice the minimal sampling effort) using iNEXT (Hsieh et al., 2016). Although this sampling duration was at the lower end of the recommended sampling duration (see S.1.2.1), an inspection of Fig. S1 revealed that at 8 sampling days, for each additional sampling day the Mean Rank Shift changed by less than 0.1 on average. Moreover, the Mean Rank Shift decreased towards the zero asymptote as more sampling days were added. As such, the change in the overall relationship between the soundscape richness and richness of soniferous species at longer sampling durations was likely minimal.

For each of the sites, after rarefaction/extrapolation, we computed the soundscape richness and assessed the relationship with the richness of soniferous species. As the sampling regime influences the number of OSUs which can be detected in acoustic trait space, we divided the soundscape richness values by the total number of detectable OSUs in this space to get the percentage of space occupied. Finally, we computed the Pearson correlation coefficient and R^2 -value for a simple linear regression model between the soundscape richness and the richness of soniferous species (Fig. S2).

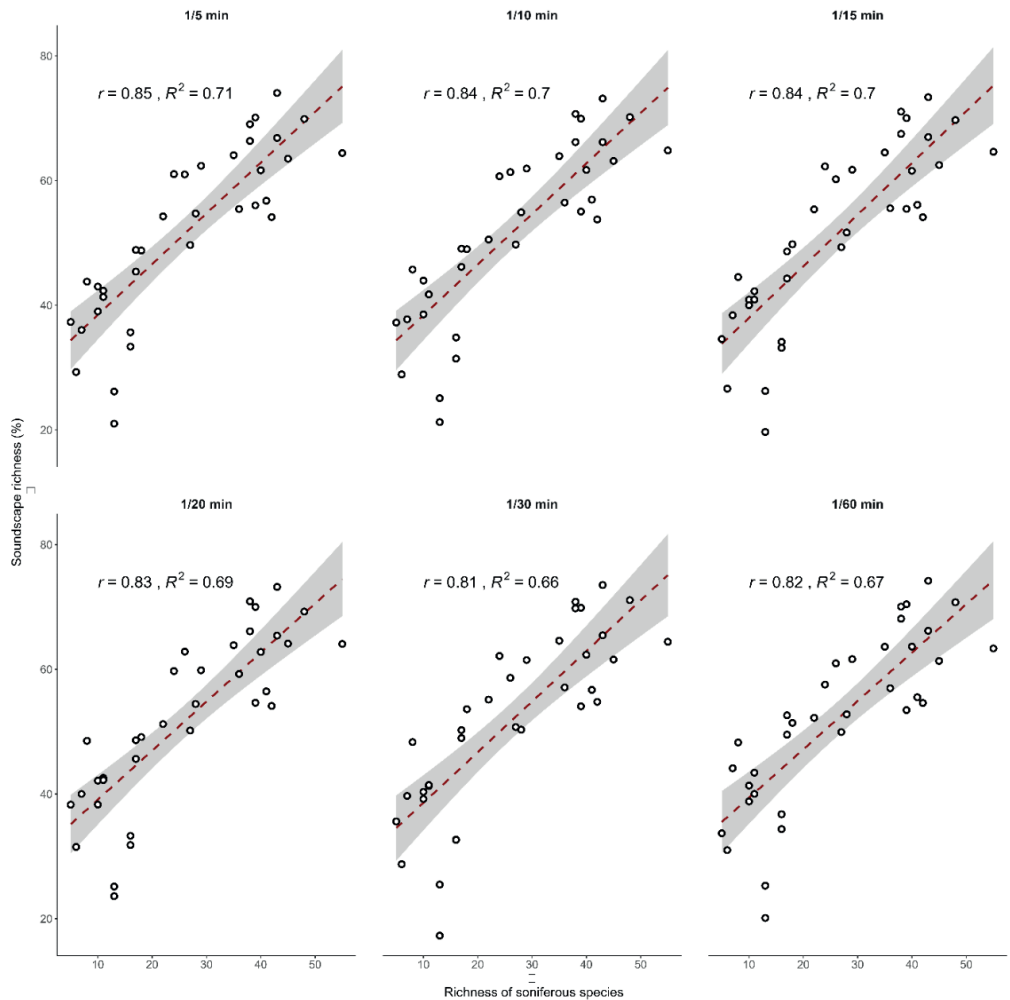


Figure S2: Relationships between the soundscape richness (as the percentage of acoustic trait space occupied by OSUs) and the richness of soniferous species for a wide range of sampling regimes. Pearson correlation coefficients and associated p -values, which are given for each sampling regime ($p < 0.001$ in all instances), show that the predictive power of soundscape richness is largely invariant in relation to these sampling regimes.

The scatterplots and associated Pearson correlation coefficients (Fig. S2) revealed that, at equal sampling effort, the relationship between the soundscape richness and the richness of soniferous species remained high ($r \geq 0.81$) even for the sparse sampling regimes. This was contrary to previous findings reported in the literature (e.g. Bradfer-Lawrence et al., 2019), which found that intense sampling regimes (e.g. continuous sampling) were required to capture soundscapes reliably – suggesting the workflow described here is robust and can pick up on ecological patterns, even at sampling regimes of lower intensity.

S.2: Assessing the effect of window length on soundscape diversity metrics

As with time-frequency bins in spectrograms, the resolution of OSUs in the frequency domain of acoustic trait space is dictated by the sampling rate and window length with which the Fast Fourier Transformation is performed. The data of the empirical case study was acquired using a 44,100 Hz sampling rate and then truncated at 11,025 Hz. As such, it is the choice of window length that dictates the resolution in the frequency domain. The choice of window length determines the sensitivity of the CVR index values to different types of sound and depends on the soniferous community in the study area of interest. A window length of 256 (e.g. Campos-Cerqueira et al., 2020), 512 (Gasc et al., 2013; Rodriguez et al., 2013; Eldridge et al., 2018; Burivalova et al., 2018; Phillips et al., 2018) and 1024 samples (e.g. Machado et al., 2017) have all been used to capture the audible soundscape in a range of environments.

Here, we investigated the effect of window length choice on the proposed soundscape diversity metrics and their relationship with the richness of soniferous species in the landscape. To do so, we computed the CVR index for each one sound minute file using a sampling rate of 44,100 Hz and a window length of 128, 256, 512 and 1024 samples. For each of these window lengths, we applied the same analytical workflow as described in the main body of this manuscript. We calculated the soundscape richness and assessed its relationship with the richness of soniferous species using the Pearson correlation test and R^2 -value for a simple linear regression model.

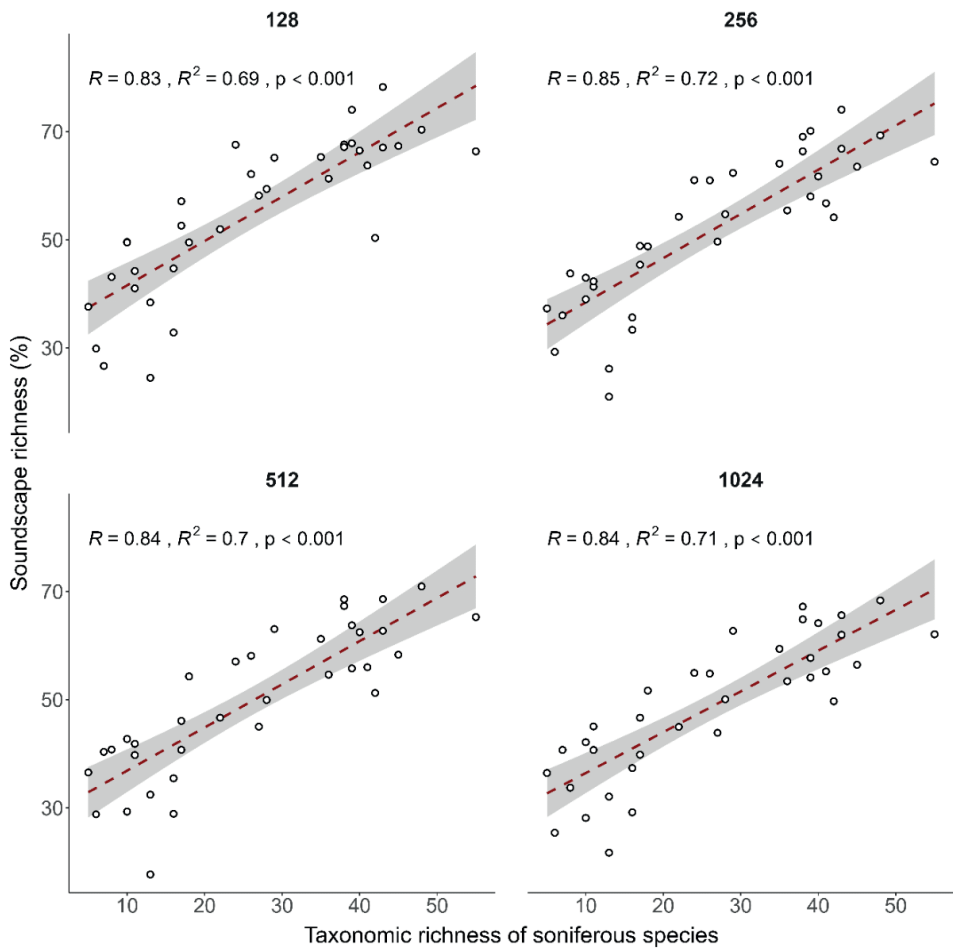


Figure S3: A set of scatterplots showing the relationship between the soundscape richness (as the percentage of the total number of detectable OSUs) and the richness of soniferous species for a set of window lengths ($wl = 128; 256; 512; 1024$). For each window length, the Pearson correlation coefficient (r) and R^2 -value are provided ($p < 0.001$ in all instances).

We found that the choice of window length had a negligible impact on the observed relationship between the soundscape richness and the richness of soniferous species (Fig. S3) – suggesting the proposed soundscape richness metric is sensitive to ecological patterns regardless of these methodological variations. For future studies, we advise the use of a 256-sample window length, as this has been previously used in the literature and provides the highest correlation with the richness of sound-producing organisms.

S.3: Assessing the effect of threshold choice on the soundscape richness – species richness relationship

The 3 dB amplitude threshold used to calculate the CVR index and the binarisation threshold used here are both aimed at removing the influence of low-amplitude and transient or short-duration noise on the soundscape diversity metrics described in this study, thus increasing the sensitivity to the soniferous species richness.

Choosing the binarisation threshold which is used to obtain detection / non-detection values for each OSU in the 24-hour acoustic trait space constitutes an important step in our workflow. The choice of this threshold value depends on the sound transmission characteristics of the habitat under investigation, and the amount and type of background noise in the environment.

Several thresholding approaches exist to achieve this objective. For instance, in Burivalova et al. (2018), a range of amplitude threshold values were trialled, looking for the value which yielded a near-normal distribution of the variable of interest across all sites in the study. In Aide et al. (2017), a fixed threshold value was used across all sites to determine the presence of sound. Here, we investigated various approaches and how they influenced the observed relationship between the soundscape richness and the richness of soniferous species. The preferred thresholding method is the one that increases the sensitivity of the proposed metrics to the richness of soniferous species.

3.1. Applying a constant threshold value across all sites

For our first approach, we applied a constant threshold value for all sites in the study. We applied the same analytical workflow as described in the main text and S.6, however, to assess which constant threshold value yields the best relationship between the soundscape richness and the richness of soniferous species, we trialled a range of constant threshold values between 0.01 and 0.5 at 0.01 intervals. For each of these threshold values, we calculated the soundscape richness. Finally, per Burivalova et al. (2018), we assessed which of the threshold values yielded the best near-normal distribution of soundscape richness values, and which of the threshold values yielded the best correlation with the richness of soniferous species.

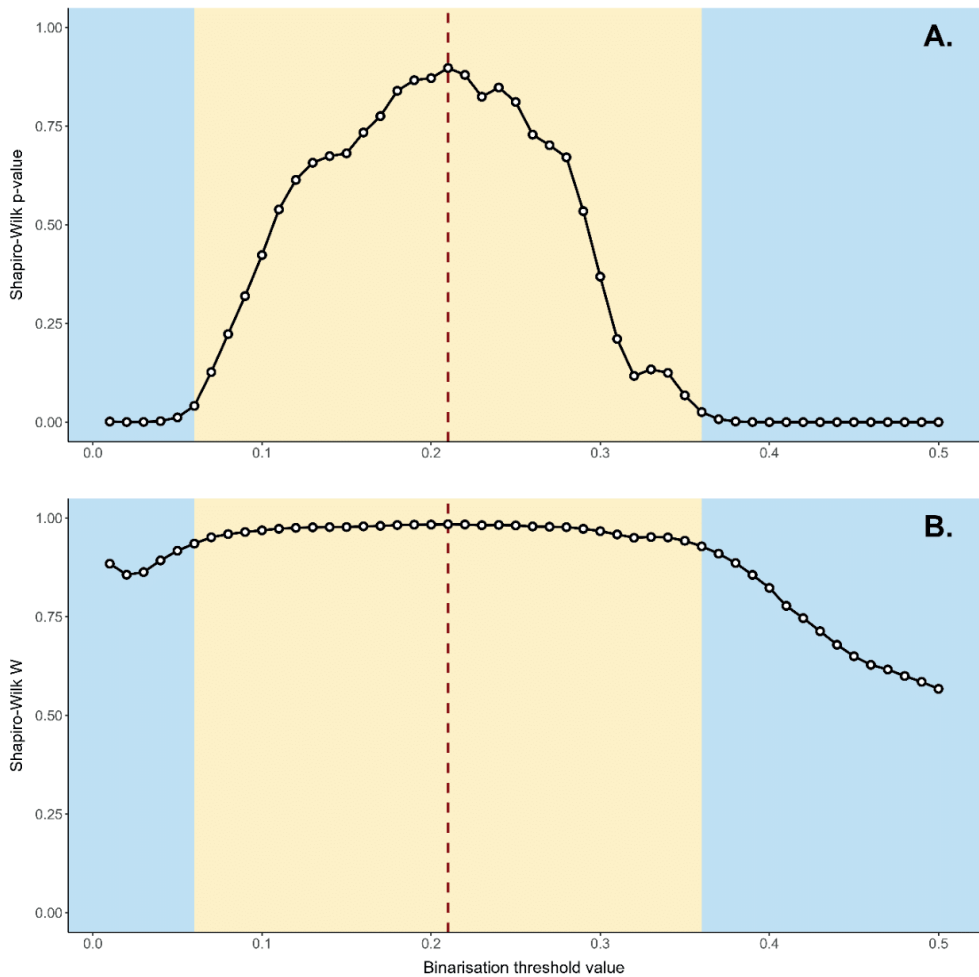


Figure S4: **A.** The relationship between the binarisation threshold value and the p-values acquired from the Shapiro-Wilk normality test performed on the soundscape richness data obtained at each threshold value; **B.** The relationship between the binarisation threshold value and the W-values acquired from the Shapiro-Wilk normality test performed on the soundscape richness data obtained at each threshold value. The dashed red line represents the threshold value for which the resulting soundscape richness values are most normally distributed (highest p- and W-values). The shaded blue area represents the threshold values for which the resulting soundscape richness values are not normally distributed (p -value < 0.05), whereas the shaded yellow area represents threshold values resulting in normally distributed soundscape richness values.

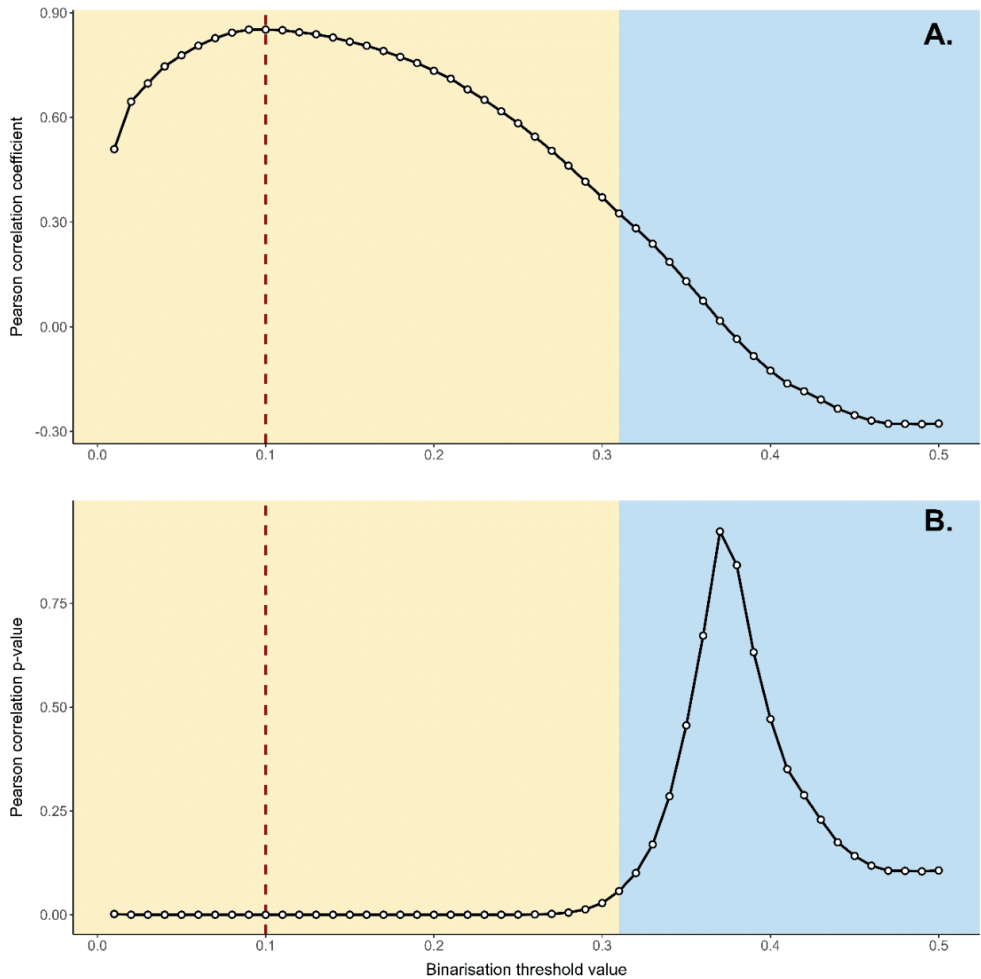


Figure S5: **A.** The relationship between the binarisation threshold value and Pearson's correlation coefficient (r) obtained from the Pearson correlation test between the resulting soundscape richness and the richness of soniferous species.; **B.** The relationship between the binarisation threshold value and the p -value obtained from the Pearson correlation test between the resulting soundscape richness and the richness of soniferous species. The dashed red line represents the threshold value (threshold = 0.10) for which the correlation between the soundscape richness and richness of soniferous species is highest ($r = 0.85$). The shaded blue area represents the values for which the correlation is not significant, whereas the shaded yellow area represents the values for which correlations are significant.

The most normal distribution of soundscape richness values was obtained at a constant binarisation threshold of 0.21 (Figs. S4A and S4B; $r = 0.71$; $R^2 = 0.51$; $p < 0.001$), yet this value does not correspond to the binarisation threshold which yields the highest correlation with the richness of soniferous species (threshold = 0.1; $r = 0.85$; $R^2 = 0.72$; $p < 0.001$; Figs. S5A and S5B). In the next section, we investigated the use of site-dependent thresholding using binarisation algorithms.

3.2. Applying a site-dependent threshold using binarisation algorithms

For our second approach, instead of applying a constant binarisation threshold, we applied a site-dependent threshold to each of the plots described in the main text. To determine the threshold value for each plot, we made use of the binarisation algorithms available in the *autothresholdr* R-package (v1.3.11; Landini et al., 2017 – for algorithm descriptions, consult: <https://imagej.net/plugins/auto-threshold>). Every binarisation algorithm provides a unique binarisation threshold per plot, and unlike the previous method, threshold values can be variable between plots. We omitted the following binarisation algorithms from the analysis, as they were not suitable for our type of data: “Intermodes”, “MaxEntropy”, “Minimum”, “Yen”. Finally, we assessed which of the binarisation algorithms produced the best relationship between the soundscape richness and the richness of soniferous species using the Pearson correlation coefficient and R²-value for a simple linear regression model.

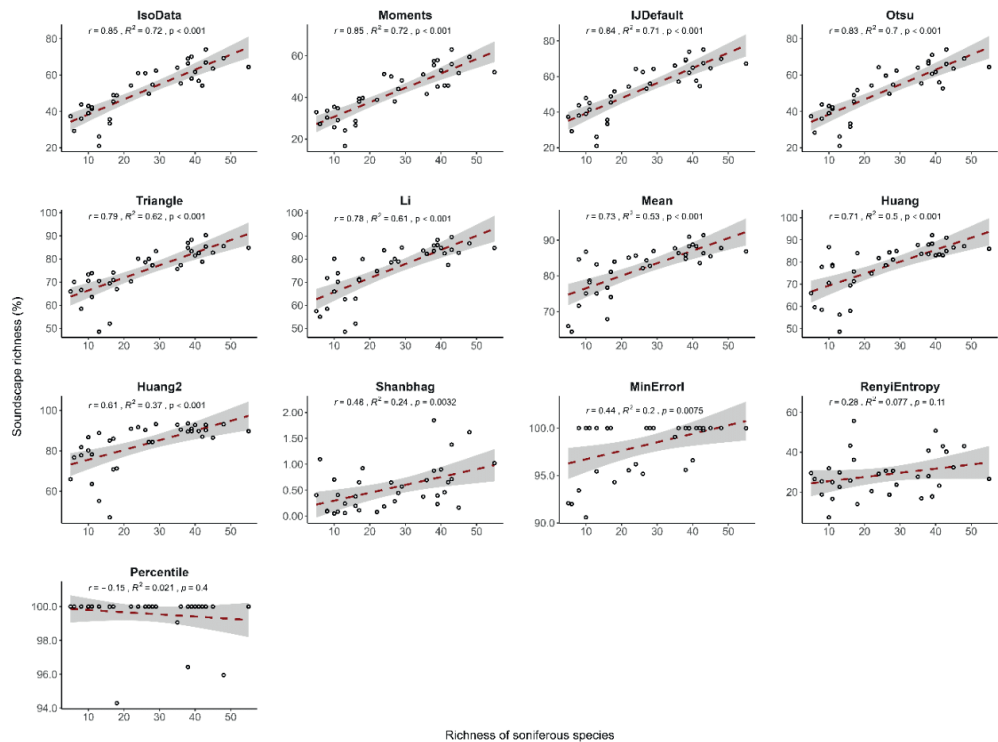


Figure S6: A set of scatterplots displaying the relationship between the soundscape richness (as the percentage of the total number of detectable OSUs) and the richness of soniferous species for the various binarisation algorithms available in the ‘autothresholdr’ R-package (Landini et al. 2017). The Pearson correlation coefficient (r) and R²-values are given for each binarisation algorithm.

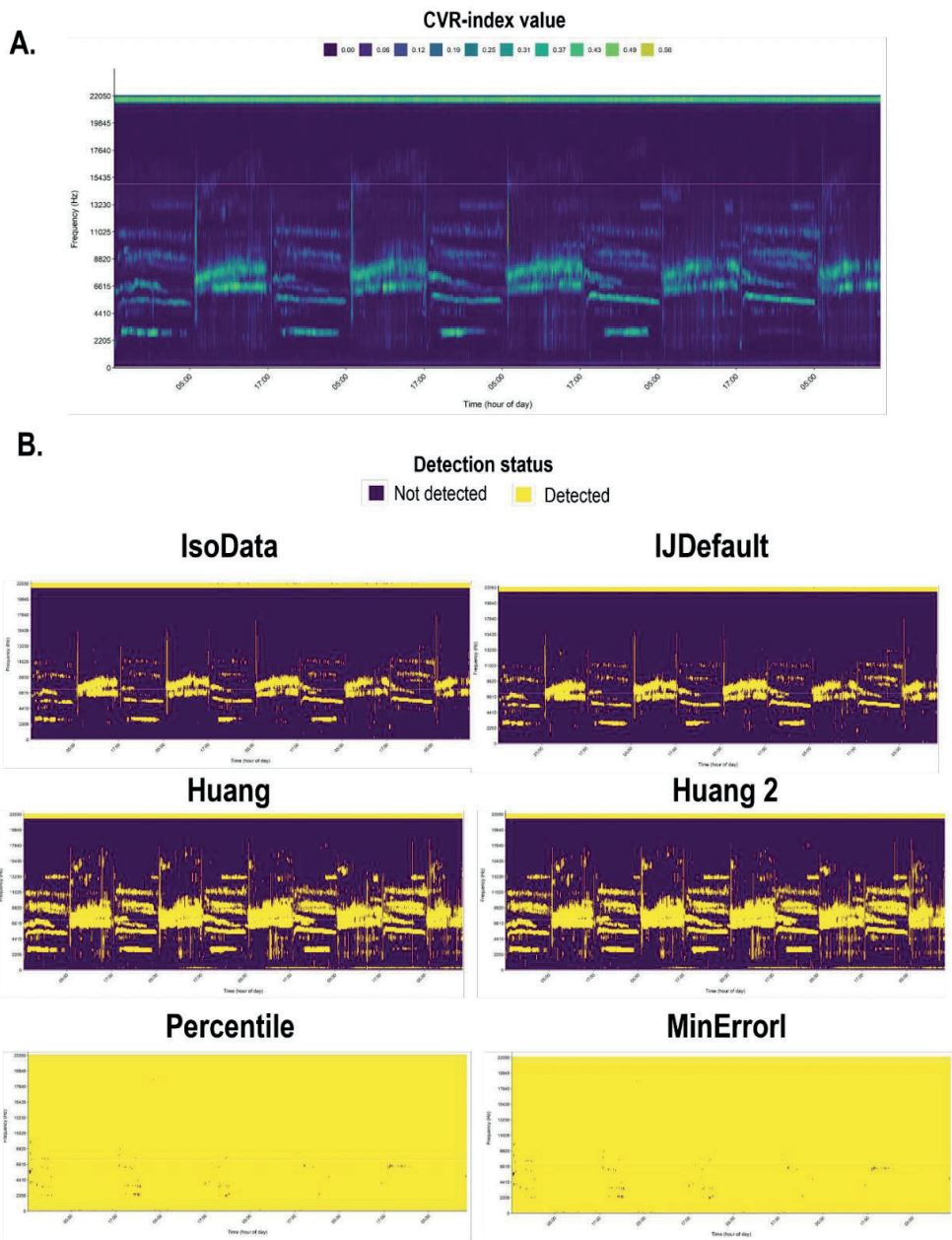


Figure S7: A visual representation of the pre- (A.) and post-binarisation (B.) soundscapes using a subset of binarisation methods available in the 'autothreshold' R-package (Landini et al. 2017) for one of the sites in the study period. Post-binarisation plots are ranked from high ("IJDefault" and "IsoData"), to medium ("Huang" and "Huang 2") and low ("Percentile" and "MinError1") correlation with species richness. Visual inspection of pre- and post-binarisation plots provides insight into how the acoustic structure is captured and which threshold stringency results in good correlation with species richness.

We found high Pearson correlation coefficients ($r > 0.80$) for the relationship between the soundscape diversity and the richness of soniferous species using the 'IsoData', 'Moments', 'IJDefault' and 'Otsu' binarisation

algorithms (Fig. S6), the value of which was similar to the correlation coefficients found for constant binarisation thresholds (Fig. S5). A visual inspection of the pre- and post-binarisation plots (Fig. S7) revealed that the more stringent thresholding methods (e.g. *"IsoData"* and *"JJDefault"*), where more sound is removed, resulted in higher correlations with species richness.

The binarisation algorithms produce a unique binarisation threshold per plot that is determined by the distribution of CVR-values in the acoustic trait space, which in turn is influenced by the soniferous community, amount and type of background noise, and sound transmission characteristics of the habitat. As such, these binarisation algorithms generate data-driven threshold values. Conversely, although we found that a thresholding value of around 0.1 worked well for the plots in our study, other habitats with differing sound transmission characteristics, noise levels, or acoustic communities might have a different optimal threshold value. As such, since the threshold value for binarisation algorithms is determined directly by the acoustic fingerprint of the plot, we recommend using one of the binarisation algorithms highlighted above. Further research in a wider variety of habitats is needed to confirm that the 'IsoData' algorithm performs the best consistently.

S.4. A framework for decomposing soundscape diversity into its alpha, beta, and gamma components

In addition to quantifying the soundscape richness (0D), diversity (qD with $q = 1, 2, \dots$), and evenness (${}^2D / {}^0D$) components, the workflow proposed in this manuscript can be used to decompose the regional metacommunity diversity (γ -diversity) into its local diversities (α -diversity) and a community turnover component (β -diversity). Moreover, it can be used to generate several measures of similarity or dissimilarity and overlap. Here, we outlined the theoretical framework for decomposing the soundscape diversity into its alpha, beta, and gamma components. In S.5.5, we provided a working example of this theoretical framework in practice.

The framework of Hill numbers follows a multiplicative relationship to decompose the soundscape diversity into its various components (Eqn. 1):

$$(1) \quad {}^qD_\gamma = {}^qD_\alpha \times {}^qD_\beta$$

$$(2) \quad {}^qD_\alpha = \frac{1}{N} \left\{ \sum_{i=1}^S \sum_{j=1}^N (w_j p_{ij})^q \right\}^{\frac{1}{(1-q)}}$$

$$(3) \quad {}^qD_\gamma = \left\{ \sum_{i=1}^S \left(\sum_{j=1}^N (w_j p_{ij}) \right)^q \right\}^{\frac{1}{(1-q)}}$$

$$(4) \quad {}^qD_\beta = \frac{{}^qD_\gamma}{{}^qD_\alpha}$$

Here, N refers to the total number of sub-systems (soundscapes), j refers to each individual sub-system, and w_j represents the relative weight given to each sub-system in the system. If all soundscapes are weighted equally, w_j equals $1/N$. The alpha diversity is the Hill number of the averaged basic sums of the soundscapes (Eqn. 2). The gamma diversity is computed by taking the average of the relative abundance of each OSU across the soundscapes in the system and calculating the Hill number of the pooled system (Eqn. 3). The beta diversity captures the degree of heterogeneity in the OSU composition across sites (Eqn. 4). It ranges from 1 to N and quantifies the relationship between the regional and local diversity, that is, how many times more diverse is the whole system in the effective number of OSUs compared to the sub-systems on average (Alberdi & Gilbert,

2019). The beta diversity can also be seen as the effective number of completely distinct soundscapes in the system (Tuomisto, 2010).

The framework of Hill numbers also allows us to define several measures of similarity between soundscapes in the wider system. Because beta diversity ranges between 1- N , it is not independent of the number of soundscapes in the system, and can thus not be used as a measure of similarity directly (Alberdi & Gilbert, 2019). Instead, to compare the relative compositional difference between soundscapes across multiple systems with a different number of soundscapes, some simple transformations can be performed on the beta diversity to remove the dependence on the number of soundscapes (Jost, 2007; Chao et al., 2012; Chiu et al., 2014; Alberdi & Gilbert, 2019).

$$(5) \quad C_{qN} = \frac{\left[\left(\frac{1}{qD_{\beta}} \right)^{(q-1)} - \left(\frac{1}{N} \right)^{(q-1)} \right]}{\left[1 - \left(\frac{1}{N} \right)^{(q-1)} \right]}$$

$$(6) \quad U_{qN} = \frac{\left[\left(\frac{1}{qD_{\beta}} \right)^{(1-q)} - \left(\frac{1}{N} \right)^{(1-q)} \right]}{\left[1 - \left(\frac{1}{N} \right)^{(1-q)} \right]}$$

Equations (5) and (6) are measures of overlap between soundscapes. The local or Sørensen-type overlap (C_{qN}) quantifies the effective average proportion of a soundscape's OSUs which are shared across all soundscapes (Chiu et al., 2014). It captures the overlap between soundscapes from the sub-system's perspective (Alberdi & Gilbert, 2019). For N soundscapes each having S equally common OSUs and sharing A OSUs between them, this function reduces to $C_{qN}=A/S$. The regional or Jaccard-type overlap (U_{qN}) quantifies the effective proportion of shared OSUs in a pooled assemblage of soundscapes, and thus captures the overlap between soundscapes from a regional perspective. Assume N soundscapes in a region with S unique and equally abundant OSUs. Here, R OSUs are shared between all soundscapes and the remaining OSUs ($S-R$) are distributed evenly among N soundscapes. In this scenario, Eqn. 8 reduces to $U_{qN} = R/S$.

$$(7) \quad V_{qN} = \frac{(N - qD_{\beta})}{(N - 1)}$$

$$(8) S_{qN} = \frac{\left(\frac{1}{qD_{\beta}} - \frac{1}{N}\right)}{\left(1 - \frac{1}{N}\right)}$$

Equations (7) and (8) are measures of turnover in OSUs between soundscapes (Harrison et al., 1992; Jost, 2007). The local or Sørensen-type turnover complement (V_{qN}) quantifies the normalised OSU turnover rate with respect to the average soundscape (Alberdi & Gilbert, 2019). It measures the proportion of a typical soundscape which changes as one goes from one soundscape to the next (Harrison et al., 1992; Chao et al., 2012; Jost, 2007). The regional or Jaccard-type turnover complement (S_{qN}) quantifies the proportion of the regional soundscape diversity contained in the average assemblage and is a measure of regional homogeneity. All of the aforementioned similarity indices can be transformed into metrics of dissimilarity by taking their one-complement ($1 - X_{qN}$) (Alberdi & Gilbert, 2019).

S.5: Simulating artificial soundscapes to demonstrate the soundscape diversity workflow's desirable properties

In this section, we used simulated artificial soundscapes to construct simple examples which illustrate that the proposed soundscape diversity framework abides by a set of fundamental criteria for trait-based diversity indices and behave in an ecologically intuitive manner. To do so, we adopted some of the criteria relevant to our workflow outlined in Ricotta (2005), Villéger et al. (2008) and Mouchet et al. (2010), and added to these some key behaviours we deemed fundamental for our workflow to work as required (Table S2). As suggested in Villéger et al. (2008), here it is not important that each index matches each criterion, but rather that the ensemble of the indices does. In section S.5.1, we discussed the criteria which can be confirmed without a need for explicit testing. Further on, in sections S.5.2 – S.5.6, we used simulated artificial soundscapes to prove that the workflow abided by the fundamental properties we desire.

Table S2: A summary of some desired criteria and properties for the soundscape diversity indices described in this workflow. A green tick mark indicates the index follows the criterion, whereas a red tick mark indicates it does not. For criterion 4, two symbols are provided, indicating whether that soundscape diversity metric follows this criterion for the closest other metric in the table, looking from left to right. For instance, the soundscape richness is not independent from the soundscape diversity at $q=2$ but is independent from the soundscape evenness.

Criterion	Soundscape richness (0D)	Soundscape diversity (1D , 2D , ...)	Soundscape evenness (${}^2D / {}^0D$)
(1) The indices can only have positive values (see section 5.1)	✓	✓	✓
(2) The indices can be strictly contained between 0 – 1 (see section 5.1)	✓	✓	✓
(3) The indices are independent of the species richness (see section 5.1)	✓	✓	✓
(4) The indices are independent of one another (see section 5.3)	✗ ✓	✗ ✗	✓ ✗
(5) The indices are monotonous (see section 5.2)	✓	✓	✗
(6) The indices abide by the replication principle (see section 5.4)	✓	✓	✗
(7) The indices can be decomposed into alpha, beta, and gamma components (see section 5.6)	✓	✓	✗

5.1. Fundamental properties of trait-based diversity indices

Several of the desired properties of our soundscape diversity workflow were fulfilled because of how the workflow and diversity indices have been set up, and thus did not need explicit testing. For instance, all our indices were

strictly positive and could be constrained between 0-1. The soundscape richness and diversity (at $q = 1, 2, \dots$) could be constrained between 0-1 by dividing the diversity value by the maximum possible detectable OSUs in the acoustic trait space. The soundscape evenness values were constrained between 0-1 by default. Moreover, the criterion of independence from the species richness was true for all indices, as we did not use any taxonomic information in our workflow. As such, any potential correlation between the diversity measures and the species richness stemmed from underlying processes of species assembly, and not inherent correlations stemming from how the metrics are computed. In the next section, we tested the remaining criteria and behaviours using simulated soundscapes.

5.2. The soundscape richness, evenness and diversity are monotonous

The criterion of monotonicity states that a subset of the community should always have a lower diversity value than the total community. To test this, we created 100 simplified simulated soundscapes sampled using a 1 min / 5 min sampling regime (resulting in 288 temporal bins in a 24-hour period), and a 0 – 11,025 Hz frequency domain generated using a 256-frame window length (resulting in 64 frequency bins). In this case, the total number of detectable OSUs was 18,432 (288 * 64). We considered each soundscape to be completely filled, having a soundscape richness of 18,432 OSUs. For every simulated soundscape, the relative abundance values of OSUs were sampled so that the number of highly abundant OSUs in the community (relative abundance = 1) ranges from 1-100% of OSUs – the remainder of OSUs being rare (relative abundance = 0.01). By doing so, we altered the proportion of dominant species in the community, thus creating one hundred evenness classes for each soundscape. For each of these 100 soundscapes, we subsetted the soundscape using sample sizes ranging between 1-99% of the total soundscape richness at 1% increments. Then, for each sample size, we randomly sampled the correct number of OSUs 100 times, resulting in a total of 1,000,000 replicates (100 soundscapes with different evenness values * 100 subset sizes * 100 replicates). We calculated the soundscape richness, diversity ($q=2$), and evenness (${}^2D / {}^0D$) for each soundscape. To test whether each of the metrics abides by the criterion of monotonicity, we subtracted the richness, diversity, and evenness metrics for each subsetted soundscape from their respective original soundscape metrics. If any negative values are present in the data, this suggests the soundscape diversity metric of the subsetted soundscape was larger than that of the original soundscape, and thus the criterion of monotonicity does not hold.

As expected, the monotonicity criterion held true for the soundscape richness and soundscape diversity (Fig. S8), as a subset of OSUs could never be richer than the total pool. For the evenness, however, the criterion of monotonicity did not hold, as a subset of OSUs could result in a higher evenness value than the total pool if the relative abundances of the subset were more even (Fig. S8).

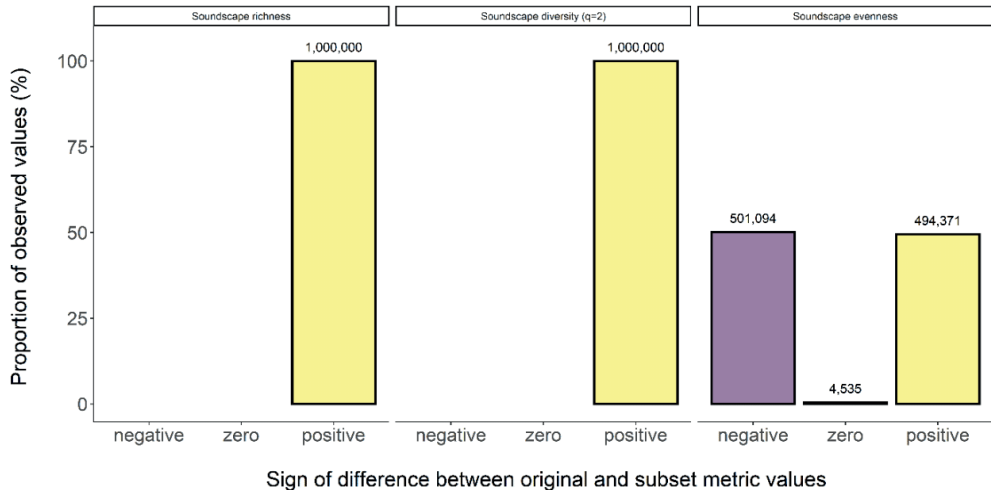


Figure S8: A barplot displaying the proportion of observations that had a negative, zero or positive sign for the difference between the soundscape richness, diversity (q=2) and evenness of the original soundscape and the respective metric of the subsetting soundscape. Negative values indicate the value of the subset metric was larger than the original value, and thus the metric does not abide by the criterion of monotonicity. Above each bar, the raw number of observations for that sign is displayed.

5.3. Soundscape diversity metrics are independent of one another

For our next criterion, we wanted to assess whether our soundscape diversity metrics are strictly independent of one another, capturing unique aspects of acoustic trait space usage. To test this, we generated simulated soundscapes with randomised variation in the trait values. We considered the same simplified acoustic trait space as in section 5.2, consisting of 18,432 detectable OSUs. We considered one hundred soundscape richness classes (1-100% of OSUs detected). For each of these richness classes, the equivalent number of OSUs in acoustic trait space was generated. For instance, for the acoustic trait space with 18,432 potential OSUs, the 10% richness class resulted in $0.1 \times 18,432 = 1,843$ OSUs. As before, for each richness class, the relative abundance values of OSUs were sampled so that the number of highly abundant species in the community (relative abundance = 1) ranges from 1-100% of OSUs – the remainder of OSUs being rare (relative abundance = 0.01). As such, we have created 10,000 replicates along the richness-evenness range. The

soundscape richness, diversity and evenness were computed for these 10,000 datasets, and the Pearson correlation coefficient and R^2 -value for a simple linear regression model were calculated for each combination of indices to assess independence. We expected the soundscape richness and evenness to be strictly independent of one another, capturing unique aspects of the soundscape. Conversely, as the soundscape diversity at $q=2$ incorporates both aspects of the soundscape richness and evenness, we expected it to be positively correlated with an increasing soundscape richness and evenness.

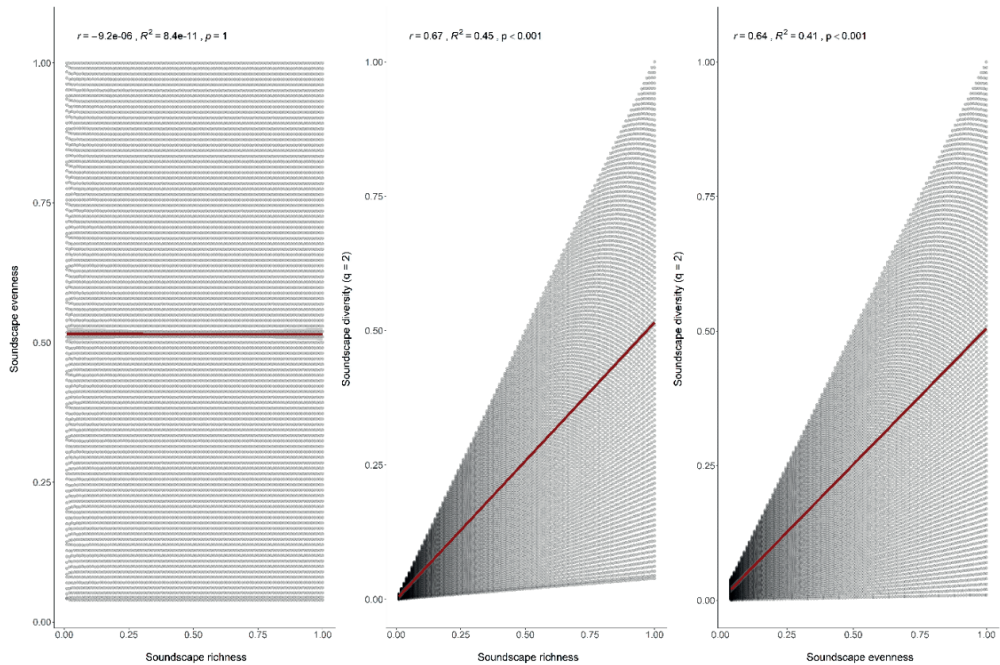


Figure S9: The relationship between the soundscape diversity variables (soundscape richness, evenness, and diversity) for 10,000 simulated soundscapes with richness values ranging between 1-100% of the total number of detectable OSUs, and relative abundance values sampled so that the evenness value covers the range from 0-1. The Pearson correlation coefficient ($r < 0.001$) and associated R^2 -value ($R^2 < 0.001$) reveal there is no relationship between the soundscape richness and evenness, confirming they are strictly independent. The soundscape diversity at $q = 2$ is positively correlated with both the soundscape richness ($r = 0.67$) and the soundscape evenness ($r = 0.64$).

The Pearson correlation coefficient and associated R^2 -value obtained for the simulated soundscapes demonstrated that the soundscape richness and evenness were independent of one another (Fig. S9), thus satisfying our independence criterion. Moreover, as expected, the soundscape diversity at $q=2$ demonstrated a positive relationship with both the soundscape richness and evenness, being sensitive to changes in both.

5.4. Soundscape metrics abide by the replication principle

For our next test, we wanted to test whether the diversity indices described in this study abide by some fundamental behaviours required for biodiversity indices. The replication principle states that for two equally diverse communities with identical relative abundance distributions and no shared species, the diversity of the pooled community assemblage should be twice as high (Hill, 1973; Jost, 2006). Inversely, when the number of OSUs in the system is reduced by half, so should the diversity. Yet, classical diversity indices such as the Shannon and Simpson indices do not follow this intuitive notion of diversity. For these indices, the change in index values is not proportional to the change in the underlying diversity of the system. As such, treating these diversity indices as diversity values can lead to gross misinterpretation of results (Alberdi & Gilbert, 2019). Hill numbers follow the replication principle, which makes changes in their magnitude easily interpretable and ensures that the beta diversity, computed as the ratio between alpha and gamma, accurately reflects the compositional similarity of soundscapes.

Here, we demonstrated that the soundscape diversity indices (qD with $q = 0, 1, 2, \dots$) proposed in this study abided by the replication principle. To do so, we modified a real-life soundscape which was generated for one of the sites in the case study, to create three artificial soundscapes. The first two artificial soundscapes we made to be equally diverse with an identical relative abundance distribution, but no shared species. To achieve this, for the OSUs occurring between 12:00h – 23:59h in the real-life soundscape, we set the incidence values to zero, thus generating a half-filled soundscape that represents our first artificial soundscape (Fig. S10 – soundscape 1). Next, to generate our second artificial soundscape with an equal diversity and relative abundance distribution but no shared OSUs, we copied the OSUs and their relative abundance values occurring between 00:00h – 11:59h to the period from 12:00h – 23:59h. Next, we set the incidence values for the OSUs occurring between 00:00h – 11:59h to zero (Fig. S10 – soundscape 2). This way, our second artificially generated soundscape contained the exact diversity and relative abundance distribution of OSUs, but no shared OSUs. For our final artificial soundscape, we pooled artificial soundscapes 1 and 2 (Fig. S10 – pooled soundscape).

To demonstrate that the diversity of the pooled assemblage is twice the diversity of the sub-soundscapes (soundscapes 1 and 2), we computed the soundscape diversity ($q = 0, 1, 2$), as well as equivalent classical diversity indices, the Shannon and Simpson diversity indices, for all artificially generated soundscapes.

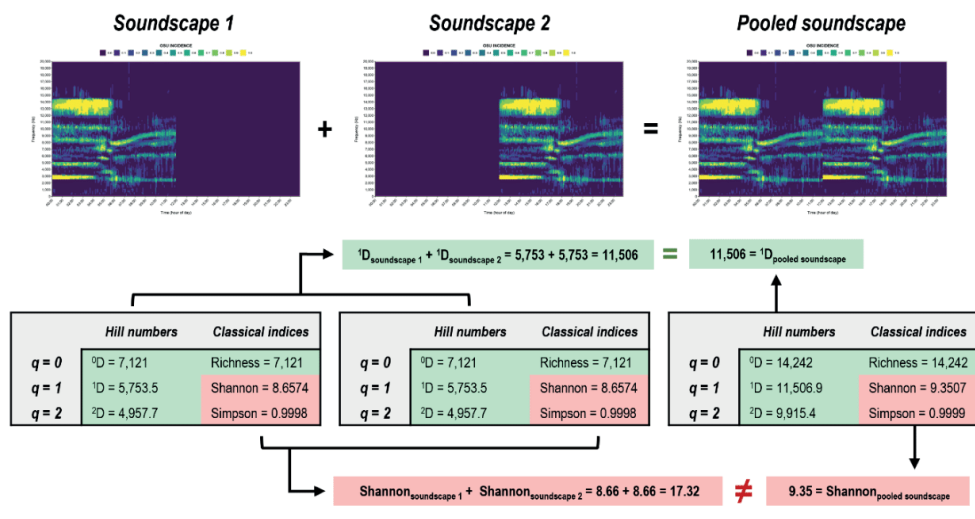


Figure S10: A visual representation of our workflow's adherence to the replication principle, demonstrated using artificial soundscapes. The replication principle states that, for two soundscapes that are equally diverse and have an identical relative abundance distribution, but without any species in common (soundscape 1 and soundscape 2), the diversity of the pooled soundscape should be twice as high. We demonstrate this holds true for the Hill numbers applied to our workflow (green shaded areas), but not for the equivalent classical diversity indices (red shaded areas).

Using these artificially generated soundscapes, we demonstrated that the soundscape diversity metrics proposed in this study abide by the replication principle, whereas the Shannon and Simpson indices which are commonly used in soundscape research did not.

5.5. Diversity profiles

Even when diversity metrics abide by the replication principle, a single diversity metric only portrays part of the information. The perceived diversity of a soundscape depends on the importance the researcher gives to the commonness or rarity of OSUs, which is modulated by parameter q . For instance, one soundscape might have a higher richness but lower evenness than another – information that is lost when only looking at a single index. Diversity profiles plot Hill numbers in function of the parameter q , thus providing an accurate graphical representation of the shape of the acoustic community – or a type of soundscape fingerprint (Fig. S11). They provide insight into the change in perceived soundscape diversity as the emphasis shifts from rare to common OSUs, graphically illustrating the evenness and degree of dominance in the community (Leinster & Cobbold, 2012; Chao et al., 2014). The left-hand side of the diversity profile yields information about the soundscape richness, valuing rare and common species equally. The right-hand side gives information about the diversity of

common or dominant OSUs. Thus, they allow researchers to investigate the diversity of the soniferous community from multiple perspectives, providing a more comprehensive method for inter-soundscape comparison than any single index (Chao & Jost, 2015).

We demonstrated the utility of diversity profiles by generating a set of four simulated soundscapes with an equal soundscape richness, but varying soundscape diversity and evenness. To do so, we used one of the soundscapes we previously produced in the case study and modified the relative abundance distribution of the OSUs in the community to simulate different degrees of soundscape evenness. We simulated four soundscapes along the evenness gradient by modifying the OSU abundances so that the number of highly abundant species in the community (relative abundance = 1) ranged from 25%, 50%, 75% and 100% of OSUs. The remainder of rare OSUs were obtained by randomly sampling their relative abundance along a range of 0.01-0.5 using a 0.01 interval. For each of these simulated soundscapes along the evenness gradient, we computed the soundscape diversity along a range of diversity orders q from 0.01-5.0 at 0.01 intervals. Finally, to produce the soundscape diversity profiles, we plotted the soundscape diversity in function of diversity order q for the four simulated soundscapes with differing evenness (Fig. S11). In addition to the soundscape diversity profile, we provided a graphical representation of the acoustic trait space for each of the simulated soundscapes.

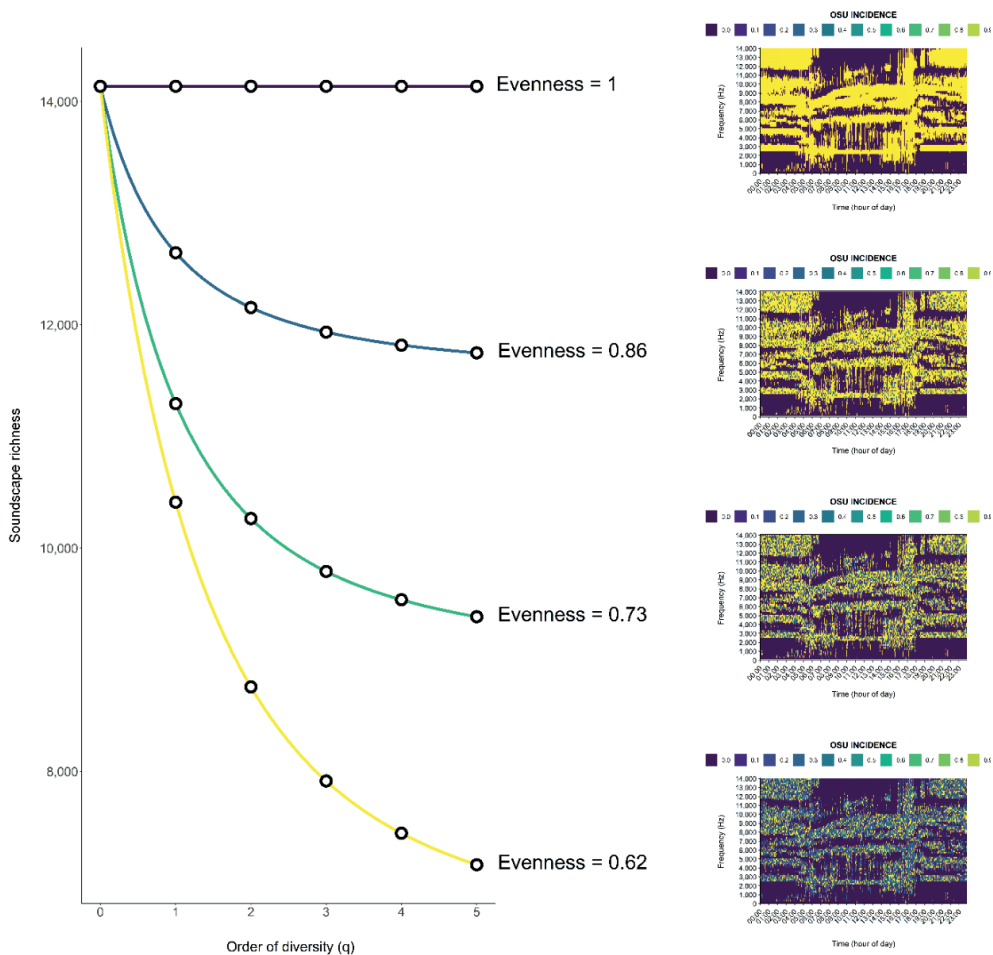


Figure S11: A soundscape diversity profile displaying the change in the soundscape diversity in function of the order of diversity (q) for four soundscapes with differing evenness (${}^0D/{}^2D$) values. The lower the evenness of the soundscape, the more rapidly the soundscape diversity drops in function of the order of diversity.

5.6. Soundscape diversity can be decomposed into its alpha, beta, and gamma components

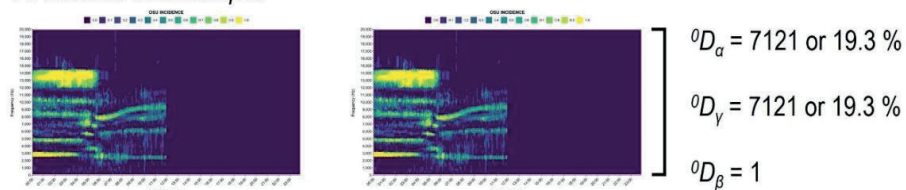
The soundscape diversity can be assessed with reference to the wider ecological system by breaking it down into its respective alpha, beta and gamma components (Whittaker, 1960). Within the framework of Hill numbers, these components take a simple multiplicative relationship in which gamma equals alpha times beta.

To illustrate the meaning of these components, in the following example (Fig. S12) we computed the alpha, beta and gamma components for three hypothetical scenarios: (i) a system comprised of two identical and equally

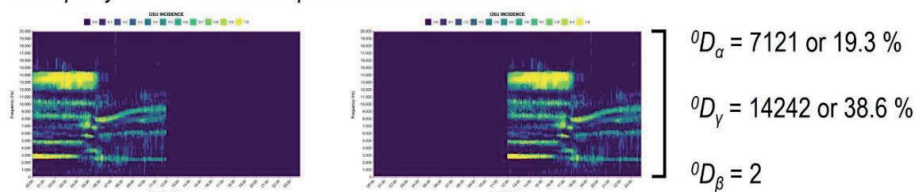
diverse soundscapes (Fig. S12A); (ii) a system comprised of two unique but equally diverse soundscapes (Fig. S12B); (iii) a system comprised of two partially overlapping soundscapes (Fig. S12C). To create these hypothetical scenarios, we used the same artificial soundscapes generated in section S.5.4. For the first scenario, we replicated the same soundscape twice (soundscape 1 and soundscape 1), and computed the alpha, beta, and gamma components for the system. For the second scenario, we took the two equally diverse soundscapes with no common OSUs (soundscape 1 and soundscape 2) and computed the three components. Finally, for the third scenario, we computed alpha, beta and gamma for a system comprised of soundscape 1 and the pooled soundscape, which partially overlaps the former.

When two soundscapes were identical, alpha equalled gamma and thus beta equalled 1. When two soundscapes were equally diverse but unique, gamma was double alpha, and thus beta equalled 2. When two soundscapes overlapped partially, beta ranged between 1 and N (the total number of soundscapes). In this case, beta could be seen as the effective number of equally large and completely distinct soundscapes in the overall system – or a measure of how many times more diverse the whole system (gamma) was in the effective number of OSUs compared to its soundscapes on average.

A. Identical soundscapes



B. Equally diverse soundscapes with no shared OSUs



C. Partially overlapping soundscapes

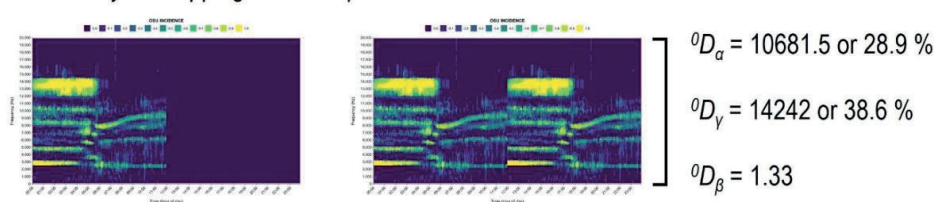


Figure S12: A simple example illustrating soundscape diversity partitioning for three scenarios: **A.** Two equally diverse and completely identical soundscapes with the same relative abundance distribution. In this scenario, gamma equals alpha, and beta – or the number of equally large and completely distinct soundscapes – is one. **B.** Two equally diverse but unique soundscapes. In this scenario, gamma is twice alpha, and the number of distinct soundscapes (beta) is 2 – or the number of subsystems. **C.** Two partially overlapping soundscapes, one of which is twice as diverse as the other. In this scenario, beta ranges between 1 and N (the number of soundscapes).

S.6. Additional case study information

6.1: A note on data collection

Before assessing the soundscape diversity, acoustic data needs to be collected. For this, several decisions need to be made. First, the sampling rate and bit depth of the acoustic recorder need to be chosen. These parameters will dictate the frequency and amplitude resolution. The sampling rate should be twice the desired maximal frequency, a principle known as the Nyquist-Shannon sampling theorem. In this study, the sampling rate needs to be a minimum of 44,100, as we are interested in sounds up to 22,050 Hz. The choice of sampling rate and bit depth also constitutes a trade-off between the desired resolution on the one hand, and the available storage on the memory card and the battery life of the sensor on the other hand, as higher sampling rates and bit depths are more storage- and energy-demanding. Next, the recording schedule and duration for each site should be determined. For soundscape studies, sound files are usually collected for 1-minute durations. If multiple soundscapes are to be compared in the same study, the same recording schedule should be used. The soundscape can be recorded either continuously or using a regular-interval sampling regime (1 min/5 min; 10 min/30 min; etc.). However, sparse sampling regimes are generally discouraged as they require the soundscape to be recorded for long periods before the soundscape variability is captured adequately, which in turn introduces issues related to seasonal variation (Bradfer-Lawrence et al., 2019). In S.1, we provide recommendations regarding the choice of sampling duration and regime using our workflow.

6.2. Site selection

Acoustic data were collected at the Balbina Hydroelectric Reservoir (BHR) in Brazilian Amazonia (1°40'S, 59°40'W). Surveys were conducted between July and December 2015, the local dry season, sampling 151 plots at 78 sampling sites (74 forest islands and 4 continuous forest sites) in the mainland (Bueno et al., 2020). At each plot, a single acoustic recorder was deployed at 1.5 m height and set to record the soundscape for 1-minute every 5-min for 5-9 consecutive days at a sampling rate of 44.1 kHz using the ARBIMON Touch application. For the purposes of this case study, only the plots for which data on the richness of soniferous species was available were retained (see section 6.3. for further details). Moreover, all plots located in riparian habitats near streams were removed from the dataset. Additionally, the sound recordings for all plots were visually inspected using long-duration false-colour spectrograms (LDFCSs) (see Towsey et al., 2016; Towsey et

al., 2018), and plots with signs of microphone failure or persistent noise were removed. If multiple plots were present at the same site, data were aggregated across plots, resulting in a final sample size of 35 sites. For more detailed information on data collection through passive acoustic monitoring, see Bueno et al. (2020).

Table S3: Overview of the sites and their respective sub-plots included in the case study

Island name	Plot name	Island name	Plot name
Abusado	Abusado	Jabuti	Jabuti_A
Adeus	Adeus_A		Jabuti_B
	Adeus_B		Jabuti_C
Aline	Aline	Jiquitaia	Jiquitaia
Andre	Andre	Joaninha	Joaninha
Arrepiado	Arrepiado	Martelo	Martelo_B
Bacaba	Bacaba_B		Martelo_C
Beco_do_Catitu	Beco_do_Catitu_A	Mascote	Mascote_A1
	Beco_do_Catitu_B		Mascote_A2
	Beco_do_Catitu_D		Mascote_B1
	Beco_do_Catitu_E		Mascote_B2
Cafundo	Cafundo	Moita	Moita_A
CF_Grid	CF_Grid_CampTrail_A		Moita_B
		CF_Grid_NS3_1200	Palhal
CF_Loreno	CF_Loreno_A	Panema	Panema
	CF_Loreno_B	Pe_Torto	Pe_Torto
CF_WABA	CF_WABA_B	Piquia	Piquia
	CF_WABA_C	Pontal	Pontal_B
Cipoal	Cipoal_A		Pontal_C
	Cipoal_B	Porto_Seguro	Porto_Seguro_B
	Cipoal_C		Porto_Seguro_C
Coata	Coata	Relogio	Porto_Seguro_D
Formiga	Formiga		Relogio_B
Furo_de_Santa_Luzia	Furo_de_Santa_Luzia_B	Sapupara	Sapupara_A
	Furo_de_Santa_Luzia_C		Sapupara_B
Fuzaca	Fuzaca_B	Torem	Torem
	Fuzaca_C	Tristeza	Tristeza_A
	Fuzaca_D		Tristeza_B
Garrafa	Garrafa		Tristeza_C
Gaviao_real	Gaviao_real_A	Tucumari	Tucumari_A
	Gaviao_real_B		Tucumari_B
	Gaviao_real_C		Tucumari_C
	Gaviao_real_D		

6.3. Compound richness of soniferous species

To assess the relationship between the soundscape diversity metrics and the species richness of sound-producing organisms in the study area, we calculated the compound richness of three major vocalising groups in

tropical rain forests: (i) anurans; (ii) birds; and (iii) primates. Below, we outlined how the species richness for each of these groups was determined.

6.3.1. Anuran data

The anuran species richness was determined using passive acoustic monitoring data obtained at BHR. Per plot, a subset of 62 1-minute recordings was selected for aural identification of anuran species, taking the first 1-minute of recording every 10-min over 5 hours between 17:00h-22:01h during sampling days 2 and 4. In each sound recording, anuran species were identified using both aural identification and visual inspection of spectrograms by a trained expert (GSM) using the RFCx Arbimon II Visualizer Tool (<https://arbimon.rfcx.org/>). All species identifications were cross-validated by a second reviewer (ILK) to ensure accuracy, and species records were discarded if they could not be readily identified or if spectrograms were inadequate.

6.3.2. Bird data

The detection history of species in the audio recordings was acquired through three steps. First, an expert (MC-C) manually searched for species in recordings from two non-consecutive days in each plot and created a preliminary list of species and a call template for each species detected. Second, in the RFCx-ARBIMON platform, we used the template matching procedure to classify the audio recordings. In this step, we created two audio playlists: a) all diurnal (05:00h - 18:00h) recordings and b) all nocturnal (18:00h - 05:00h) recordings. All bird templates, except for *Glaucidium hardyi* were assigned to the nocturnal playlist. The classification of recordings based on the pattern matching procedures searches through the audio data (all 1-minute recordings) for acoustic signals and detects regions that have a high correlation with a template that has been selected by the user. All regions of interest (ROIs) with values above the selected correlation threshold (0.1) were presented as potential detections for posterior validations (LeBien et al., 2020). We then used a filter to display only the best matches per plot per day. The selection of a low threshold resulted in a high number of false positives, though the number of false negatives was negligible. In the third step, one of us (MC-C) manually reviewed the template matching results using a filter that displays only the best matches per plot and per day. In this step, we annotated the results as either positive or negative, indicating the corresponding species presence or absence. This ensured that the final data set used in the analyses only included expert verified detections and the exclusion of all false positive detections.

6.3.3. Primate data

The primate data was compiled from Benchimol and Peres (2015). In this study, vertebrate surveys including primates were conducted on 37 islands and 3 continuous forest sites. Primate surveys were conducted based on diurnal line-transect censuses, although some species were also detected using a systematic camera-trapping programme (Benchimol & Peres, 2021). For each of the sites, one to five line-transects of variable length were cut based on the island size and shape. For the continuous forest sites, three parallel 4-km transects were established with a 1-km separation. At each of the sites, line-transect surveys were conducted by expert observers, walking the transects at a constant speed (~ 1 km/h) in the morning (06:15h - 10:30h) and afternoon (14:00h - 17:30h) following a standard protocol (Peres & Cunha, 2011). For each sampling year of the study (2011 and 2012), four line-transect surveys were conducted per site, each of which was separated by 30 sampling days to minimize the impact of time of day and seasonality.

In addition to the line-transect surveys, sign surveys for vertebrate activity were conducted on the return walks, and species identifications were recorded. Moreover, to supplement these surveys, Reconyx HC 500 Hyperfire camera traps were deployed at each site. For each sampling site, two to ten camera traps were deployed at 30-40 cm height, separating individual camera traps at an approximate distance of 500 m depending on island size and shape. For the continuous forest sites, 15 camera traps were deployed, installing five camera traps per transect. All camera trap stations were active for 30 days in each sampling year, taking a sequence of five photos for every detection event, and using 15-second intervals between consecutive detections. Camera trapping efforts were always temporally separated from line-transect surveys to prevent disturbance of the local fauna. All data from line-transect surveys, sign surveys and camera trapping were compiled into presence-absence data per island for the species known to present in the study area.

6.3.4. Compound species richness

A subset of the species richness data was taken, including only the sites and plots outlined in section 6.3 (Table S3). For sampling sites containing multiple plots, the site-wide species richness was calculated for each taxonomic group. Finally, for each site, the richness values for the anurans, birds and primates were summed to

obtain the compound richness of soniferous species. This metric of species richness was compared against the soundscape diversity metrics to assess their behaviour along this ecological gradient (Table S4).

Table S4: Soundscape diversity and species richness data for 35 sites at the Balbina Hydroelectric Reservoir

Site	Soundscape diversity data		Species richness data			
	soundscape richness (%)	soundscape evenness	anuran richness	bird richness	primate richness	compound richness
Abusado	35.66	0.67	9	4	3	16
Adeus	61.04	0.69	7	15	2	24
Aline	42.99	0.62	4	6	0	10
Andre	26.17	0.60	9	3	1	13
Arrepiado	33.37	0.64	5	10	1	16
Bacaba	48.78	0.68	4	10	4	18
Beco_do_Catitu	66.84	0.71	17	20	6	43
Cafundo	45.40	0.77	7	10	0	17
CF_Grid	61.72	0.74	12	21	7	40
CF_Loreno	69.05	0.73	10	21	7	38
CF_Waba	64.08	0.69	12	16	7	35
Cipoal	63.52	0.68	13	25	7	45
Coata	49.67	0.64	10	15	2	27
Formiga	39.02	0.67	7	3	0	10
Furo_de_Santa_Luzia	62.37	0.69	7	17	5	29
Fuzaca	56.76	0.72	16	18	7	41
Garrafa	21.01	0.63	6	6	1	13
Gaviao_real	54.15	0.71	13	24	5	42
Jabuti	70.12	0.73	11	21	7	39
Jiquitaia	43.79	0.61	1	4	3	8
Joaninha	36.04	0.65	4	3	0	7
Martelo	66.36	0.70	10	21	7	38
Mascote	69.31	0.73	13	28	7	48
Moita	54.73	0.67	7	17	4	28
Palhal	41.33	0.65	3	6	2	11
Panema	37.32	0.76	3	2	0	5
Pe_Torto	42.34	0.66	3	7	1	11
Piquia	48.87	0.66	7	9	1	17
Pontal	55.44	0.67	10	21	5	36
Porto_Seguro	64.42	0.71	21	27	7	55
Relogio	54.26	0.67	8	8	6	22
Sapupara	66.99	0.69	10	11	5	26
Torem	29.29	0.77	3	2	1	6
Tristeza	74.06	0.76	13	23	7	43
Tucumari	58.01	0.67	9	26	4	39

6.4. Soundscape diversity data

To derive the soundscape diversity metrics, the set of recordings described in section 3.1 of the main text was used (see Table S3). Per plot, we quantified the presence of sound in the acoustic trait space by computing the CVR index for each 1-minute file using a 256-frame window length (see S.2. for more information on window length choice) and 44,100 Hz sampling rate. This measure quantifies the fraction of cells in each noise-reduced frequency bin that exceed a 3 dB amplitude value. Next, we concatenated the CVR files chronologically per plot. Then, we determined a binarisation threshold for each plot using the 'IsoData' binarisation algorithm in the 'autothresholdr' R-package (v1.3.11; Landini et al. 2017; see S3 for more details). Using this site-specific threshold, we binarised the CVR-values to obtain a detection (1) / non-detection (0) variable for each OSU (see S.3. for a detailed breakdown of thresholding methods). After, we separated the binarised spectral index files into 24-hour samples (288 files using a 1 min/5 min sampling regime) of the soundscape. Furthermore, we subsetted the frequency domain to include only the sounds below 11,025 Hz. Finally, an OSU-by-sample incidence matrix for each plot was obtained. For sampling sites containing multiple plots, the obtained OSU-by-sample incidence matrices were grouped across plots. We then computed the soundscape richness and evenness as described in the main manuscript.

References:

- Aide, T.M., Hernández-Serna, A., Campos-Cerqueira, M., Acevedo-Charry, O., Deichmann, J. (2017). Species Richness (of Insects) Drives the Use of Acoustic Space in the Tropics. *Remote Sensing* 9(11), 1096-1108. <https://doi.org/10.3390/rs9111096>.
- Alberdi, A., Gilbert, M.T.P. (2019). A guide to the application of Hill numbers to DNA-based diversity analyses. *Molecular Ecology Resources* 19(4), 804–817. <https://doi.org/10.1111/1755-0998.13014>.
- Baty, F., Ritz, C., Charles, S., Brutsche, M., Flandrois, J-P., Delignette-Muller, M-L. (2015). A toolbox for nonlinear regression in R: the package nlstools. *Journal of Statistical Software* 66(5), 1–21. <https://doi.org/10.18637/jss.v066.i05>

- Benchimol, M., Peres, C.A. (2015). Widespread Forest Vertebrate Extinctions Induced by a Mega Hydroelectric Dam in Lowland Amazonia. *PLOS One* 10(7), e0129818. <https://doi.org/10.1371/journal.pone.0129818>.
- Benchimol, M., Peres, C.A. (2021). Determinants of population persistence and abundance of terrestrial and arboreal vertebrates stranded in tropical forest land-bridge islands. *Conservation Biology* 35(3), 870–883. <https://doi.org/10.1111/cobi.13619>.
- Bradfer-Lawrence, T., Gardner, N., Bunnefeld, L., Bunnefeld, N., Willis, S.G., Dent, D.H. (2019). Guidelines for the use of acoustic indices in environmental research. *Methods in Ecology and Evolution* 10(10), 1796–1807. <https://doi.org/10.1111/2041-210X.13254>.
- Bueno, A.S., Masseli, G.S., Kaefer, I.L., Peres, C.A. (2020). Sampling design may obscure species–area relationships in landscape-scale field studies. *Ecography* 43(1), 107–118. <https://doi.org/10.1111/ecog.04568>.
- Burivalova, Z., Towsey, M., Boucher, T., Truskinger, A., Apelis, C., Roe, P., Game, E.T. (2018). Using soundscapes to detect variable degrees of human influence on tropical forests in Papua New Guinea. *Conservation Biology* 32(1), 205–215. <https://doi.org/10.1111/cobi.12968>.
- Campos-Cerqueira, M., Mena, J.L., Tejada-Gómez, V., Aguilar-Amuchastegui, N., Gutierrez, N., Aide, T.M. (2020). How does FSC forest certification affect the acoustically active fauna in Madre de Dios, Peru? *Remote Sensing in Ecology and Conservation* 6(3), 274–285. <https://doi.org/10.1002/rse2.120>.
- Chao, A., Chiu, C-H., Hsieh, T.C. (2012). Proposing a resolution to debates on diversity partitioning. *Ecology* 93(9), 2037–2051. <https://doi.org/10.1890/11-1817.1>.
- Chao, A., Chiu, C-H., Jost, L. (2014). Unifying Species Diversity, Phylogenetic Diversity, Functional Diversity, and Related Similarity and Differentiation Measures Through Hill Numbers. *Annual Review of Ecology, Evolution, and Systematics* 45(1), 297–324. <https://doi.org/10.1146/annurev-ecolsys-120213-091540>.
- Chao, A., Jost, L. (2012). Coverage-based rarefaction and extrapolation: standardizing samples by completeness rather than size. *Ecology* 93(12), 2533–2547. <https://doi.org/10.1890/11-1952.1>.
- Chao, A., Jost, L. (2015). Estimating diversity and entropy profiles via discovery rates of new species. *Methods in Ecology and Evolution* 6(8), 873–882. <https://doi.org/10.1111/2041-210X.12349>.

- Chiu, C.-H., Jost, L., Chao, A. (2014). Phylogenetic beta diversity, similarity, and differentiation measures based on Hill numbers. *Ecological Monographs* 84(1), 21–44. <https://doi.org/10.1890/12-0960.1>.
- Eldridge, A., Guyot, P., Moscoso, P., Johnston, A., Eyre-Walker, Y., Peck, M. (2018). Sounding out ecoacoustic metrics: Avian species richness is predicted by acoustic indices in temperate but not tropical habitats. *Ecological Indicators* 95(1), 939–952. <https://doi.org/10.1016/j.ecolind.2018.06.012>.
- Gasc, A., Sueur, J., Jiguet, F., Devictor, V., Grandcolas, P., Burrow, C., Depraetere, M., Pavoine, S. (2013). Assessing biodiversity with sound: Do acoustic diversity indices reflect phylogenetic and functional diversities of bird communities? *Ecological Indicators* 25, 279–287. <https://doi.org/10.1016/j.ecolind.2012.10.009>.
- Hallett, L.M., Jones, S.K., MacDonald, A.M., Jones, M.B., Flynn, D.F.B., Ripplinger, J., Slaughter, P., Gries, C., Collins, S.L. (2016). codyn : An R package of community dynamics metrics. *Methods in Ecology and Evolution* 7(10), 1146–1151. <https://doi.org/10.1111/2041-210X.12569>.
- Harrison, S., Ross, S.J., Lawton, J.H. (1992). Beta Diversity on Geographic Gradients in Britain. *The Journal of Animal Ecology* 61(1), 151–158. <https://doi.org/10.2307/5518>.
- Hill, M.O. (1973). Diversity and Evenness: A Unifying Notation and Its Consequences. *Ecology* 54(2), 427–432. <https://doi.org/10.2307/1934352>.
- Hsieh, T.C., Ma, K.H., Chao, A. (2016). iNEXT: an R package for rarefaction and extrapolation of species diversity (Hill numbers). *Methods in Ecology and Evolution* 7(12), 1451–1456. <https://doi.org/10.1111/2041-210X.12613>.
- Jost, L. (2006). Entropy and diversity. *Oikos* 113(2), 363–375. <https://doi.org/10.1111/j.2006.0030-1299.14714.x>.
- Jost, L. (2007). Partitioning diversity into independent alpha and beta components. *Ecology* 88(10), 2427–2439. <https://doi.org/10.1890/06-1736.1>.
- Landini, G., Randell, D.A., Fouad, S., Galton, A. (2017). Automatic thresholding from the gradients of region boundaries. *Journal of microscopy* 265(2), 185–195. <https://doi.org/10.1111/jmi.12474>.

- LeBien, J., Zhong, M., Campos-Cerqueira, M., Velev, J.P., Dodhia, R., Ferres, J.L., Aide, T.M. (2020). A pipeline for identification of bird and frog species in tropical soundscape recordings using a convolutional neural network. *Ecological Informatics* 59, 101113. <https://doi.org/10.1016/j.ecoinf.2020.101113>.
- Leinster, T., Cobbold, C.A. (2012). Measuring diversity: The importance of species similarity. *Ecology* 93(3), 477–489. <https://doi.org/10.1890/10-2402.1>.
- Machado, R.B., Aguiar, L., Jones, G. (2017). Do acoustic indices reflect the characteristics of bird communities in the savannas of Central Brazil? *Landscape and Urban Planning* 162, 36–43. <https://doi.org/10.1016/j.landurbplan.2017.01.014>.
- Mouchet, M.A., Villéger, S., Mason, N.W.H., Mouillot, D. (2010). Functional diversity measures: an overview of their redundancy and their ability to discriminate community assembly rules. *Functional Ecology* 24(4), 867–876. <https://doi.org/10.1111/j.1365-2435.2010.01695.x>.
- Peres, C.A., Cunha, A.A. (2011). Manual para censo e monitoramento de vertebrados de médio e grande porte por transecção linear em florestas tropicais. Wildlife Conservation Society.
- Phillips, Y.F., Towsey, M., Roe, P. (2018). Revealing the ecological content of long-duration audio-recordings of the environment through clustering and visualisation. *PLOS One* 13(3), e0193345. <https://doi.org/10.1371/journal.pone.0193345>.
- R Core Team (2020). R: A Language and Environment for Statistical Computing. Vienna, Austria. Available online at <https://www.r-project.org/>.
- Ricotta, C. (2005). A note on functional diversity measures. *Basic and Applied Ecology* 6(5), 479–486. <https://doi.org/10.1016/j.baae.2005.02.008>.
- Rodríguez, A., Gasc, A., Pavoine, S., Grandcolas, P., Gaucher, P., Sueur, J. (2014). Temporal and spatial variability of animal sound within a neotropical forest. *Ecological Informatics* 21, 133–143. <https://doi.org/10.1016/j.ecoinf.2013.12.006>.

- Towsey, M., Truskinger, A., Roe, P. (2016). QUT Ecoacoustics | Long-duration Audio-recordings of the Environment. QUT Ecoacoustics Group. Available online at <https://research.ecosounds.org/research/eadm-towsey/long-duration-audio-recordings-of-the-environment>.
- Towsey, M., Znidersic, E., Broken-Brow, J., Indraswari, K., Watson, D.M., Phillips, Y., Truskinger, A., Roe, P. (2018). Long-duration, false-colour spectrograms for detecting species in large audio data-sets. *Journal of Ecoacoustics* 2(1), 1-13. <https://doi.org/10.22261/JEA.IUSWUI>.
- Tuomisto, H. (2010). A diversity of beta diversities: Straightening up a concept gone awry. Part 1. Defining beta diversity as a function of alpha and gamma diversity. *Ecography* 33(1), 2-22. <https://doi.org/10.1111/j.1600-0587.2009.05880.x>.
- Villéger, S., Mason, N.W.H., Moullot, D. (2008). New multidimensional functional diversity indices for a multifaceted framework in functional ecology. *Ecology* 89(8), 2290–2301. <https://doi.org/10.1890/07-1206.1>.
- Whittaker, R.H. (1960). Vegetation of the Siskiyou Mountains, Oregon and California. *Ecological Monographs* 30(3), 279–338. <https://doi.org/10.2307/1943563>.



CHAPTER II

Extending species-area relationships to the realm of ecoacoustics:
The Soundscape-Area Relationship

II Extending species-area relationships to the realm of ecoacoustics: The Soundscape-Area Relationship

Authors

Thomas Luypaert^{1*}, Anderson S. Bueno², Torbjørn Haugaasen¹, Carlos A. Peres^{3,4}

Affiliations

¹ Faculty of Environmental Sciences and Natural Resource Management, Norwegian University of Life Sciences, Ås, Norway

² Instituto Federal de Educação, Ciência e Tecnologia Farroupilha, Júlio de Castilhos, RS, Brazil

³ School of Environmental Sciences, University of East Anglia, Norwich, United Kingdom

⁴ Instituto Juruá, Manaus, AM, Brazil

***Corresponding authors**

Thomas Luypaert (thomas.luypaert@nmbu.no / thomas.luypaert@outlook.com)

Keywords:

Ecoacoustics, soundscape ecology, acoustic indices, habitat fragmentation, insularisation, island biogeography, Soundscape-Area Relationships (SSAR), macroecology

Abstract

The rise in species richness with area is one of the few ironclad ecological relationships. Yet, little is known about the spatial scaling of alternative dimensions of diversity. Here, we provide empirical evidence for a relationship between the richness of acoustic traits emanating from a landscape, or soundscape richness, and island size, which we term the Soundscape-Area Relationship (SSAR). We show a positive relationship between the gamma soundscape richness and island size. This relationship breaks down at the smallest spatial scales, indicating a small-island effect. Moreover, we demonstrate a positive spatial scaling of the plot-scale alpha soundscape richness, but not the beta soundscape turnover, suggesting disproportionate effects as an underlying mechanism. We conclude that the general scaling of biodiversity can be extended into the realm of ecoacoustics, implying soundscape metrics are sensitive to fundamental ecological patterns and useful in disentangling their complex mechanistic drivers.

1. Introduction

The Island biogeography theory (IBT; MacArthur and Wilson 1967) posits that the species richness in insular systems is modulated by the interplay between island size and isolation. These factors influence the extinction-colonisation dynamics on islands, leading to two foundational observations: (i) smaller islands hold fewer species than larger islands (species-area relationship or SAR); and (ii) less isolated islands hold more species than more isolated islands (species-isolation relationship or SIR; Giladi et al. 2014).

The spatial scaling of species richness with area (SAR) is one of the oldest, best-documented, and most ubiquitous ecological patterns (Arrhenius 1921; Gleason 1922; Connor and McCoy 1979; Rosenzweig 1995; Lomolino 2000; Drakare et al. 2006; Matthews et al. 2016). Although SARs can take many different forms, here we will focus on the Island Species-Area Relationship (ISAR or Type IV SAR), which quantifies the increase in species richness with increasing island or habitat patch size (Scheiner 2003). The relationship is typically positive, except for particularly small islands, where stochastic processes overcome the effect of area on species richness (the small island effect; Niering 1963; Lomolino 2000). Yet, there is considerable ambiguity regarding the underlying mechanisms that shape, regulate, and maintain the SAR across space despite its importance to conservation biogeography (Scheiner et al. 2011; Chase et al. 2019; Gooriah 2020).

The null hypothesis is that ISARs result solely from sampling effects. Firstly, ISAR patterns could be caused by sampling artefacts (Preston 1962; Schoereder et al. 2004), with larger islands requiring a larger sampling effort to properly describe their species richness. Consequently, more individuals are sampled, which by chance alone increases the number of species detected (Hill et al. 1994). Secondly, passive sampling effects dictate that species richness in island systems is controlled by ecological sampling processes, in which larger islands represent a larger sample of the original species pool than small islands and, by probability, sample more species (Chase et al. 2019). Alternatively, ISARs may result from biological differences linked to island size. According to the theory of disproportionate effects, island size affects the biological processes regulating species richness (Schoereder et al. 2004). Extinction rates are inversely proportional to population sizes, and the number of individuals an island can sustain is proportional to island size, resulting in higher extinction rates and reduced species richness on small islands. Moreover,

disproportionate effects can emerge through reduced colonisation rates (e.g., through target effects), edge-effects, and reduced trophic levels (see Chase et al. 2019). Finally, the theory of heterogeneity effects posits that island size influences the compositional heterogeneity of species because larger islands contain a wider spectrum of unique habitats, each with a distinct set of species, thereby increasing species richness (Williams 1964).

In contrast to SARs, evidence for the SIR is limited (but see Giladi et al. 2014). The SIR can be attributed to the effects of lower immigration from source habitat patches, leading to reduced rescue effects, higher extinction rates, and, ultimately, lower species richness (Helmus et al. 2014). In patchy habitat systems, however, immigrants travel predominantly from nearby habitat patches rather than a mainland area (Fahrig 2013). Hence, patch isolation depends on the total area of surrounding habitat and isolation can be defined as the landscape-scale habitat amount. Under this whole-landscape context, SARs and SIRs can merely result from the sample area effect: larger and less isolated patches are often surrounded by larger local landscape-scale habitat amounts, which contain more individuals, and by extension, more species (the habitat amount hypothesis or HAH; Fahrig 2013). In summary, the importance of the patch-scale habitat amount and isolation (following the IBT) versus the local landscape-scale habitat amount (following the HAH) will depend on the degree to which patches behave as closed units to the inhabiting community, which is determined by the hostility of the matrix and the dispersal ability of the taxonomic group under investigation. However, elucidating which ecological mechanisms operate at different scales has proven challenging. Additionally, investigations into spatial biodiversity patterns in insular systems have traditionally been restricted to taxonomic species richness, overlooking other dimensions of biodiversity (Galiana et al. 2022; Gonzalez et al. 2020).

One alternative dimension of biodiversity can be derived from the field of ecoacoustics, which makes use of the soundscape, or the combination of all ambient sounds in the landscape, to make inferences about landscape-scale ecological processes (Farina and Gage 2017). The premise is that changes in ecosystems and their organisms that are linked to ecological processes or disturbances will be reflected by the sounds emanating from the landscape (Stowell and Sueur 2020). However, rather than deriving taxonomic information by identifying species' calls, ecoacoustic methods detect ecological signals through acoustic indices (Sueur et al. 2014). These mathematical equations extract information on the diversity of

acoustic traits by quantifying the amplitude variation across the time-frequency domain of sound files (Eldridge et al. 2018). If these metrics respond consistently and predictably to underlying changes in the ecosystem, acoustic indices could be used to lift the veil on landscape-scale processes (Bradfer-Lawrence et al. 2020). Indeed, acoustic indices have been successfully applied to answer ecological questions such as identifying habitat disturbances (e.g., Burivalova et al. 2018), distinguishing habitat types (e.g., Bormpoudakis et al. 2013), and assessing landscape configuration (e.g., Fuller et al. 2015). Moreover, the soundscape richness metric described in Luypaert et al. (2022) was positively correlated with the species richness of sound-producing organisms. Yet, the spatial scaling of these acoustic indices and the mechanisms that govern them in space have received surprisingly little attention (but see Tucker et al. 2014; Fuller et al. 2015; Müller et al. 2020; Han et al. 2022).

Here, we examine the spatial variation in soundscape richness using the world's largest man-made tropical forest archipelago. In doing so, we aim to assess the relative importance of island size and isolation on soundscape richness, and elucidate which mechanisms drive this relationship.

2. Methods

2.1. Data collection

2.1.1. A multi-scale sampling protocol to uncover spatial biodiversity patterns

Much of the contention relating to the ecological mechanisms driving biodiversity patterns in insular systems is linked to methodological inconsistencies (Chase et al. 2019; Gooriah 2020). For instance, many studies have investigated ISARs using uniform sampling protocols (an invariant sampling effort across the island size gradient), characterising the relationship between the island-wide richness and island size (Schoereder et al. 2004; Chase et al. 2019). Although this approach is useful in capturing the shape of ISARs while dealing with confounding non-biological sampling processes, it can tell us little about the potential ecological mechanisms driving observed patterns. Equalising sampling efforts for varying island (or habitat patch) sizes may obscure variation in habitat diversity, thereby missing out on important beta-diversity effects (e.g., heterogeneity effects; Schoereder et al. 2004). Moreover, by focusing on island-wide patterns in biological

richness, local-scale (alpha) biodiversity patterns are overlooked (e.g., disproportionate effects).

To elucidate which ecological mechanisms underlie spatial patterns of biodiversity in our study system, we employed a modified version of the generalised multi-scale and multi-metric framework outlined in Chase et al. (2019). We used a standardised spatial sampling design, scaling the number of plots per island with island size (Fig. 1C). By pooling sampling plots per island, we can derive the island-wide gamma soundscape richness. This metric can be used to assess the relative importance of island size versus isolation. We further examine the soundscape richness at sub-island scales to shed light on the ecological mechanisms governing ISARs. To account for sampling artefacts, we compare the unrarefied and rarefied gamma soundscape richness. Moreover, to discern whether the soundscape-area relationship is not just the result of passive sampling, we investigate the soundscape richness at both local plot scales (alpha soundscape richness) and between-plot turnover (beta soundscape turnover). If island size affects processes of biodiversity regulation (disproportionate effects), we expect the local-scale alpha soundscape richness to positively covary with island size. Conversely, if ISARs result from higher habitat diversity on larger islands (heterogeneity effects), we expect soundscape turnover between plots to positively covary with island size.

2.1.2. Acoustic sampling

Acoustic data were collected at the Balbina Hydroelectric Reservoir (BHR) in Brazilian Amazonia (Fig. 1). The BHR is one of the largest hydroelectric reservoirs on Earth and was formed when the Uatumã River, a tributary of the Amazon, was dammed in 1987 (Fearnside 1989). This flooding event turned the hilltops of the former primary forest into > 3,500 islands covering an area of approximately 300,000 ha and ranging in size from 0.2 to 4,878 ha (Benchimol and Peres 2015a).

Long-duration acoustic surveys were conducted at the BHR between July and December 2015, sampling 74 forest islands (see Bueno et al. 2020). The number of sampling plots per island ranged from 1 to 7 and increased with island size (see S1 for details). At each sampling plot, a passive acoustic sensor was deployed on a tree trunk at 1.5 m above ground with the microphone pointing downward. Each acoustic sensor consisted of an LG smartphone enclosed within a waterproof case with an external connector linked to an omnidirectional microphone and was set to

record 1 in every 5 min at a sampling rate of 44.1 kHz for 4-10 days using the ARBIMON Touch application (ARBIMON, <https://arbimon.rfcx.org/>). Due to poor recording quality, and to retain a proportional sampling scheme, several sites were excluded from the study (see S1), finally retaining 69 sampling plots (1-4 plots per island) on 49 islands (0.45 - 668.03 ha; Fig. S1; Table S1).

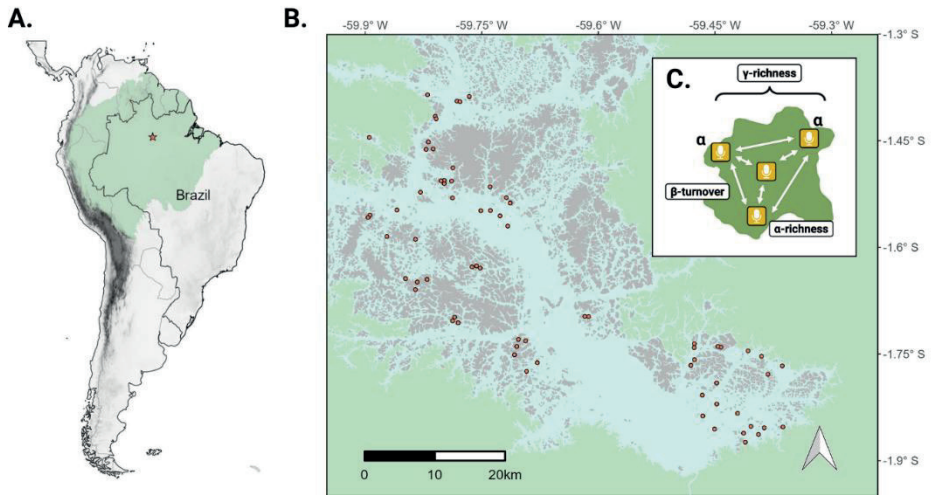


Figure 1: **A.** Location of the Balbina Hydroelectric Reservoir (BHR; orange star) in central Amazonia (light green), Brazil. **B.** A detailed overview of the BHR (blue) showing over >3,500 hilltop islands (grey), surrounded by continuous forest (green). For this study, 69 sites (orange) were sampled on 49 islands. **C.** An overview of the spatial sampling design employed in this study. The green area represents an island, with multiple acoustic sampling plots in yellow. This sub-island scale sampling design allows to quantify not only the island-wide gamma soundscape richness, but also the local-scale alpha soundscape richness and beta turnover components.

2.2. Calculating model variables

2.2.1. Response variable - a metric of soundscape richness

To quantify the diversity of acoustic traits emanating from the landscape, we followed the analytical pipeline outlined in Luypaert et al. (2022) to calculate the soundscape richness acoustic index. This metric is positively correlated with the species richness of sound-producing BHR organisms (Luypaert et al. 2022). To

capture ecological patterns without the need for species identification, the pipeline quantifies the richness of Operational Sound Units (OSUs), a unit of measurement that groups sound by their shared acoustic traits in the time-frequency domain of the acoustic space in which species produce sound.

Briefly, we equalised the sampling effort across all sampling plots to 5 sampling days (Supplementary Materials S2). Next, we calculated the acoustic cover (CVR) spectral index for each 1-min sound file at every plot (i.e., recording station) using a sampling rate of 44,100 Hz and a window length of 256 frames. For each plot, the spectral CVR-index files were concatenated chronologically into a time-by-frequency data frame of CVR-index values. We then determined the detection/non-detection of OSUs per 24h sample of each soundscape by converting the raw CVR-index values into a binary variable using the 'IsoData' binarisation algorithm. In doing so, we obtained an OSU-by-sample incidence matrix per plot, capturing the detection/non-detection of OSUs for each 24h soundscape sample in the 5-day acoustic survey. This matrix forms the base of all subsequent soundscape richness computations.

To quantify the island-wide gamma soundscape richness, we pooled the OSU-by-sample incidence matrices across all sampling plots on each island. Next, we calculated the unrarefied island-wide gamma soundscape richness by counting the number of unique OSUs detected on each island. Moreover, we investigated the spatial scaling of soundscape richness using the: (i) rarefied gamma soundscape richness; (ii) alpha soundscape richness; and (iii) beta soundscape turnover.

2.2.2. Predictor variables

Island size corresponds to the total forest cover per island. We downloaded a classified image from MapBiomas (30m resolution; MapBiomas Project- Collection 2 of the Annual Series of Land Use and Land Cover Maps of Brazil, accessed in 2015 through mapbiomas.org; Souza et al. 2020) and calculated the amount of 'dense forest' per island (pixel value 3), as other pixel values contained either heavily degraded or non-forest cover types (Bueno et al. 2020).

For the isolation metric, we followed MacDonald et al. (2018), using QGIS to calculate island isolation as the proportion of water (1 – proportion of land area) within a range of buffer sizes calculated from the island perimeter. To determine the

optimal scale-of-effect for our isolation variable (see Jackson and Fahrig 2015), we trialled 40 different buffer sizes (50-2000m at 50m intervals), choosing the spatial scale at which the isolation metric attains the strongest relationship with soundscape richness. The highest correlation between the soundscape richness and our isolation metric was attained at a scale-of-effect of 650 m (see S3 for a detailed overview).

2.3. Patch- vs landscape-scale effects on soundscape richness

Although debated (see Tjørve 2003, 2012; Triantis et al. 2012), ISARs are most often mathematically approximated by the power law function (Arrhenius 1921), defined as $S = cAz$, where S is the number of species units, A is the habitat patch area, and c and z represent the slope and intercept of the equation in log-log space. The power-law model provides the best ISAR fits at intermediate spatial scales, such as in our study system (He and Legendre 1996; Triantis et al. 2012; Matthews et al. 2016). We compare the strength and slope of a potential soundscape-area relationship to conventional ISAR studies for a range of taxonomic groups in the study area using a power-law model framework. All power-law models were fitted using the 'lin_pow' function of the 'sars' R-package (v1.3.5 - Matthews et al. 2019) using a \log_{10} transformation.

In addition to island size, we examine the influence of island isolation (i.e., the inverse of landscape-scale habitat amount). To assess the relative importance of these two predictors, we first used partial regression plots to visually explore each variable's influence on the unrarefied soundscape richness while accounting for the other variable. Next, we assessed whether there was an interaction between island size and isolation using conditioning scatterplots. Finally, we fitted a series of linear models and used an information theoretic approach for model selection (Burnham and Anderson 2004):

- (1) $\log_{10}(\text{gamma soundscape richness}) \sim \log_{10}(\text{island size}) + \text{isolation} + \log_{10}(\text{island size}) * \text{isolation}$
- (2) $\log_{10}(\text{gamma soundscape richness}) \sim \log_{10}(\text{island size})$
- (3) $\log_{10}(\text{gamma soundscape richness}) \sim \log_{10}(\text{island size}) + \text{isolation}$
- (4) $\log_{10}(\text{gamma soundscape richness}) \sim \text{isolation}$
- (5) $\log_{10}(\text{gamma soundscape richness}) \sim 1$

As our predictor variables were correlated with one another (see S4.2), we checked for multicollinearity between the predictors by calculating the Variance Inflation Factor (VIF) using the 'vif' function from the 'car' R-package (Fox and Weisberg 2019 - version 3.1-0). We observed a VIF of 1.44, which is within the acceptable range to retain both predictor variables (Johnston et al. 2018). For each model, we tested whether the following assumptions were met: (i) a normal distribution of residuals; (ii) homoscedasticity of residuals; (iii) a zero-mean of residuals; and (iv) independence of residual terms (Supplementary Material S4).

2.4. Decomposing the ecological mechanisms underlying ISARs

Due to stochastic effects, species-area relationships often break down at very small scales, a phenomenon known as the small island effect. As such, we checked for the presence of a small-island effect by comparing four ISAR models for the unrarefied gamma soundscape richness using the 'sar_threshold' function from the 'sars' R-package (v1.3.5 - Matthews et al. 2019): (i) a continuous one-threshold model; (ii) a left-horizontal one-threshold model; (iii) a power-law model without the small-island effect; and (iv) an intercept-only model. We performed model selection using several metrics (small-sample correct Akaike Information Criterion (AICc), Bayesian Information Criterion (BIC) and adjusted R^2). If a small-island effect was detected, we excluded all islands below the threshold value from subsequent analyses investigating soundscape richness-area patterns (Supplementary Material S5).

To account for potential sampling artefacts due to an unequal sampling effort, we calculated the rarefied gamma soundscape richness per island. Here, we employed both temporal-effort-based and plot-based rarefaction to calculate the rarefied gamma soundscape richness, rarefying the sampling effort of the pooled OSU-by-sample incidence matrix to five sampling days and 1 plot per island, respectively (Supplementary Material S2). We tested for the role of disproportionate effects by assessing the relationship between plot-scale alpha soundscape richness and island size. We sub-sampled the total dataset to obtain a uniform sampling regime consisting of one plot per island, ensuring all plots had equal weight on the final alpha soundscape richness-area relationship by repeating the sub-sampling process until all possible combinations of 1-plot subsets across all islands were generated at 110,592 subsets. To assess whether heterogeneity effects were driving SSARs, we assessed the relationship between the beta soundscape turnover and island size. We

calculated the beta soundscape turnover per island using the multiplicative framework provided by Hill numbers, whereby beta is calculated by dividing the regional (unrarefied island-wide gamma) soundscape richness by the average local (alpha) soundscape richness. The beta-turnover captures the degree of heterogeneity in the OSU composition across plots and ranges from 1 to N, where N is the number of plots per island. The beta-turnover can be seen as the effective number of completely distinct soundscapes per island (Tuomisto 2010). As the beta-turnover cannot be computed for islands containing a single sampling plot, 1-plot islands were removed from the data (remaining islands = 13). Next, we subsampled the total dataset to obtain a uniform sampling regime consisting of two plots per island. As before, we repeated the sub-sampling process until all possible combinations of two-plot subsets across all islands in the study were generated (# subsets = 972). We calculated the beta soundscape turnover by dividing the gamma soundscape richness (pooled richness across 2 plots) by the alpha soundscape richness (mean richness across 2 plots).

The relationship between the soundscape richness (rarefied gamma, alpha and beta) and island size was quantified by fitting power-law models.

3. Results

3.1. The effect of island size and isolation on soundscape richness

When controlling for the effect of isolation, island size still explains a significant proportion of the variation ($R^2 = 0.44$; Fig. 2-A1), showing a strong positive relationship between the island size (\log_{10}) and unrarefied gamma soundscape richness ($\log_{10} x$). Conversely, when controlling for the effect of island size, isolation does not explain any more meaningful additional variation ($R^2 = 0.04$; Fig. 2-A2). Conditioning scatterplots indicated that there was an interaction between island size and isolation on the unrarefied gamma soundscape richness, with isolation acting as a modulator variable (Fig. 2B). In increasingly isolated islands, the effect of island size on the gamma soundscape richness becomes shallower and eventually negative on the most isolated islands. Model selection confirmed the negative area \times isolation interaction (interaction term: -0.73). The most parsimonious model (model 1) describes the change in unrarefied gamma soundscape richness as a function of island size, isolation, and the area \times isolation interaction ($AICc = -79.1$; $R^2_{adj} = 0.64$; Table 1). The model conforms to most

underlying assumptions, but the residuals show a slight deviation from normality (Table S2; Fig. S7).

Table 1: Output of five models compared using an information-theoretic approach. Parameter significance codes: **** = $p < 0.001$; *** = $p < 0.01$; ** = $p < 0.05$; * = $p < 0.1$; “ ” = $p > 0.01$.

Model	Integer	Isolation	Island size (log ₁₀)	Isolation * island size (log ₁₀)	df	R ² _{adj}	AICc	delta
1	0.56****	0.71****	0.85***	-0.73****	5	0.64	-79.1	0.00
2	1.28****		0.14****		3	0.45	-61.6	17.55
3	1.12****	0.18	0.15****		4	0.46	-61.0	18.12
4	1.64****	-0.28*			3	0.05	-34.6	44.50
5	1.42****				2		-33.4	45.70

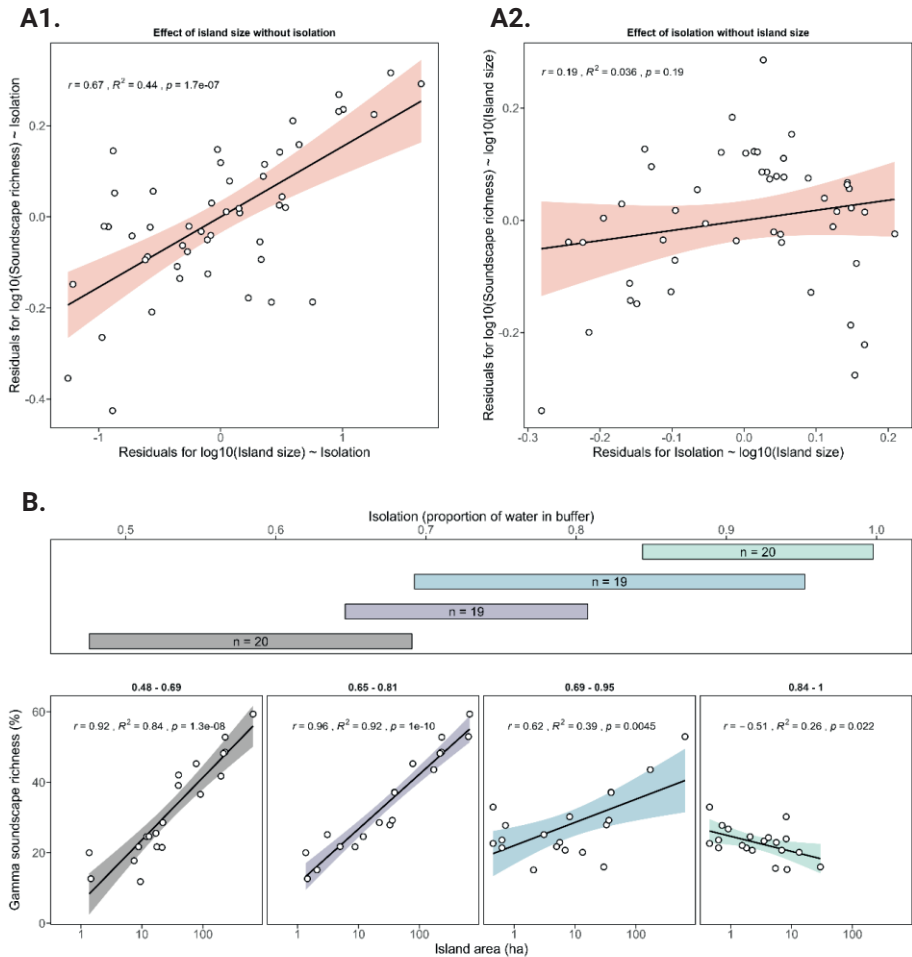


Figure 2: **A.** Partial regression plots showing the relationship between island size (**A1**) and isolation (**A2**), and the unrarefied soundscape richness, considering the variation accounted for by the other variable; **B.** Scatterplots showing the relationships between the unrarefied gamma soundscape richness and island size ($\log_{10} x$) conditioned on island isolation, which is divided into four equal-sized classes with 50% overlap between neighbouring classes.

3.2. Ecological mechanisms underlying ISARs

We find evidence for a small island effect, as indicated by the comparable support for continuous one-threshold and left-horizontal one-threshold models with threshold values at 9.40 and 12.68 ha, respectively (Supplementary Material S5, Fig. S9). As we were interested in the island size effect on soundscape richness and its underlying mechanisms, we excluded all islands smaller than the lowest of these threshold values (9.40 ha) from all subsequent analyses (44 plots retained on 24 islands). In doing so, the power-law model showed a substantially improved positive relationship between island size and the gamma soundscape richness in log-log space (Fig. 3A; $R^2_{\text{adj}} = 0.71$; z-value = 0.28; $\log_{10} c = 1.03$) compared to the full dataset (Fig. 3A; $R^2_{\text{adj}} = 0.45$; z-value = 0.14; $\log_{10} c = 1.28$). Although slightly weaker, this relationship persisted when accounting for unequal sampling effort using either temporal-effort-based rarefaction (Fig. 3-B1; $R^2_{\text{adj}} = 0.54$; z-value = 0.17; $\log_{10} c = 1.15$) or plot-based rarefaction (Fig. 3-B2; $R^2_{\text{adj}} = 0.40$; z-value = 0.13; $\log_{10} c = 1.20$). At the plot-scale, the power-law model showed a positive log-log relationship between island size and the alpha soundscape richness (Fig. 4A;), but not the beta soundscape turnover (Fig. 4B; $R^2_{\text{adj}} = 0.00$; z-value = 0.00; $\log_{10} c = 0.14$).

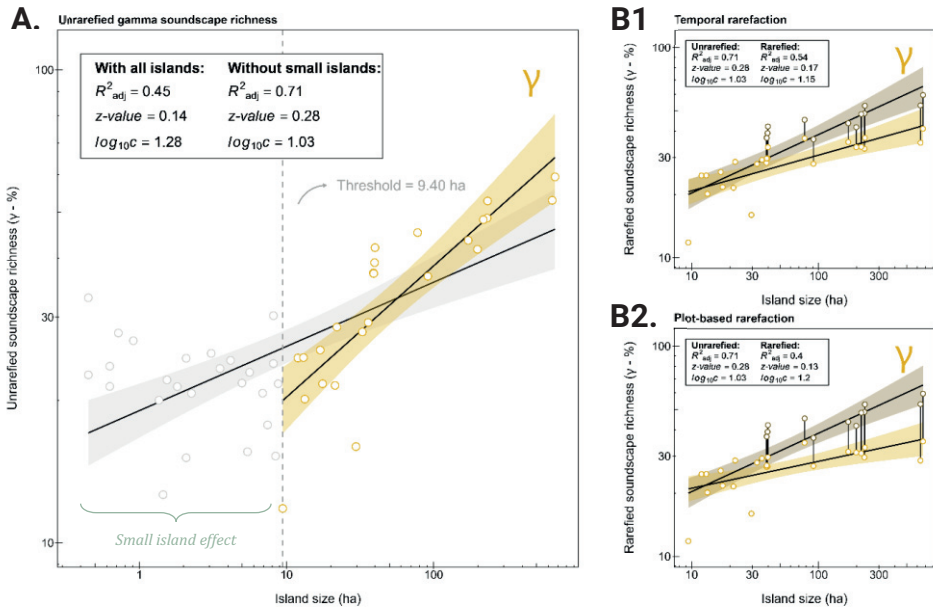


Figure 3: **A.** Relationship between (\log_{10}) island size and the (\log_{10}) unrarefied gamma soundscape richness for all islands ($n = 49$; light grey) and for islands larger than the 9.4-ha small-island threshold ($n = 24$; yellow). **B1.** Relationship between (\log_{10}) island size and the unrarefied (brown) and rarefied (yellow) (\log_{10}) gamma soundscape richness, using temporal effort-based rarefaction (5 sampling days/island) for the islands larger than 9.4 ha. **B2.** Relationship between (\log_{10}) island size and the (\log_{10}) unrarefied (brown) and rarefied (yellow) gamma soundscape richness using plot-based rarefaction (1 plot/island) for the islands larger than 9.4 ha. For islands with a single plot, the unrarefied and rarefied values are equal, and thus only the rarefied values (yellow) are shown.

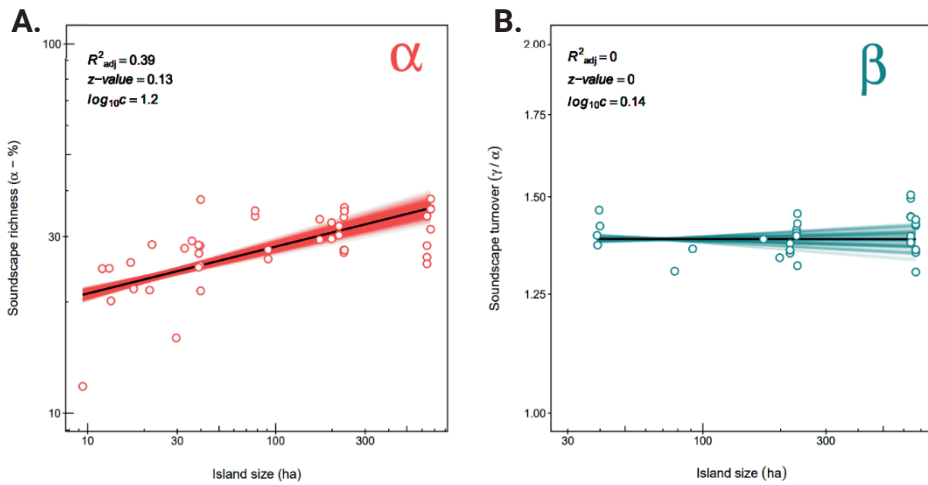


Figure 4: Scatterplots showing the log-log relationship between island size and (A) plot-scale alpha soundscape richness, and (B) beta soundscape turnover. For both plots, solid black lines represent a linear regression fitted to all the data combined (all subset combinations) and coloured lines represent linear regressions fitted to each individual subset (red: 1-plot-per-island subsets; blue: 2-plot-per-island subsets). Due to the large number of subsets for the alpha soundscape richness, only ~10% of subsets were selected for plotting.

Table 2: Slope- (z) and R^2 -values for log-log linear power law models fitted to different dimensions of biological richness, including the soundscape richness (this study), and the species richness derived using direct sampling of vocally-active terrestrial vertebrates (other studies) at the Balbina archipelagic landscape. Since semi-log linear models were reported in the anuran literature, for comparability, the raw data presented in the paper's supplementary material was used to construct log-log linear power models retroactively. For forest birds, no rarefaction was performed since the sampling design had a uniform sampling effort across all islands in the study.

Richness type	Effort	z-value	R ² -value	Model type	# islands	Size range (ha)	Reference
Soundscape richness	Unrarefied	0.28	0.71	Log-log linear	24	9.42 – 668	This study
	Rarefied	0.17 / 0.13	0.54 / 0.40				
Small mammals	Rarefied	0.29	0.69	Log-log linear	25	0.83 – 1,466	Palmeirim et al. (2018)
Frogs	Rarefied	0.18	0.40	Log-log linear	74	0.45 – 1,699	Bueno et al. (2020)
Large vertebrates	Unrarefied	0.29	0.89	Log-log linear	37	0.83 – 1,690	Benchimol & Peres (2015)
Forest birds	Uniform	0.41	0.74	Log-log linear	33	0.63 – 1,699	Bueno et al. (2019)

4. Discussion

In insular systems, local species richness is governed by island size and isolation, a well-known tenet of island biogeography theory. Here, we extended this ecological paradigm to the realm of ecoacoustics, testing the relative importance of island size and island isolation as predictors of the spectro-temporal richness of acoustic traits emanating from the landscape, or soundscape richness. Moreover, we decomposed the soundscape richness at sub-island scales and assessed its relationship with island size to gain insights into the ecological mechanisms that drive observed spatial patterns of acoustic trait diversity.

Overall, our best-fit model provides support for a strong positive effect of island size on the unrarefied gamma soundscape richness. Moreover, a strong negative interaction term in the model vindicates the strength of the soundscape richness \times island size relationship, which decreases in increasingly isolated islands (Fig. 2B; Table 1). This negative interaction is at odds with expectations from the theory of island biogeography (MacArthur and Wilson 1967; Kadmon and Allouche 2007) and a study on Euglossine bees at BHR (Storck-Tonon and Peres 2017), where decreasing immigration rates associated with increasing isolation steepened the ISAR curve. Yet, our island size and isolation variables were negatively correlated, indicating that highly connected small islands and highly isolated large islands were largely missing from the dataset. As we demonstrate a small-island effect, it is plausible that the flattening of the ISAR slope for highly isolated (and small) islands results from stochastic effects obscuring ISAR patterns on small islands, or vice versa.

When we disregard any potential interaction effect, we find that a model containing only island size as a predictor best described the variation in the unrarefied gamma soundscape richness (Table 1; model 2; $R^2_{adj} = 0.44$; z -value = 0.13; $\log_{10}c = 1.28$). As we measured the island isolation as the inverse of the landscape-scale habitat amount, the absence of an isolation effect suggests that the sampling effect underlying the habitat amount hypothesis (Fahrig 2013) is not the driving mechanism behind the soundscape richness gradient. Indeed, the importance of island- versus landscape-scale factors in governing species richness regulation in insular systems is dependent on the degree of 'islandness' of the habitat patches, which in turn depends on the matrix permeability and species dispersal abilities (Bueno and Peres 2019). The lack of a landscape-scale habitat amount effect (HAH) is expected at the BHR, as the habitat patches are separated by an inhospitable open-water matrix that is largely prohibitive to between-patch dispersal for many taxonomic groups (Bueno et al. 2020). In fact, the absence of isolation effects has previously been described for birds (Aurélio-Silva et al. 2016), large vertebrates (Benchimol and Peres 2015b), lizards (Palmeirim et al. 2017) and harvestmen (Tourinho et al. 2020) at the BHR.

ISAR patterns have been repeatedly demonstrated for species-richness and are consistent with several theoretical predictions (MacArthur and Wilson 1967; Connor and McCoy 1979). However, to my knowledge, this represents the first empirical evidence of a positive relationship between whole-island (gamma)

soundscape richness and island size, referred to here as the SoundScape-Area Relationship (SSAR). This term had been previously coined by de Camargo et al. (2019), but these authors derived traditional taxonomic richness data from sound files, thereby capturing a conventional species-area relationship using acoustic methods, which does not fully justify the use of a novel term. Yet, positive ISARs can emerge through a range of mechanisms, including sampling effects (sampling artefacts and passive sampling), disproportionate effects, and heterogeneity effects. We disentangled which of these mechanisms generated the SSAR by dissecting the soundscape richness at various spatial scales.

Prior to assessing the mechanisms underlying observed SSARs, we examined the small-island threshold, below which island size exerts little or no effect on soundscape richness. A piecewise regression revealed the presence of a small-island effect (threshold = 9.4 ha). Small islands at the BHR are affected by severe edge effects, including windfalls and episodic wildfires, which markedly reduce structural forest habitat complexity and resource availability (Benchimol and Peres 2015a). The stochasticity associated with these edge effects can obscure the effect of island size on soundscape richness, leading to the breakdown of the ISARs at small spatial scales. Indeed, operational small-island effects have previously been suggested in our study area for several sound-producing vertebrate taxa. For instance, for anurans, ISARs had weak inferential power below 100 ha (Bueno et al. 2020). Similarly, both large vertebrates and understory birds had much shallower or non-existent ISARs below 10 ha (Benchimol and Peres 2015b; Bueno and Peres 2019). Once islands smaller than 9.40 ha were excluded, the relationship between the unrarefied gamma soundscape richness and island size displayed a much-improved fit ($R^2_{\text{adj}} = 0.71$; $z\text{-value} = 0.28$; $\log_{10} c = 1.03$).

We found a positive relationship between island size and soundscape richness for both the temporal (Fig. 3-B1; $R^2_{\text{adj}} = 0.54$; $z\text{-value} = 0.17$; $\log_{10} c = 1.15$) and plot-based rarefaction (Fig. 3-B2; $R^2_{\text{adj}} = 0.40$; $z\text{-value} = 0.13$; $\log_{10} c = 1.20$), suggesting the relationship is driven by underlying mechanisms beyond sampling artefacts. As expected, the slope and R^2 -values of the SSARs are slightly weaker than most studies based on species richness of known sound-producing taxa reported in the BHR literature (Table 2). This is expected, as acoustic indices can be sensitive to non-target sounds, including abiotic sounds such as rain, wind, or vegetation turbulence (Gasc et al. 2015), thereby introducing undesirable variability into the model. Moreover, the strength of the effect and explanatory power of SAR-models are

sensitive to the range of island sizes under consideration, with both z - and R^2 -values increasing as larger islands are included (Bueno et al. 2020). The largest island included in this study (668 ha) was smaller than those in other SAR-studies at the BHR (approx. 1,500 ha), thus potentially depressing the observed slope and R^2 -values of the log-log linear model.

Alpha soundscape richness showed a positive relationship with island size (Fig. 4A; $R^2_{adj} = 0.39$; z -value = 0.13; $\log_{10} c = 1.20$), indicating that SSARs were at least partly generated by disproportionate (Schoereder et al. 2004) or heterogeneity effects (e.g., through spillover effects - see Giladi et al. 2014). The fact that island size was unrelated to beta soundscape turnover (Fig. 4B; $R^2_{adj} = <0.01$; z -value = <0.01 ; $\log_{10} c = 0.14$) rules out heterogeneity effects, validating disproportionate effects as the main biological mechanism underlying the SSAR. This suggests that island size affects processes that regulate soundscape richness at a local scale. A meta-analysis of plant ISARs found that ~40% of all studies demonstrated a positive relationship between the alpha species richness and island size (Giladi et al. 2014). Moreover, Chase et al. (2019) found that disproportionate effects were an important SAR-generating mechanism for orthopterans and lizards, but not for shrubs. Here, the authors posited that the importance of disproportionate effects versus sampling effects is dictated by the type of matrix and taxa under investigation. For assemblages isolated by hostile matrices, or taxa exhibiting severe dispersal limitation, local processes likely outweigh regional sampling effects, leading to disproportionate effects. Indeed, the vast open-water matrix at BHR typically deters gap-crossing movements, further explaining the importance of disproportionate effects in generating the observed SSARs.

In addition to shedding light on the ecological mechanisms that modulate soundscape richness along a landscape gradient, we can elucidate which mechanisms generate acoustic trait diversity. The strong positive relationship between island size and plot-scale alpha soundscape richness, and the absence of a relationship with beta soundscape turnover, suggest that the landscape-scale richness of acoustic traits is unlikely governed by environmental filtering for optimal sound propagation (acoustic adaptation hypothesis). Otherwise, we would expect the composition of acoustic traits to be uniquely adapted to each habitat and showcase minimal overlap (Mullet et al. 2017). Instead, soundscape richness is much more likely a function of the species richness of sound-producing organisms, as posited by the acoustic niche hypothesis (Krause 1993). Indeed, a strong positive

relationship between soundscape richness and taxonomic richness of vocally-active organisms (frogs, birds, and primates) has previously been shown at the BHR (Luypaert et al. 2022).

The acoustic niche hypothesis states that, over evolutionary timescales, undisturbed ecosystems acquire an equilibrium between sounds in the landscape, resulting in soundscapes with high spectro-temporal complexity and signal diversity, and minimal overlap (Eldridge et al. 2016; Krause 1993; Pijanowski et al. 2011a; Pijanowski et al. 2011b). In fragmented landscapes such as the one in this study, this equilibrium is disturbed, and locally-adapted species are lost from the ecosystem as land-bridge islands become smaller. Previous work at the BHR has shown that, along the island size gradient, forest habitat specialists tend to be lost or replaced with habitat generalists, leading to functional impoverishment (Palmeirim et al. 2017). In the context of the acoustic niche hypothesis, it is plausible that acoustically optimised species are lost from their ecosystem and replaced with generalists that are poorly adapted to the specific acoustic environment they inhabit, leading to overlap in acoustic signals, readily detectable gaps in the soundscape, and ultimately, a lower soundscape richness on more defaunated forest islands.

Although rarely assessed, previous work in Amazonian fragmented landscapes shows that, for large-bodied forest vertebrates, the abundance of nearly all species decreased with either habitat patch (Michalski and Peres 2007) or island size (Benchimol and Peres 2021). Moreover, island size also affects the operational group size of several vocal species, such as primates and trumpeters, which exhibit smaller groups on small islands (Benchimol and Peres 2021). It is likely that these abundance-area relationships also contribute to the observed soundscape-area relationship. For social species, calling rates for both populations (Payne et al. 2003) and individuals (Radford and Ridley 2008; Fernandez et al. 2017) are positively correlated with group size. Moreover, group-living animals exhibiting more complex socioecology produce more complex vocal repertoires, as individuals have to navigate more vocal interactions within and between social groups (Teixeira et al. 2019). The simplified acoustic environment resulting from severe defaunation on smaller islands most likely leads to less elaborate vocal repertoires with lower spectro-temporal complexity and signal diversity. Moreover, for vocalisations associated with competition for resources, a lower abundance of conspecifics on smaller islands may also lead to a reduction in calling rates due to competitive release (Radford and Ridley 2008).

5. Conclusion

This study adds to the growing body of literature on ecoacoustics. We provide evidence for a positive relationship between the richness of acoustic features in a landscape, or the soundscape richness, and island size – which we term the SoundScape Area Relationship (SSAR). We demonstrate that the unrarefied and rarefied gamma soundscape richness, and plot-scale alpha soundscape richness, scale positively with island size, while beta soundscape turnover does not. This suggests that disproportionate effects, but not heterogeneity effects, play an important role in the spatial scaling of soundscape richness at the Balbina Hydroelectric Reservoir. Moreover, we show that this relationship breaks down at the smallest spatial scales, a phenomenon known as the small-island effect. The observed small island threshold corresponds with those previously demonstrated in the study area, confirming that the soundscape metrics we adopted can effectively capture true ecological patterns in the complex acoustic environment characteristic of tropical rainforests.

These findings have broader implications for understanding the effects of habitat fragmentation and insularisation on biodiversity. Our study demonstrates that the consequences of anthropogenic habitat destruction and fragmentation extend beyond species loss to a general reduction in the complexity of ecological communities, including the impoverishment of natural soundscapes, with potential consequences for the functioning of ecosystems. The systematic scaling of soundscape richness with area suggests that acoustic communities experience a predictable simplification with habitat destruction. By measuring soundscape richness at a range of spatial scales, we can unravel complex ecological patterns and their driving factors, demonstrating the value of soundscape analysis as a non-invasive and efficient method for assessing spatial biodiversity patterns.

6. References

- Arrhenius, O.** (1921). Species and Area. *The Journal of Ecology*, 9(1), p.95.
- Aurélio-Silva, M.; Anciães, M.; Henriques, L.M.P.; Benchimol, M.; Peres, C.A.** (2016). Patterns of local extinction in an Amazonian archipelagic avifauna following 25 years of insularization. *Biological Conservation*, 199, pp.101-109.
- Benchimol, M.; Peres, C.A.** (2015a). Edge-mediated compositional and functional decay of tree assemblages in Amazonian forest islands after 26 years of isolation. *The Journal of Ecology*, 103(2), pp.408-420.
- Benchimol, M.; Peres, C.A.** (2015b). Widespread Forest Vertebrate Extinctions Induced by a Mega Hydroelectric Dam in Lowland Amazonia. *PLOS ONE*, 10(7), e0129818.
- Benchimol, M.; Peres, C.A.** (2021). Determinants of population persistence and abundance of terrestrial and arboreal vertebrates stranded in tropical forest land-bridge islands. *Conservation Biology*, 35(3), pp.870-883.
- Bormpoudakis, D.; Sueur, J.; Pantis, J.D.** (2013). Spatial heterogeneity of ambient sound at the habitat type level: ecological implications and applications. *Landscape Ecology*, 28(3), pp.495-506.
- Bradfer-Lawrence, T.; Bunnefeld, N.; Gardner, N.; Willis, S.G.; Dent, D.H.** (2020). Rapid assessment of avian species richness and abundance using acoustic indices. *Ecological Indicators*, 115, p.106400.
- Bueno, A.S.; Masseli, G.S.; Kaefer, I.L.; Peres, C.A.** (2020). Sampling design may obscure species–area relationships in landscape-scale field studies. *Ecography*, 43(1), pp.107-118.
- Bueno, A.S.; Peres, C.A.** (2019). Patch-scale biodiversity retention in fragmented landscapes: Reconciling the habitat amount hypothesis with the island biogeography theory. *Journal of Biogeography*, 46(3), pp.621-632.
- Burivalova, Z.; Towsey, M.; Boucher, T.; Truskinger, A.; Apelis, C.; Roe, P.; Game, E.T.** (2018). Using soundscapes to detect variable degrees of human influence on tropical forests in Papua New Guinea. *Conservation Biology*, 32(1), pp. 205-215.
- Burnham, K.P.; Anderson, D.R.** (2004). Multimodel inference: understanding AIC and BIC in model selection. *Sociological methods & research*, 33(2), pp.261-304.

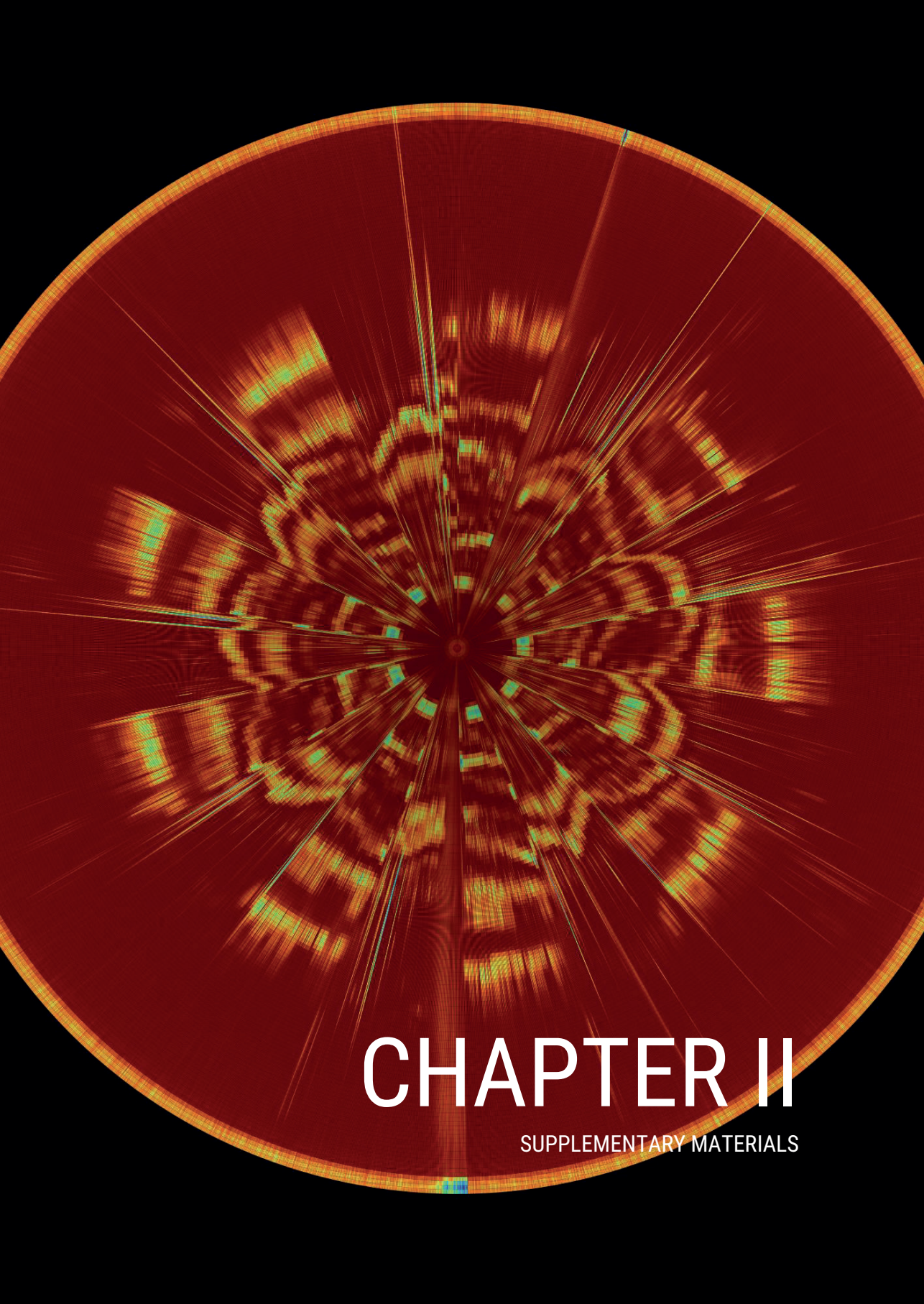
- Chase, J.M.**; Gooriah, L.; May, F.; Ryberg, W.A.; Schuler, M.S.; Craven, D.; Knight, T.M. (2019). A framework for disentangling ecological mechanisms underlying the island species–area relationship. *Frontiers of Biogeography*, 11(1). e40844
- Connor, E.F.**; McCoy, E.D. (1979). The Statistics and Biology of the Species-Area Relationship. *The American Naturalist*, 113(6), pp.791-833.
- de Camargo, U.**; Roslin, T.; Ovaskainen, O. (2019). Spatio-temporal scaling of biodiversity in acoustic tropical bird communities. *Ecography*, 42(11), pp.1936-1947.
- Drakare, S.**; Lennon, J.J.; Hillebrand, H. (2006). The imprint of the geographical, evolutionary and ecological context on species-area relationships. *Ecology letters*, 9(2), pp.215-227.
- Eldridge, A.**; Casey, M.; Moscoso, P.; Peck, M. (2016). A new method for ecoacoustics? Toward the extraction and evaluation of ecologically-meaningful soundscape components using sparse coding methods. *PeerJ*, 4, e2108.
- Eldridge, A.**; Guyot, P.; Moscoso, P.; Johnston, A.; Eyre-Walker, Y.; Peck, M. (2018). Sounding out ecoacoustic metrics: Avian species richness is predicted by acoustic indices in temperate but not tropical habitats. *Ecological Indicators*, 95, pp.939-952.
- Fahrig, L.** (2013). Rethinking patch size and isolation effects: the habitat amount hypothesis. *Journal of Biogeography*, 40(9), pp.1649-1663.
- Farina, A.**; Gage, S.H. (2017). *Ecoacoustics: The ecological role of sounds*: John Wiley & Sons.
- Fearnside, P.M.** (1989). Brazil's Balbina Dam: Environment versus the legacy of the Pharaohs in Amazonia. *Environmental Management*, 13(4), pp.401-423.
- Fernandez, M.S.A.**; Vignal, C.; Soula, H.A. (2017). Impact of group size and social composition on group vocal activity and acoustic network in a social songbird. *Animal Behaviour*, 127, pp.163-178.
- Fox, J.**; Weisberg, S. (2019). *An R Companion to Applied Regression*. Third edition. Thousand Oaks CA. Sage.
- Fuller, S.**; Axel, A.C.; Tucker, D.; Gage, S.H. (2015). Connecting soundscape to landscape: Which acoustic index best describes landscape configuration? *Ecological Indicators*, 58, pp.207-215.

- Galiana, N.;** Lurgi, M.; Bastazini, V.A.; Bosch, J.; Cagnolo, L.; Cazelles, K.; Claramunt-López, B.; Emer, C.; Fortin, M.J.; Grass, I.; Hernández-Castellano, C. (2022). Ecological network complexity scales with area. *Nature ecology & evolution*, 6(3), pp.307-314.
- Gasc, A.;** Pavoine, S.; Lellouch, L.; Grandcolas, P.; Sueur, J. (2015). Acoustic indices for biodiversity assessments: Analyses of bias based on simulated bird assemblages and recommendations for field surveys. *Biological Conservation*, 191, pp.306-312.
- Giladi, I.;** May, F.; Ristow, M.; Jeltsch, F.; Ziv, Y. (2014). Scale-dependent species-area and species-isolation relationships: a review and a test study from a fragmented semi-arid agro-ecosystem. *Journal of Biogeography*, 41(6), pp.1055-1069.
- Gleason, H.A.** (1922). On the Relation Between Species and Area. *Ecology* 3(2), pp.158-162.
- Gonzalez, A.;** Germain, R.M.; Srivastava, D.S.; Filotas, E.; Dee, L.E.; Gravel, D.; Thompson, P.L.; Isbell, F.; Wang, S.; Kéfi, S.; Montoya, J. (2020). Scaling-up biodiversity-ecosystem functioning research. *Ecology Letters*, 23(4), pp.757-776.
- Gooriah, L.D.** (2020). Disentangling the mechanisms underlying the island species-area relationship (ISAR). PhD thesis. Universitäts- Und Landesbibliothek Sachsen-Anhalt, Martin-Luther Universität - Chase, J.; Kostas A.; Triantis, I.H.
- Han, P.;** Zhao, Y.; Kang, Y.; Ding, P.; Si, X. (2022). Island biogeography of soundscapes: Island area shapes spatial patterns of avian acoustic diversity. *Journal of Biogeography*, 0, pp.1-11.
- He, F.;** Legendre, P. (1996). On Species-Area Relations. *The American Naturalist*, 148(4), pp.719-737.
- Helmus, M.R.;** Mahler, D.L.; Losos, J.B. (2014). Island biogeography of the Anthropocene. *Nature*, 513(7519), pp. 543-546.
- Hill, J.L.;** Curran, P.J.; Foody, G.M. (1994). The Effect of Sampling on the Species-Area Curve. *Global Ecology and Biogeography Letters*, 4(4), p.97.
- Jackson, H.B.;** Fahrig, L. (2015). Are ecologists conducting research at the optimal scale? *Global Ecology and Biogeography*, 24(1), pp.52-63.
- Johnston, R.;** Jones, K.; Manley, D. (2018). Confounding and collinearity in regression analysis: a cautionary tale and an alternative procedure, illustrated by studies of British voting behaviour. *Quality and Quantity*, 52(4), pp.1957-1976.

- Kadmon, R.**; Allouche, O. (2007). Integrating the effects of area, isolation, and habitat heterogeneity on species diversity: a unification of island biogeography and niche theory. *The American Naturalist*, 170(3), pp.443-454.
- Krause, B.L.** (1993). The niche hypothesis: a virtual symphony of animal sounds, the origins of musical expression and the health of habitats. *The Soundscape Newsletter*, 6, pp.6-10.
- Lomolino, M.V.** (2000). Ecology's Most General, Yet Protean Pattern: The Species-Area Relationship. *Journal of Biogeography*, 27(1), pp.17-26.
- Luypaert, T.**; Bueno, A.S.; Masseli, G.S.; Kaefer, I.L.; Campos-Cerqueira, M.; Peres, C.A.; Haugaasen, T. (2022). A framework for quantifying soundscape diversity using Hill numbers. *Methods in Ecology and Evolution*, 13(10), pp.2262-2274.
- MacArthur, R.H.**; Wilson, E.O. (1967). *The theory of island biogeography*. Princeton university press.
- MacDonald, Z.G.**; Anderson, I.D.; Acorn, J.H.; Nielsen, S.E. (2018). Decoupling habitat fragmentation from habitat loss: butterfly species mobility obscures fragmentation effects in a naturally fragmented landscape of lake islands. *Oecologia*, 186(1), pp.11-27.
- Matthews, T.J.**; Triantis, K.A.; Rigal, F.; Borregaard, M.K.; Guilhaumon, F.; Whittaker, R.J. (2016). Island species-area relationships and species accumulation curves are not equivalent: an analysis of habitat island datasets. *Global Ecology and Biogeography*, 25(5), pp.607-618.
- Matthews, T.J.**; Triantis, K.A.; Whittaker, R.J.; Guilhaumon, F. (2019). sars: an R package for fitting, evaluating and comparing species-area relationship models. *Ecography*, 42(8), pp.1446-1455.
- Michalski, F.**; Peres, C.A. (2007). Disturbance-mediated mammal persistence and abundance-area relationships in Amazonian forest fragments. *Conservation Biology*, 21(6), pp.1626-1640.
- Müller, S.**; Shaw, T.; Güntert, D.; Helmbold, L.; Schütz, N.; Thomas, L.; Scherer-Lorenzen, M. (2020). Ecoacoustics of small forest patches in agricultural landscapes: acoustic diversity and bird richness increase with patch size. *Biodiversity*, 21(1), pp.48-60.

- Mullet**, T.C.; Farina, A.; Gage, S.H. (2017). The Acoustic Habitat Hypothesis: An Ecoacoustics Perspective on Species Habitat Selection. *Biosemiotics*, 10(3), pp.319-336.
- Niering**, W.A. (1963). Terrestrial Ecology of Kapingamarangi Atoll, Caroline Islands. *Ecological Monographs*, 33(2), pp.131-160.
- Palmeirim**, A.P.; Vieira, M.V.; Peres, C.A. (2017). Non-random lizard extinctions in land-bridge Amazonian forest islands after 28 years of isolation. *Biological Conservation*, 214, pp.55-65.
- Payne**, K.B.; Thompson, M.; Kramer, L. (2003). Elephant calling patterns as indicators of group size and composition: the basis for an acoustic monitoring system. *African Journal of Ecology*, 41(1), pp.99-107.
- Pijanowski**, B.C.; Farina, A.; Gage, S.H.; Dumyahn, S.L.; Krause, B.L. (2011a). What is soundscape ecology? An introduction and overview of an emerging new science. *Landscape Ecology*, 26(9), pp.1213-1232.
- Pijanowski**, B.C.; Villanueva-Rivera, L.J.; Dumyahn, S.L.; Farina, A.; Krause, B.L.; Napolitano, B.M.; Gage, S.H.; Pieretti, N. (2011). Soundscape ecology: the science of sound in the landscape. *BioScience*, 61(3), pp.203-216.
- Preston**, F. W. (1962). The Canonical Distribution of Commonness and Rarity: Part I. *Ecology*, 43(2), p.185.
- Radford**, A.N.; Ridley, A.R. (2008). Close calling regulates spacing between foraging competitors in the group-living pied babbler. *Animal Behaviour*, 75 (2), pp.519-527.
- Rosenzweig**, M.L. (1995). Species diversity in space and time. Cambridge University Press.
- Scheiner**, S.M. (2003). Six types of species-area curves. *Global Ecology and Biogeography*, 12(6), pp.441-447.
- Scheiner**, S.M.; Chiarucci, A.; Fox, G.A.; Helmus, M.R.; McGlenn, D.J.; Willig, M.R. (2011). The underpinnings of the relationship of species richness with space and time. *Ecological Monographs*, 81(2), pp.195-213.
- Schoederer**, J.H.; Galbiati, C.; Ribas, C.R.; Sobrinho, T.G.; Sperber, C.F.; DeSouza, O.; Lopes-Andrade, C. (2004). Should we use proportional sampling for species-area studies? *Journal of Biogeography*, 31(8), pp. 1219-1226.

- Souza, C.M.**; Shimbo, J.; Rosa, M.R.; Parente, L.L.; Alencar, A.; Rudorff, B.F.T., Hasenack, H.; Matsumoto, M.G.; Ferreira, L.; Souza-Filho, P.W.; de Oliveira, S.W. (2020). Reconstructing Three Decades of Land Use and Land Cover Changes in Brazilian Biomes with Landsat Archive and Earth Engine. *Remote Sensing*, 12(17), p.2735.
- Storck-Tonon, D.**; Peres, C.A. (2017). Forest patch isolation drives local extinctions of Amazonian orchid bees in a 26 years old archipelago. *Biological Conservation*, 214, pp.270-277.
- Stowell, D.**; Sueur, J. (2020). Ecoacoustics: acoustic sensing for biodiversity monitoring at scale. *Remote Sensing in Ecology and Conservation*, 6(3), pp.217-219.
- Sueur, J.**; Farina, A.; Gasc, A.; Pieretti, N.; Pavoine, S. (2014). Acoustic Indices for Biodiversity Assessment and Landscape Investigation. *Acta Acustica*, 100(4), pp.772-781.
- Teixeira, D.**; Maron, M.; Rensburg, B.J. (2019). Bioacoustic monitoring of animal vocal behavior for conservation. *Conservation Science and Practice*, 1(8), e72.
- Tjørve, E.** (2003). Shapes and functions of species-area curves: a review of possible models. *Journal of Biogeography*, 30(6), pp.827-835.
- Tjørve, E.** (2012). Arrhenius and Gleason revisited: new hybrid models resolve an old controversy. *Journal of Biogeography*, 39(4), pp.629-639.
- Tourinho, A.L.**; Benchimol, M.; Porto, W.; Peres, C.A.; Storck-Tonon, D. (2020). Marked compositional changes in harvestmen assemblages in Amazonian forest islands induced by a mega dam. *Insect Conservation Diversity*, 13(5), pp.432-444.
- Triantis, K.A.**; Guilhaumon, F.; Whittaker, R.J. (2012). The island species-area relationship: biology and statistics. *Journal of Biogeography*, 39(2), pp.215-231.
- Tuomisto, H.** (2010). A diversity of beta diversities: straightening up a concept gone awry. Part 1. Defining beta diversity as a function of alpha and gamma diversity. *Ecography*, 33(1), pp.2-22.
- Williams, C. B.** (1964). *Patterns in the balance of nature*. Academic Press, London.



CHAPTER II

SUPPLEMENTARY MATERIALS

Supplementary material 1: Data collection

1.1. Collection of acoustic data

The study system

Hydroelectric reservoirs represent an excellent study system to assess the spatial scaling of biodiversity. On the one hand, they constitute a rapidly emerging threat to Neotropical rainforest ecosystems (Finer and Jenkins 2012; Emer et al. 2013; Fearnside 2006). On the other hand, hydroelectric reservoirs are considered a perfect experimental system to study the effects of island area while controlling for confounding effects. For instance, they allow us to capitalise on the fact that all patches were formed simultaneously due to a single disturbance event. Moreover, they have a uniform and largely untraversable matrix, a spatial scale comparable to terrestrial patches and were formed recently enough so that evolution and species adaptation have yet to take effect.

Our study was conducted at the Balbina Hydroelectric Reservoir (BHR) in Brazilian Amazonia (1°40'S, 59°40'W; Fig. 1), one of the largest hydroelectric reservoirs on Earth. The reservoir was formed when a tributary of the Amazon, the Uatumã River, was dammed in 1987, turning the former hilltops of primary continuous forest into > 3,500 islands spanning an area of approximately 300,000 ha (Fearnside 2006). The artificial tropical rainforest archipelago now contains islands spanning a wide range of sizes, ranging from 0.2 to 4,878 ha (Benchimol and Peres 2015). The area's vegetation is characterised by a submontane dense ombrophilous (terra firme) forest. Moreover, the forest structure of larger islands resembles a continuous forest, with large-seeded and canopy tree species dominating assemblies. Conversely, smaller islands are dominated by pioneer species due to edge effects

(Benchimol and Peres 2015). Finally, virtually all islands lack perennial streams due to the submergence of lowland areas.

Data collection: see Bueno and Peres (2019) for a detailed overview of data collection

Acoustic surveys were conducted between July and December 2015, recording long-duration acoustic data at 151 plots on 74 islands and 4 continuous forest sites. As mentioned in the main text, the number of plots per area was proportional to the habitat area associated with each plot and varied between 4-10 for continuous forest sites and 1-7 for islands. At each plot, a passive acoustic sensor (an LG smartphone enclosed in a waterproof case linked to an external omnidirectional microphone) was attached to a tree trunk at 1.5 m height and set to record the soundscape for 1 minute every 5 minutes for 4-10 days at a sampling rate of 44,100 Hz using the ARBIMON Touch application (ARBIMON, <https://arbimon.rfcx.org/>).

Site selection

Several islands and sampling plots were removed from this study: (i) mainland sites; (ii) riparian habitats; (iii) plots with microphone failure; and (iv) plots with overly noisy recordings. Due to the removal of these plots from the study data, some islands deviated from the proportional sampling regime. We rectified this by retroactively removing islands that deviated from the proportional sampling regime ($r = 0.87$; $R^2 = 0.75$ $p < 0.001$; Fig. S1). Ultimately, we retained 69 plots on 49 islands for further analysis (Table S1).

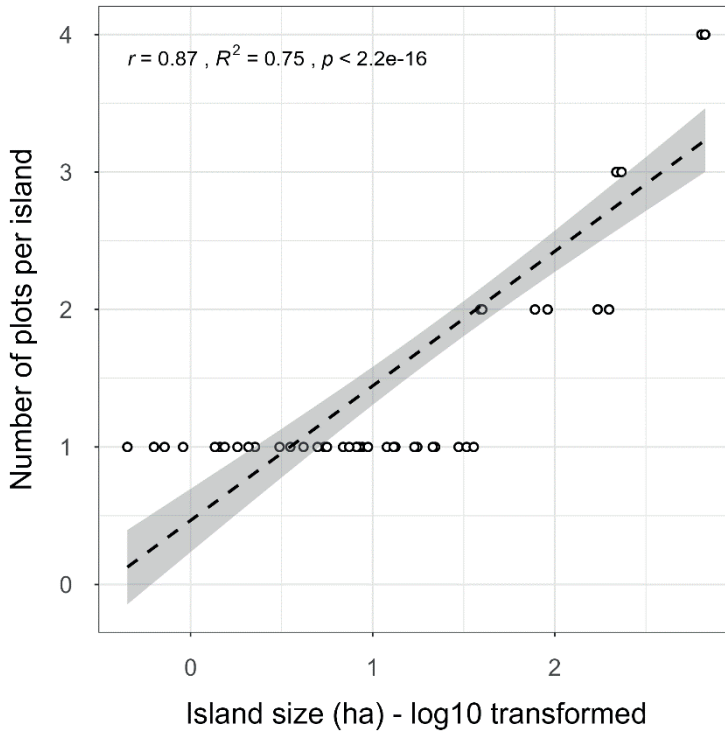


Figure S1: A scatterplot with regression line showing the proportional relationship between the island size (\log_{10} transformed) and the number of acoustic sampling plots per island ($r = 0.87$; $R^2 = 0.75$; $p < 0.001$ for the final set of islands used in the study).

Table S1: An overview of the sites included in the study

Island name	Plot name	Latitude	Longitude	Area (ha)	Island name	Plot name	Latitude	Longitude	Area (ha)
10_626	10_626	-1.75309	-59.39003	8.78	Abandonada_left	Abandonada_left	-1.39418	-59.78186	8.15
10_709	10_709	-1.80791	-59.46624	5.43	Abandonada_right	Abandonada_right	-1.39513	-59.77795	0.45
12_28	12_28	-1.85177	-59.4038	8.42	Abusado	Abusado	-1.76217	-59.67862	13.31
12_9	12_9	-1.5057	-59.79838	11.96	Aline	Aline	-1.54838	-59.75128	2.08
15_188	15_188	-1.55566	-59.72653	1.81	Andre	Andre	-1.58462	-59.87211	2.08
17_697	17_697	-1.44519	-59.8948	17.57	Arrepiado	Arrepiado	-1.51483	-59.73933	7.43
185_358	185_358_A	-1.53759	-59.71342	171.73	Beco_do_Catitu	Beco_do_Catitu_A	-1.75116	-59.70799	638.66
	185_358_B	-1.53013	-59.71838	171.73		Beco_do_Catitu_B	-1.73938	-59.70495	638.66
	2_258	-1.85392	-59.38668	0.72		Beco_do_Catitu_D	-1.73166	-59.69366	638.66
2_333	2_333	-1.83704	-59.46564	0.63		Beco_do_Catitu_E	-1.72938	-59.703	638.66

2_771	2_771	-1.82046	-59.44777	0.45	Cipoal_A	-1.69814	-59.78502	217.63
2_794	2_794	-1.86325	-59.39397	0.91	Cipoal	-1.70343	-59.7876	217.63
2_87	2_87	-1.7457	-59.40742	1.45	Cipoal_C	-1.70606	-59.78051	217.63
	235_234_A	-1.4518	-59.81887	230.7	Coata	-1.48819	-59.7872	16.94
235_234	235_234_B	-1.46164	-59.81255	230.7	Formiga	-1.83339	-59.42093	1.54
	235_234_C	-1.46213	-59.82167	230.7	Furo_de_Santa_Luzia_B	-1.74046	-59.44223	198.52
3_311	3_311	-1.87406	-59.41093	1.36	Furo_do_Santa_Luzia	-1.73941	-59.44632	198.52
33_793	33_793_A	-1.53047	-59.7877	29.62	Garrafa	-1.58863	-59.83535	9.42
34_526	34_526_A	-1.86134	-59.4132	5.61	Jabuti_A	-1.62741	-59.76267	232.49
37_028	37_028_B	-1.77863	-59.38195	32.78	Jabuti_B	-1.62615	-59.75668	232.49
37_7	37_7_A	-1.5103	-59.79834	39.67	Jabuti_C	-1.6291	-59.75201	232.49
	37_7_B	-1.5063	-59.80247	39.67	Joaninha	-1.52243	-59.82888	0.63
4_746	4_746	-1.54811	-59.73888	2.26	Mascote	-1.64506	-59.82035	668.03

43_792	43_792_A	-1.73547	-59.47663	38.94	Mascote_A2	-1.6489	-59.83297	668.03
	43_792_B	-1.74108	-59.47684	38.94	Mascote_B1	-1.64406	-59.84817	668.03
44_174	44_174_A	-1.75791	-59.4764	39.12	Mascote_B2	-1.65936	-59.83546	668.03
	44_174_B	-1.766	-59.48114	39.12	Moita_A	-1.55491	-59.894	91.3
44_21	44_21_B	-1.38776	-59.76615	35.87	Moita_B	-1.55799	-59.89637	91.3
49_62	49_62_A	-1.41565	-59.80996	39.94	Palhal	-1.79071	-59.44785	21.37
	49_62_B	-1.41927	-59.80871	39.94	Panema	-1.7745	-59.69236	3.08
5_708	5_708	-1.57007	-59.71667	3.53	Pe_Torto	-1.76671	-59.36338	4.98
54_544	54_544_B	-1.85262	-59.36253	22.01	Piquia	-1.50662	-59.78885	13.04
	7_335	-1.8555	-59.4506	4.17	Sapupara_A	-1.69722	-59.61253	77.8
8_042	8_042	-1.54737	-59.85917	6.88	Sapupara_B	-1.69699	-59.61744	77.8
8_672	8_672	-1.3854	-59.81981	8.15				

Supplementary material 2: Soundscape richness

To quantify the richness of acoustic traits emanating from the landscape for each island in the study, we employed the analytical pipeline outlined in Luypaert et al. (2022) to calculate the soundscape richness acoustic index. As soundscape diversity metrics aim to capture ecological patterns without the need to isolate and identify species' vocalisations from sound files, they generally lack a unified unit of diversity measurement (*e.g.*, species). To overcome this, the pipeline groups sounds by their shared spectro-temporal properties in the 24h trait space in which species produce sound, better known as 'Operational Sounds Units' or OSUs. Using an incidence-approach, the relative abundance of these OSUs is quantified throughout the recording period and soundscape diversity metrics are calculated using the analytical framework of Hill numbers.

To assess potential patterns of soundscape richness in our insular system and elucidate which underlying mechanisms might drive these, we quantified the soundscape richness using an adapted version of the multi-scale and multi-metric framework outlined in Chase et al. (2019). We analysed the spatial biodiversity scaling using four soundscape metrics at various spatial scales: (i) the unrarefied island-wide gamma soundscape richness; (ii) the rarefied island-wide gamma soundscape richness; (iii) the local plot-scale alpha soundscape richness; and (iv) a beta soundscape turnover metric between plots per island.

2.1. Gamma soundscape richness

Unrarefied gamma soundscape richness

To assess the relative importance of island size versus island isolation (*i.e.*, the proportion of water surrounding the island), and uncover the shape of the island soundscape-area relationship (SSAR), firstly, we quantified the unrarefied island-wide gamma soundscape richness. To do so, we pooled the OSU-by-sample incidence matrices across all plots per island. Per example, for an island consisting of 4 sampling plots with 5 sampling days each, pooling the OSU-by-sample incidence matrices across all plots (each matrix consisting of 5 columns of OSU detection (1) / non-detection (0) data for that sample) would result in a pooled matrix consisting of 20 columns (soundscape samples) containing OSU incidence data. Using the pooled OSU-by-sample incidence matrix per island, we quantified the unrarefied gamma soundscape richness by counting how many unique OSUs were detected across all soundscape samples.

Rarefied gamma soundscape richness

As we employed a proportional sampling scheme, for which larger islands were sampled more intensely, we might expect a positive relationship between the unrarefied gamma soundscape richness and our predictor variables because of sampling effects (sampling artefacts). To account for this unequal sampling effort among islands, we adopted a rarefaction procedure to calculate the rarefied gamma soundscape richness per island. The framework outlined by Chase et al. (2019) employs an individual-based rarefaction framework to equalise the sampling effort

between islands. However, due to the nature of the soundscape richness metric used here, for which we renounced the isolation and identification of individual vocalisations from sound files, this type of individual-based abundance data is not available. Instead, the soundscape richness metric was calculated using sampling-unit-based incidence data. As such, to equalise the sampling effort among islands, we employed a sample-based rarefaction procedure.

For our workflow, what exactly constitutes a sample of the soundscape in the OSU-by-sample incidence matrix is dependent on the scale at which we regard the soundscape. At a plot scale, each 24h period in the acoustic survey represents a sample of the soundscape for which we determine the detection (1) / non-detection (0) of OSUs. As such, when performing sample-based rarefaction, the temporal sampling effort (number of 24h sampling periods in the acoustic survey) is equalised.

However, when regarding the soundscape richness on an island scale, we have multiple sampling plots per island, each with its own OSU-by-sample incidence matrix. When rarefying the sampling effort at this scale, what constitutes a sample of the soundscape can be viewed in one of two ways. If we do not take the spatial heterogeneity between plots into account and assume that OSUs are distributed randomly across the island, we can pool the OSU-by-sample incidence matrices across all plots on the island into one island-scale OSU-by-sample incidence matrix and equalise the sampling effort between islands using the number of 24h soundscape samples. However, if habitat heterogeneity influences the presence and distribution of OSUs across the island, we expect that an increase in the number of

plots per island will inflate the number of detected OSUs. In this case, rather than treating each 24h sampling period in the acoustic survey as a soundscape sample, we should treat each plot as a sample of the soundscape and rarefy the sampling effort using the number of plots per island. In this study, to account for the potential confounding influence of sampling artefacts on the soundscape-area relationship, we rarefied the island-wide gamma soundscape richness using both the temporal- and plot-based rarefaction procedures.

For the temporal rarefaction, we pooled the OSU-by-sample incidence matrices across all plots per island and rarefied the sampling effort between islands to 5 sampling days. For the plot-based rarefaction, we converted each plot's OSU-by-sample incidence matrix to a vector containing the detection (1) / non-detection (0) of OSUs at that plot across the whole acoustic survey. Then, we constructed a novel island-scale OSU-by-sample incidence matrix with plots as samples. We performed plot-based rarefaction to one plot per island. The results of the relationship between island size and the rarefied soundscape richness are presented in the main text (section 3.2).

Supplementary Material 3: Calculating the isolation variable

To examine the degree to which landscape-scale habitat amount (or island isolation) was informative, we follow the approach outlined in MacDonald et al. (2018).

Accordingly, isolation was quantified for all islands in the study by calculating the proportion of water (1 – the proportion of land area) within a range of buffer sizes calculated from the island edge. To determine the optimal scale-of-effect for our isolation variable (Jackson and Fahrig 2015), we considered 40 different buffer sizes, ranging from 50 to 2000 m at 50-m intervals.

The computation of the isolation metric was performed using a combination of the open-source QGIS software (QGIS Association 2022 - version 3.2.2) and the R environment (R Core Team 2022 - version 4.1.2).

3.1. Deriving the total land area shapefiles for islands in the study

First, we downloaded a land cover map for Brazil in 2015 (the time at which the surveys were conducted) using the ‘MapBiomias’ online download tool (collection 2 https://storage.googleapis.com/mapbiomas-public/brasil/collection-6/lclu/coverage/brasil_coverage_2015.tif). Next, the MapBiomias GeoTIFF raster file was uploaded into QGIS and clipped to contain the study landscape (BHR). The ‘identify features’ tool was used to sample the raster values corresponding to the water matrix within the Hydroelectric Reservoir (value = 33). We then used the ‘raster calculator’ to binarise the raster values, setting the water matrix values to 0, and all surrounding land area to 1. The binary matrix was then converted to a set of polygon shapefiles using the ‘polygonize’ function. To retain only the land area as

polygons and remove the water matrix from the shapefile, the attribute table of the polygonised binary raster data was edited, removing all shapefiles containing zero values. This shapefile was merged with the previously generated 'island forest area' shapefile to get the final islands shapefile for the study area. To do so, we used the 'merge' and 'dissolve' functions and patched any holes within polygons using the 'delete holes' function. A visual inspection of the island shapefiles with an ESRI satellite base map revealed an excellent approximation of island shapes at the BHR.

3.2. Generating the buffer rings around the islands in the study

We further isolated individual islands from the final shapefiles of all islands using the 'multipart to singleparts' function and selected the islands in the study area based on the coordinates of the sampling plots using the 'select by location' function. For all islands included in the study area, we generated 40 buffers around each focal island using a range of buffer sizes calculated from the island edge (from 50m to 2000m at 50m intervals). Since we want the buffers to exclude the original island from the buffer area, we used the 'multi-ring buffer' QGIS plugin function. For each buffer size, we calculated the total area covered by the buffer using the attribute table field calculator. Next, to calculate the area covered by land (island or mainland) within each buffer area, we used the 'clip' function, clipping the buffer shapefiles with the shapefile of all islands. Then, we calculated the total land area within each buffer using the attribute table field calculator. The attribute tables were exported from QGIS and imported into R for further analysis. For each island and buffer size, the proportion of land within the buffer area was calculated by dividing the land area by the total area of the buffer. Finally, the proportion of water

within the buffer area was calculated (proportion of water = 1 – the proportion of land). In doing so, we obtained a metric of isolation (proportion of water within the surrounding buffer) which can range from 0 to 1 for 40 different buffer sizes around each of the islands in this study, where lower values indicate less isolated islands and higher values indicate more isolated islands.

3.3. Determining the scale-of-effect

To determine the spatial scale at which the isolation metric attains the strongest relationship with soundscape richness, we calculated the correlation between the unrarefied island-wide gamma soundscape richness and the proportion of water for each of the 40 buffer sizes under investigation.

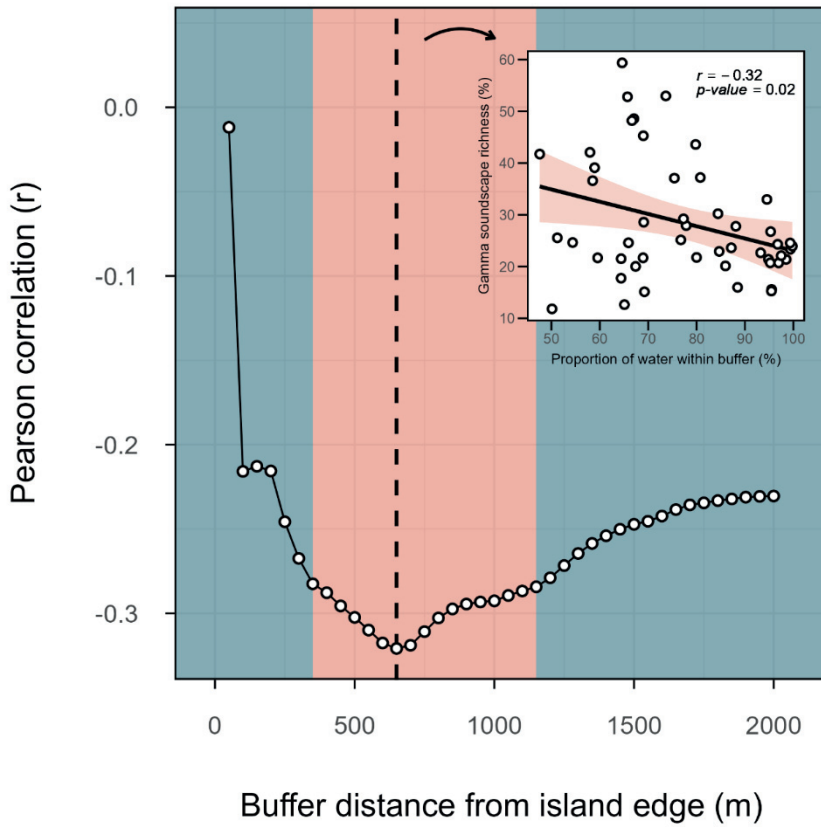


Figure S2: A visual representation of the spatial scale at which the landscape-scale isolation metric derived in this study (proportion of water within the buffer area of each island) attains the highest correlation value with the soundscape richness metric (unrarefied gamma soundscape richness); this is better known as the ‘scale-of-effect’ (Jackson and Fahrig 2015). The blue shading represents buffer distances for which the correlation between soundscape richness and the isolation metric was not significant ($p > 0.05$), whereas orange shading represents significant correlations. The highest correlation value was reached at a buffer distance of 650 m. The inset plot displays the correlation between the soundscape richness and our isolation metric at the scale-of-effect (650 m).

The highest correlation between soundscape richness and our isolation metric was attained at a scale-of-effect of 650 m (Fig. S2). At this spatial scale, we observed a

significant negative correlation between the degree of island isolation and soundscape richness ($r = -0.32$; $p < 0.05$).

Supplementary Material 4: Modelling island size versus isolation

The highest correlation between soundscape richness and our isolation metric was attained at a scale-of-effect of 650 m (Fig. S2). At this spatial scale, we observed a significant negative correlation between the degree of island isolation and soundscape richness ($r = -0.32$; $p < 0.05$).

4.1. Checking variable distributions

Before modelling the data, we assessed the distribution of the three variables under investigation (unrarefied gamma soundscape richness, island size, and island isolation) using raincloud plots and Quantile-Quantile plots (Fig. S3, S4 and S5). We observed a right-skewed distribution for the gamma soundscape richness and island area (Fig. S3 and S4). To account for this, these variables were log-transformed ($\log_{10} x$).

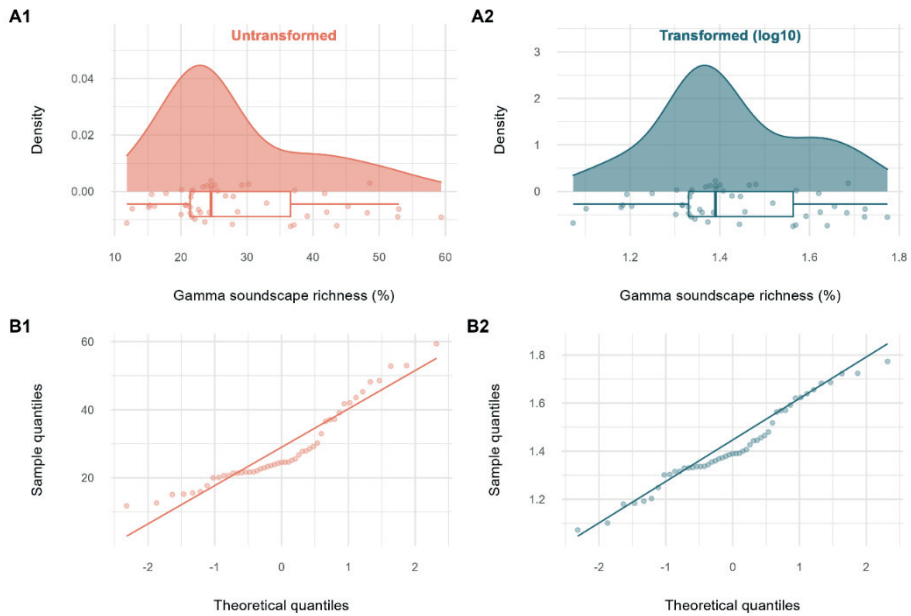


Figure S3: A visual representation of the distribution of unrarefied gamma soundscape richness using (A) density plots and (B) quantile-quantile plots for both untransformed (1; orange) and log₁₀-transformed (2; blue) data.

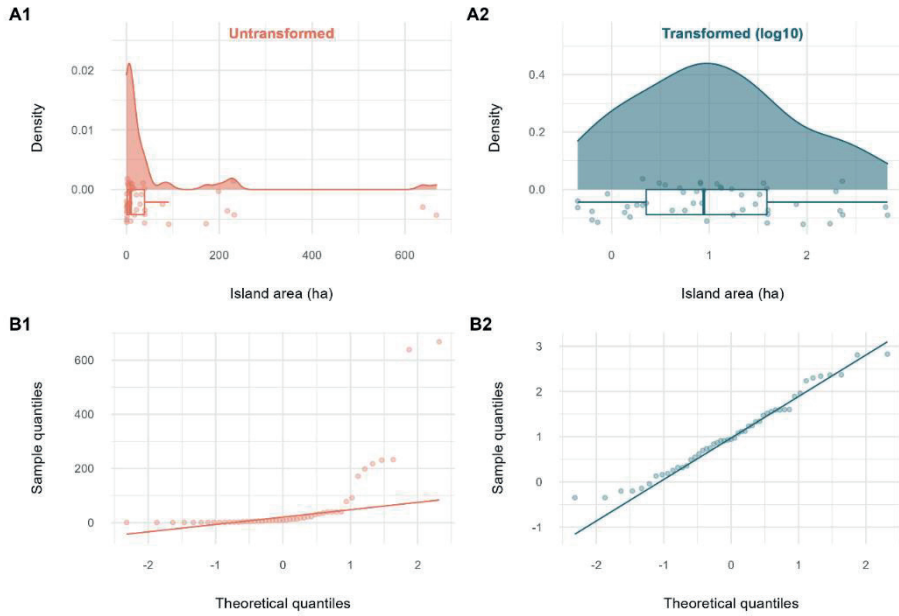


Figure S4: A visual representation of the distribution of the island size variable using (A) density plots and (B) quantile-quantile plots for both untransformed (1; orange) and log₁₀-transformed (2; blue) data.

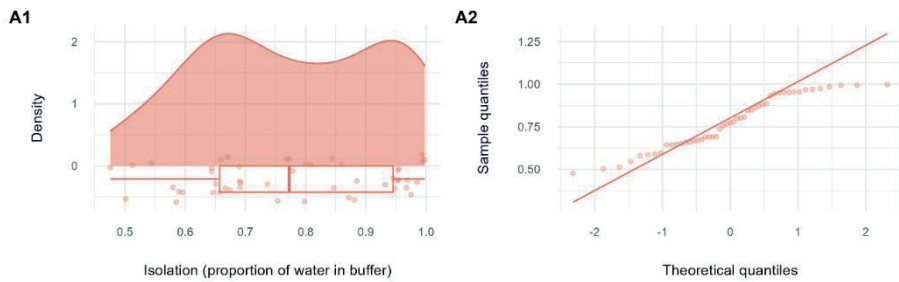


Figure S5: A visual representation of the distribution of the isolation variable (proportion of water within buffer) using (A1) density plots and (A2) quantile-quantile plots.

4.2. Exploring the relationship between predictor variables

In fragmented landscapes, there is often a correlation between the island size and isolation, with smaller islands also being more isolated, or larger islands more connected. As this correlation could have consequences for subsequent modelling procedures, first, we explored the relationship between the size and isolation for the islands contained in the study (Fig. S6).

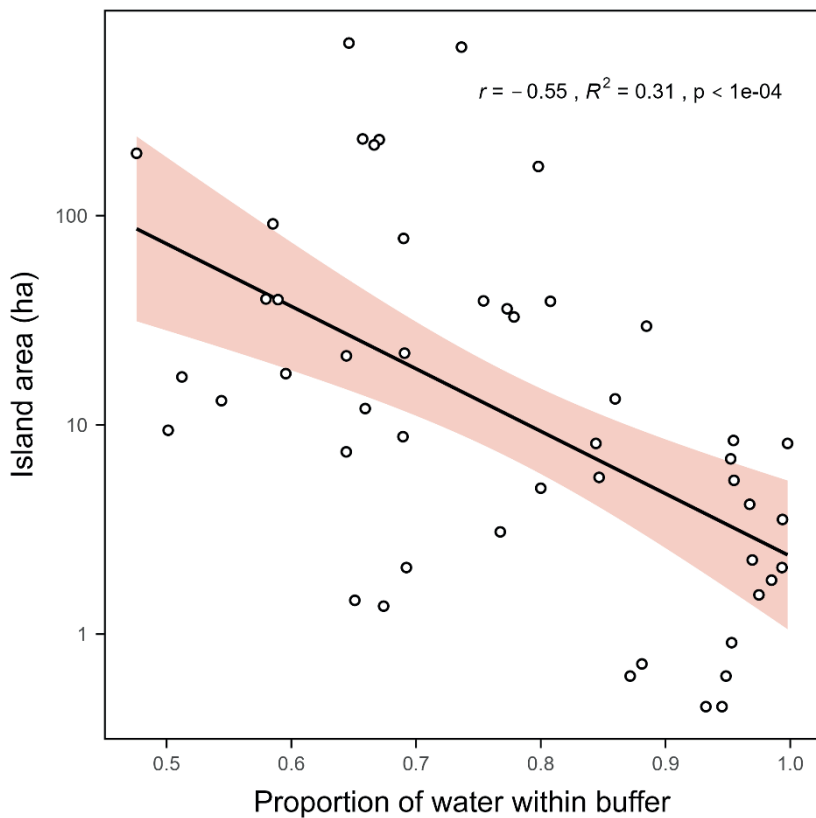


Figure S6: A scatterplot displaying the relationship between the island area (ha – \log_{10} scale) and island isolation (proportion of water within 650 m buffer around the island edge).

Indeed, as anticipated, our two predictor variables have a strong and negative correlation, a typical observation in fragmented landscapes. Our study system is missing highly connected small islands and highly isolated large islands. We will keep this in the back of our minds as we continue our analysis.

4.3. Exploring the relationship between predictor and response variables using partial regression plots

Before fitting our linear regression models, we visually explored the relationship between the unrarefied gamma soundscape richness, and the island size and isolation. However, when using regressions that involve multiple potential predictor variables, the use of bivariate plots to show the relationship between $X \sim Y$ may be misleading, as the regression coefficients may change in magnitude and sign when more than one predictor influences the response variable (Moya-Laraño and Corcobado 2008). Instead, we made use of partial regression plots (also known as added variable plots or adjusted variable plots), which allowed us to plot the effects of area and isolation separately while accounting for the variation taken up by the other variable (Fig. 3A).

Say we are interested in the relationship between $\log_{10}(\text{soundscape richness}) \sim \log_{10}(\text{island size})$, the plot displays the relationship between the residuals of a model between $\log_{10}(\text{soundscape richness}) \sim \text{isolation}$ and the residuals of a model between $\log_{10}(\text{island size}) \sim \text{isolation}$. In doing so, the plot shows the relationship of $\log_{10}(\text{island size})$ on the soundscape richness while eliminating the effect of isolation. Similarly, if we are interested in the relationship between $\log_{10}(\text{soundscape richness}) \sim \text{isolation}$, the plot displays the relationship between

the residuals of a model between $\log_{10}(\text{soundscape richness}) \sim \log_{10}(\text{island size})$ and the residuals of a model between isolation $\sim \log_{10}(\text{island size})$.

4.4. Assessing the presence of an interaction effect between island size and isolation

In addition to visually exploring the relationship between the predictors and the response variable, we were also interested in assessing whether an interaction effect between our continuous predictor variables existed. To test this, we made use of a conditioning plot (also known as a co-plot), a type of scatterplot that shows the relationship between two variables when 'conditioned' on a third variable. In our case, we visualised the potential interaction between the island size and isolation by plotting the relationship between the $\log_{10}(\text{soundscape richness}) \sim \log_{10}(\text{island size})$ for four classes along the isolation range, where each isolation class contained approximately the same number of data points and had a 50% overlap with its neighbouring classes (Fig. 3B).

The conditioning plot shows that the strength of the positive relationship between the unrarefied gamma soundscape richness (\log_{10}) and island size (ha - \log_{10}) decreases with increasing isolation. This is suggestive of a negative interaction effect between the island area and isolation. As such, we included a model with an interaction term when fitting linear models in the next section.

4.5. Fitting linear models

For model fitting, first, we constructed a global model using the following equation:

$$(1) \log_{10}(\text{gamma soundscape richness}) \sim \log_{10}(\text{island area}) + \text{isolation} + \log_{10}(\text{island area}) * \text{isolation}$$

As we know our predictor variables are correlated with each other (Fig. S6), we checked for multicollinearity between the predictors by calculating the Variance Inflation Factor (VIF) for the model without an interaction term (model 3) using the 'vif' function from the 'car' R-package (Fox and Weisberg 2019 - version 3.1-0). We observed a VIF of 1.44, which is within the acceptable range to retain both predictor variables in the model (Johnston et al. 2018).

Next, we fitted four other candidate models:

$$(2) \log_{10}(\text{gamma soundscape richness}) \sim \log_{10}(\text{island area})$$

$$(3) \log_{10}(\text{gamma soundscape richness}) \sim \log_{10}(\text{island area}) + \text{isolation}$$

$$(4) \log_{10}(\text{gamma soundscape richness}) \sim \text{isolation}$$

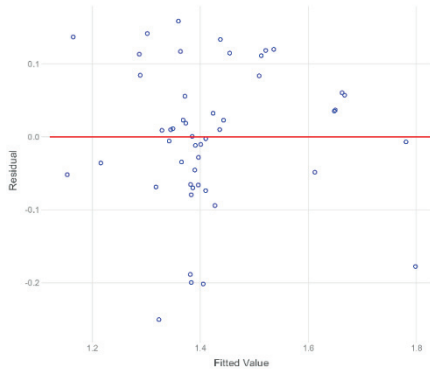
$$(5) \log_{10}(\text{gamma soundscape richness}) \sim 1$$

4.6. Testing model assumptions

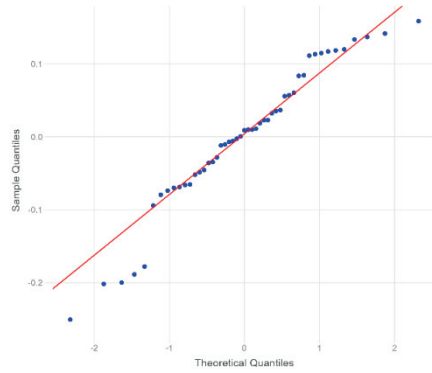
For each of these models, we assessed whether the following assumptions were met: (i) a normal distribution of residuals; (ii) homoscedasticity of residuals; (iii) a

zero-mean of residuals; and (iv) independence of residual terms. We found that all models had a near-zero mean of residuals and independence of residual terms (Table S2). For model 4, the residuals displayed heteroscedasticity, as indicated by the Studentized Breusch-Pagan test. Furthermore, for model 1, the Shapiro-Wilkinson test suggests that the residuals deviate from the assumption of normality slightly, however, this is not confirmed by the Kolmogorov-Smirnov test (Table S2; Fig. S7).

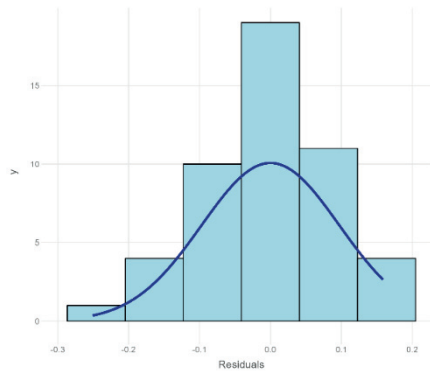
Residual vs Fitted Values



Normal Q-Q Plot



Residual Histogram



Residual Box Plot

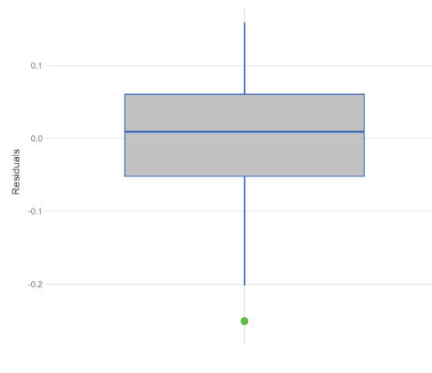
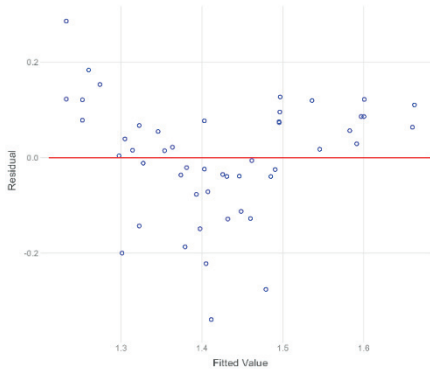
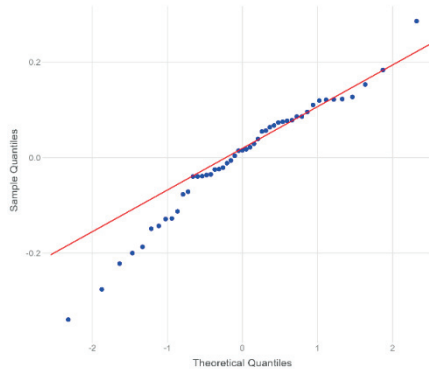


Figure S7: Diagnostic plots showing the residual-vs-fitted plot, residuals qq-plot, residuals boxplot and residuals histogram in clockwise order from the top left to the bottom left for the best fitting model (model 1).

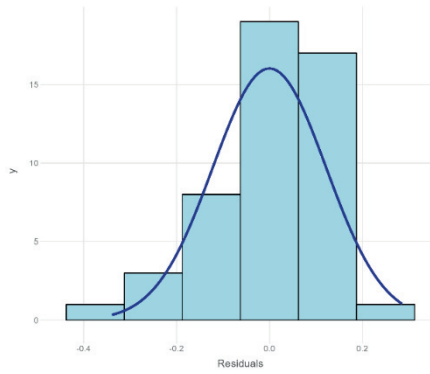
Residual vs Fitted Values



Normal Q-Q Plot



Residual Histogram



Residual Box Plot

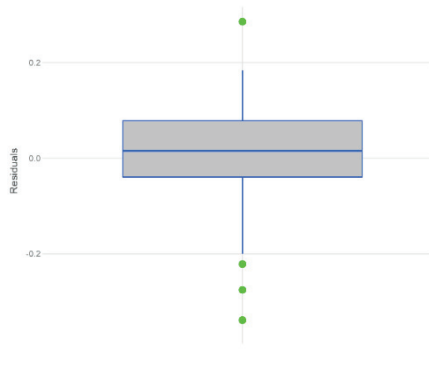


Figure S8: Diagnostic plots showing the residual-vs-fitted plot, residuals qq-plot, residuals boxplot and residuals histogram in clockwise order from the top left to the bottom left for the second-best fitting model (model 2).

Table S2: A diagnostic table for five fitted models with results for the following model assumption tests: (i) normal distribution of residuals; (ii) homoscedasticity of residuals; (iii) a zero-mean of residuals; and (iv) independence of residuals terms. Green indicates the assumption is met, orange indicates a marginal acceptance of the assumption, and red indicates the assumption is not met.

	Normality of residuals		Homoscedacity of residuals	Zero mean residuals	Independent residuals
	Shapiro-Wilk test	Kolmogorov-Smirnov test	Studentized Breusch-Pagan test		Durbin-Watson test
Model 1	W = 0.95; p = 0.05	KS = 0.08; p = 0.85	BP = 0.62; p = 0.89	Mean = $-1.54 * 10^{-18}$	D-W = 1.76; p = 0.40
Model 2	W = 0.97; p = 0.18	KS = 0.13; p = 0.36	BP = 1.59; p = 0.21	Mean = $-9.55 * 10^{-19}$	D-W = 1.89; p = 0.70
Model 3	W = 0.97; p = 0.20	KS = 0.10; p = 0.66	BP = 1.30; p = 0.52	Mean = $3.15 * 10^{-18}$	D-W = 1.89; p = 0.77
Model 4	W = 0.98; p = 0.78	KS = 0.06; p = 0.99	BP = 9.05; p = 0.003	Mean = $-2.26 * 10^{-18}$	D-W = 2.22; p = 0.44
Model 5	W = 0.97; p = 0.16	KS = 0.12; p = 0.40	NA	Mean = $-3.57 * 10^{-19}$	D-W = 2.13; p = 0.70

Supplementary material 5: The small-island effect

The perceived slope of the species-area relationship is sensitive to the scale at which ISARs are considered. According to Lomolino and Weiser (2001), untransformed ISARs should exhibit a sigmoidal form with three distinct phases: (i) at very small spatial scales, a phase with no strong relationship between the species richness and island size (the small-island effect or SIE); (ii) at intermediate scales, a phase with a rapid rise in richness with increasing island size; and (iii) at large scales, a phase with a flattening of the slope towards an asymptote, as the number of species per island reaches the levels of the mainland species pool. Each of these phases is delineated by a turnover point at which the predominant mechanisms that govern species richness in space change.

For our assessment of potential soundscape-area relationships and the mechanisms driving them, we were only interested in the effect of the island area on soundscape richness (phase 2). As such, we tested whether there was a spatial scale below which the effect of island area on the soundscape richness broke down (the small island effect). To do so, we used breakpoint linear regression, following the criteria outlined in Dengler (2010) for robust SIE detection: (i) a goodness-of-fit measure that penalised the model complexity; (ii) inclusion of at least three relevant SIE models (a linear, left-horizontal, and continuous one-threshold model); (iii) model selection in the same S-space; and (iv) inclusion of islands with zero-richness. We employed the 'sar_threshold' function in the 'sars' R-package (Matthews et al. 2019) to fit four SIE models: (i) a continuous one-threshold model; (ii) a left-horizontal one-threshold model; (iii) a log-log linear model (log10); and (iv) an intercept-only

model. As the scales considered in this study ranged from small to intermediate, and to avoid overfitting, we did not test for the presence of phase 3 using two-threshold models. We selected the best model fit while penalising for added model complexity by considering the sample-size-correct Akaike Information Criterion (AICc), Bayesian Information Criterion (BIC) and the adjusted R^2 value.

Considering all model selection factors, we found a comparable fit for the continuous one-threshold and left-horizontal one-threshold models with thresholds at 9.40 and 12.68 ha respectively (Table S3; Fig S9). As such, we used the smaller of both threshold values (threshold = 9.40 ha) as our cut-off for the small island effect in our study. Thus, for all subsequent analyses investigating species-area patterns, we will include only the islands above 9.40 ha.

Table S3: A table containing the small island effect (SIE) model output.

	AIC	AICc	BIC	R^2	R^2 - adj	Threshold (\log_{10} - ha)	Threshold (ha)
Continuous one-threshold	303.42	304.82	312.88	0.82	0.81	0.97	9.40
Left-horizontal	304.41	305.32	311.98	0.81	0.80	1.10	12.68
Linear power-law	342.75	343.28	348.43	0.56	0.53	NA	NA
Intercept-only	380.86	381.12	384.64	0.00	0.00	NA	NA

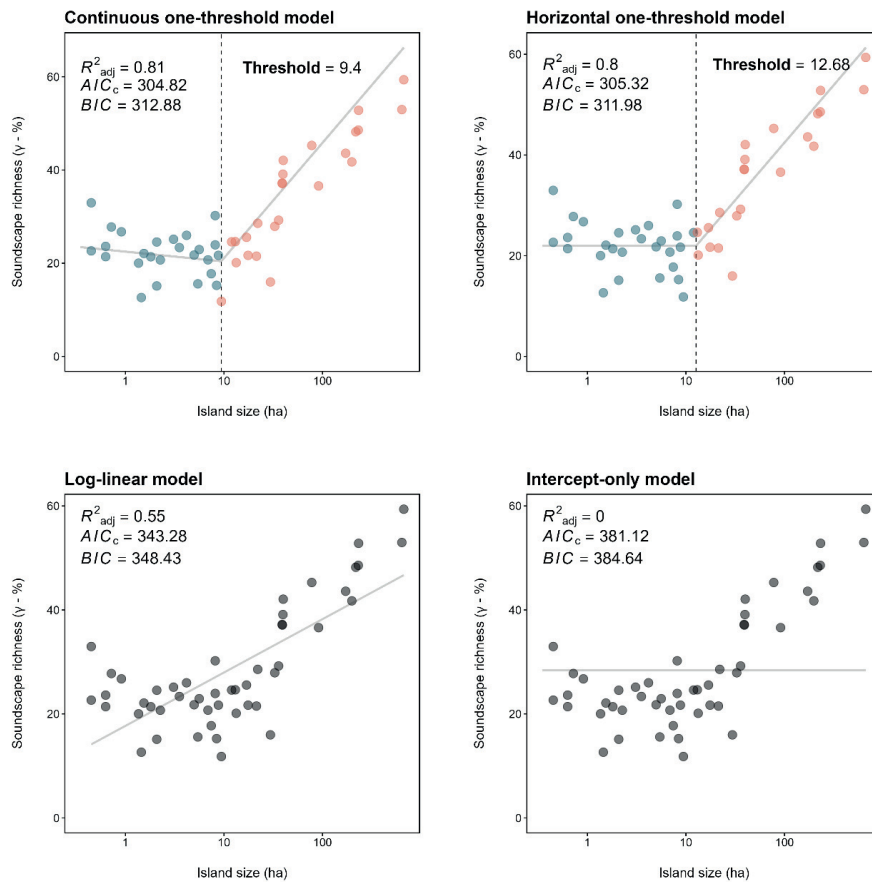
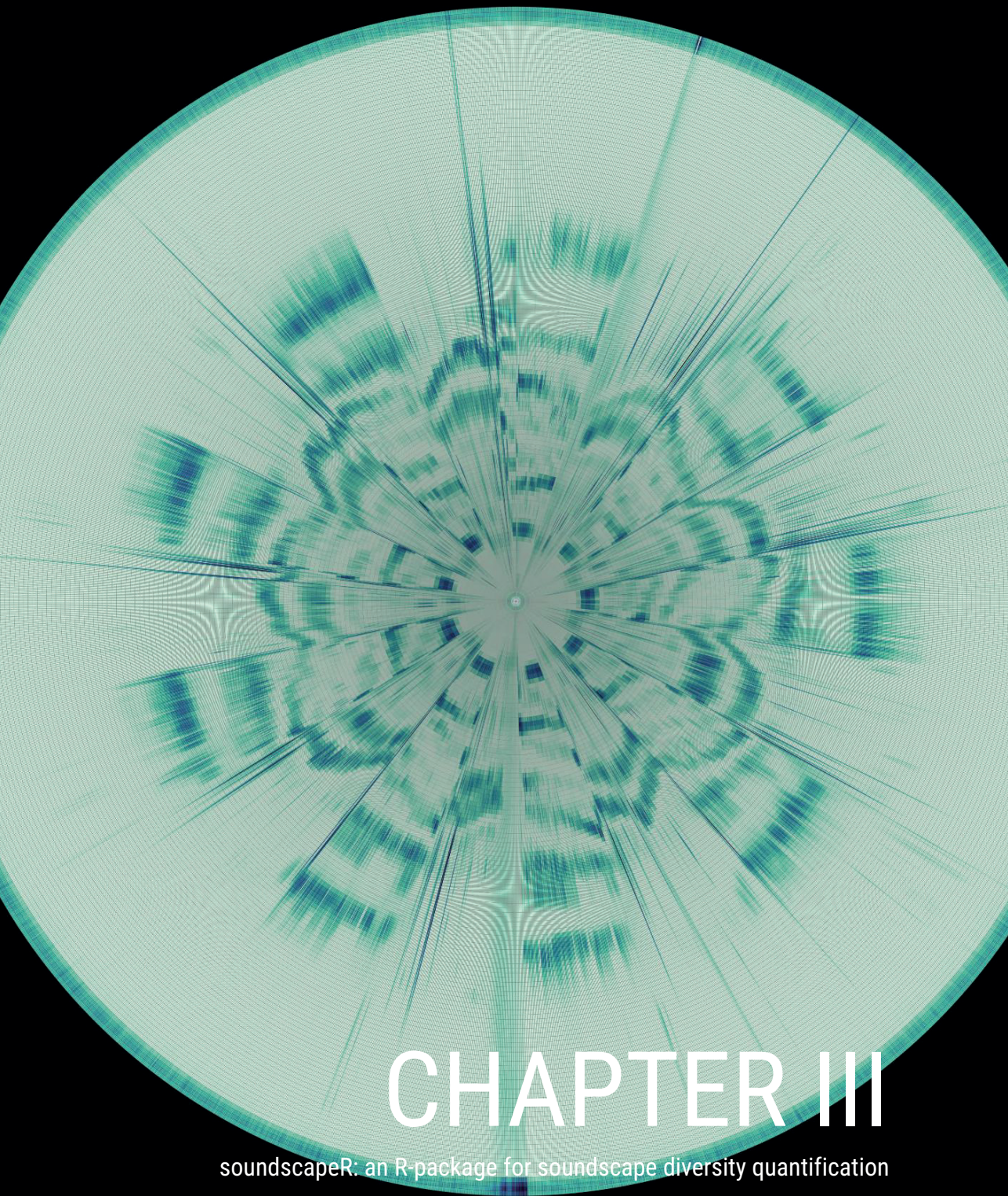


Figure S9: A series of scatterplots with fitted lines (light grey) showing the relationship between the unrarefied gamma soundscape richness and island size (\log_{10}) for four models: (i) a continuous one-threshold model; (ii) a horizontal one-threshold model; (iii) a log-linear model; and (iv) and intercept-only model. The blue and orange dots indicate data points below and above the model's threshold respectively, with the dashed black line indicating the island size threshold for that model. Grey dots indicate the model did not include any threshold

References

- Benchimol, M.;** Peres, C.A. (2015). Edge-mediated compositional and functional decay of tree assemblages in Amazonian forest islands after 26 years of isolation. *Journal of Ecology*, 103(2), pp.408-420.
- Bueno, A.S.;** Peres, C.A. (2019). Patch-scale biodiversity retention in fragmented landscapes: Reconciling the habitat amount hypothesis with the island biogeography theory. *Journal of Biogeography*, 46(3), pp.621-632.
- Chase, J.M.;** Gooriah, L.; May, F.; Ryberg, W.A.; Schuler, M.S.; Craven, D.; Knight, T.M. (2019). A framework for disentangling ecological mechanisms underlying the island species–area relationship. *Frontiers of Biogeography*, 11(1). e40844
- Dengler, J.** (2010). Robust methods for detecting a small island effect. *Diversity and Distributions*, 16(2), pp.256-266.
- Emer, C.;** Venticinque, E.M.; Fonseca, C.R. (2013). Effects of dam-induced landscape fragmentation on Amazonian ant–plant mutualistic networks. *Conservation Biology*, 27(4), pp.763-773.
- Fearnside, P.M.** (2006). Dams in the Amazon: Belo Monte and Brazil’s hydroelectric development of the Xingu River Basin. *Environmental management*, 38, pp.16-27.
- Finer, M.;** Jenkins, C.N. (2012). Proliferation of hydroelectric dams in the Andean Amazon and implications for Andes-Amazon connectivity. *Plos One*, 7(4), p.e35126.
- Fox, J.;** Weisberg, S. (2019). *An R Companion to Applied Regression*. Third edition. Thousand Oaks CA. Sage.
- Jackson, H.B.;** Fahrig, L. (2015). Are ecologists conducting research at the optimal scale? *Global Ecology and Biogeography* 24(1), pp.52–63.
- Johnston, R.;** Jones, J.; Manley, D. (2018). Confounding and collinearity in regression analysis: a cautionary tale and an alternative procedure, illustrated by studies of British voting behaviour. *Quality & Quantity* 52(4), pp.1957-1976.
- Lomolino, M.V.;** Weiser, M.D. (2001). Towards a more general species-area relationship: diversity on all islands, great and small. *Journal of biogeography*, pp.431-445.

- Luypaert**, T.; Bueno, A.S.; Masseli, G.S.; Kaefer, I.L.; Campos-Cerqueira, M.; Peres, C.A.; Hugaasen, T. (2022). A framework for quantifying soundscape diversity using Hill numbers. *Methods in Ecology and Evolution*, 13(10), pp.2262-2274.
- MacDonald**, Z.G.; Anderson, I.D.; Acorn, J.H.; Nielsen, S.E. (2018). Decoupling habitat fragmentation from habitat loss: butterfly species mobility obscures fragmentation effects in a naturally fragmented landscape of lake islands. *Oecologia* 186(1), pp. 11–27.
- Matthews**, T.J.; Triantis, K.A.; Whittaker, R.J.; Guilhaumon, F. (2019). sars: an R package for fitting, evaluating and comparing species–area relationship models. *Ecography*, 42(8), pp.1446-1455.
- Moya-Laraño**, J.; Corcobado, G. (2008). Plotting partial correlation and regression in ecological studies. *Web Ecology*, 8(1), pp.35-46.
- R Core Team** (2021). R: A language and environment for statistical computing. R Foundation for Statistical Computing, Vienna, Austria. <https://www.R-project.org/>



CHAPTER III

soundscapeR: an R-package for soundscape diversity quantification

III soundscapeR: An R-package for the exploration, visualisation, diversity quantification and comparison of soundscapes

Authors

Thomas Luypaert^{1*}, Anderson S. Bueno², Tom Bradfer-Lawrence³, Carlos A. Peres^{4,5},

Torbjørn Haugaasen¹

Affiliations

¹ Faculty of Environmental Sciences and Natural Resource Management, Norwegian University of Life Sciences, Ås, Norway

² Instituto Federal de Educação, Ciência e Tecnologia Farroupilha, Júlio de Castilhos, RS, Brazil

³ Centre for Conservation Science, Royal Society for the Protection of Birds (RSPB), Edinburgh, UK

⁴ School of Environmental Sciences, University of East Anglia, Norwich, United Kingdom

⁵ Instituto Juruá, Manaus, AM, Brazil

*Corresponding authors

Thomas Luypaert (thomas.luypaert@nmbu.no / thomas.luypaert@outlook.com)

Keywords:

Acoustic indices, Acoustic niche usage, Biodiversity monitoring, Ecoacoustics, Hill numbers, Passive Acoustic Monitoring (PAM), R package, Software, Soundscape analysis

Abstract

1. As passive acoustic monitoring technologies continue to gain popularity, the amount of environmental sound recordings has greatly increased. However, researchers still face challenges in extracting ecologically relevant information from these recordings. To overcome the species identification bottleneck, researchers often use acoustic indices, which provide a summary of the spectral and temporal distribution of the energy in acoustic recordings. Although these indices have been broadly applied, methods for analysing big ecoacoustic datasets are still evolving.
2. In a recent publication, we introduced an analytical pipeline that combines the statistical framework of Hill numbers with the computation of acoustic diversity indices, granting us novel insights into acoustic niche usage. Despite the potential of this approach for ecological research, there is currently no software tool available for its implementation.
3. To address this gap, we present `soundscapeR`, an R package that provides an analytical pipeline for exploring, visualising, quantifying, and comparing soundscapes. Specifically designed to process long-duration acoustic recordings of the environment, the package provides flexible functions that allow for the quantification of soundscape diversity across a range of diversity types, scales, and spectro-temporal subsets. Additionally, the package includes a suite of customisable visualisation tools that simplify the exploration of large acoustic datasets.
4. We demonstrate the utility of `soundscapeR` by applying the package to an acoustic dataset from Brazilian Amazonia. Our case study illustrates the

potential of soundscapeR to provide novel insights into acoustic niche usage and to help elucidate the relationships among soundscapes.

1. Introduction

Passive Acoustic Monitoring (PAM) tools have been widely adopted in recent years (Sugai et al. 2019b), yet the effective extraction of ecological information from large acoustic datasets remains a major analytical bottleneck (Gibb et al. 2019; Vella et al. 2022). This has encouraged the development of ecoacoustics, which characterises ecosystems using the collective sounds emanating from the landscape, known as the soundscape (Sueur and Farina 2015). The soundscape encompasses all sounds of biological origin (biophony), as well as those generated by geophysical (geophony) and human (anthropophony) activities (Pijanowski et al. 2011a). Rather than relying on species identification, soundscape analyses aim to establish a relationship between the diversity of acoustic signals in the soundscape and the ecological processes affecting biological communities (Bradfer-Lawrence et al. 2019). Acoustic indices summarise the distribution of acoustic energy across the time and frequency dimensions of sound files, thus condensing information from large acoustic datasets (Eldridge et al. 2018).

At least 65 acoustic indices exist (Buxton et al. 2018), and several software tools have been developed for their computation, including online software (e.g., ecoSound-web: Darras et al. 2020b; ARBIMON: Aide et al. 2013), R-packages (e.g., seewave: Sueur et al. 2008b; soundecology: Villanueva-Rivera et al. 2018b), or terminal-based programs (e.g., AnalysisPrograms: Towsey et al. 2021). Acoustic indices can be classified based on the temporal scale over which the values are calculated. For instance, some of the most widely used indices (e.g., Acoustic Complexity Index or Bioacoustic Index) are generally computed over relatively

short periods (e.g., 1-minute sound files; Truskinger and Towsey 2019a).

Conversely, other metrics, such as the Acoustic Space Use (ASU, available in ARBIMON), quantify acoustic diversity patterns over 24h periods (Aide et al. 2017), offering a different perspective on the use of the acoustic trait space.

In a recent publication, we presented an analytical pipeline that falls in the second category (Luypaert et al. 2022), quantifying soundscape diversity patterns over a 24h period. We proposed three soundscape diversity metrics (soundscape richness, evenness, and diversity) that retain information in both the temporal and frequency dimensions, incorporate the temporal incidence of sound, and integrate the diversity calculations with the mathematically unified framework of Hill numbers. These metrics can be used to calculate diversity values at a range of scales (alpha, beta, gamma) and for spectro-temporal subsets, providing an intuitive way to gain novel insights into acoustic niche usage. We previously demonstrated a positive relationship between soundscape richness and evenness and the taxonomic richness of sound-producing species (Luypaert et al. 2022). Additionally, we showed that soundscape richness is sensitive to one of the most fundamental patterns in ecology: the positive scaling of richness with island size, which we termed the soundscape-area relationship (Luypaert et al. 2023).

In this paper, we introduce soundscapeR, an R-package designed to facilitate the implementation of our approach, with functions aiding the exploration, visualisation, diversity quantification, and comparison of soundscapes. The package allows the user to quantify soundscape diversity across a range of diversity types, scales, and spectro-temporal subsets. The package also features a suite of

customisable visualisation tools, simplifying the visual exploration of large acoustic datasets.

2. Package description

2.1. Installation and documentation

The `soundscapeR` package can be installed from GitHub using the `'install_github'` function from the `remotes` R- package (Csárdi et al. 2021):
`remotes::install_github("ThomasLuybaert/soundscapeR")`. We also provide a comprehensive vignette, which contains specific use cases for all the functions in the package: thomasluybaert.github.io/soundscapeR_vignette.

2.2. Data

The `soundscapeR` package is designed to work with long-duration soundscape recordings collected using either continuous or regular-interval (*e.g.*, 1 minute every 5 minutes) sampling regimes using a 1-minute file length (see Truskinger and Towsey 2019). Although the `soundscapeR` functions can handle ultrasonic data in principle, the application of acoustic indices (and CVR in particular) has not been widely used with ultrasonic data. For guidance on soundscape data collection, see Metcalf et al. (2023).

To demonstrate the utility of `soundscapeR`, we analyse a dataset from Brazilian Amazonia consisting of soundscape recordings from two islands in the Balbina Hydroelectric Reservoir (see Bueno et al. 2020): *Andre* Island (2.08 ha) and *Mascote* Island (668.03 ha). The number of plots at which we collected soundscape data was proportional to island size: 1 plot at Andre Island and 4 plots at Mascote Island,

totalling 5 plots. At each of these plots, sound was recorded for 1 minute every 5 minutes for 5 days (1440 1-min sound files per plot) using a 44,100 Hz sampling rate.

The raw sound files for these islands can be downloaded from Data Dryad:

<https://datadryad.org/stash/share/JUnmstefWNy3UUkjk086mA3iGKxOrSI9iHsLzmPo0s>

The R code supporting this case study can be found in Supplementary Materials 2.

2.3. Workflow overview

In this section, we outline a step-by-step approach for using the `soundscapeR` package to implement the workflow presented in Luypaert et al. (2022). Moreover, we present a range of visualisation tools that allow the user to explore and compare soundscapes.

The Hill-based diversity quantification of soundscapes presented in Luypaert et al. (2022) consists of three key steps:

Step 1: Grouping sounds into Operational Sound Units (OSUs) and assessing OSU presence in each sample of the 24h acoustic trait space.

Step 2: Evaluating the prevalence (or incidence) of OSUs across the recording period.

Step 3: Quantifying the soundscape diversity using the framework of Hill numbers.

To simplify the use of our package, we have created an S4-object called a 'soundscape' object (see Table S1). This data object has slots containing all relevant metadata and data objects generated during the workflow (steps 1 and 2 above). The soundscape object serves as the basis for all downstream functions in the workflow (step 3 above). Hence, metadata only need to be entered once and is remembered downstream. Additionally, all chosen parameters in the workflow are stored by the soundscape object and can be easily accessed. Finally, the slots containing the various metadata and data objects have strict expectations of what each data input looks like, minimising the chance of accidental errors. To perform the steps described above, as well as conduct additional analyses, the functions in the `soundscapeR` package can be divided into four categories (Fig. 1):

1. Functions for file management:

`ss_find_files` and `ss_assess_files`

2. Functions for preparing the soundscape object (steps 1 and 2):

`ss_index_calc` and `ss_create`

3. Functions for visualising and quantifying the diversity of a single soundscape (step 3) `ss_heatmap`, `ss_diversity`, `ss_evenness`, and `ss_diversity_plot`

4. Functions for comparing the diversity of multiple soundscapes:

`ss_compare`, `ss_pcoa`, `ss_divpart`, and `ss_pairedis`

A comprehensive summary of the functions currently available in `soundscapeR` is provided in Table S2.

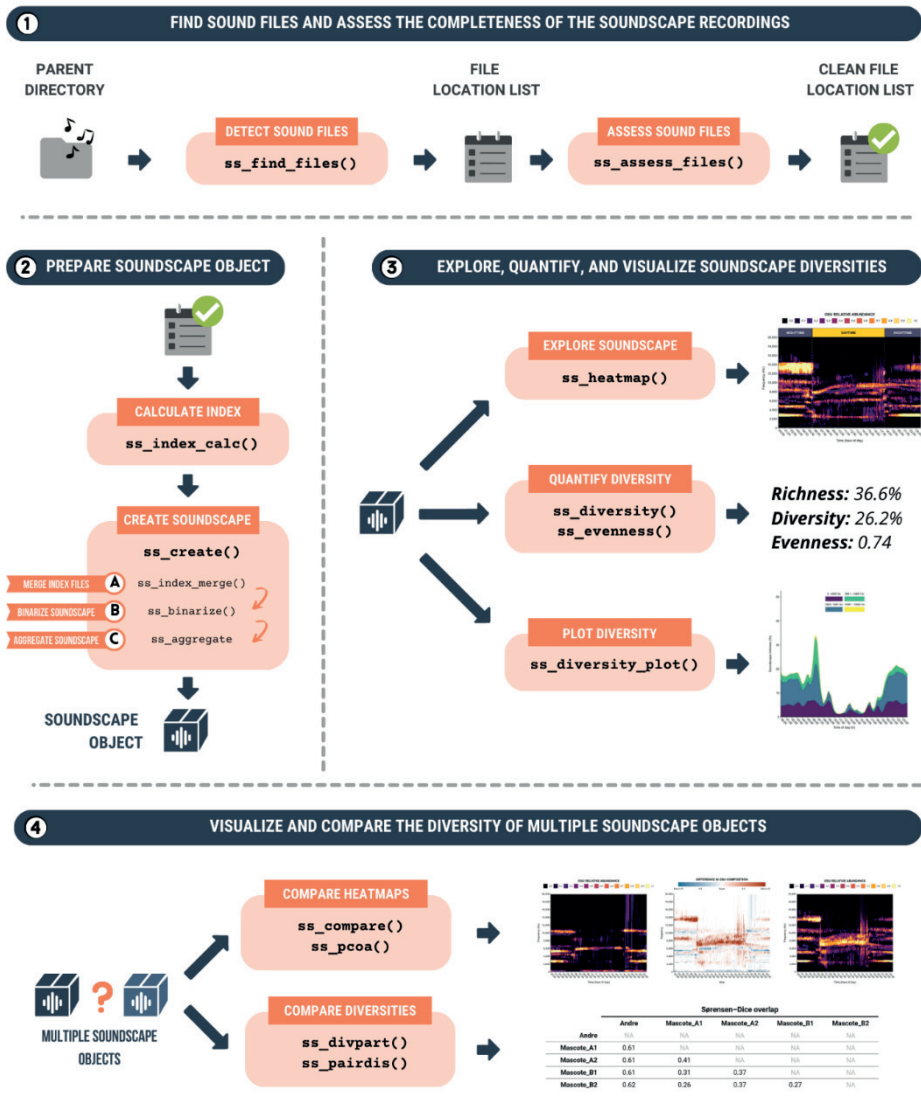


Figure 1: An overview of the soundscapeR workflow. The suite of functions in soundscapeR can be divided into four categories: (1) file management; (2) soundscape preparation; (3) exploring the diversity of a single soundscape; and (4) comparing the diversity of multiple soundscapes.

3. Function descriptions

3.1. File management: `ss_find_files` and `ss_assess_files`

We assume the user has successfully collected soundscape recordings at one or multiple sites and that these files are stored on the user's device, external hard drive, or High-Performance Computing platform.

The `ss_find_files` function automatically detects all sound files within a specified parent directory and subdirectories. The function returns a list of vectors containing the location of each sound file for each site or period. Next, `ss_assess_files` is applied to the `ss_find_files` output. This function automatically detects the temporal sampling regime (*i.e.*, continuous or regular-interval) that was used to record the soundscape and uses this information to identify missing files. Furthermore, the function can be used to exclude any sound files that are not part of a full sampling day (24h period). The result of this process is a cleaned list of vectors with sound file locations.

```
fileloc <- ss_find_files(parent_directory = output_dir)
fileloc <- ss_assess_files(file_locs = fileloc, full_days
= TRUE)
```

3.2. Preparing a soundscape object: `ss_index_calc` and `ss_create`

To quantify the soundscape diversity in the 24h acoustic trait space, a novel unit of diversity measurement called the Operational Sound Unit (OSU) was introduced by Luypaert et al. (2022). OSUs group all sounds occurring into a 24h sample of the soundscape by their shared spectro-temporal properties. Like time-frequency bins

in a spectrogram, OSUs divide the acoustic trait space into discrete spectro-temporal bins, allowing for a comprehensive representation of the distribution of sounds in the soundscape.

To compute the OSUs, the Acoustic Cover (CVR) spectral acoustic index (formerly called 'Activity' or 'ACTsp'; Towsey 2017) is employed to capture the acoustic characteristics of sound in 1-minute recordings. The CVR index generates a vector of values, where each value corresponds to a frequency bin in a 1-minute spectrogram. These values indicate the proportion of cells in a noise-reduced frequency bin that exceed a 3-dB threshold, ranging from 0 to 1. To perform this task, we input the sound file locations (obtained using `ss_find_files` and `ss_assess_files`) into the `ss_index_calc` function. This function calculates the CVR index for each sound file in a folder and saves the output as a `'csv'` file in a user-specified directory.

To calculate the CVR indices for each 1-min file of Andre Island, we use:

```
ss_index_calc(file_list = fileloc[["Andre "]],  
              window = 256,  
              parallel = FALSE)
```

After index computation, we use `ss_create` to create a soundscape object. This function is a wrapper that applies three sub-functions in sequence. First, `ss_index_merge` performs chronological concatenation of the previously calculated CVR index into a time-frequency data frame. Second, `ss_binarize` converts the raw CVR values into a binary detection (1)/ non-detection (0) variable for each day in the recording period using a threshold determined with the IsoData binarisation algorithm (see the package documentation for available binarisation

options). Last, `ss_aggregate` calculates the incidence (or relative abundance) of each time-frequency bin in a 24h period (each bin is an OSU) across all sampled days. Although each of these sub-functions can be used individually, in most cases, the `ss_create` function will meet the user's needs in a single step. The `ss_create` function returns an S4 soundscape object (Table S1) that contains all the information required for subsequent diversity quantification using Hill numbers (OSUs presence and relative abundance), as well as relevant metadata and workflow parameter choices.

To create a soundscape object, we can use:

```
# Direct method

Andre_soundscape <-
  ss_create(fileloc = paste0(output_dir, "/Andre"),
            samplerate = 44100,
            window = 256,
            index = "CVR",
            date = "2015-10-10",
            lat = -1.58462,
            lon = -59.87211,
            method = "IsoData",
            output = "incidence_freq")

# Step-by-step

#1. Merge CVR files

Andre_soundscape_merged <-
  ss_index_merge(fileloc = paste0(output_dir, "/Andre"),
                 samplerate = 44100,
                 window = 256,
                 index = "CVR",
                 date = "2015-10-10",
                 lat = -1.58462,
```

```
lon = -59.87211)
```

```
#2. Binarise CVR values
```

```
Andre_soundscape_binarized <-  
  ss_binarize(merged_soundscape = Andre_soundscape_merged,  
             method = "IsoData")
```

```
3. Calculate OSU incidence
```

```
Andre_soundscape_aggregated <-  
  ss_aggregate(binarized_soundscape =  
Andre_soundscape_binarized,  
               output = "incidence_freq")
```

3.3. Example dataset

The raw sound files of our case study data are too large to include in the package as example data. If we repeat phase 1 (file management) and phase 2 (soundscape preparation) for both case study islands, we obtain a list of soundscape objects that can be used for all downstream analyses. This data is included in the `soundscapeR` package to support all downstream code examples and can be loaded as follows:

```
data(balbina)
```

For additional information on the dataset, use:

```
?balbina
```

The remaining functions in the `soundscapeR` package can be classified into two types: (i) functions for exploring and visualising the diversity of a single soundscape; and (ii) functions for visualising and contrasting the diversity of multiple soundscapes.

3.4. Exploring the diversity of a single soundscape

In this section, we will access the soundscape for one of our islands in the list using:

```
balbina[["Andre"]]
```

3.4.1. The *ss_heatmap* function

The `ss_heatmap` function generates a visual heatmap representation of the presence and abundance of OSUs within the soundscape. It offers considerable flexibility, including the ability to: (i) automatically annotate the heatmap with local sunrise and sunset times, (ii) subset acoustic trait space to a specific spectro-temporal region of interest, (iii) display the heatmap using either cartesian or polar coordinate systems, (iv) modify the visual aesthetics of the heatmap, such as the colour palette and axis labels, and (v) produce interactive heatmaps to explore OSU values.

To produce a heatmap for the Andre Island soundscape (Fig. 2), we can use:

```
# Regular heatmap with annotation

ss_heatmap(soundscape_obj = balbina[["Andre"]],
           type = "regular",
           annotate = TRUE)

# Polar heatmap with annotation

ss_heatmap(soundscape_obj = balbina[["Andre"]],
           type = "polar",
           annotate = TRUE)
```

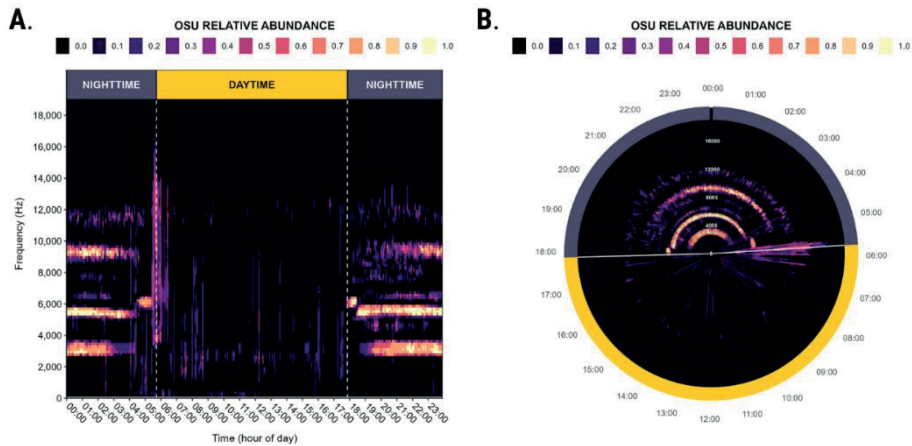


Figure 2: Two heatmaps produced using the `ss_heatmap` function. The heatmaps show the presence and prevalence (or relative abundance) of OSUs for the Andre Island soundscape. The annotation argument allows the user to automatically annotate the heatmap with the time of sunrise and sunset (vertical dashed lines; grey = night; yellow = day), and the boundary between the audible and ultrasonic frequencies (dashed horizontal lines). **A.** A regular heatmap. **B.** A polar heatmap.

3.4.2. The `ss_diversity` and `ss_evenness` functions

The `ss_diversity` function computes the richness and diversity of the soundscape using Hill numbers (Table 1). The `q`-parameter can be adjusted to modify the impact of common or rare OSUs on diversity values. The `ss_evenness` function computes soundscape evenness (Table 1). Both functions allow soundscape diversity metrics to be calculated at various spectro-temporal scales by specifying custom time-frequency limits, computing the soundscape metrics for various built-in diurnal-phase presets (dawn, day, dusk, night), or for every individual recording in the 24h cycle. The resulting diversity metrics can be returned in two ways: (i) as the effective number of OSUs (`output = "raw"`), where the maximum number of detectable OSUs in the soundscape equals the number of soundscape time-

frequency bins; or (ii) the percentage of the acoustic trait space that is saturated with sound (`output = "percentage"`), where the number of detected OSUs is divided by the number of detectable OSUs and multiplied by 100.

To calculate the soundscape richness, diversity, and evenness of Andre Island, we can use:

```
# Richness
SSR <- ss_diversity(soundscape_obj = balbina[["Andre"]],
                    qvalue = 0,
                    subset = "total",
                    output = "percentage")
# Diversity
SSD <- ss_diversity(soundscape_obj = balbina[["Andre"]],
                    qvalue = 2,
                    subset = "total",
                    output = "percentage")
# Evenness
SSE <- ss_evenness(soundscape_obj = balbina[["Andre"]],
                   subset = "total")
```


Table 1: An overview of the soundscape diversity metrics that can be computed using the *soundscapeR* package. Note that the equation for the soundscape evenness was updated compared to Luypaert et al. (2022) to reflect recommendations in Chao and Ricotta (2019) and Chao et al. (2020).

Name	Abbreviation	Equation	Code example value
Soundscape richness	SSR	$SSR = \left(\sum_{i=1}^s p_i^q \right)^{\frac{1}{(1-q)}}$ with $q = 0$	15.13%
Soundscape diversity	SSD	$SSD = \left(\sum_{i=1}^s p_i^q \right)^{\frac{1}{(1-q)}}$ with $q > 0$	10.67%
Soundscape evenness	SSE	$SSE = \frac{(SSD^{q=2} - 1)}{(SSR^{q=0} - 1)}$	0.70

3.4.3. The *ss_diversity_plot* function

The *ss_diversity_plot* function produces area plots showing the variation in soundscape richness or diversity by the time of day. The soundscape metrics can be shown for the full frequency range (`type = "total"`) or the relative contribution of different frequency bins with user-specified width (`type = "frequency"`, `"normfreq"` or `"linefreq"`). Moreover, the function allows the user to: (i) calculate the temporal variation in soundscape metrics for user-specified time-frequency subsets; (ii) apply a moving average filter of user-specified width; and (iii) produce interactive plots to explore diversity values.

To calculate the four different diversity plot types for Andre Island (Fig. 3), we can use:

```
# Total
ss_diversity_plot(soundscape_obj = balbina[["Andre"]],
                  qvalue = 0,
                  graphtype = "total",
                  maxfreq = 20000,
                  smooth = TRUE,
                  movavg = 20)

# Frequency
ss_diversity_plot(soundscape_obj = balbina[["Andre"]],
                  qvalue = 0,
                  graphtype = "frequency",
                  maxfreq = 20000,
                  nbins = 4,
                  smooth = TRUE,
                  movavg = 20)

# Normalised frequency
ss_diversity_plot(soundscape_obj = balbina[["Andre"]],
                  qvalue = 0,
                  graphtype = "normfreq",
                  maxfreq = 20000,
                  nbins = 4,
                  smooth = TRUE,
                  movavg = 20)

# Line frequency
ss_diversity_plot(soundscape_obj = balbina[["Andre"]],
                  qvalue = 0,
                  graphtype = "linefreq",
                  maxfreq = 20000,
                  nbins = 4,
                  smooth = TRUE,
                  movavg = 20,
                  timeinterval = "4 hours")
```

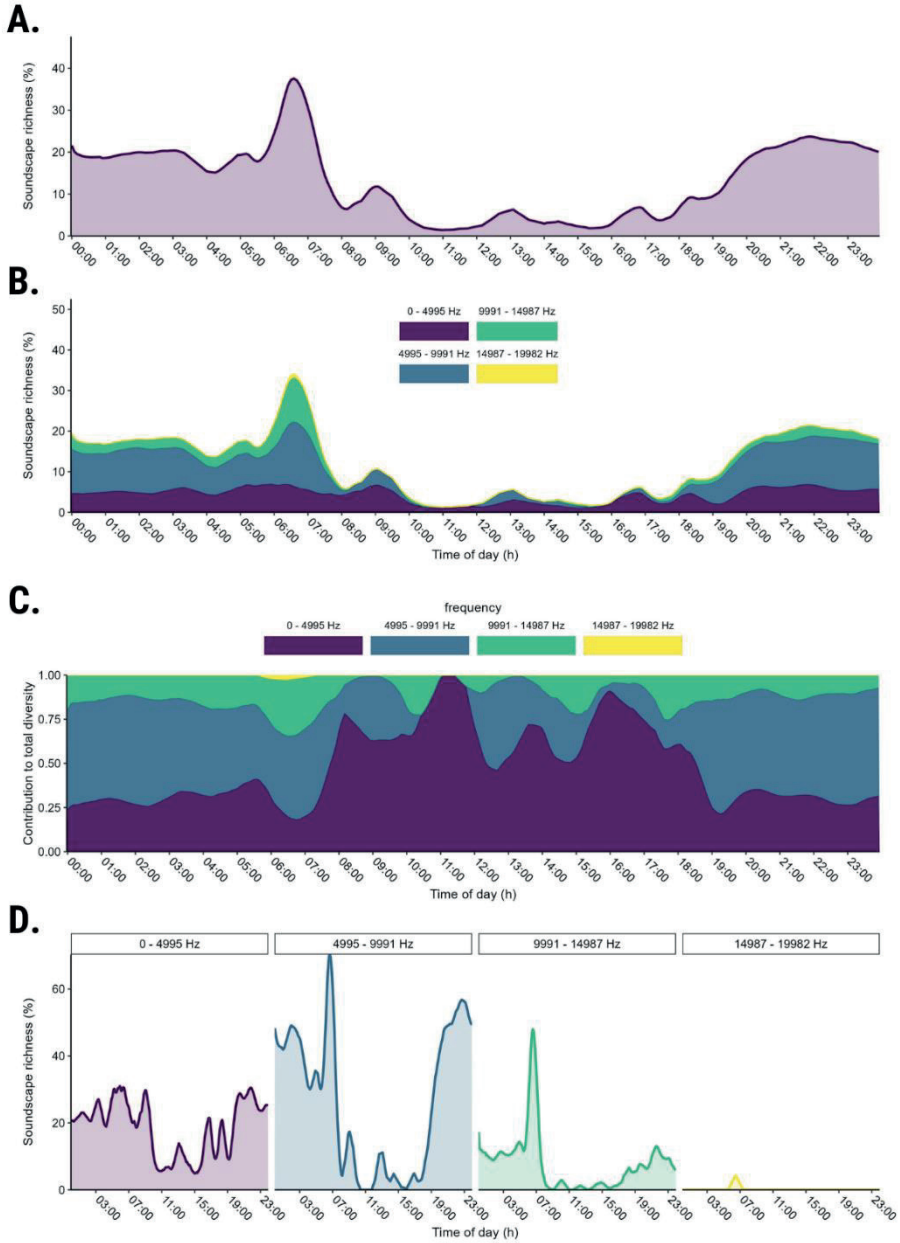


Figure 3: A summary of the plot types available using the `ss_diversity_plot` function. Each plot shows the variation in soundscape richness by the time of day. A. Soundscape richness for the total soundscape (`graphtype = "total"`). B. The contribution of four frequency bins to soundscape richness (`graphtype =`

"frequency"). C. The proportional contribution of four frequency bins to soundscape richness (`graphtype = "normfreq"`). D. The individual variation in soundscape richness for four frequency bins (`graphtype = "linefreq"`).

3.5. Comparing the diversity of multiple soundscapes

3.5.1. The `ss_compare` and `ss_pcoa` functions

The `ss_compare` function takes two soundscape objects and produces differential soundscape heatmaps contrasting the difference in OSU presence and prevalence between the soundscapes. Like the `ss_heatmap` function, the visual appearance of the heatmaps produced by `ss_compare` is customisable.

To compare the soundscapes of Andre Island and one of the plots on Mascote Island (Fig. 4), we can use:

```
ss_compare(soundscape_obj_A = balbina[["Andre"]],
           soundscape_obj_B = balbina[["Mascote_A1"]],
           type = "regular")
```

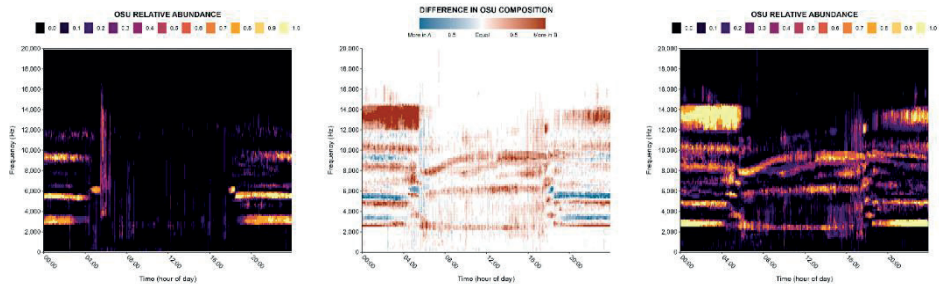


Figure 4: A differential heatmap produced using the `ss_compare` function. The differential heatmap (middle) displays the differences in the OSU presence and prevalence (or relative abundance) between soundscape A (left) and soundscape B (right). Colder colours (blue) indicate OSUs were found more in soundscape A, whereas warmer colours (red) indicate OSUs were found more in soundscape B. When OSU prevalence was equal in both soundscapes, pixels are coloured white.

The `ss_pcoa` function takes a list of soundscape objects and uses a Principal Coordinate Analysis (PCoA) to plot the soundscapes in two-dimensional space based on the Bray-Curtis dissimilarity in the OSU composition.

To produce a PCoA plot of our soundscapes (Fig. 5), we can use:

```
ss_pcoa(soundscape_list = balbina,  
        grouping = c("Andre", "Mascote", "Mascote",  
                    "Mascote", "Mascote"),  
        screeplot = TRUE)
```

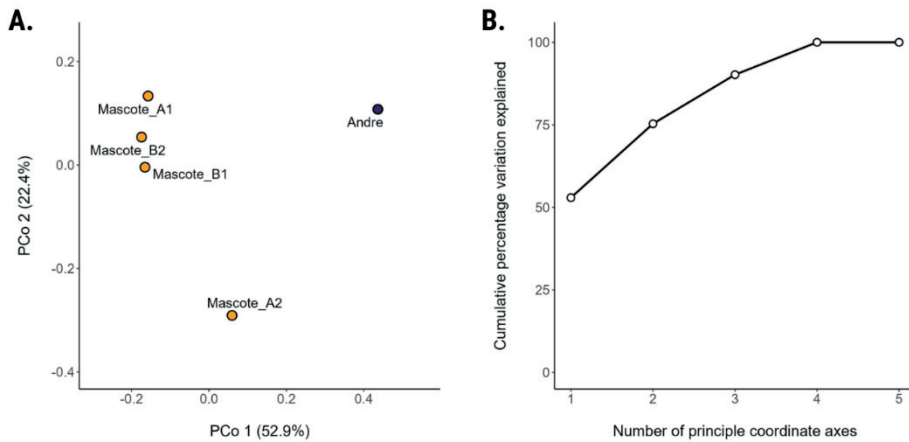


Figure 5: **A.** Principal Coordinate Plot produced using the `ss_pcoa` function showing the relationship between the soundscapes in two-dimensional space, based on pairwise Bray-Curtis dissimilarity between the OSU composition of the soundscapes. **B.** Screeplot showing the cumulative percentage of the variation explained as additional principal coordinate axes are added.

3.5.2. The `ss_divpart` and `ss_pairdis` function

The `ss_divpart` function takes a list of soundscape objects and performs multi-level diversity partitioning, decomposing the soundscape diversity into its respective alpha, beta and gamma diversities following a multiplicative relationship

based on Hill numbers (Luyypaert et al. 2022). As a default, the function partitions the diversity based on a two-level hierarchical structure (Level 1: alpha; Level 2: gamma), however, a multi-tier hierarchical structure can be supplied using the "hier_table" argument. Moreover, the diversity can be partitioned for a range of *q-values* (0-n) and time-frequency subsets.

To partition the soundscape richness and diversity ($q = 0, 1, 2$) into its alpha, beta and gamma components using a two-level hierarchical structure (Table 2), we can use:

```
ss_divpart(soundscape_list = balbina,
           qvalue = 0)
```

```
ss_divpart(soundscape_list = balbina,
           qvalue = 1)
```

```
ss_divpart(soundscape_list = balbina,
           qvalue = 2)
```

Table 2: A table produced using the *ss_divpart* function, showing the diversity components at the sub-system scale (alpha), the whole-system scale (gamma), and the between-system turnover (beta). The soundscape richness and diversities were decomposed using a two-level hierarchical structure.

	Hierarchical levels	# sub-systems (N1)	# systems (N2)	Alpha	Beta	Gamma
q = 0	2	5	1	31.4	57.2	1.82
q = 1	2	5	1	24.9	40.6	1.63
q = 2	2	5	1	20.1	31.0	1.54

The `ss_pairdis` function takes a list of soundscape objects and computes the pairwise dissimilarities among soundscapes as the complement of the: (i) Sørensen–Dice overlap; (ii) Jaccard overlap; (iii) Sørensen–Dice turnover; or (iv) Jaccard-subset turnover.

To compute the pairwise dissimilarities between our soundscapes based on the soundscape richness (Table 3), we can use:

```
ss_pairdis(soundscape_list = balbina,
           qvalue = 0)
```

Table 3: Pairwise dissimilarities (range: 0-1) between the five case study soundscapes, produced using the `ss_pairdis` function. Dissimilarity values were computed for all dissimilarity equations, but only the Sørensen–Dice and Jaccard overlap are displayed.

Sørensen–Dice overlap					
	Andre	Mascote_A1	Mascote_A2	Mascote_B1	Mascote_B2
Andre	NA	NA	NA	NA	NA
Mascote_A1	0.61	NA	NA	NA	NA
Mascote_A2	0.61	0.41	NA	NA	NA
Mascote_B1	0.61	0.31	0.37	NA	NA
Mascote_B2	0.62	0.26	0.37	0.27	NA

Jaccard overlap					
	Andre	Mascote_A1	Mascote_A2	Mascote_B1	Mascote_B2
Andre	NA	NA	NA	NA	NA
Mascote_A1	0.76	NA	NA	NA	NA
Mascote_A2	0.75	0.58	NA	NA	NA
Mascote_B1	0.76	0.48	0.54	NA	NA
Mascote_B2	0.76	0.42	0.54	0.43	NA

4. Summary

The R-package soundscapeR offers a streamlined and accessible workflow for exploring, visualising, quantifying, and comparing soundscapes through the analytical framework of Hill numbers. With a minimal background in ecoacoustics, users can gain insight into patterns in large acoustic datasets. Users can visually explore the presence and prevalence of sound across entire soundscapes and time-frequency subsets. Additionally, users can visually contrast multiple soundscapes, efficiently uncovering differences in acoustic features. By utilising Hill numbers, a variety of soundscape diversity metrics can be easily quantified at various scales and orders of diversity. The package provides a means to partition system-wide diversity into its diversity components and quantify and visualise pairwise dissimilarity among soundscapes. In summary, soundscapeR is a valuable tool that simplifies the exploration and analysis of big acoustic data.

5. References

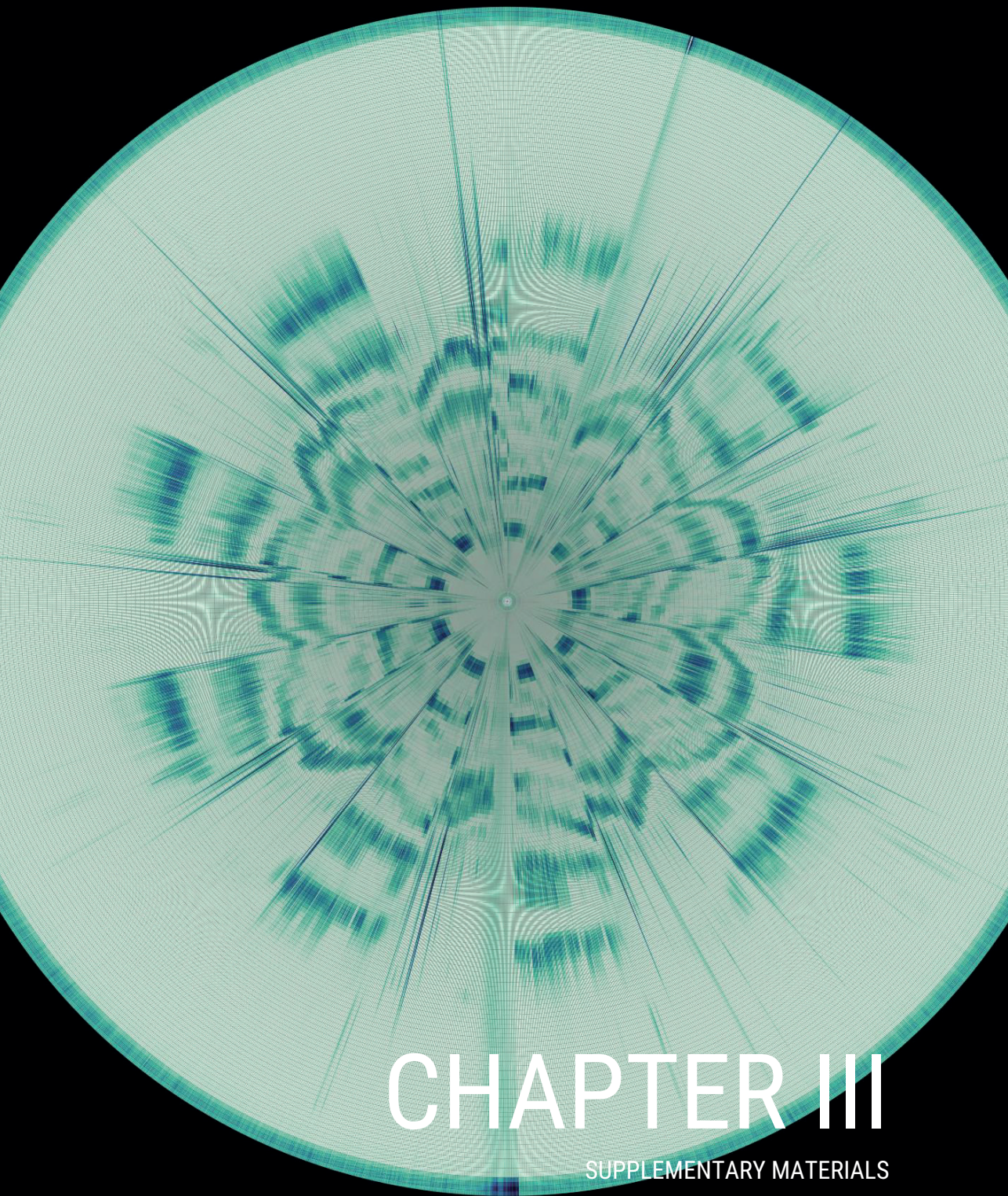
- Aide**, T.M.; Hernández-Serna, A.; Campos-Cerqueira, M.; Acevedo-Charry, O.; Deichmann, J.L. (2017). Species richness (of insects) drives the use of acoustic space in the tropics. *Remote Sensing*, 9(11).
- Aide**, T.M.; Corrada-Bravo, C.; Campos-Cerqueira, M.; Milan, C.; Vega, G.; Alvarez, R. (2013). Real-time bioacoustics monitoring and automated species identification. *PeerJ*, 1, e103.
- Bradfer-Lawrence**, T.; Gardner, N.; Bunnefeld, L.; Bunnefeld, N.; Willis, S.G.; Dent, D.H. (2019). Guidelines for the use of acoustic indices in environmental research. *Methods in Ecology and Evolution*, 10(10), pp.1796-1807.
- Bueno**, A.S.; Masseli, G.S.; Kaefer, I.L.; Peres, C.A. (2020). Sampling design may obscure species–area relationships in landscape-scale field studies. *Ecography*, 43(1), pp.107-118.
- Buxton**, R.T.; McKenna, M.F.; Clapp, M.; Meyer, E.; Stabenau, E.; Angeloni, L.M.; Crooks, K.; Wittemyer, G. (2018). Efficacy of extracting indices from large-scale acoustic recordings to monitor biodiversity. *Conservation Biology*, 32(5), pp.1174-1184.
- Chao**, A.; Kubota, Y.; Zelený, D.; Chiu, C-H; Li, C-F; Kusumoto, B; Yasuhara, M.; Thorn, S.; Wei, C.L.; Costello, M.J.; Colwell, R.K. (2020). Quantifying sample completeness and comparing diversities among assemblages. *Ecological Research*, 35(2), pp.292-314.
- Chao**, A.; Ricotta, C. (2019). Quantifying evenness and linking it to diversity, beta diversity, and similarity. *Ecology*, 100(12), e02852.
- Csárdi**, G.; Hester, J.; Wickham, H.; Chang, W.; Morgan, M.; Tenenbaum, D. (2021). remotes: R Package Installation from Remote Repositories. <https://cran.r-project.org/web/packages/remotes/index.html>.
- Darras**, K.F.A.; Pérez, N.; Mauladi; Dilong, L.; Hanf-Dressler, T.; Markolf, M.; Wanger, T.C. (2020). ecoSound-web: an open-source, online platform for ecoacoustics. *F1000Research*, 9, p.1224.
- Eldridge**, A.; Guyot, P.; Moscoso, P.; Johnston, A.; Eyre-Walker, Y.; Peck, M. (2018). Sounding out ecoacoustic metrics: Avian species richness is predicted by

- acoustic indices in temperate but not tropical habitats. *Ecological Indicators*, 95, pp.939-952.
- Gibb, R.**; Browning, E.; Glover-Kapfer, P.; Jones, K. (2019). Emerging opportunities and challenges for passive acoustics in ecological assessment and monitoring. *Methods in Ecology and Evolution*, 10(2), pp.169-185.
- Luypaert, T.**; Bueno, A.S.; Masseli, G.S.; Kaefer, I.L.; Campos-Cerqueira, M.; Peres, C.A.; Haugaasen, T. (2022). A framework for quantifying soundscape diversity using Hill numbers. *Methods in Ecology and Evolution*, 13(10), pp.2262-2274.
- Luypaert, T.**; Bueno, A.S.; Haugaasen, T.; Peres, C.A. (2023). Extending species-area relationships into the realm of ecoacoustics: The soundscape-area relationship. *bioRxiv*.
- Metcalf, O.C.**; Abrahams, C.; Ashington, B.; Baker, E.; Bradfer-Lawrence, T.; Browning, E.; Carruthers-Jones, J.; Darby, J.; Dick, J.; Eldridge, A.; Elliott, D. (2023). Good practice guidelines for long-term ecoacoustic monitoring in the UK. UK Acoustics Network.
- Pijanowski, B.C.**; Farina, A.; Gage, S.H.; Dumyahn, S.L.; Krause, B.L. (2011). What is soundscape ecology? An introduction and overview of an emerging new science. *Landscape ecology*, 26, pp.1213-1232.
- Sueur, J.**; Aubin, T.; Simonis, C. (2008). Seewave, A free modular tool for sound analysis and synthesis. *Bioacoustics*, 18(2), pp.213-226.
- Sueur, J.**; Farina, A. (2015). Ecoacoustics: The Ecological Investigation and Interpretation of Environmental Sound. *Biosemiotics*, 8(3), pp.493-502.
- Sugai, L.S.M.**; Silva, T.S.F.; Ribeiro, J.W.; Llusia, D. (2019). Terrestrial Passive Acoustic Monitoring: Review and Perspectives. *BioScience*, 69(1), pp.15-25.
- Towsey, M.** (2017): The calculation of acoustic indices derived from long-duration recordings of the natural environment. Technical Report. Available online at https://eprints.qut.edu.au/110634/1/QUTePrints110634_TechReport_Towsey_2017August_AcousticIndices%20v3.pdf
- Towsey, M.**; Truskinger, A.; Cottman-Fields, M.; Roe, P. (2021). QutEcoacoustics/audio-analysis: Ecoacoustics Audio Analysis Software v21.7.0.4: Zenodo.

Truskinger, A.; Towsey, M. (2019). QUT Ecoacoustics | Why do we analyze data in 1-minute chunks? Available online at <https://research.ecosounds.org/2019/08/09/analyzing-data-in-one-minute-chunks.html>.

Vella, K.; Capel, T.; Gonzalez, A.; Truskinger, A.; Fuller, S.; Roe, P. (2022). Key Issues for Realizing Open Ecoacoustic Monitoring in Australia. *Frontiers in Ecology and Evolution*, 9, p.1010.

Villanueva-Rivera, L.J., Pijanowski, B.C. (2018). Package 'soundecology'. R package version, 1(3), p.3.



CHAPTER III

SUPPLEMENTARY MATERIALS

**soundscapeR: An R-package for the exploration, visualisation, diversity
quantification and comparison of soundscapes**

Supplementary Materials 1

Table S1: A table showing the formalised structure of an S4 soundscape object, consisting of 18 slots containing relevant data and metadata about the soundscape and the parameter choices used in the pipeline. The slots can be accessed in R using: `soundscape_object@slotname`.

Andre Island		
Slot	Type	Description
first_day	POSIXct	The first day of the recording period for the soundscape object.
lat	double	The latitude where the soundscape recordings were collected (decimal degrees).
lon	double	The longitude where the soundscape recordings were collected.
tz	character	The time zone in which the soundscape recordings were collected.
sunrise	POSIXct	The time of sunrise.
sunset	POSIXct	The time of sunset.
fileloc	character	The full-length path to where the raw sound files are stored.
index	character	The spectral acoustic index used to determine the presence of sound.
samplerate	double	The sampling rate used to record the soundscape (in Hz).
window	double	The window length used for the Fast Fourier Transformation.
binarization_method	character	The methods used for CVR-index binarisation.
threshold	double	The threshold that was used for the binarisation step.

output	character	“incidence_freq”	The way the OSU incidence data is displayed. Options are ‘raw’ for the absolute OSU count, or ‘incidence_freq’ for the proportion of times OSUs were detected.	
merged_df	data.frame	15:55:00 16:00:00 16:05:00 ...	A data frame containing the raw CVR-index values per sound files (columns) and frequency bin (rows).	
		22050 0.19408888 0.18264127 0.18909356 ...		
		21877 0.45009887 0.48069518 0.49037361 ...		
		21705 0.49172651 0.50431887 0.50005203 ...		
		21533 0.31439276 0.34571756 0.31616193 ...		
		...		
binarized_df	data.frame	15:55:00 16:00:00 16:05:00 ...	A data frame containing the binarised OSU detection/non-detection values, obtained by binarising the merged_df data frame.	
		22050 1 1 1 ...		
		21877 1 1 1 ...		
		21705 1 1 1 ...		
		21533 1 1 1 ...		
		...		
aggregated_df	data.frame	15:55:00 16:00:00 16:05:00 ...	A data frame containing the incidence frequency per OSU across the recording period (displayed here as the proportional incidence value).	
		22050 0.6 1.0 0.6 ...		
		21877 1.0 1.0 1.0 ...		
		21705 1.0 1.0 1.0 ...		
		21533 1.0 1.0 1.0 ...		
		...		
aggregated_df_per_time	list	00:00:00 00:00:00 00:00:00 00:00:00 00:00:00	A list showing the daily incidence of OSUs for each unique time in the recording period. Here, an example is shown for the OSU incidence for the top four frequency bins at midnight (00:00:00) across the recording period (5 days).	
		22050 0 1 0 1 1		
		21877 1 1 1 1 1		
		21705 1 1 1 1 1		
		21533 1 1 1 1 1		

effort_per_time	list	Time	Number of soundscape samples
		00:00:00	5
		00:05:00	5
		00:10:00	5

A list showing the number of soundscape samples (soundscape recordings across a 24h period) per unique time. An example is shown between midnight (00:00:00) and 10 past midnight (00:10:00).

Table S2 : A summary table describing the functions available in the *soundscapeR* R package and associated dependencies, ordered in the sequence of use in the workflow.

Function name		Description	Dependencies
File management	<code>ss_find_files</code>	Takes the path to a parent directory and recursively looks for all directories and subdirectories containing .wav files. The full-length path to each discovered .wav file is saved in a named list maintaining the directory structure.	Base R (R Core Team 2022)
	<code>ss_assess_files</code>	Takes the output list of the 'ss_find_files' function and performs several checks on the files. The function automatically detects the sampling regime of all files and checks whether the time interval between adjacent files in a folder deviates from the expected sampling regime (<i>e.g.</i> , due to missing files). Moreover, the function allows the user to subset the number of files per folder to contain only full sampling days (remove partially sampled days from the study).	Base R (R Core Team 2022)
Prepare soundscapes	<code>ss_index_calc</code>	Takes the output of <code>ss_find_files</code> or <code>ss_assess_files</code> and calculates the spectral acoustic indices.	tuneR (Ligges et al. 2023); seewave (Sueur et al. 2008b); zoo (Zeileis and Grothendieck 2005); terra (Hijmans 2023); tidyR (Wickham et al. 2023b); parallel (R Core Team 2022); doSNOW (Weston 2022a); progress (Csárdi and FitzJohn 2019); foreach (Weston 2022b); assertthat (Wickham 2019).

<code>ss_create</code>	A wrapper function that combines the functions below to create an <code>S4</code> <code>soundscape</code> object:	
<code>ss_merge_index</code>	Takes the output directory where the CVR-index files were saved during the <code>ss_index_calc</code> step. Per <code>soundscape</code> sample (all sound files in the recording period at a single site), concatenates the spectral index vectors (computed using the <code>ss_index_calc</code> function) for each 1-min sound file chronologically. The function produces an <code>S4</code> <code>soundscape</code> object that contains slots with some relevant metadata, as well as a data frame with the time of day as columns and frequency bins as rows and CVR values as cells.	assertthat (Wickham 2019); data.table (Dowle and Srinivasan 2022); lutz (Teucher 2019); hms (Müller 2022); stringr (Wickham 2022); suncalc (Thieurmel and Elmarhraoui 2022); methods (R Core Team 2022).
<code>ss_binarize</code>	Takes the output of <code>ss_merge_index</code> and separates acoustically active OSUs from background noise by converting each OSU's raw spectral index values into a binary detection (1)/non-detection (0) variable. To determine the binarisation threshold, several thresholding methods are available, either using the image thresholding tools available in the <code>autothresholdr</code> package (Landini, Randell, Fouad, & Galton, 2017), modal subtraction, or a custom threshold value.	assertthat (Wickham 2019); autothresholdr (Landini et al. 2017); methods (R Core Team 2022)
<code>ss_aggregate</code>	Takes the output of <code>ss_binarize</code> and calculates the incidence frequency of each Operational Sound Unit (OSU) across the recording period. Returns an <code>S4</code> 'soundscape' object.	assertthat (Wickham 2019); hms (Müller 2022); rlist (Ren 2021); methods (R Core Team 2022)

Single soundscape diversity assessment	Multi-soundscape diversity comparison
<p><code>ss_heatmap</code></p> <p>Takes a soundscape object and produces a visual heatmap representation of the acoustic trait space, showing the OSU presence and prevalence during the recording period.</p>	<p><code>ss_compare</code></p> <p>Takes two soundscape objects. Produces a differential soundscape heatmap to visually contrast the difference in the OSU presence and prevalence between two soundscapes.</p>
<p><code>ss_diversity</code></p> <p>Takes a soundscape object and computes the soundscape richness (SSR; $q = 0$) or soundscape diversity (SSD; $q > 0$) using the statistical framework of Hill numbers.</p>	<p><code>ss_pcoa</code></p> <p>Takes a list of soundscape objects. Uses Principal Coordinate Analysis (PCoA) to plot the soundscapes in a two-dimensional space based on the Bray-Curtis dissimilarity in the OSU composition.</p>
<p><code>assertthat</code> (Wickham 2019); <code>reshape2</code> (Wickham 2007); <code>viridis</code> (Garnier et al. 2021); <code>ggplot2</code> (Wickham 2016); <code>grid</code> (R Core Team 2022); <code>scales</code> (Wickham and Seidel 2022); <code>plotly</code> (Sievert 2020)</p>	<p><code>assertthat</code> (Wickham 2019); <code>reshape2</code> (Wickham 2007); <code>viridis</code> (Garnier et al. 2021); <code>ggplot2</code> (Wickham 2016); <code>grid</code> (R Core Team 2022); <code>scales</code> (Wickham and Seidel 2022); <code>plotly</code> (Sievert 2020), <code>patchwork</code> (Pedersen 2022)</p>
<p><code>assertthat</code> (Wickham 2019); <code>hms</code> (Müller 2022); <code>hilldiv</code> (Alberdi and Gilbert 2019)</p>	<p><code>assertthat</code> (Wickham 2019); <code>vegan</code> (Oksanen et al. 2007); <code>stats</code> (R Core Team 2022); <code>tidyr</code> (Wickham et al. 2023b); <code>ggplot2</code> (Wickham 2016); <code>ggrepel</code> (Slowikowski 2023); <code>viridis</code> (Garnier et al. 2021); <code>grid</code> (R Core Team 2022); <code>patchwork</code> (Pedersen 2022)</p>
<p><code>ss_evenness</code></p> <p>Takes a soundscape object and computes the soundscape evenness (SSE) using the statistical framework of Hill numbers.</p>	<p><code>ss_diversity_plot</code></p> <p>Takes a soundscape object and produces area plots to visualise the variation in the soundscape richness and diversity in a 24h period.</p>
<p><code>assertthat</code> (Wickham 2019); <code>hms</code> (Müller 2022); <code>hilldiv</code> (Alberdi and Gilbert 2019)</p>	<p><code>assertthat</code> (Wickham 2019); <code>stringr</code> (Wickham 2022); <code>pracma</code> (Borchers 2022); <code>ggplot2</code> (Wickham 2016); <code>scales</code> (Wickham and Seidel 2022); <code>grid</code> (R Core Team 2022); <code>plotly</code> (Sievert 2020); <code>dplyr</code> (Wickham et al. 2023a); <code>viridis</code> (Garnier et al. 2021); <code>hms</code> (Müller 2022); <code>hilldiv</code> (Alberdi and Gilbert 2019)</p>

<code>ss_divpart</code>	Takes a list of soundscape objects. Performs multi-level diversity partitioning, decomposing the soundscape richness or diversity into its respective alpha, beta and gamma components following the multiplicative relationships of Hill numbers.	<code>assertthat</code> (Wickham 2019); <code>hms</code> (Müller 2022); <code>dplyr</code> (Wickham et al. 2023); <code>stats</code> (R Core Team 2022); <code>hilldiv</code> (Alberdi and Gilbert 2019)
<code>ss_pairdis</code>	Takes a list of soundscape objects. Computes the pairwise distance between soundscape objects in the list using one of: Sørensen–Dice overlap; Jaccard overlap; Sørensen–Dice turnover; Jaccard-subset turnover.	<code>assertthat</code> (Wickham 2019); <code>hms</code> (Müller 2022); <code>dplyr</code> (Wickham et al. 2023); <code>stats</code> (R Core Team 2022); <code>hilldiv</code> (Alberdi and Gilbert 2019)

References

- Alberdi, A.**; Gilbert, M.T.P. (2019). hilldiv: an R package for the integral analysis of diversity based on Hill numbers. Biorxiv, p.545665.
- Borchers, H. W.** (2022). pracma: Practical Numerical Math Functions. Available online at <https://CRAN.R-project.org/package=pracma>.
- Csárdi, G.**; FitzJohn, R. (2019). progress: Terminal Progress Bars. Available online at <https://CRAN.R-project.org/package=progress>.
- Dowle, M.**; Srinivasan, A. (2022). data.table: Extension of 'data.frame'. Available online at <https://CRAN.R-project.org/package=data.table>.
- Garnier, S.**; Ross, N.; Rudis, B.; Filipovic-Pierucci, A.; Galili, T.; Greenwell, B. (2021). viridis: Zenodo.
- Hijmans, R. J.** (2023). terra: Spatial Data Analysis. Available online at <https://CRAN.R-project.org/package=terra>.
- Landini, G.**; Randell, D. A.; Fouad, S.; Galton, A. (2017). Automatic thresholding from the gradients of region boundaries. *Journal of Microscopy* 265(2), pp.185–195.
- Ligges, U.**; Krey, S.; Mersmann, O.; Schnackenberg, S. (2023). tuneR: Analysis of Music and Speech. Available online at <https://CRAN.R-project.org/package=tuneR>.
- Müller, K.** (2022). hms: Pretty Time of Day. Available online at <https://CRAN.R-project.org/package=hms>.
- Oksanen, J.**; Kindt, R.; Legendre, P.; O'Hara, B.; Stevens, M. Henry H. (2007). The vegan package. *Community ecology*, 10, p.719.
- Pedersen, T. L.** (2022). patchwork: The Composer of Plots. Available online at <https://CRAN.R-project.org/package=patchwork>.
- R Core Team** (2022). R: A Language and Environment for Statistical Computing. Vienna, Austria. Available online at <https://www.R-project.org/>.
- Ren, K.** (2021). rlist: A Toolbox for Non-Tabular Data Manipulation. Available online at <https://CRAN.R-project.org/package=rlist>.
- Sievert, C.** (2020). Interactive Web-Based Data Visualization with R, plotly, and shiny. Available online at <https://plotly-r.com>.
- Slowikowski, K.** (2023). ggrepel: Automatically Position Non-Overlapping Text Labels with 'ggplot2'. Available online at <https://CRAN.R-project.org/package=ggrepel>.
- Sueur, J.**; Aubin, T.; Simonis, C. (2008). Seewave: a free modular tool for sound analysis and synthesis. *Bioacoustics*, 18, pp.213-226.

- Teucher, A.** (2019). lutz: Look Up Time Zones of Point Coordinates. Available online at <https://CRAN.R-project.org/package=lutz>.
- Thieurmél, B.; Elmarhraoui, A.** (2022). suncalc: Compute Sun Position, Sunlight Phases, Moon Position and Lunar Phase. Available online at <https://CRAN.R-project.org/package=suncalc>.
- Weston, S.** (2022a). doSNOW: Foreach Parallel Adaptor for the 'snow' Package. Available online at <https://CRAN.R-project.org/package=doSNOW>.
- Weston, S.** (2022b). foreach: Provides Foreach Looping Construct. Available online at <https://CRAN.R-project.org/package=foreach>.
- Wickham, H.** (2007). Reshaping Data with the reshape Package. *Journal of Statistical Software*, 21(12), pp.1-20. Available online at <http://www.jstatsoft.org/v21/i12/>.
- Wickham, H.** (2016). ggplot2: Elegant Graphics for Data Analysis: Springer-Verlag New York. Available online at <https://ggplot2.tidyverse.org>.
- Wickham, H.** (2019). assertthat: Easy Pre and Post Assertions. Available online at <https://CRAN.R-project.org/package=assertthat>.
- Wickham, H.** (2022). stringr: Simple, Consistent Wrappers for Common String Operations. Available online at <https://CRAN.R-project.org/package=stringr>.
- Wickham, H.; François, R.; Henry, L.; Müller, K.; Vaughan, D.** (2023a). dplyr: A Grammar of Data Manipulation. Available online at <https://CRAN.R-project.org/package=dplyr>.
- Wickham, H.; Seidel, D.** (2022). scales: Scale Functions for Visualization. Available online at <https://CRAN.R-project.org/package=scales>.
- Wickham, H.; Vaughan, D.; Girlich, M.** (2023b). tidyr: Tidy Messy Data. Available online at <https://CRAN.R-project.org/package=tidyr>.
- Zeileis, A.; Grothendieck, G.** (2005). zoo: S3 Infrastructure for Regular and Irregular Time Series. *Journal of Statistical Software*, 14(6), pp.1-27.

soundscapeR: An R-package for the exploration, visualisation, diversity quantification and comparison of soundscapes

Supplementary Materials 2

```
#####  
# Welcome!  
# This R scripts support the analysis outlined in Luypaert  
et # al. (2023): soundscapeR: An R-package for the  
exploration, # visualisation, diversity quantification and  
comparison of # soundscapes.  
# Feel free to follow along all the workflow's steps that  
we # presented in the soundscapeR paper using the  
instructions # provided below.  
# To dive into the functions with greater detail, consult  
# the package vignette available online here:  
# thomasluypaert.github.io/soundscapeR_vignette  
# !) If you don't want to wait for the index computation  
# step, which is the most time-consuming skip ahead to  
# 'PART 2: EXPLORE, VISUALISE AND QUANTIFY DIVERSITY'  
#####  
  
# 0. PRIORS -----  
# Before we get started, if you haven't done so already,  
# download and install the soundscapeR R-package using the  
# code provided below.  
remotes::install_github("ThomasLuypaert/soundscapeR")  
  
library(soundscapeR)  
  
# For the sake of the code demonstration, we assume you  
have # downloaded and unzipped the raw sound files and  
saved them # in a directory called 'output_dir'.  
  
# 1. PART 1: CREATE SOUNDSCAPE OBJECTS -----  
  
# 1.1. Download the raw sound files  
  
# Download link:  
https://datadryad.org/stash/share/JUnmste-fWNY3UUkjko86mA3iGKxOrSI9iHsLzmPo0s  
  
# Instruction: Download the raw sound files from the link  
# above and unzip the downloaded folder  
# Instruction: Go inside the unzipped directory and copy  
the # file path to the output_dir object below
```

```

# Instruction: Inside the unzipped directory, you will
find 5 # zipped folders. Unzip each of these to the same
location.
# Instruction: Now proceed with the code below.

output_dir <-
"PASTE_THE_FULL_PATH_TO_THE_LOCATION_OF_THE_DOWNLOADED_AND
_UNZIPPED_FILES_HERE"

# 1.2. Load metadata

metadata <- read.csv(file = paste0(output_dir,
"/metadata.csv"))

# 1.3. Search for the raw sound files in the folders

fileloc <- ss_find_files(parent_directory = output_dir)

# 1.4. Check if everything is in order with the files

fileloc <- ss_assess_files(file_locs = fileloc, full_days
= TRUE)

names(fileloc) <- c("Andre", "Mascote_A1", "Mascote_A2",
"Mascote_B1", "Mascote_B2")

# 1.5. Add the folder path to each soundscape to the
metadata

metadata$folderloc <- sapply(fileloc, function(x)
dirname(x[1]))

# 1.6. Calculate the CVR index for each 1-min file at
Andre Island

# Note: This step might take a while... You can speed it
up
# by setting parallel = TRUE.

# Note: If you need to interrupt your index computation,
you # can do so without problems. Just resume the
calculation
# later and the function will automatically detect where
it
# left off.

# Note: If you have access to a High-Performance Computing
# (HPC) platform, this will speed up the process

```

```

# considerably, especially if you're dealing with large
# studies

ss_index_calc(file_list = fileloc[["Andre"]],
              window = 256,
              parallel = FALSE)

# 1.7. Create a soundscape object for Andre Island

# Direct way

Andre_soundscape <-
  ss_create(fileloc = metadata$folderloc[1],
            samplerate = 44100,
            window = 256,
            index = "CVR",
            date = metadata$first_day[1],
            lat = metadata$lat[1],
            lon = metadata$lon[1],
            method = "IsoData",
            output = "incidence_freq")

# Step-by-step

Andre_soundscape_merged <-
  ss_index_merge(fileloc = metadata$folderloc[1],
                samplerate = 44100,
                window = 256,
                index = "CVR",
                date = metadata$first_day[1],
                lat = metadata$lat[1],
                lon = metadata$lon[1])

Andre_soundscape_binarized <-
  ss_binarize(merged_soundscape = Andre_soundscape_merged,
             method = "IsoData")

Andre_soundscape_aggregated <-
  ss_aggregate(binarized_soundscape =
Andre_soundscape_binarized,
              output = "incidence_freq")

# Great work! We've successfully created a soundscape
# object # for Andre Island. In the next section, we'll
# demonstrate
# how we can use these soundscape objects to explore,
# visualise, quantify, and compare the soundscape

```

```

diversity of # these sites. To get the soundscapes of the
other islands,
# we can load a list of soundscape objects saved in the
# soundscapeR package

data("balbina")

# 2. PART 2: EXPLORE, VISUALISE AND QUANTIFY DIVERSITY ---

# 2.2. Make heatmaps

heatmap_1 <- ss_heatmap(soundscape_obj =
balbina[["Andre"]],
                        type = "regular",
                        annotate = TRUE)

heatmap_2 <- ss_heatmap(soundscape_obj =
balbina[["Andre"]],
                        type = "polar",
                        annotate = TRUE)

# 2.3. Compute the soundscape metrics for various diurnal-
phase subsets

ss_diversity(soundscape_obj = balbina[["Andre"]],
             qvalue = 0,
             subset = "total") # Richness

ss_diversity(soundscape_obj = balbina[["Andre"]],
             qvalue = 2,
             subset = "total") # Diversity

ss_evenness(soundscape_obj = balbina[["Andre"]],
            subset = "total") # Evenness

# 2.4. Calculate four different diversity plot types for
Andre island

# Total
ss_diversity_plot(soundscape_obj = balbina[["Andre"]],
                 qvalue = 0,
                 graphtype = "total",
                 maxfreq = 20000,
                 smooth = TRUE,
                 movavg = 20)

# Frequency

```

```

diversity_plot_2 <- ss_diversity_plot(soundscape_obj =
balbina[["Andre"]],
    qvalue = 0,
    graphtype = "frequency",
    maxfreq = 20000,
    nbins = 4,
    smooth = TRUE,
    movavg = 20)

# Normalised frequency
ss_diversity_plot(soundscape_obj = balbina[["Andre"]],
    qvalue = 0,
    graphtype = "normfreq",
    maxfreq = 20000,
    nbins = 4,
    smooth = TRUE,
    movavg = 20) +

    guides(fill = guide_legend(nrow = 1,
        title.position = "top",
        title.hjust = 0.5,
        title.vjust = 0.5,
        label.position = "top",
        label.hjust = 0.5))

# Line frequency
ss_diversity_plot(soundscape_obj = balbina[["Andre"]],
    qvalue = 0,
    graphtype = "linefreq",
    maxfreq = 20000,
    nbins = 4,
    smooth = TRUE,
    movavg = 20,
    timeinterval = "4 hours")

# 2.5. Compare the soundscapes of Andre island and
Mascote_A1

diff_heatmap <-
    ss_compare(soundscape_obj_A = balbina[["Andre"]],
        soundscape_obj_B = balbina[["Mascote_A1"]],
        type = "regular",
        maxfreq = 20000,
        timeinterval = "4 hours")

```

```
# 2.6. Produce a PCAO plot showing the five sites on two islands:
```

```
ss_pcoa(soundscape_list = balbina,  
        grouping = c("Andre", "Mascote", "Mascote",  
"Mascote", "Mascote"),  
        screeplot = TRUE)
```

```
# 2.7. Partition the soundscape diversity using a two-level hierarchy
```

```
ss_divpart(soundscape_list = balbina,  
           qvalue = 0)
```

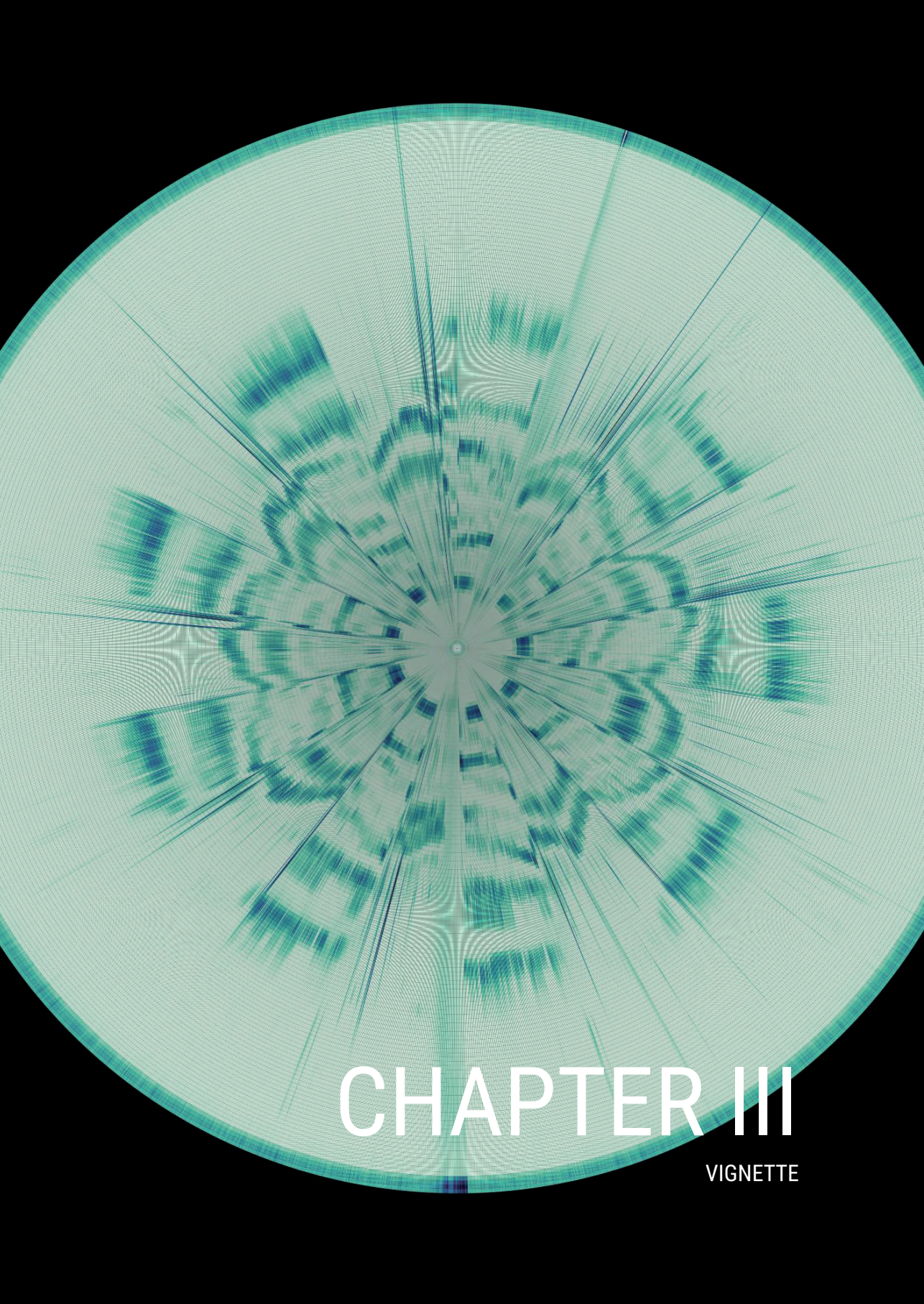
```
ss_divpart(soundscape_list = balbina,  
           qvalue = 1)
```

```
ss_divpart(soundscape_list = balbina,  
           qvalue = 2)
```

```
# 2.8. Compute pairwise dissimilarities between soundscapes
```

```
ss_pairdis(soundscape_list = balbina,  
           qvalue = 0, )
```

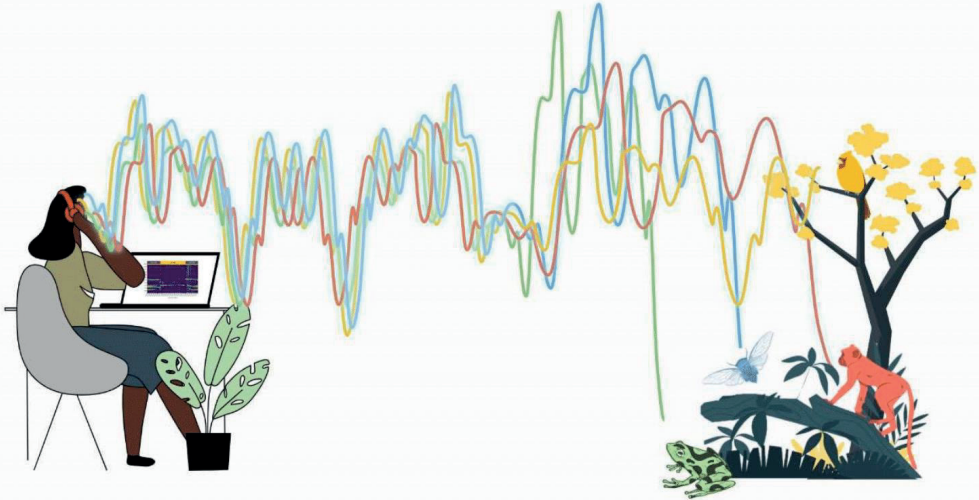
8 Appendices



CHAPTER III

VIGNETTE

soundscapeR R-package



Welcome!

Hi there!

Welcome to the case study vignette of the `soundscapeR` R-package. Here, we demonstrate the use of the functions contained in the package using data from a real-world ecological system. The goal of `soundscapeR` is to provide a standardized analytical pipeline for the computation, exploration, visualization, diversity quantification and comparison of soundscapes using Hill numbers. The package is designed to work with either continuous or regular-interval long-duration acoustic recordings, and can quantify the diversity of soundscapes using a range of different diversity types (richness, evenness & diversity), spatial scales (alpha, beta and gamma diversities), and spectro-temporal subsets.



If you are unfamiliar with the `soundscapeR` workflow, head on over to [Luypaert et al. \(2022\)](#) and take a look at the theoretical concepts. Moreover, additional background information can be found on the [GitHub landing page](#) for this R-package.

Without further ado, let's get started!

Case study data

The study system

For the case study presented here, we will be comparing the soundscapes of two islands of differing size in the Balbina Hydroelectric Reservoir (BHR; Fig. 1) in the Brazilian Amazon. The BHR is one of the largest hydroelectric reservoirs on Earth and was formed when a tributary of the Amazon, the Uatumã River, was dammed in 1987, turning the former hilltops of primary continuous forest into > 3,500 islands spanning an area of approximately 300,000 ha (Buono and Peres 2019). The artificial tropical rainforest archipelago now contains islands spanning a wide range of sizes, ranging from 0.2 to 4,878 ha.



Figure 1: An aerial photograph of the Balbina Hydroelectric Reservoir, showcasing a highly fragmented landscape consisting of many islands of different sizes. Picture credit belongs to Luke Gibson.

Long-duration acoustic data was collected at 151 plots on 74 islands (size range: 0.45-1699 ha) and 4 continuous forest sites at the BHR between July and December 2015. The number of plots per island was proportional to the habitat area associated with each island, and varied between 4-10 for continuous forest sites and 1-7 for islands. At each plot, a passive acoustic sensor (an LG smartphone enclosed in a waterproof case linked to an external omnidirectional microphone) was attached to a tree trunk at 1.5m height and set to record the soundscape for 1 minute every 5 minutes for 4-10 days at a sampling rate of 44,100 Hz using the [ARBIMON Touch application](#).

Why the BHR?

Previous work has shown that the soundscape diversity metrics that can be computed using the [soundscapeR](#) R-package are a good proxy for the taxonomic diversity at the Balbina Hydroelectric Reservoir (Luypaert et al. 2022). Moreover, more recently, we showed that the soundscape richness is sensitive to one of the most fundamental patterns in ecology, the positive scaling of richness with island size, which we termed the soundscape-area relationship (SSAR - see Luypaert et al. 2023).

Clearly, the BHR is an informative system to explore how soundscapes can be used to uncover ecology's secrets. As such, in this case study, we investigate the soundscapes of two islands of differing size to demonstrate the steps in

such, in this case study, we investigate the soundscapes of two islands of differing size to demonstrate the steps in the `soundscaper` workflow.

The selected islands

For this case study, we will be looking at the soundscapes of two islands at the BHR: **Andre island** (2.08 ha) and **Mascote island** (668.03 ha). Since the number of plots at which we collected soundscape data is proportional to the island size, we will use acoustic data for 1 plot at Andre island and 4 plots at Mascote island (Fig. 2). At each of these plots, sound was recorded for 1 minute every 5 minutes for 5 days (1440 1-min sound files per plot).



Figure 2: A schematic representation of the islands used in this case study.

The raw sound files for these 5 plots on 2 island can be downloaded from the online repository [here](#).

The workflow

Before we start

Before starting the practical part of the case study, first, we will download and install the `soundscaper` R-package from GitHub and load it into R.

If you haven't already installed the package, uncomment the first command below and run the code chunk:

```
# devtools::install_github(repo = "ThomasLuypaert/soundscaperR")  
  
library(soundscaperR)
```


Workflow overview

The Hill-based diversity quantification of soundscapes presented in [Luypaert et al. \(2022\)](#) consists of three key steps:

- **Step 1:** Grouping sounds into Operational Sound Units (OSUs) and evaluating OSU presence in each sample of the 24h acoustic trait space
- **Step 2:** Assessing the prevalence (or incidence) of OSUs across the recording period
- **Step 3:** Quantifying the soundscape diversity using the framework of Hill numbers

To simplify the use of the `soundscaper` package, we created an S4-object which we term a '`soundscape`' object. This data object has a formally defined structure consisting of slots, containing all relevant metadata and data objects that are generated during the workflow (step 1 and 2). The soundscape object forms the basis on which all functions downstream in the workflow are applied (step 3). Using this object-oriented programming approach ensures that metadata only needs to be entered once and is remembered downstream. Moreover, all chosen parameters in the workflow are stored by the soundscape object and can be accessed easily. Finally, the slots containing the various metadata and data objects have strict expectations of what each data input looks like, thus minimizing the chance of accidental errors.

Take a look at Figure 3 for an overview of the `soundscaper` workflow:

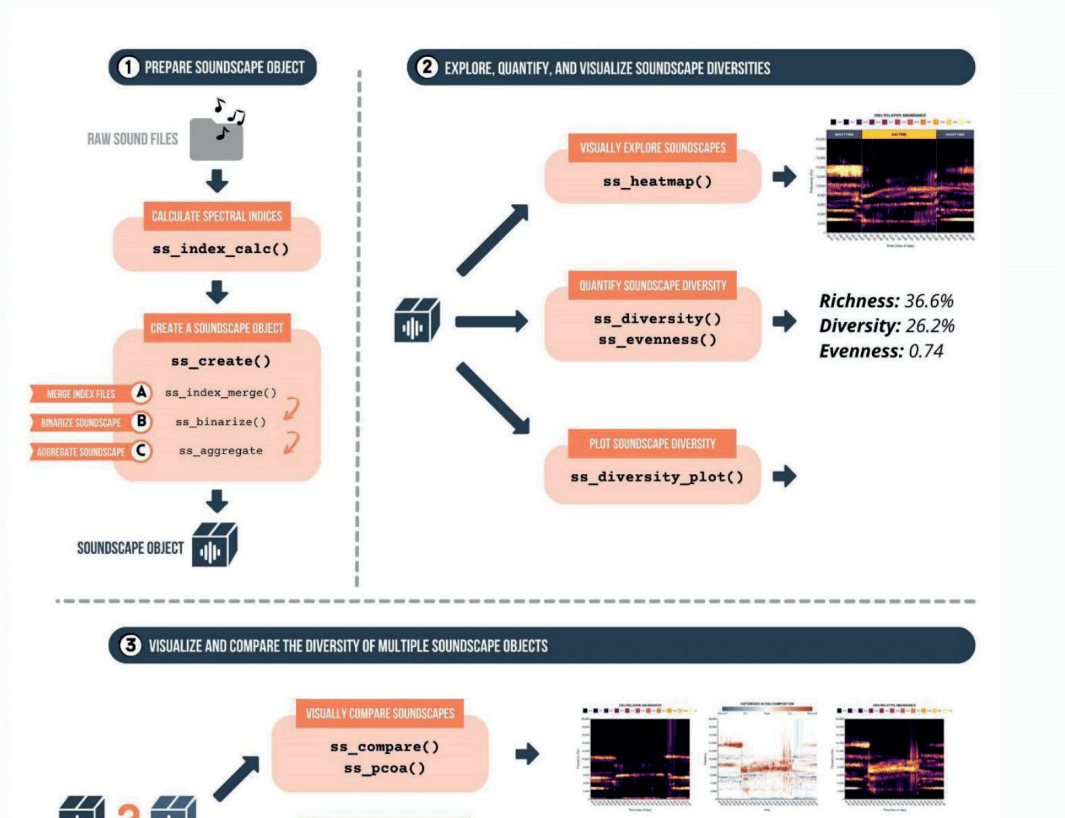




Figure 3: A schematic overview of the `soundscapeR` workflow

As you can see, there are three phases to the `soundscapeR` workflow:

- **Phase 1:** Prepare a soundscape object using the `ss_index_calc` function for index calculation and the `ss_create` function for calculating OSU presence and incidence across the recording period
- **Phase 2:** Explore the diversity of a single soundscape using the `ss_heatmap`, `ss_diversity`, `ss_evenness`, and `ss_diversity_plot` functions
- **Phase 3:** Compare the diversity of multiple soundscapes using the `ss_compare`, `ss_pcoa`, `ss_divpart`, and `ss_pairdis` functions

Below, we will go over each of these phases and show you how to use each function using the case study data outlined above.

Phase I: Preparing soundscapes

1.1. The `ss_index_calc` function

A. In theory

To quantify the presence of OSUs in each day of the recording period, first, we will make use the **Acoustic Cover (CVR)** spectral acoustic index (also known as *ACT_{sp}* in the [Towsey 2017](#) technical report) to capture the acoustic properties of sound in our 1-minute recordings. Per sound file, this index captures the fraction of cells in each noise-reduced frequency bin whose value exceeds a 3 dB threshold. By using this spectral acoustic index, we greatly condense the amount of information contained in these sound files while retaining important data on their time-frequency features. For more information on spectral acoustic indices and their use, check out [this](#) website.

To calculate these spectral indices, we will use the `ss_index_calc()` function. This function calls on the 'AnalysisPrograms' software tool, developed by the QUT Ecoacoustic group, to compute a series of spectral acoustic indices.

Let's take a look at the input parameters of the `ss_index_calc` function:

Function input parameters

- **fileloc:**
The full-length path to the folder containing the sound files for which to compute indices. In our case, for each plot, we stored the sound files in a separate folder which we will supply to the `fileloc` argument.
- **outputloc:**
The full-length path to the location where you wish to save the output files. Defaults to the same location as

the fileloc.

- **samplerate:**

The number of times the sound was sampled each second. This is a fixed parameter determined by your recording setup, although downsampling to a lower sampling rate is possible.

- **window:**

A variable of the Fast Fourier Transformation, expressed as the number of samples. The window size of choice depends on the fundamental frequency, intensity and change of the signal of interest, and influences the temporal and frequency resolution of the analysis. The window size is generally a power of 2.

- **parallel:**

A boolean flag (TRUE or FALSE) indicating whether parallel processing should be enabled for index computation. Set to FALSE by default.

In case the duration of each sound file is longer than 1 minute, the function cuts the files into 1-minute segments before index calculation.

B. In practice

Below, you can find the code to calculate the CVR-index for all sound files in a folder.

```
# ss_index_calc(fileloc = "filepath_here",
#               outputloc = "filepath_here",
#               samplerate = 44100,
#               window = 256,
#               parallel = FALSE)
```

Because the index calculation can be time consuming, for the purposes of this vignette, here we will download the CVR-index 'csv' files we previously calculated from the [KNB repository](#):

```
# 1. Download the metajam package

# install.packages("metajam")

# 2. Set folder location to save data

setwd("G:/soundscapeR_case_study")

dir.create(paste0(getwd(), "/case_study_data"))
```

```
## Warning in dir.create(paste0(getwd(), "/case_study_data")):
## 'G:\soundscapeR_case_study\case_study_data' already exists
```

```
output_dir <- paste0(getwd(), "/case_study_data")

# 3. Download data and metadata

# metajam::download_d1_data(data_url = "https://knb.ecoinformatics.org/knb/d1/mn/v2/object/urn%3Auuid%3Acfcc67
#
# # 4. Unzip
#
# to_unzip <- list.files(output_dir, full.names = TRUE)
#
```



```
# sapply(to_unzip, function(x) unzip(zipfile = x,exdir = output_dir, overwrite = TRUE))

# Specify the folder locations

folder_locs <- list.dirs(path = output_dir, recursive = FALSE)
```

In addition to the sound data, we will also require some metadata for the downstream analysis, so let's prepare a metadata object.

Make a metadata object:

```
island_metadata <- data.frame(plot = c("Andre", "Mascote_A1", "Mascote_A2", "Mascote_B1", "Mascote_B2"),
  first_day = c("2015-10-10", rep("2015-10-16", 4)),
  lat = c(-1.58462, -1.64506, -1.6489, -1.64406, -1.65936),
  lon = c(-59.87211, -59.82035, -59.83297, -59.84817, -59.83546),
  folder_locs = folder_locs)
```

1.2. The `ss_create` function

A. In theory

Following index computation, we use the `ss_create` function to create a *soundscape* object.

The `ss_create` function is a wrapper function combining the functionality of three functions in sequence:

- `ss_index_merge`: Performs chronological concatenation of the CVR index files into a time-frequency-index value data frame
- `ss_binarize`: Converts the raw CVR values of OSUs into a binary detection (1)/ non-detection (0) variable for each day in the recording period
- `ss_aggregate`: Calculates the incidence of OSUs across all sampled days

Although each of these sub-functions can be used individually, in most cases, the `ss_create` function will cover the needs of the user in a single step.

Let's take a look at the input parameters for the `ss_create` function:

Function input parameters

- **fileloc:**
The full-length path to the folder containing the sound files for which to compute indices. In our case, for each plot, we stored the sound files in a separate folder which we will supply to the fileloc argument.
- **samplerate:**
The number of times the sound was sampled each second. This is a fixed parameter determined by your recording setup, although downsampling to a lower sampling rate is possible.
- **window:**
A variable of the Fast Fourier Transformation, expressed as the number of samples. The window size of choice depends on the fundamental frequency, intensity and change of the signal of interest, and influences the

temporal and frequency resolution of the analysis. The window size is generally a power of 2.

- **index:**
The acoustic index of interest. Options are “BGN”, “PMN”, “CVR”, “EVN”, “ENT”, “ACI”, “OSC”, “SPT”, “RHZ”, “RVT”, “RPS” and “RNG”. For a brief description of indices, consult the `ss_index_calc` documentation. Note that the soundscape diversity metrics that can be calculated downstream have only been tested using the Acoustic Cover (CVR) index.
- **date:**
The first day of the recording period. Used for managing time-objects in R. Formatted as “YYYY-mm-dd”.
- **lat:**
The latitude of the site at which the sound files were collected. Coordinates should be specified in decimal degrees as a numerical variable.
- **lon:**
The longitude of the site at which the sound files were collected. Coordinates should be specified in decimal degrees as a numerical variable.
- **method:**
The algorithm used to determine the threshold. Options are “IJDefault”, “Huang”, “Huang2”, “Intermodes”, “IsoData”, “Li”, “MaxEntropy”, “Mean”, “MinErrorI”, “Minimum”, “Moments”, “Otsu”, “Percentile”, “RenyiEntropy”, “Shanbhag”, “Triangle”, “Yen”, and “Mode”. To specify a custom threshold, use `method=“Custom”` in combination with the `value` argument. Consult http://imagej.net/Auto_Threshold for more information on algorithm methodologies.
- **value:**
Optional argument used to set a custom threshold value for binarization - used in combination with `method=“Custom”`.
- **output:**
Determines whether the function returns the raw total number of detections per time during the recording period (`output = “raw”`), or the incidence frequency (total number of detections / number of recordings for that time - `output = “incidence_freq”`).

The `ss_create` function returns an S4 *soundscape* object.

B. In practice

Now that we know which input parameters to provide, let’s give this a try. We will prepare the soundscape objects for our five plots on the two islands described above. We can use the `lapply` function to iterate over the metadata we previously saved.

Let’s run the `ss_create` function:

```
soundscape_list <-  
  
lapply(X = 1:nrow(island_metadata), function(x)  
  ss_create(fileloc = island_metadata$folder_locs[x],  
            samplerate = 44100,  
            window = 256,  
            index = "CVR",  
            date = island_metadata$first_day[x],  
            lat = island_metadata$lat[x],  
            lon = island_metadata$lon[x],  
            method = "IsoData",  
            output = "incidence_freq"))  
  
names(soundscape_list) <- c("Andre", "Mascote_A1", "Mascote_A2", "Mascote_B1", "Mascote_B2")
```

Doing so, we will get a list of soundscape objects for further analysis. But before we proceed with phase two of the pipeline, let's have a closer look at this 'soundscape' object in the next section!

1.3. Introducing the `soundscape` object

As we previously mentioned, the `ss_create` function requires us to provide some additional metadata information, as well as several parameters on how the data should be processed. Using the `ss_create` function, we are creating a new type of data object which stores all the relevant information, and will form the basis on which all subsequent functions in the workflow are performed!

Let's take a look at this newly created object for Andre island:

```
# Let's see what class this object is:
summary(soundscape_list[["Andre"]])
```

```
##      Length      Class      Mode
##          1 soundscape      S4
```

This new data object is an 'S4' object of the class `soundscape`.

```
# Let's see what sort of information this object holds
soundscape_list[["Andre"]]
```

```
##
## 1. Soundscape metadata
##
##   Sampling point metadata:
##
##   First day of recording: 2015-10-10
##   Latitude of sampling point: -1.58462
##   Longitude of sampling point: -59.87211
##   Time zone of sampling point: America/Manaus
##   Sunrise time at sampling point: 05:43:36
##   Sunset time at sampling point: 17:51:47
##
##   Acoustic index metadata:
##
##   Path to raw sound files: G:/soundscapeR_case_study/case_study_data/Andre
##   Spectral index used: CVR
##   Sampling rate of the recording: 44100 Hz
##   Window size used in FFT: 256 samples
##   Frequency resolution: 172.2656 Hz
##   Temporal resolution: 0.005804989 ms
##
##   Data frame binarization metadata:
##
##   Used binarization algorithm: IsoData
##   Binarization threshold: 0.16
##
##   Aggregated data frame metadata:
##
```

```

## Output format: incidence_freq
## Data frame frequency range: 172 - 22050 Hz
## Data frame time range: 00:00:00 - 23:55:00
##
## 2. Soundscape data
##
## Merged data frame data:
##
## Columns 1 to 5 and rows 1 to 5 displayed
##
##      15:55:00  16:00:00  16:05:00  16:10:00  16:15:00
## 22050 0.19408888 0.18264127 0.18909356 0.18763659 0.20761786
## 21877 0.45009887 0.48069518 0.49037361 0.48579457 0.51306067
## 21705 0.49172651 0.50431887 0.50005203 0.50993860 0.51930482
## 21533 0.31439276 0.34571756 0.31616193 0.33884900 0.32802581
## 21360 0.01966906 0.02580914 0.01821209 0.02435217 0.01842023
##
## Binarized data frame data:
##
## Columns 1 to 5 and rows 1 to 5 displayed
##
##      15:55:00 16:00:00 16:05:00 16:10:00 16:15:00
## 22050      1      1      1      1      1
## 21877      1      1      1      1      1
## 21705      1      1      1      1      1
## 21533      1      1      1      1      1
## 21360      0      0      0      0      0
##
## Aggregated data frame data:
##
## Aggregated data frame:
##
## Columns 1 to 5 and rows 1 to 5 displayed
##
##      00:00:00 00:05:00 00:10:00 00:15:00 00:20:00
## 22050      0.6      1      0.6      0.6      1
## 21877      1.0      1      1.0      1.0      1
## 21705      1.0      1      1.0      1.0      1
## 21533      1.0      1      1.0      1.0      1
## 21360      0.0      0      0.0      0.0      0
##
## Aggregated data frame per time:
##
## First list element displayed: 00:00:00
##
## Columns 1 to 5 and rows 1 to 5 displayed
##
##      00:00:00 00:00:00.1 00:00:00.2 00:00:00.3 00:00:00.4
## 22050      0      1      0      1      1
## 21877      1      1      1      1      1
## 21705      1      1      1      1      1
## 21533      1      1      1      1      1
## 21360      0      0      0      0      0
##
## Number of soundscape samples per time (sampling effort):
##
## List elements 1 to 5 displayed
##
## $`00:00:00`
## [1] 5
##
## $`00:05:00`
## [1] 5
##
## $`00:10:00`

```



```
## [1] 5
##
## $`00:15:00`
## [1] 5
##
## $`00:20:00`
## [1] 5
```

As we can see, this objects holds two types of information:

- **Metadata:** Information regarding the data collection and which parameters where used in the different steps of preparing the soundscape object
- **Soundscape information:** Various intermediate data objects that are created as the `ss_create` function works its way through the index concatenation, binarization and computation of OSU abundance steps.

To access the information stored in this object, we will use the '@' symbol.

Let's take a look at which types of data are stored in the object so far:

```
# Let's check what sort of data collection metadata is stored in the object
print(paste0("First day of data collection: ", soundscape_list[["Andre"]]@first_day))
```

```
## [1] "First day of data collection: 2015-10-10"
```

```
print(paste0("Latitude at data collection site: ", soundscape_list[["Andre"]]@lat))
```

```
## [1] "Latitude at data collection site: -1.58462"
```

```
print(paste0("Longitude at data collection site: ", soundscape_list[["Andre"]]@lon))
```

```
## [1] "Longitude at data collection site: -59.87211"
```

```
print(paste0("Time zone at data collection site: ", soundscape_list[["Andre"]]@tz))
```

```
## [1] "Time zone at data collection site: America/Manaus"
```

```
print(paste0("Sunrise at time of data collection: ", soundscape_list[["Andre"]]@sunrise))
```

```
## [1] "Sunrise at time of data collection: 2015-10-10 05:43:36"
```

```
print(paste0("Sunset at time of data collection: ", soundscape_list[["Andre"]]@sunset))
```

```
## [1] "Sunset at time of data collection: 2015-10-10 17:51:47"
```

The `ss_create` function has automatically calculated a set of important ecological variables, such as sunrise and sunset times, and timezones, based on the first day of recording and geographical coordinates.

Let's continue looking at the data stored in the *soundscape* object:

```
# Let's check what sort of metadata the object has stored regarding past data processing steps  
print(paste0("Where are the raw sound files located: ", soundscape_list[["Andre"]]@fileloc))
```

```
## [1] "Where are the raw sound files located: G:/soundscapeR_case_study/case_study_data/Andre"
```

```
print(paste0("What acoustic index are we using: ", soundscape_list[["Andre"]]@index, " index"))
```

```
## [1] "What acoustic index are we using: CVR index"
```

```
print(paste0("What was the samplerate used to collect the data: ", soundscape_list[["Andre"]]@samplerate, " Hz")
```

```
## [1] "What was the samplerate used to collect the data: 44100 Hz"
```

```
print(paste0("What was the window length used during the FFT: ", soundscape_list[["Andre"]]@window, " samples")
```

```
## [1] "What was the window length used during the FFT: 256 samples"
```

The *soundscape* object has recorded where our raw data files are stored, which acoustic index we're working with, what sampling rate was used during data collection, and what window length was used during the acoustic index calculation.

Let's take a look at some of the data frames we created by running the `ss_create` function:

```
head(soundscape_list[["Andre"]]@merged_df)[,1:5]
```

```
##           15:55:00  16:00:00  16:05:00  16:10:00  16:15:00  
## 22050 0.19408888 0.18264127 0.18909356 0.18763659 0.20761786  
## 21877 0.45009887 0.48069518 0.49037361 0.48579457 0.51306067  
## 21705 0.49172651 0.50431887 0.50005203 0.50993860 0.51930482  
## 21533 0.31439276 0.34571756 0.31616193 0.33884900 0.32802581  
## 21360 0.01966906 0.02580914 0.01821209 0.02435217 0.01842023  
## 21188 0.01207202 0.01800395 0.01186388 0.01592257 0.01321678
```

As we previously mentioned, the first step performed by the `ss_create` function is the chronological concatenation of the CVR-index files for a site into a time-frequency-index value data frame. This data frame is stored in the

@merged_or slot, and contains the time-of-recording as column names, the frequency bins as row names, and the CVR-index for each time-frequency pair as values. Each column contains the spectral index values of a single sound file.

Let's inspect this data frame a little closer:

```
# How many columns does the data frame contain?  
  
paste0("The data frame contains: ", ncol(soundscape_list[["Andre"]@merged_df), " columns")
```

```
## [1] "The data frame contains: 1440 columns"
```

```
# What are the column names?  
  
head(colnames(soundscape_list[["Andre"]@merged_df))
```

```
## [1] "15:55:00" "16:00:00" "16:05:00" "16:10:00" "16:15:00" "16:20:00"
```

```
tail(colnames(soundscape_list[["Andre"]@merged_df))
```

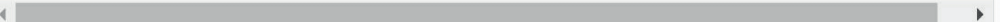
```
## [1] "15:25:00" "15:30:00" "15:35:00" "15:40:00" "15:45:00" "15:50:00"
```

As we said, the number of columns equals the number of sound files collected during the acoustic survey - in this case, 1440 sound files. The name of each column corresponds to the time of day at which the recording was collected.

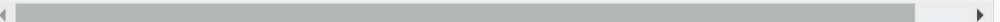
Next, let's take a look at the rows:

```
# How many rows does the data frame contain?  
  
paste0("The data frame contains: ", nrow(soundscape_list[["Andre"]@merged_df), " rows")
```

```
## [1] "The data frame contains: 128 rows"
```

```
# What do these row names look like?  
  
# The first five names  
  
paste0("The first five rownames: ", paste0(rownames(soundscape_list[["Andre"]@merged_df)[1:5], collapse = ", "  
◀  ▶
```

```
## [1] "The first five rownames: 22050, 21877, 21705, 21533, 21360"
```

```
# The last five names  
  
paste0("The last five rownames: ", paste0(rownames(soundscape_list[["Andre"]@merged_df)[123:128], collapse = "  
◀  ▶
```

```
## [1] "The last five rownames: 1033, 861, 689, 516, 344, 172"
```

The data frame contains 128 rows, each corresponding to a unique frequency bin. The frequency bins range from 0 - 22,050 Hz, and are of approximately 172 Hz width.

Now, let's inspect the CVR-index values:

```
# What is the minimum CVR-index value in our data frame?  
  
paste0("The minimum CVR-value in our data frame is: ", min(soundcape_list[["Andre"]>@merged_df))
```

```
## [1] "The minimum CVR-value in our data frame is: 0"
```

```
# What is the maximum CVR-index value in our data frame?  
  
paste0("The max CVR-value in our data frame is: ", max(soundcape_list[["Andre"]>@merged_df))
```

```
## [1] "The max CVR-value in our data frame is: 0.672286398168384"
```

As we can see, in our dataset, the CVR-index values range between 0 - 0.67. Remember, CVR-index values capture the proportion of cells in each noise-reduced frequency bin of a sound file that exceeds a 3-dB amplitude threshold. As such, the values can technically range between 0-1.

After the CVR-indices for a soundscape recording of a site have been chronologically concatenated, instead of using the raw CVR-values that we computed for every OSU in each 24h sample of the soundscape, the `ss_create` function determines a threshold value for each site, and converts the OSU's CVR-index values into a binary detection (1) / non-detection (0) variable per 24h sample based on this threshold. This step is aimed at detecting the presence of sound for every OSU in each 24h sample of acoustic trait space while removing low-amplitude or transient sounds, which potentially have a non-biological origin, from the data. In this way, we hope to capture the acoustic structure of the soundscape while removing background noise.

We can see that the *soundcape* objects produced by the `ss_create` function has some new metadata related to this binarization step:

```
# Which threshold algorithm was used for binarization?  
  
paste0("The ", soundcape_list[["Andre"]>@binarization_method, " method was used for binarization")
```

```
## [1] "The IsoData method was used for binarization"
```

```
# Which threshold was used for binarization?  
  
paste0("The threshold used for binarization was: ", soundcape_list[["Andre"]>@threshold)
```

```
## [1] "The threshold used for binarization was: 0.16"
```

Additionally, a `binarized_df` data frame was added to the object.

Let's inspect this data frame:

```
# What are the dimensions of the binarized dataframe?  
dim(soundscape_list[["Andre"]@binarized_df)
```

```
## [1] 128 1440
```

```
# What are the unique values contained in this data frame?
```

```
unique(unlist(soundscape_list[["Andre"]]@binarized_df))
```

```
## [1] 1 0
```

As expected, the new binarized data frame contains the same number of rows and columns as the `merged_df` data frame. However, whereas previously we had CVR-index values ranging between anywhere between 0-1, due to the binarization step, the values are now strictly 0 or 1.

Finally, after binarization, the `ss_create` function calculates the relative abundance of OSUs across all 24h samples of acoustic trait space for a site. For Andre island, we have five 24h samples (5 recording days) per plot.

To do this, the function uses an incidence-based approach. Previously, the `ss_create` function computed the detection (1) / non-detection (0) of each OSU in each 24h soundscape sample. Next, per OSU, the function takes the mean of this binary variable across all 24h soundscape samples to get the relative frequency by which each OSU was detected. To avoid confusion between the frequency of OSU detection and the sound frequency (in Hz), we'll refer to this OSU importance value as the '*relative abundance*'.

The *soundscape* object contains some information related to this step. Let's investigate the *soundscape* object for Andre island to see what is new.

What are the dimensions of the new '*aggregated_df*' data frame?

```
# First, let's check out the new 'aggregated_df' data frame
```

```
paste0("The aggregated_df data frame has ",  
       nrow(soundscape_list[["Andre"]]@aggregated_df),  
       " rows")
```

```
## [1] "The aggregated_df data frame has 128 rows"
```

```
paste0("The aggregated_df data frame has ",  
       ncol(soundscape_list[["Andre"]]@aggregated_df),  
       " columns")
```

```
## [1] "The aggregated_df data frame has 288 columns"
```

The number of rows in the '*aggregated_df*' data frame that was added to the *soundscape* object is still 128, one for each frequency bins resulting from the Fast Fourier Transformation. However, the number of columns in the '*aggregated_df*' data frame is 288 - that is five times less than the '*binarized_df*' data frame! Well, since we averaged the detection/non-detection values across five 24h samples of the acoustic trait space, this makes sense...

Now, what range of values do the OSU relative abundances take?

```
paste0("The relative abundance of OSUs can take the following values: ",  
       paste(sort(unique(unlist(soundscape_list[["Andre"]]@aggregated_df))), collapse = " "))
```

```
## [1] "The relative abundance of OSUs can take the following values: 0,0.2,0.4,0.6,0.8,1"
```

The relative abundance can take 6 values: 0, 0.2, 0.4, 0.6, 0.8 and 1. This makes sense. If an OSU was detected in 0 out of 5 soundscape samples, its relative abundance is 0. If an OSU was detected in 5 out of 5 soundscape samples, its relative abundance is 1. If it was detected somewhere in between, say 3 out of 5 samples, its relative abundance would be 0.6.

Great, we've got a soundscape object that contains a dataframe with our a unit of diversity measurement (OSUs) with an associated importance value (the relative abundance). We now have all the ingredients to start the next part of the workflow: exploration and diversity quantification of a single soundscape object.

The remaining functions in the `soundscapeR` package can be divided into two types:

- **Phase 2:** Functions for exploring and visualizing the diversity of a single soundscape
- **Phase 3:** Functions for visualizing and contrasting the diversity of multiple soundscapes

Phase II: Exploring a single soundscape

The `soundscapeR` package contains a range of functions to explore the diversity patterns of a single soundscape object. These include functions for visualizing the overall soundscape (`ss_heatmap`), functions for quantifying soundscape diversity metrics for a range of spectro-temporal subsets (`ss_diversity` & `ss_evenness`), and functions for visualizing diversity patterns throughout the day or for different frequency bins (`ss_diversity_plot`).

We will go deeper into each of these functions in the following section.

2.1. The `ss_heatmap` function

The `ss_heatmap` function allows us to visualize the distribution and relative abundance of OSUs in the 24h acoustic trait space. This function is a true workhorse - it is highly flexible, allowing us to subset the soundscape by specific time or frequency coordinates, portray the soundscape in either Cartesian or polar coordinates, annotate the soundscape with the sunset and sunrise time, and many more. Below, we'll provide an overview of `ss_heatmap`'s abilities.

Let's take a look at the soundscape for Andre island. We will start with the `ss_heatmap` function in it's most basic form and add progressively more advanced plotting arguments.

A basic heatmap

In it's most basic form, the `ss_heatmap` function only takes a single argument.

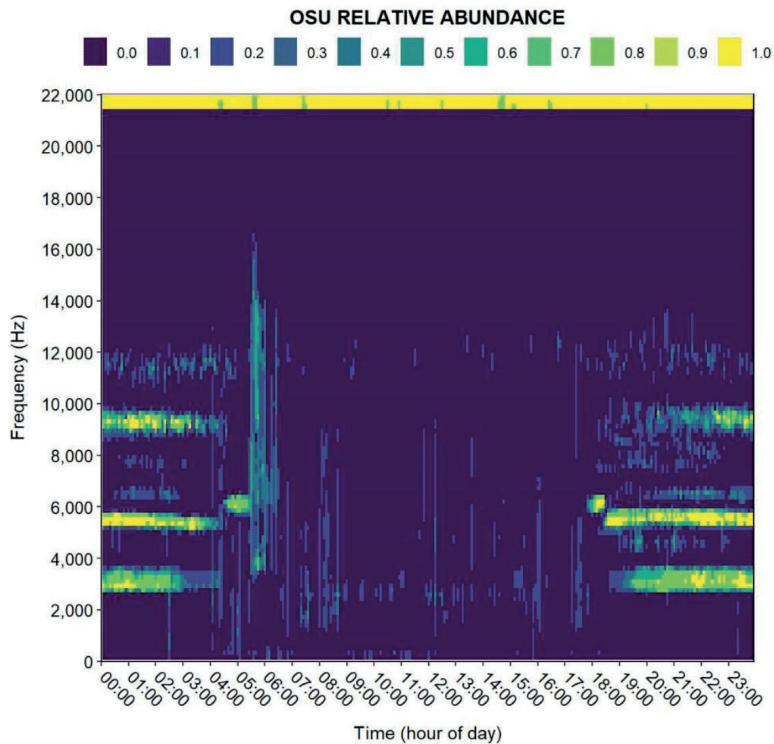
Mandatory input parameters

- `soundscape_obj`:

a *soundscape* object produced by the `ss_create` function (or `ss_index_merge`, `ss_binarize` and `ss_aggregate` functions applied in sequence).

In practice, the code looks as follows:

```
ss_heatmap(soundscape_obj = soundscape_list[["Andre"]])
```



The heatmap shows us that, above 12,000 Hz, Andre's soundscape is pretty empty. We can also see that most of the sound is present at night and the daytime soundscape is much more impoverished. The, the yellow band at the top is because the recorder was not able to record sound at this frequency - we will see how to remove this from the heatmap at a later stage.

Even in it's most simple form, the heatmap reveals quite a lot about a soundscape. Without looking at species-specific information or listening to sound files, we have just obtained ecologically relevant information from 24 full hours of recording (1440 1-minute files). Now, imagine you have many sites and longer recording periods... This is where the true value of the `soundscapeR` workflow lies!

A polar heatmap

In addition to the base heatmap we produced above, the `ss_heatmap` function also allows us to plot the heatmap in a polar coordinate system.

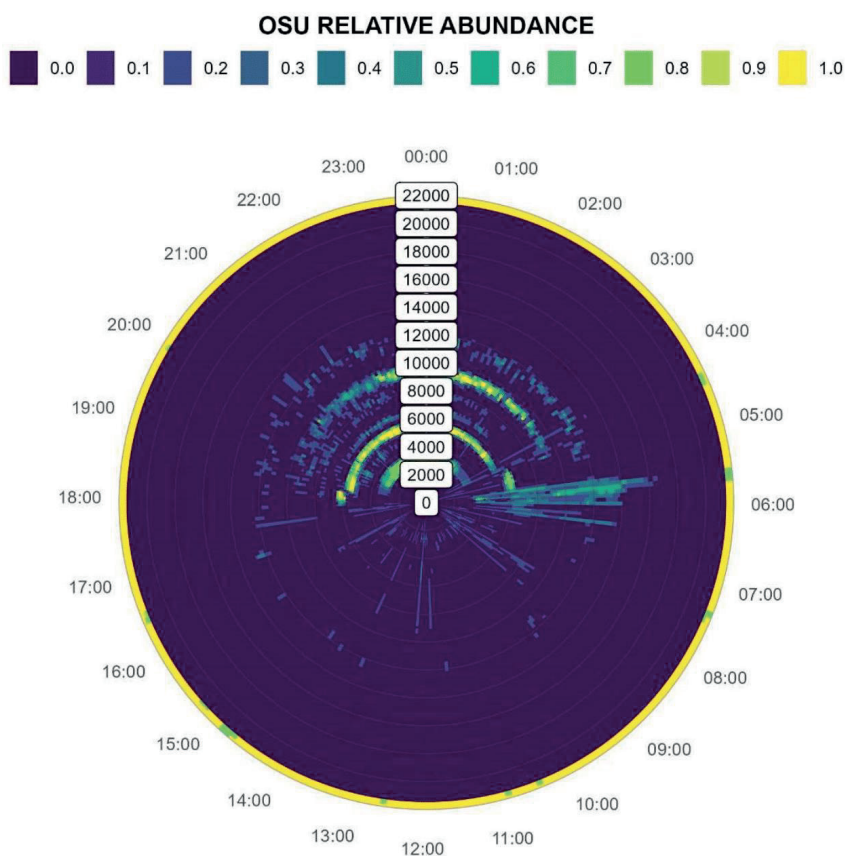
Parameters to change the coordinate system

- **type:**

A character string. One of either “regular” or “polar”. If set to “regular”, produces a regular rectangular heatmap. If set to “polar”, produces a heatmap in the polar coordinate system.

To understand what this argument does, let’s try `type = “polar”`:

```
ss_heatmap(soundscape_obj = soundscape_list[["Andre"]],  
           type = "polar")
```



The `type` arguments let’s us choose whether to plot regular (rectangular) heatmaps, like in the previous example, or polar heatmaps. And why would we want to do this, you may ask? Well, a rectangular heatmap distorts the relationships between sounds in the acoustic trait space. Imagine two sounds, one that is produced at 15,000 Hz

around 23:55h at night, and the other at 15,000 Hz at 00:05h in the morning. On our rectangular heatmap, these two sounds would be perceived as distant in the acoustic trait space, as they would be on opposite ends. From an ecological and functional perspective, these sounds are actually quite similar - they were produced at the same frequency at 10 minutes apart... The polar heatmap captures this relationship more accurately.

An annotated heatmap

Next up, let's have a look at how we can add some ecologically important variables to this plot: the time of sunrise, sunset, and if applicable, the approximate boundary between the human-audible and ultrasonic frequency spectrum.

Parameters to add ecologically relevant variables

- **annotate:**

A Boolean operator. One of either TRUE or FALSE. If set to TRUE, annotates the heatmap with sunrise and sunset times and highlights the border between the audible and ultrasonic spectrum for human hearing.

Let's try this out for the regular and polar heatmap:

```
# Regular heatmap

regular_heatmap_annotated <-
  ss_heatmap(soundcape_obj = soundcape_list[["Andre"]],
            type = "regular",
            annotate = TRUE)

# Polar heatmap

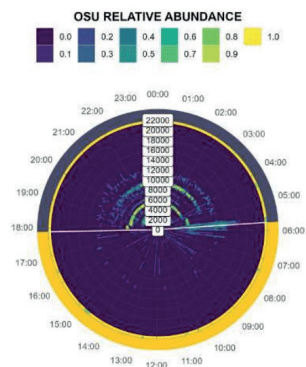
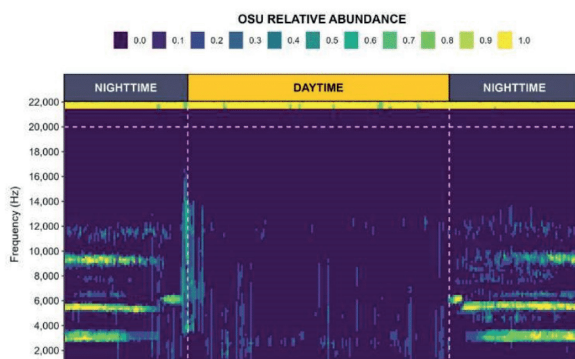
polar_heatmap_annotated <-
  ss_heatmap(soundcape_obj = soundcape_list[["Andre"]],
            type = "polar",
            annotate = TRUE)

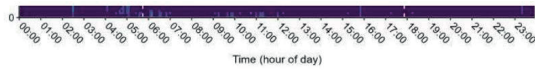
# Combine

library(patchwork)

annotated_heatmaps <- regular_heatmap_annotated + polar_heatmap_annotated

annotated_heatmaps
```





With the addition of one simple argument, the `ss_heatmap` function annotates the heatmap with the time of sunrise and sunset (stored in the `soundscape` object) and the boundary between the audible and ultrasonic spectrum. The part of the soundscape that occurs in the day is highlighted in yellow, whereas the nighttime is highlighted in blue.

Alter the axis labels

The `ss_heatmap` function also contains parameters to change the aesthetics of the axis labels.

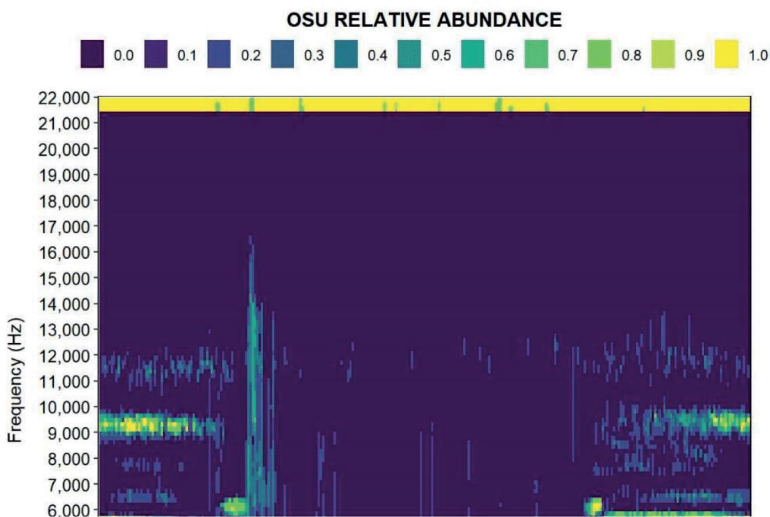
Parameters to change the axis label aesthetics

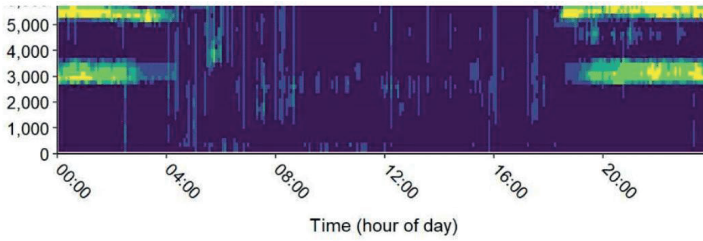
- **timeinterval:**
A time interval for the x-axis. Options can be found in the `scales::breaks_width` documentation.
- **freqinterval:**
The frequency interval for the y-axis, expressed as a numeric value.

Let's try this out for the Andre island soundscape using a regular heatmap with a 4 hour x-axis interval and 1000 Hz y-axis interval:

```
ss_heatmap(soundscape_obj = soundscape_list[["Andre"]],
           timeinterval = "4 hours",
           freqinterval = 1000)
```

```
## Warning: Removed 542 rows containing missing values (`geom_tile()`).
```





Subset the soundscape in the time or frequency domain

If we are only interested in a subset of the acoustic trait space, the `ss_heatmap` function contains a number of parameters to perform time-frequency subsetting.

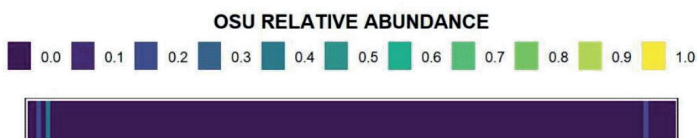
Parameters to change subset the acoustic trait space

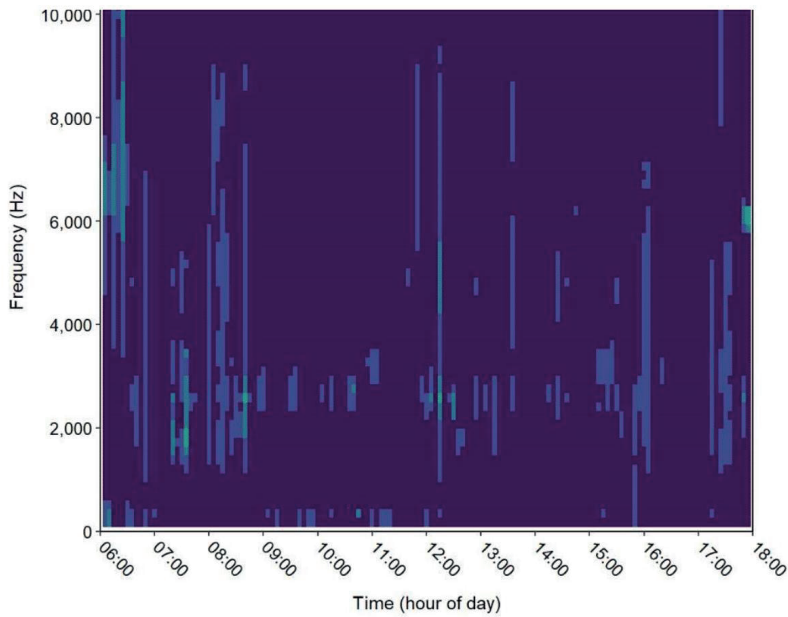
- **mintime:**
The lower time limit for the x-axis, formatted as "HH:MM:SS". Defaults to the earliest time for which data exists in the dataframe.
- **maxtime:**
The upper time limit for the x-axis, formatted as "HH:MM:SS". Defaults to the latest time for which data exists in the dataframe.
- **minfreq:**
The lower frequency limit for the y-axis as a numeric value. Defaults to zero.
- **maxfreq:**
The upper frequency limit for the y-axis as a numeric value. Defaults to zero.

Let's try visualizing the Andre island soundscape between 06:00h and 18:00h for frequencies between 0 - 11,000 Hz:

```
ss_heatmap(soundscape_obj = soundscape_list[["Andre"]],
           mintime = "06:00:00",
           maxtime = "18:00:00",
           minfreq = 0,
           maxfreq = 11000)
```

```
## Warning: Removed 27855 rows containing missing values ('geom_tile()').
```





Alter the heatmap's color aesthetics

We can also alter the color aesthetics that are mapped to the OSU relative abundance values in the heatmap.

Parameters to change the color aesthetics

- palette:**
 A character string indicating the colormap option to use. Four options are available: "magma" (or "A"), "inferno" (or "B"), "plasma" (or "C"), "viridis" (or "D", the default option) and "cividis" (or "E"). Consult [this website](#) for options.
- direction:**
 Sets the order of colors in the scale. If 1, the default, the regular order is followed. If -1, the order of colors is reversed.
- zero.black:**
 One of either TRUE or FALSE. If set to TRUE, absent OSUs with incidence zero will be colored black.

We can try to see what these do by adding them in one by one. Up first is the palette option. Let's try them all on Andre island's soundscape:

```
# Try the palettes one by one

color_1 <-
  ss_heatmap(soundscape_obj = soundscape_list[["Andre"]],
            palette = "A")

color_2 <-
```

```

ss_heatmap(soundcape_obj = soundscape_list[["Andre"]],
           palette = "B")

color_3 <-
  ss_heatmap(soundcape_obj = soundscape_list[["Andre"]],
           palette = "C")

color_4 <-
  ss_heatmap(soundcape_obj = soundscape_list[["Andre"]],
           palette = "D")

color_5 <-
  ss_heatmap(soundcape_obj = soundscape_list[["Andre"]],
           palette = "E")

# Combine into one plot

library(patchwork)

all_colors <- color_1 + color_2 + color_3 + color_4 + color_5

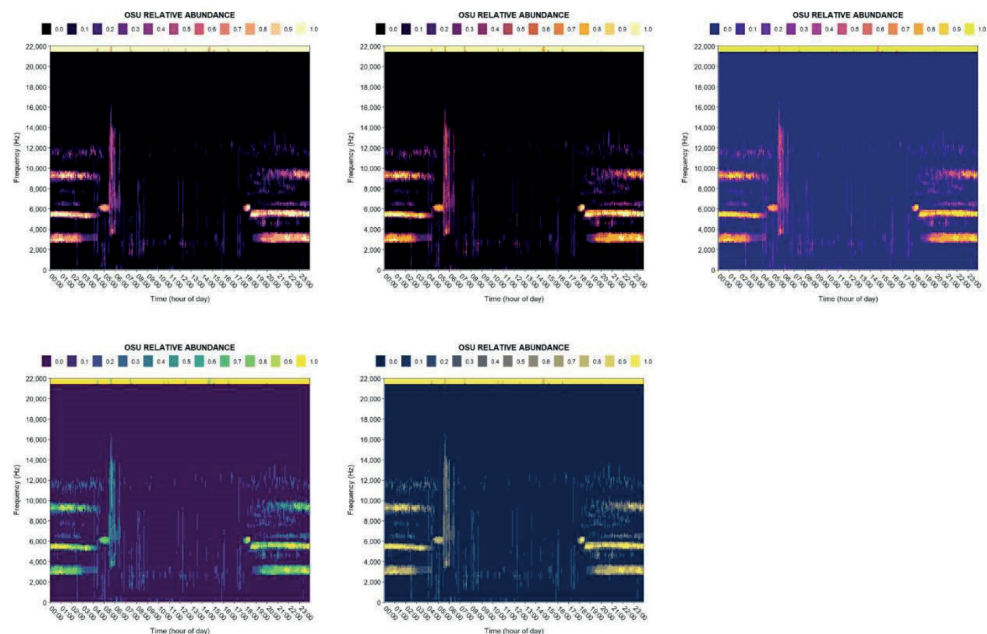
all_colors

```

```

## Warning: Removed 542 rows containing missing values (`geom_tile()`).
## Removed 542 rows containing missing values (`geom_tile()`).
## Removed 542 rows containing missing values (`geom_tile()`).
## Removed 542 rows containing missing values (`geom_tile()`).
## Removed 542 rows containing missing values (`geom_tile()`).

```



With the `palette` option, we can choose which of the *viridis* color palettes is used to visualize our soundscape.

Great, now let's test the direction variable for the "magma" color palette:

```
# Try the direction options

direction_1 <-
  ss_heatmap(soundcape_obj = soundscape_list[["Andre"]],
    palette = "magma",
    direction = 1)

direction_2 <-
  ss_heatmap(soundcape_obj = soundscape_list[["Andre"]],
    palette = "magma",
    direction = -1)

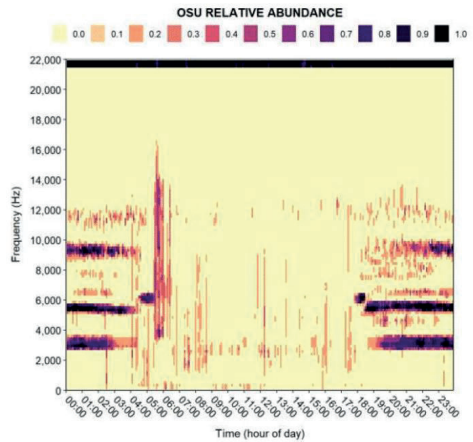
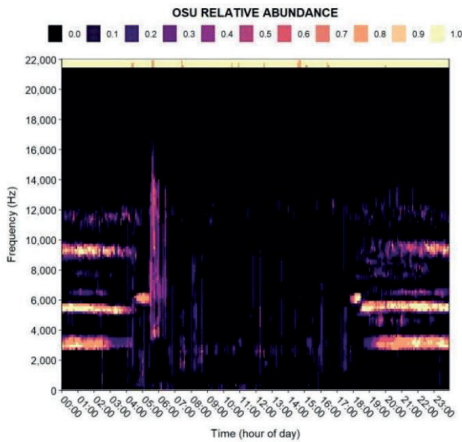
# Combine into one plot

library(patchwork)

all_directions <- direction_1 + direction_2

all_directions
```

```
## Warning: Removed 542 rows containing missing values (`geom_tile()`).
## Removed 542 rows containing missing values (`geom_tile()`).
```



The `direction` argument can be used to inverse the color scales of the viridis R-packages, switching which colors are used for low and high values respectively.

Finally, let's see what the `zero.black` variable does for the regular 'viridis' palette:

```
# Try the direction options

zero_black_off <-
  ss_heatmap(soundcape_obj = soundscape_list[["Andre"]],
```

```

palette = "viridis",
zero.black = FALSE)

zero_black_on <-
  ss_heatmap(soundcape_obj = soundscape_list[["Andre"]],
    palette = "viridis",
    zero.black = TRUE)

# Combine into one plot

library(patchwork)

zero_black_all <- zero_black_off + zero_black_on

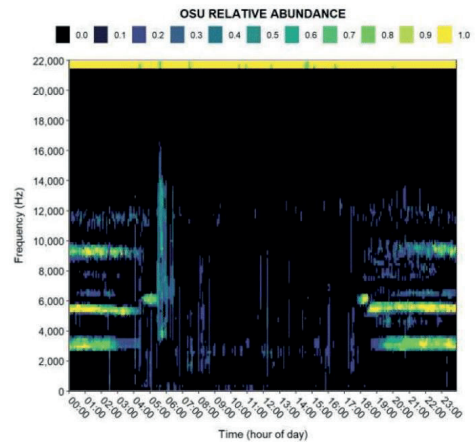
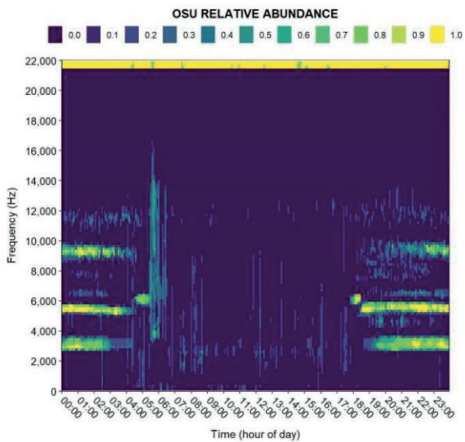
zero_black_all

```

```

## Warning: Removed 542 rows containing missing values (`geom_tile()`).
## Removed 542 rows containing missing values (`geom_tile()`).

```



The `zero.black` argument takes all OSUs for which no sound was detected (relative abundance = 0) and sets the color to zero to increase the contrast with OSUs for which sound was detected. Be careful using the `zero.black` argument with the `direction` argument for some of the color palettes.

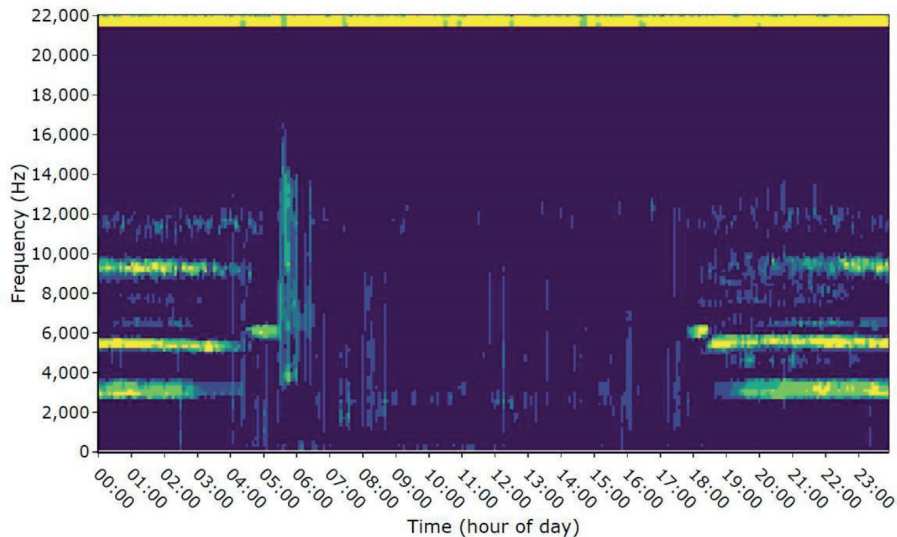
Make your heatmap interactive

The `ss_heatmap` function can also be used to make interactive heatmaps.

Parameters to make interactive heatmaps

- **interactive:**
A Boolean operator, one of either TRUE or FALSE. If set to TRUE, an interactive plot is produced using ggplotly.

Let's make an interactive regular annotated heatmap for Andre island's soundscape:



Try hovering your mouse over the interactive plot we just made. The **interactive** argument lets us query the relative abundance of each OSU for a specific time of day and frequency bin. This way, we can see which sounds were more abundant or rare. For instance, we can see that the relative abundance of the OSUs around 5,340 Hz between 00:00h and 03:00h had a relative abundance of 1, meaning they were detected in every sample. Conversely, we can see that the vertical banding we picked up on between 19:00-20:00h only have a relative abundance of 0.2 - they were detected in only 1 out of 5 sampling days. This strengthens our suspicion that the vertical band may have been created by a non-biological event, such as a rainstorm.

Save your heatmap

Finally, the `ss_heatmap` function contains a number of arguments for saving your plot.

Parameters to save the plot

- **save:**
A Boolean operator - one of either TRUE or FALSE. If set to TRUE, saves the plot using ggsave using the the 'dir', 'filename' and 'device' arguments.
- **dir:**
Path of the directory to save plot to: path and filename are combined to create the fully qualified file name. Defaults to the working directory. For more information consult ggsave.
- **filename:**
The file name without the extension. For more information consult ggsave.
- **device:**
Device to use. Can either be a device function (e.g. png()), or one of "eps", "ps", "tex" (pictex), "pdf", "jpeg", "tiff", "png", "bmp", "svg" or "u2p" (windows only). Defaults to "png". For more information consult ggsave.

png, bmp, svg or wmf (windows only). Defaults to png. For more information consult ggsave.

- **width:**
If save=TRUE, expresses the width of the saved image in millimeters. Defaults to 100 mm.
- **height:**
If save=TRUE, expresses the height of the saved image in millimeters. Defaults to 100 mm.

These arguments rely on the `ggsave` function from the `ggplot2` package. For additional information of how to save your `soundscaper` heatmap, consult the `ggsave` documentation.

2.2. A note on Hill numbers

Now that we know how to visually explore the diversity of our soundscape, let's get to quantifying how much diversity we're actually dealing with using the various soundscape metrics available in the `soundscaper` package.

To calculate the soundscape metrics, we use the analytical framework of **Hill numbers**. In brief, Hill numbers provide a unified statistical framework to measure biological diversity in all its facets. The framework is highly robust and flexible, allowing us to quantify different dimensions of diversity (e.g. taxonomic, functional, phylogenetic and soundscape diversity). Doing so, we can answer common scientific questions by measuring, estimating, partitioning, and comparing different diversity types using a common analytical framework. Although a plethora of indices has been proposed to measure diversity, there is a growing consensus that Hill numbers are the most appropriate framework to separate system diversity into its various components.

Want to know more about Hill numbers? For a deep dive, visit [this website](#) and [this GitHub tutorial](#)!

For an overview of the benefits of Hill numbers over conventional diversity indices, expand the section below. If you're familiar with Hill numbers, feel free to skip over this part.

[CLICK HERE TO LEARN MORE ABOUT THE ADVANTAGES OF HILL NUMBERS](#)

Now that we know why we use Hill numbers, let's have a look at how we can compute our soundscape metrics.

2.3. The `ss_diversity` and `ss_evenness` functions

The `ss_diversity` function is used to compute the soundscape richness and diversity values. The user can modulate the importance of common or rare OSUs on the diversity values using the q-parameter (order of diversity).

The `ss_evenness` function is used to compute the soundscape evenness. In [Luypaert et al. \(2022\)](#), we mentioned the soundscape evenness was calculated as $2D$ (soundscape diversity with $q = 2$)/ OD (soundscape richness with $q = 0$), following [Jost et al. \(2010\)](#). However, based on recent [publications](#), a more proper way to calculate the soundscape evenness is: $(2D - 1) / (OD - 1)$. Therefore, from here on out, we will only use the latter equation for the calculation of the soundscape evenness.

Both functions allow the soundscape metrics to be computed at a range of different scales and resolutions. For instance, the user can specify custom time-frequency limits, calculate the soundscape metrics for various built-in diurnal-phase presets (dawn, dusk, day, night), or track the soundscape metrics at each unique time of day.

The soundscape richness and diversity for the whole soundscape

In their most basic forms, both the `ss_diversity` and `ss_evenness` functions are used to compute soundscape metrics for the whole soundscape. For this, the `ss_diversity` function requires three main input parameters.

Mandatory function input parameters

- **soundscape_obj:**
a *soundscape* object produced by the `ss_create` function (or `ss_index_merge`, `ss_binarize` and `ss_aggregate` functions applied in sequence).
- **qvalue:**
A positive integer or decimal number (≥ 0), most commonly between 0-3. This parameter modulates the sensitivity of diversity values to the relative abundance of Operational Sound Units (OSUs). A value of 0 corresponds to the richness, a value of 1 is the equivalent effective number of OSUs for the Shannon index, a value of 2 is the equivalent effective number of OSUs for the Simpson index.
- **output:**
A character string. Indicates the format in which the soundscape diversity is expressed. Options are "percentage" (the fraction between the observed soundscape diversity and the maximum possible soundscape diversity), or "raw" (the number of acoustically active OSUs in the soundscape). Defaults to "percentage".

Let's look at an example of what the various arguments are and change about the index computation. First, we will use the `ss_diversity` function to calculate the soundscape richness ($q=0$) and diversity (at $q=1$ and $q=2$) for the *soundscape_obj* of Andre island. We want the output as the 'effective number of OSUs'.

Let's try out the code:

```
# Soundscape richness  
  
ss_diversity(soundscape_obj = soundscape_list[["Andre"]],  
            qvalue = 0,  
            output = "raw")
```

```
## [1] 5577
```

```
# Soundscape diversity at q=1  
  
ss_diversity(soundscape_obj = soundscape_list[["Andre"]],  
            qvalue = 1,  
            output = "raw")
```

```
## [1] 4532.245
```

```
# Soundscape diversity at q=2  
  
ss_diversity(soundscape_obj = soundscape_list[["Andre"]],  
            qvalue = 2,
```

```
output = "raw")
```

```
## [1] 3931.819
```

As we can see, the higher the *q-value*, the less importance is given to rare OSUs (with a low relative abundance), and thus the lower the soundscape diversity metric.

Next, let's calculate the same soundscape diversity metrics, but display the output as the percentage of the trait space that is filled with OSUs:


```
# Soundscape richness

ss_diversity(soundscape_obj = soundscape_list[["Andre"]],
             qvalue = 0,
             output = "percentage")
```

```
## [1] 15.12858
```

```
# Soundscape diversity at q=1

ss_diversity(soundscape_obj = soundscape_list[["Andre"]],
             qvalue = 1,
             output = "percentage")
```

```
## [1] 12.2945
```

```
# Soundscape diversity at q=2

ss_diversity(soundscape_obj = soundscape_list[["Andre"]],
             qvalue = 2,
             output = "percentage")
```

```
## [1] 10.66574
```

The `output` argument allows us to modulate how the diversity value is returned and is one of either `"raw"` or `"percentage"`. The `"raw"` option displays the soundscape diversity as the effective number of OSUs in the soundscape, whereas the `"percentage"` option returns the soundscape diversity as the number of detected OSUs divided by the total number of detectable OSUs, which is conceptually similar to the **soundscape saturation** index described in [Burivalova et al. \(2018\)](#), but calculated over a 24h period. The latter allows us to compare the soundscape diversity between soundscapes with different dimensions (a different number of total detectable OSUs due to differences in the sampling regimes and window length).

The soundscape evenness for the whole soundscape

In contrast to the `ss_diversity` function, the `ss_evenness` function only has one mandatory input argument.

Mandatory function input parameters

- **soundscape_obj:**
a *soundscape* object produced by the `ss_create` function (or `ss_index_merge`, `ss_binarize` and `ss_aggregate` functions applied in sequence).

As we can see, the `ss_evenness` function only requires a `soundscape` object produced by the `ss_create` function (or

by using the `ss_index_merge`, `ss_binarize` and `ss_aggregate` functions in sequence).

We will use the `ss_evenness` function to calculate the soundscape evenness:

Let's try out the code:

```
# Soundscape evenness  
  
ss_evenness(soundscape_obj = soundscape_list[["Andre"]])
```

```
## [1] 0.7049532
```

The evenness describes the equitability of abundances. Here, since 2D represents the number of dominant OSUs in the soundscape, this evenness ratio represents the proportion of dominant OSUs.

The soundscape metrics for temporal subsets

In addition to calculating the soundscape richness, diversity and evenness for the whole soundscape, we can also compute the soundscape metrics for different temporal subsets of the soundscape.

Parameters for temporal soundscape subsetting

- **subset:**
The diurnal phase for which the soundscape diversity is computed. Options are 'total', 'day', 'night', 'dawn', 'dusk' and 'tod' (time of day - for each unique time in the day).
- **mintime:**
A positive integer or decimal number (≥ 0), most commonly between 0-3. This parameter modulates the sensitivity of diversity values to the relative abundance of Operational Sound Units (OSUs). A value of 0 corresponds to the richness, a value of 1 is the equivalent effective number of OSUs for the Shannon index, a value of 2 is the equivalent effective number of OSUs for the Simpson index.
- **maxtime:**
A character string. Indicates the format in which the soundscape diversity is expressed. Options are "percentage" (the fraction between the observed soundscape diversity and the maximum possible soundscape diversity), or "raw" (the number of acoustically active OSUs in the soundscape). Defaults to "percentage".
- **dawnstart:**
A character string. Indicates the format in which the soundscape diversity is expressed. Options are "percentage" (the fraction between the observed soundscape diversity and the maximum possible soundscape diversity), or "raw" (the number of acoustically active OSUs in the soundscape). Defaults to "percentage".
- **dawnend:**
A character string. Indicates the format in which the soundscape diversity is expressed. Options are "percentage" (the fraction between the observed soundscape diversity and the maximum possible soundscape diversity), or "raw" (the number of acoustically active OSUs in the soundscape). Defaults to "percentage".
- **duskstart:**
A character string. Indicates the format in which the soundscape diversity is expressed. Options are

“percentage” (the fraction between the observed soundscape diversity and the maximum possible soundscape diversity), or “raw” (the number of acoustically active OSUs in the soundscape). Defaults to “percentage”.

- **duskend:**

A character string. Indicates the format in which the soundscape diversity is expressed. Options are “percentage” (the fraction between the observed soundscape diversity and the maximum possible soundscape diversity), or “raw” (the number of acoustically active OSUs in the soundscape). Defaults to “percentage”.

Let's calculate the soundscape richness, but for different temporal subsets by using the *subset* argument:

```
# Soundscape richness

# subset = 'day'

ss_diversity(soundscape_obj = soundscape_list[["Andre"]],
             qvalue = 0,
             output = "percentage",
             subset = "day")
```

```
## [1] 9.364298
```

```
# subset = 'night'

ss_diversity(soundscape_obj = soundscape_list[["Andre"]],
             qvalue = 0,
             output = "percentage",
             subset = "night")
```

```
## [1] 21.05524
```

```
# subset = 'dawn'

ss_diversity(soundscape_obj = soundscape_list[["Andre"]],
             qvalue = 0,
             output = "percentage",
             subset = "dawn")
```

```
## [1] 22.43924
```

```
# subset = 'dusk'

ss_diversity(soundscape_obj = soundscape_list[["Andre"]],
             qvalue = 0,
             output = "percentage",
             subset = "dusk")
```

```
## [1] 8.767361
```

The `subset` argument uses the metadata contained in the `soundscape` object (the sunrise and sunset times) to subset the soundscapes by different diurnal phases, including `'day'`, `'night'`, `'dawn'` and `'dusk'`. We can see that the soundscape richness at Andre island was the highest at night and dawn, but the lowest during the day and around dusk.

Let's try this for the soundscape evenness:

```
# Soundscape evenness

# subset = 'day'

ss_evenness(soundscape_obj = soundscape_list[["Andre"]],
            subset = "day")
```

```
## [1] 0.6612279
```

```
# subset = 'night'

ss_evenness(soundscape_obj = soundscape_list[["Andre"]],
            subset = "night")
```

```
## [1] 0.7251704
```

```
# subset = 'dawn'

ss_evenness(soundscape_obj = soundscape_list[["Andre"]],
            subset = "dawn")
```

```
## [1] 0.7056203
```

```
# subset = 'dusk'

ss_evenness(soundscape_obj = soundscape_list[["Andre"]],
            subset = "dusk")
```

```
## [1] 0.6265451
```

We can see that the soundscape evenness metric is less variable than the soundscape richness, but still showed differences between the different diurnal phases. For instance, we find that the soundscape had a lower evenness during the day compared to the night time. This suggests there was a higher proportion of dominant OSUs during the night.

By default, the dawn period is calculated as the time of sunrise + 1.5h, and the dusk period is calculated as the time of sunset - 1.5h. We can use the `'dawnstart'`, `'dawnend'`, `'duskstart'` and `'duskend'` arguments to alter the duration of the dawn and dusk period.

Let's try this for the soundscape richness using a dawn and dusk period that starts 1 hour before sunrise/sunset, and ends one hours after:

```
# Soundscape richness
```

```
# Soundscape richness
ss_diversity(soundcape_obj = soundscape_list[["Andre"]],
             qvalue = 0,
             subset = "dawn",
             dawnstart = 3600,
             dawnend = 3600)
```

```
## [1] 28.1901
```

```
ss_diversity(soundcape_obj = soundscape_list[["Andre"]],
             qvalue = 0,
             subset = "dusk",
             duskstart = 3600,
             duskend = 3600)
```

```
## [1] 11.6862
```

As you can see, by changing the time of dawn and dusk, we get slightly different soundscape richness values. It is important to consider what period of dawn/dusk is ecologically meaningful for your study system.

Finally, we can also use the `subset` argument to calculate the soundscape metrics for each unique time of day for which we collected sound files. Let's do this for the soundscape richness:

```
# Soundscape richness
head(ss_diversity(soundcape_obj = soundscape_list[["Andre"]],
                 qvalue = 0,
                 output = "percentage",
                 subset = "tod", n = 24)
```

```
##   soundscape_div time_of_day
## 1      22.65625    00:00:00
## 2      17.18750    00:05:00
## 3      19.53125    00:10:00
## 4      20.31250    00:15:00
## 5      17.18750    00:20:00
## 6      21.09375    00:25:00
## 7      21.09375    00:30:00
## 8      20.31250    00:35:00
## 9      22.65625    00:40:00
## 10     21.87500    00:45:00
## 11     19.53125    00:50:00
## 12     20.31250    00:55:00
## 13     21.09375    01:00:00
## 14     21.09375    01:05:00
## 15     25.00000    01:10:00
## 16     22.65625    01:15:00
## 17     17.18750    01:20:00
## 18     21.09375    01:25:00
## 19     21.09375    01:30:00
## 20     21.09375    01:35:00
## 21     21.09375    01:40:00
## 22     21.09375    01:45:00
## 23     22.65625    01:50:00
## 24     22.65625    01:55:00
```


We get 288 soundscape richness values (24 values shown here), one for each unique time at which we collected sound during our recording period. This can reveal patterns in the soundscape richness throughout the day.

Aside from the *subset* argument, we can also perform temporal subsetting of the soundscape using custom time limits by using the *mintime* and *maxtime* arguments. Let's try this out by calculating the soundscape richness between 11:00 and 13:00:

```
ss_diversity(soundscape_obj = soundscape_list[["Andre"]],
             qvalue = 0,
             output = "percentage",
             mintime = "11:00:00",
             maxtime = "13:00:00")
```

```
## [1] 6.9375
```

The soundscape metrics for frequency subsets

We can also calculate the soundscape richness, diversity and evenness for user-specified frequency subsets.

Parameters for frequency soundscape subsetting

- **minfreq:**
A numeric value indicating the lower frequency limit for which to compute the soundscape diversity. If set to default, uses the lowest available frequency in the dataframe.
- **maxfreq:**
A numeric value indicating the upper frequency limit for which to compute the soundscape diversity. If set to default, uses the highest available frequency in the dataframe.
- **freqseq:**
A logical operator (TRUE/FALSE). If set to FALSE, will compute the diversity for the entire frequency range of the soundscape. If set to TRUE, will compute the diversity per frequency-bin of user-defined width (number of bins determined by *nbins* argument).
- **nbins:**
A numeric argument. If *freqseq* is set to TRUE, determines the number of the frequency-bins by which to divide the frequency range to compute the soundscape diversity.

Let's try subsetting the soundscape between 0 - 10,000 Hz and 10,000 - 20,000 Hz, and calculating the soundscape richness:

```
# Soundscape richness

# 0 - 10,000 Hz

ss_diversity(soundscape_obj = soundscape_list[["Andre"]],
             qvalue = 0,
             output = "percentage",
             minfreq = 0,
```

```
maxfreq = 10000)
```

```
## [1] 22.62931
```

```
# 10,000 - 20,000 Hz
```

```
ss_diversity(soundcape_obj = soundcape_list[["Andre"]],  
             qvalue = 0,  
             output = "percentage",  
             minfreq = 10000,  
             maxfreq = 20000)
```

```
## [1] 3.861351
```

We can see that the soundscape richness is much higher below 10,000 Hz, suggesting there is more vocal activity there.

Finally, we can also divide the frequency spectrum into a user-specified number of bins, and calculate the soundscape metrics for each frequency bin.

Let's try this for the soundscape richness, dividing the frequency spectrum into 20 bins:

```
ss_diversity(soundcape_obj = soundcape_list[["Andre"]],  
             qvalue = 0,  
             output = "percentage",  
             freqseq = TRUE,  
             nbins = 20)
```

```
##   soundscape_div   freq_interval  
## 1     5.0347222      0 - 1033 Hz  
## 2     8.6805556    1033 - 2067 Hz  
## 3    36.4583333    2067 - 3273 Hz  
## 4    21.9907407    3273 - 4306 Hz  
## 5    32.5396825    4306 - 5512 Hz  
## 6    31.7708333    5512 - 6546 Hz  
## 7    12.9629630    6546 - 7579 Hz  
## 8    16.7658730    7579 - 8785 Hz  
## 9    36.4583333    8785 - 9819 Hz  
## 10   6.1921296    9819 - 10852 Hz  
## 11   20.1967593   11025 - 12058 Hz  
## 12   6.6550926   12058 - 13092 Hz  
## 13   2.3809524   13092 - 14298 Hz  
## 14   0.6944444   14298 - 15331 Hz  
## 15   0.4960317   15331 - 16537 Hz  
## 16   0.0000000   16537 - 17571 Hz  
## 17   0.0000000   17571 - 18604 Hz  
## 18   0.0000000   18604 - 19810 Hz  
## 19   0.0000000   19810 - 20844 Hz  
## 20   50.0000000  20844 - 21877 Hz
```

We can see that, above 12,000 Hz, the soundscape richness values drop steeply. Indeed, this is confirmed by the visual exploration of our heatmap we produced earlier, where we saw practically no sound above this frequency cut-off.

Clearly the `ss_diversity` and `ss_evenness` functions are highly flexible, allowing the user to tease apart when and

clearly, the `ss_diversity` and `ss_richness` functions are highly flexible, allowing the user to subset apart metrics where sound is present for a soundscape of interest. Yet, although this is certainly useful, it can be hard to get a grasp of the patterns at hand with so many subsetting options. This is where the `ss_diversity_plot` function comes in, producing a range of different visualization options that allow for an easier assessment of temporal and frequency patterns in the soundscape metrics.

2.3. The `ss_diversity_plot` function

The `ss_diversity_plot` function produces plots showing the variation in soundscape richness and diversity metrics by time-of-day and frequency subsets. Like the `ss_diversity` function, the `ss_diversity_plot` function takes three basic arguments: `'soundscape_obj'`, `'qvalue'` and `'output'` (see above).

Additionally, the `ss_diversity_plot` function can be used to create four types of plots by specifying the `graphtype` argument.

Parameters for smoothing the temporal diversity patterns

- **graphtype:**

The type of plot which is produced. There are four options.

- **graphtype = "total":**

An area chart showing the soundscape diversity by time-of-day for the entire frequency range.

- **graphtype = "frequency":**

A stacked area chart showing the relative contribution of frequency bins with user-defined width to the total soundscape diversity by time-of-day.

- **graphtype = "normfreq":**

A percentage stacked area chart showing the normalized relative contribution of frequency bins with user-defined width to the soundscape diversity by time-of-day.

- **graphtype = "linefreq":**

A line chart showing the relative contribution of frequency bins with user-defined width to the soundscape diversity by time-of-day.

Let's have a look at these plotting options one by one.

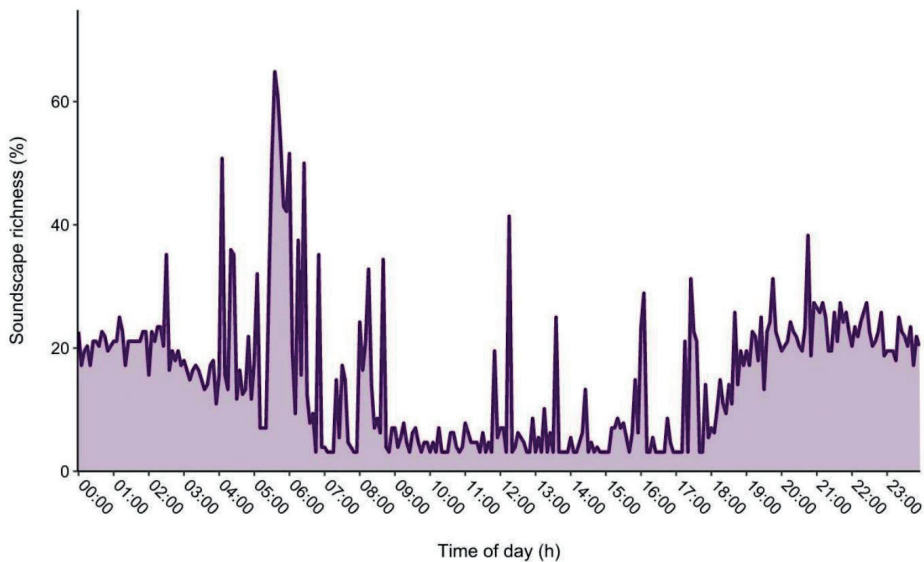
2.3.1. The `ss_diversity_plot` function with `graphtype = "total"`

Let's start by producing a plot showing the temporal patterns in the soundscape richness using the `graphtype = "total"` option:

```
# Temporal patterns in the soundscape richness

ss_diversity_plot(soundscape_obj = soundscape_list[["Andre"]],
                 qvalue = 0,
                 graphtype = "total",
                 output = "percentage",
                 smooth = FALSE)
```

```
## Warning: Removed 1 rows containing missing values (`geom_text()`).
```



This type of plot shows the variation in the soundscape richness throughout a 24-hour period, similar to using the `ss_diversity` function with `subset = "tod"` (like we did before). As you can see, there is a general trend showing a higher soundscape richness during the night, and a lower soundscape richness during the day. Moreover, there is a clear peak in the soundscape richness around dawn. Still, there is a lot of short-term variability that seems to obscure this pattern. Note that, in the command we used here, we specified an additional argument: `smooth = FALSE`.

Parameters for smoothing the temporal diversity patterns

- **smooth:**
One of either TRUE or FALSE. If set to TRUE, applies a moving average filter for smoothing the diversity by time-of-day.
- **movavg:**
If `smooth=TRUE`, determines the width of the moving average filter. Consult `movavg` for more information.

We can use the `smooth` and `movavg` arguments to apply a smoothing function to the data. This will smoothen out short-term variability and make longer-term patterns more clear.

Let's give this a shot. We will turn on the smoothing function using the `smooth` argument and specify how much smoothing will occur using three different `movavg` values:

```
# movavg = 6

plot_1 <- ss_diversity_plot(soundscape_obj = soundscape_list[["Andre"]],
  qvalue = 0,
  graphtype = "total",
  output = "percentage",
  smooth = TRUE,
```

```
      movavg = 6,  
      timeinterval = "4 hours") +  
  
ggplot2::scale_y_continuous(limits = c(0, 50),  
                           expand = c(0,0))
```

```
## Scale for y is already present.  
## Adding another scale for y, which will replace the existing scale.
```

```
# movavg = 12  
  
plot_2 <- ss_diversity_plot(soundscene_obj = soundscene_list[["Andre"]],  
                           qvalue = 0,  
                           graphtype = "total",  
                           output = "percentage",  
                           smooth = TRUE,  
                           movavg = 12,  
                           timeinterval = "4 hours")+  
  
ggplot2::scale_y_continuous(limits = c(0, 50),  
                           expand = c(0,0))
```

```
## Scale for y is already present.  
## Adding another scale for y, which will replace the existing scale.
```

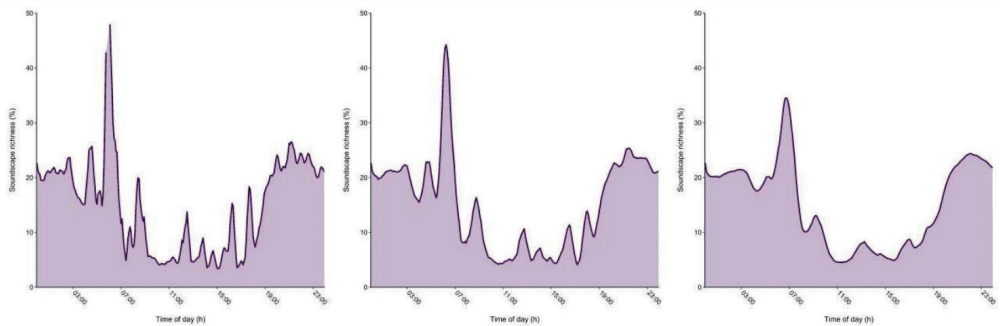
```
# movavg = 24  
  
plot_3 <- ss_diversity_plot(soundscene_obj = soundscene_list[["Andre"]],  
                           qvalue = 0,  
                           graphtype = "total",  
                           output = "percentage",  
                           smooth = TRUE,  
                           movavg = 24,  
                           timeinterval = "4 hours")+  
  
ggplot2::scale_y_continuous(limits = c(0, 50),  
                           expand = c(0,0))
```

```
## Scale for y is already present.  
## Adding another scale for y, which will replace the existing scale.
```

```
# Combine plots  
  
library(patchwork)  
  
plot_total <- plot_1 + plot_2 + plot_3  
  
plot_total
```

```
## Warning: Removed 3 rows containing non-finite values (`stat_align()`).
```

```
## Warning: Removed 1 rows containing missing values (`geom_text()`).
## Removed 1 rows containing missing values (`geom_text()`).
## Removed 1 rows containing missing values (`geom_text()`).
```



Note: As you can see, we added an additional `timeinterval` argument to format the x-axis to our liking. For a description on how to use this argument, please consult the `ss_heatmap` section above.

We can see that, as indicated before, the soundscape richness is high throughout the night and dawn period, and then drops steeply during the day. We can observe a slight peak just around mid-day. Finally, the soundscape richness starts increasing again after sunset (**remember:** you can see at what time sunset occurs for your soundscape by accessing the metadata contained in the soundscape object using `soundscape_name@sunset`).

Like before, using the `ss_diversity_plot` function, we can also subset the frequencies that are used to calculate the soundscape richness using the `minfreq` and `maxfreq` arguments (see before).

Let's have a look at the temporal patterns in the soundscape richness for three different parts of the frequency spectrum (below 2,000 Hz, between 2,000-8,000 Hz and above 8,000 Hz)

```
# Below 2,000 Hz

plot_1 <- ss_diversity_plot(soundscape_obj = soundscape_list[["Andre"]],
  qvalue = 0,
  graphtype = "total",
  output = "percentage",
  smooth = TRUE,
  movavg = 24,
  maxfreq = 2000,
  timeinterval = "4 hours")+

ggplot2::scale_y_continuous(limits = c(0, 55),
  expand = c(0,0))
```

```
## Scale for y is already present.
## Adding another scale for y, which will replace the existing scale.
```

```
# Between 2,000 - 8,000 Hz

plot_2 <- ss_diversity_plot(soundscape_obj = soundscape_list[["Andre"]],
  qvalue = 0,
  graphtype = "total",
  output = "percentage",
  smooth = TRUE,
  movavg = 24,
```

```

    minfreq = 2000,
    maxfreq = 8000,
    timeinterval = "4 hours")+

ggplot2::scale_y_continuous(limits = c(0, 55),
                           expand = c(0,0))

```

```

## Scale for y is already present.
## Adding another scale for y, which will replace the existing scale.

```

```

# Above 8,000 Hz

plot_3 <- ss_diversity_plot(soundscape_obj = soundscape_list[["Andre"]],
                           qvalue = 0,
                           graphtype = "total",
                           output = "percentage",
                           smooth = TRUE,
                           movavg = 24,
                           minfreq = 8000,
                           timeinterval = "4 hours")+

ggplot2::scale_y_continuous(limits = c(0, 55),
                           expand = c(0,0))

```

```

## Scale for y is already present.
## Adding another scale for y, which will replace the existing scale.

```

```

# Combine the plots

plot_total <- plot_1 + plot_2 + plot_3

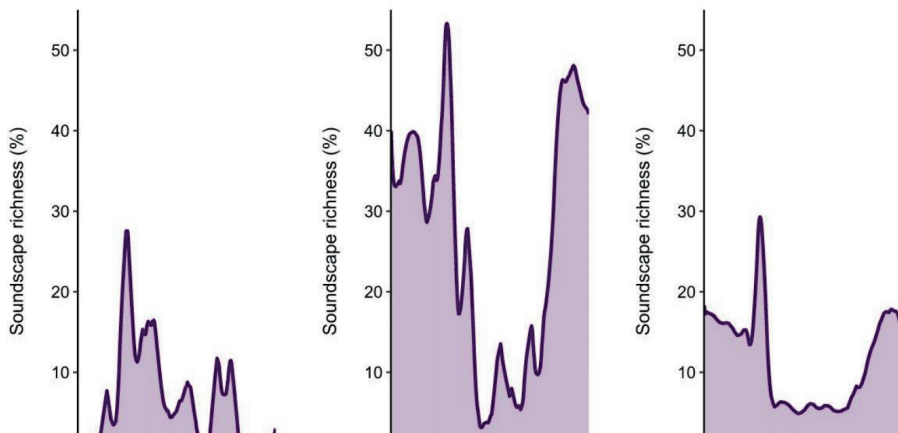
plot_total

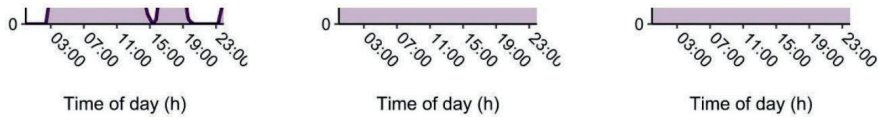
```

```

## Warning: Removed 1 rows containing missing values (`geom_text()`).
## Removed 1 rows containing missing values (`geom_text()`).
## Removed 1 rows containing missing values (`geom_text()`).

```





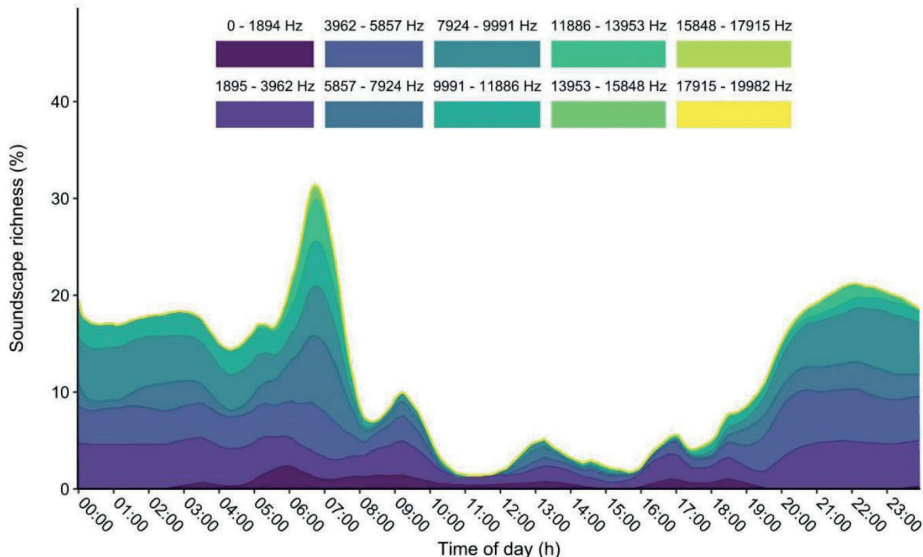
Note that, even though our different frequency subsets have a different number of detectable OSUs (different width of frequency bins), we can directly compare the soundscape richness values by using `output = "percentage"`. We can see quite different temporal patterns emerge for the three parts of the frequency spectrum. Below 2,000 Hz, we find a clear peak around dawn, and several moment where sound is completely absent. The other two frequency bins under consideration (2,000-8,000 Hz and > 8,000 Hz) show the general pattern we observed earlier, with a higher soundscape richness in the night, a peak at dawn, and a lower richness in the day. Still, we can see that, overall, more sound is present between 2,000-8,000 Hz (max soundscape richness = > 50%) compared to the frequency range above 8,000 Hz (max soundscape richness = < 30%).

Clearly, this function is very useful for providing a visual representation of the variation in our soundscape metrics throughout the 24h period in which species can vocalize. Let's have a look at the next `graphtype` option.

2.3.2. The `ss_diversity_plot` function with `graphtype = "frequency"`

Let's have a look at what the `graphtype = "frequency"` option does:

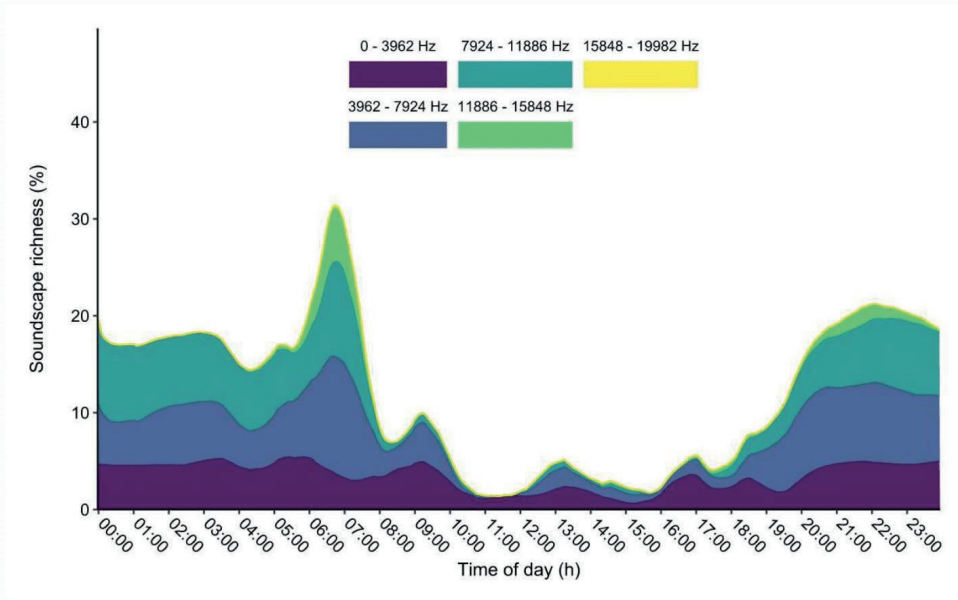
```
ss_diversity_plot(soundscape_obj = soundscape_list[["Andre"]],
                 qvalue = 0,
                 graphtype = "frequency",
                 output = "percentage",
                 smooth = TRUE,
                 movavg = 24,
                 maxfreq = 20000)
```



The `graphtype = "frequency"` option shows the variation in the soundscape richness throughout the day for a user-specified number of frequency bins. The function requires the same `freqseq` and `nbins` arguments we saw for the `ss_diversity` function (see earlier). For instance, here we can see that, around dawn, a wider variety of frequencies is present in the soundscape than during the other periods.

Let's try this again, but use fewer frequency bins for better comparisons:

```
ss_diversity_plot(soundcape_obj = soundscape_list[["Andre"]],
  qvalue = 0,
  graphtype = "frequency",
  output = "percentage",
  smooth = TRUE,
  movavg = 24,
  maxfreq = 20000,
  nbins = 5)
```



We can see patterns we established before: low frequencies peak around dawn. Additionally, frequencies between approx. 8,000-12,000 Hz are more common at night and almost absent during the day.

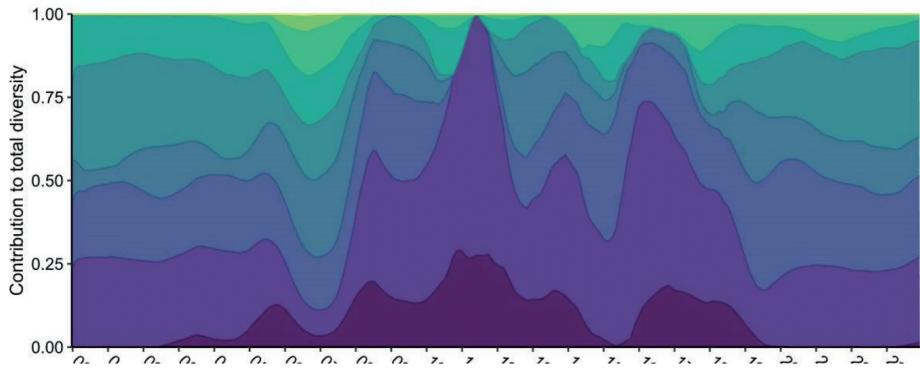
Next up, let's have a look at the `graphtype = "normfreq"` option.

2.3.3. The `ss_diversity_plot` function with `graphtype = "normfreq"`

Let's have a look at what the `graphtype = "normfreq"` option does:

```
ss_diversity_plot(soundcape_obj = soundscape_list[["Andre"]],
  qvalue = 0,
  graphtype = "normfreq",
  output = "percentage",
  smooth = TRUE,
  movavg = 24,
  maxfreq = 20000)
```





0:00 1:00 2:00 3:00 4:00 5:00 6:00 7:00 8:00 9:00 0:00 1:00 2:00 3:00 4:00 5:00 6:00 7:00 8:00 9:00 0:00 1:00 2:00 3:00
Time of day (h)

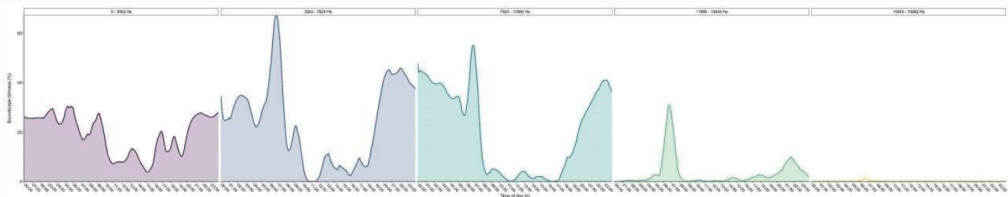
By setting the `graphtype = "normfreq"` option, we are producing a plot similar to the `graphtype = "frequency"` option. However, instead of showing the absolute contribution of frequency bins to the total soundscape richness value, here, we are showing the normalized contribution. This way, we can better see how the amount of active OSUs in each frequency bin changes throughout the day.

Finally, let's have a look at our final option: `graphtype = "linefreq"`.

2.3.3. The `ss_diversity_plot` function with `graphtype = "linefreq"`

Let's have a look at what the `graphtype = "linefreq"` option does:

```
ss_diversity_plot(soundscape_obj = soundscape_list[["Andre"]],  
                 qvalue = 0,  
                 graphtype = "linefreq",  
                 output = "percentage",  
                 smooth = TRUE,  
                 movavg = 24,  
                 maxfreq = 20000,  
                 nbins = 5)
```



The `graphtype = "linefreq"` option produces a graph similar to the `graphtype = "total"` option, but allows the user to specify the number of bins in which to divide the frequency spectrum. Here, in one glance, we can explore the temporal patterns in the soundscape richness for different frequency bands.

Phase III: Comparing multiple soundscapes

In addition to containing functions to assess the diversity patterns of a single soundscape, the `soundscapeR` package also contains a range of functions to explore and contrast the diversity patterns between multiple soundscapes. These include functions for visualizing the differences in OSU presence and relative abundance between two soundscapes (`ss_compare`), functions that perform dimensionality reduction to plot the Bray-Curtis dissimilarity between soundscapes in a two-dimensional space (`ss_pcoa`), functions for decomposing the soundscape diversity of a study area into its alpha, beta and gamma components (`ss_divpart`), and functions to compute the pairwise diversity and dissimilarity values between the soundscapes in the system (`ss_pairdis`).

We will go deeper into each of these functions in the following section.

3.1. The `ss_compare` function

The `ss_compare` function works in a very similar way to the `ss_heatmap` function and requires many of the same arguments. However, instead of portraying the presence and relative abundance of OSUs for a single soundscape, the `ss_compare` function is used to contrast OSUs between two soundscapes. To do so, the function creates a differential heatmap that visually illustrates the differences between two soundscapes.

Like the `ss_heatmap` function, `ss_compare` offers the option to subset the soundscape by specific time or frequency coordinates, portray the soundscape in either Cartesian or polar coordinates, and more.

Let's have a look at the mandatory input argument.

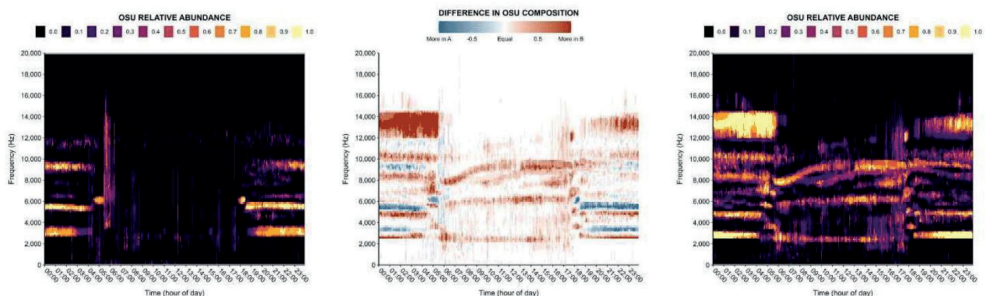
Mandatory input parameters

- **soundscape_obj_A:**
A soundscape object produced by the `ss_create` function (or `ss_index_merge`, `ss_binarize`, and `ss_aggregate` in sequence). This will be the first soundscape for comparison.
- **soundscape_obj_B:**
A soundscape object produced by the `ss_create` function (or `ss_index_merge`, `ss_binarize`, and `ss_aggregate` in sequence). This will be the second soundscape for comparison.

The remaining arguments are the same as `ss_heatmap`, except for the `annotate` argument, which cannot be specified. This is because, when contrasting two different soundscapes, the sunrise and sunset times may differ.

Let's have a look at how this works by comparing the soundscape of 'Andre' and 'Mascote_A1':

```
soundscapeR::ss_compare(soundscape_obj_A = soundscape_list[["Andre"]],  
                        soundscape_obj_B = soundscape_list[["Mascote_A1"]],  
                        maxfreq = 20000)
```



Based on the differential heatmap produced by `ss_compare`, we can see that the OSU composition between Andre island and Mascote_A1 differs quite a bit. For instance, we can see that Mascote_A1 contains more sounds between 12,000-14,000 Hz at night time (redder values indicate OSUs were more common in `soundscape_obj_B`, or Mascote_A1). Additionally, Mascote_A1 clearly contains more sound in the daytime, showing three distinct bands at approx. 2,000 Hz, 6,000 Hz, and 8,000-10,000 Hz. Conversely, we can see that Andre island contains sound in places where little sound is present for Mascote_A1 (bluer values indicate OSUs were more common in `soundscape_obj_A`, or Andre island). For instance, the vertical peak around dawn is distinct in Andre, but not as clear in Mascote_A1. Moreover, Andre contains some sounds between 3,000-4,000 Hz and 5,000-6,000 Hz at nighttime, which are not present for Mascote_A1.

Clearly, these differential heatmaps are a useful tool to quickly compare the OSU composition between two soundscapes.

3.2. The `ss_pcoa` function

If we want to go beyond heatmaps, and assess how similar or different multiple soundscapes actually are from one another, we can use the `ss_pcoa` function. The `ss_pcoa` function can be used to create principle coordinate plots, using a dimensionality reduction approach on the OSU incidence data of multiple soundscapes to plot the distances between these soundscapes in a two-dimensional space. To do this, the function calculates the Bray-Curtis dissimilarities between the soundscapes.

Let's have a look at the mandatory arguments:

Mandatory input parameters

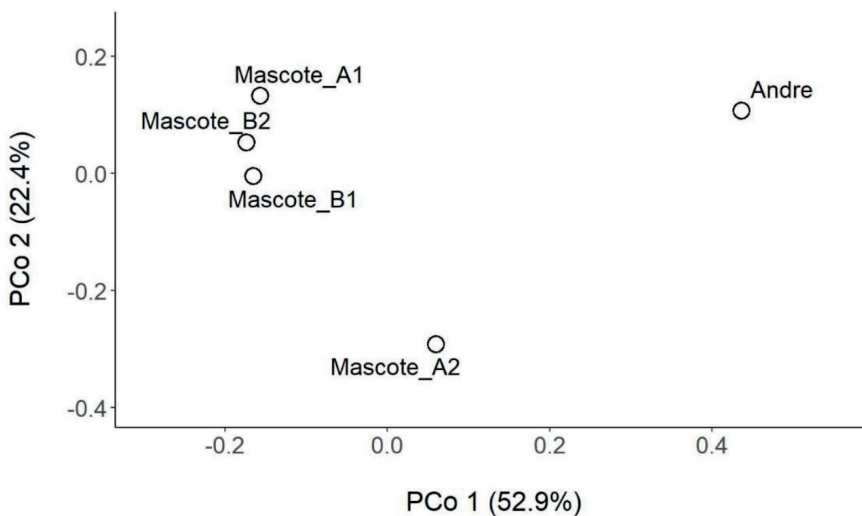
- **soundscape_list:**

A list of soundscape objects. Each object in the list should be produced using the function (or `ss_index_merge`, `ss_binarize`, and `ss_aggregate` in sequence).

In its most basic form, the `ss_pcoa` function takes a single argument: a list of soundscape object to compare.

Let's have a look at what this looks like:

```
ss_pcoa(soundscape_list = soundscape_list)
```



Great, this already reveals a lot! Based on this principle coordinate plot, we can see that the first PCo explains 52.9% of the variation between the soundscapes, and separates the plots on Mascote island from the plots on Andre island - clearly these is a difference in the soundscapes between these two islands. We can also see that a second PCo explains 22.4% of the variation and separates out plot *Mascote_A2* from the other plots on Mascote island.

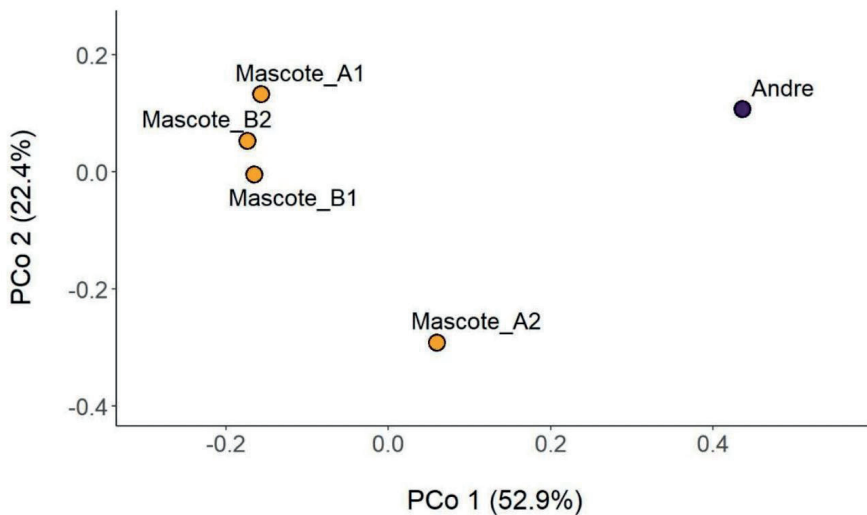
Now, let's have a look at the other plotting parameters:

Optional input parameters

- **grouping:**
A numeric or character vector indicating potential grouping of the elements in the 'soundscape_list' object. Make sure that the grouping vector has the same length as the 'soundscape_list' argument.
- **screepplot:**
A boolean operator indicating whether the function should produce a screepplot in addition to the PCoA plot. Options are: TRUE and FALSE.

Let's start of by taking a look at the *grouping* argument:

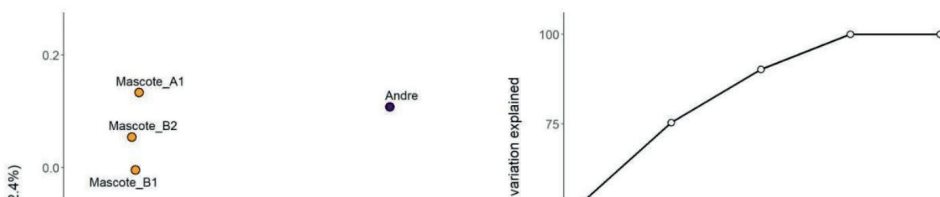
```
ss_pcoa(soundscape_list = soundscape_list,
        grouping = c("Aline", rep("Mascote", 4)))
```

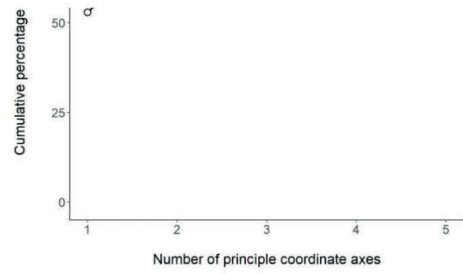
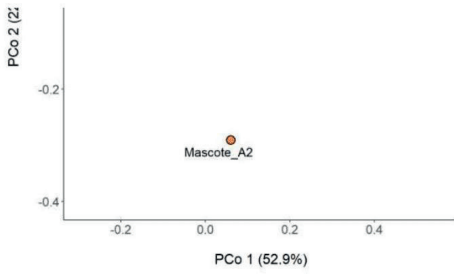


The *grouping* argument is used to indicate which soundscapes in the *soundscape_list* argument belong together, and colors them accordingly. This is already a little clearer than the previous plot.

Next, let's take a look at the *screepplot* argument:

```
ss_pcoa(soundscape_list = soundscape_list,
        grouping = c("Aline", rep("Mascote", 4)),
        screepplot = TRUE)
```





When we indicate `screplot = TRUE`, the `ss_pcoa` function produces a second plot showing the cumulative percentage of the total variation that is explained as additional PCo's are added. We can see that, at 4 PCo's, all the variation between soundscapes is captured.

3.3. The `ss_divpart` function

In addition to quantifying the soundscape richness, diversity, and evenness components, the workflow proposed in this manuscript can be used to decompose the regional metacommunity diversity (γ -diversity) into its local diversities (α -diversity) and a community turnover component (β -diversity).

To do this, we use the following multiplicative framework provided by Hill numbers:

$$(1) \quad {}^q D_\gamma = {}^q D_\alpha \times {}^q D_\beta$$

$$(2) \quad {}^q D_\alpha = \frac{1}{N} \left\{ \sum_{i=1}^S \sum_{j=1}^N (w_j p_{ij})^q \right\}^{\frac{1}{(1-q)}}$$

$$(3) \quad {}^q D_\gamma = \left\{ \sum_{i=1}^S \left(\sum_{j=1}^N (w_j p_{ij}) \right)^q \right\}^{\frac{1}{(1-q)}}$$

$$(4) \quad {}^q D_\beta = \frac{{}^q D_\gamma}{{}^q D_\alpha}$$

Here, N refers to the total number of sub-systems (soundscapes), j refers to each individual sub-system, and w_j represents the relative weight given to each sub-system in the system. If all soundscapes are weighted equally, w_j equals $1/N$. The alpha diversity is the Hill number of the averaged basic sums of the soundscapes (Eqn. 2). The gamma diversity is computed by taking the average of the relative abundance of each OSU across the soundscapes in the system and calculating the Hill number of the pooled system (Eqn. 3). The beta diversity captures the degree of heterogeneity in the OSU composition across sites (Eqn. 4). It ranges from 1 to N and quantifies the relationship between the regional and local diversity, that is, how many times more diverse is the whole system in the effective number of OSUs compared to the sub-systems on average. The beta diversity can also be seen as the effective number of completely distinct soundscapes in the system.

Now that we know the theory, let's take a look at how we can do this in practice. In its most basic form, the `ss_divpart` function takes the following arguments:

Function input parameters

- `soundscape_list`:

A list of soundscape objects of equal dimensions, each soundscape object being produced by `ss_create` (or `ss_index_merge`, `ss_binarize` and `ss_aggregate` in sequence)

- **qvalue:**

A positive integer or decimal number ($>=0$), most commonly between 0-3. This parameter modulates the sensitivity of diversity values to the relative abundance of Operational Sound Units (OSUs). A value of 0 corresponds to the richness, a value of 1 is the equivalent number of effective OSUs for the Shannon index, a value of 2 is the equivalent number of effective OSUs for the Simpson index.

Now, we can use our island system to see how the overall system soundscape diversity (gamma) differs from the local soundscape diversity (alpha), and what the soundscape turnover (beta diversity) looks like.

Let's try the code to decompose the soundscape richness into its various components:

```
ss_divpart(soundscape_list = soundscape_list,
           qvalue = 0)
```

```
## # A tibble: 1 × 7
##   levels   q alpha_l1 gamma   N1   N2 beta_l1
##   <dbl> <dbl>   <dbl> <dbl> <dbl> <dbl> <dbl>
## 1     2     0   31.4  57.2     5     1   1.82
```

We can see that the system's alpha soundscape richness is 31.4%, the average richness of the local soundscape. However, overall, the consolidated soundscape richness of the system (gamma richness) is 57.2% - almost twice as high. A lower alpha richness at each location, but higher gamma richness when taking all locations together, suggests there might be some OSU turnover going on between our soundscapes - they are not identical. Indeed, this is confirmed by the soundscape turnover (beta), which is 1.82. In theory, this value can range from 1 (all soundscapes completely identical) to 5 (all soundscapes completely distinct). Our value here suggests that there is low to moderate turnover in the OSU composition between the soundscapes in our system.

But not all soundscapes in our study system are equal - some are more similar to others. For example, we have four soundscapes from Mascote island, but only one soundscape from Aline island. We can incorporate this 'grouping' or 'hierarchical structure' into our diversity partitioning calculations.

Let's have a look at the next argument of the `ss_divpart` function:

Function input parameters

- **hier_table:**

A matrix indicating the relationship between the soundscapes in the `soundscape_list`. The first column lists the names of all the soundscapes in the `soundscape_list`, other columns can be used to group soundscapes into higher hierarchical levels. If no hierarchy table is supplied, the function defaults to a 2-level diversity partitioning.

As we can see, we can supply the `ss_divpart` function with a table indicating the hierarchy between samples.

Let's give this a try:


```

hierarchy_table <- as.matrix(
  data.frame(Sample = c("Andre", "Mascote_A1", "Mascote_A2", "Mascote_B1", "Mascote_B2"),
            grouping_1 = c("Andre", "Mascote", "Mascote", "Mascote", "Mascote")))

ss_divpart(soundscape_list = soundscape_list,
           qvalue = 0,
           hier_table = hierarchy_table)

```

```

## # A tibble: 1 × 10
##   levels   q alpha_l1 alpha_l2 gamma   N1   N2   N3 beta_l1 beta_l2
##   <dbl> <dbl> <dbl> <dbl> <dbl> <dbl> <dbl> <dbl> <dbl> <dbl>
## 1     3     0   31.4   35.5  57.2     5     2     1   1.13   1.61

```

As you can see, by defining the hierarchical relationships between the plots on our islands, the output has changed a little. We now obtain two alpha richness values, one calculated at the sample (or plot) level, and one calculated at the level of the grouping we specified (islands).

We also get two soundscape turnover values (beta), one for each grouping level:

1. $\beta_1 = \gamma\text{-islands} (35.5\%) / \alpha\text{-plots} (31.4\%) = 1.13$
2. $\beta_2 = \gamma\text{-total} (57.2\%) / \alpha\text{-islands} (35.5\%) = 1.61$

By using the *hier_table* argument, we can further decompose the soundscape metrics based on the hierarchical relationship between samples (plots).

Yet, because beta diversity ranges between 1-N, it is not independent of the number of soundscapes in the system, and can thus not be used as a measure of similarity directly. Instead, to compare the relative compositional difference between soundscapes across multiple systems with a different number of soundscapes, some simple transformations can be performed on the beta diversity to remove the dependence on the number of soundscapes. To do this, we will use the next function.

Note: We can also partition the soundscape metrics using subsets of the soundscapes using the *minfreq*, *maxfreq*, *mintime* and *maxtime* arguments we've seen before.

3.4. The `ss_pairdis` function

The framework of Hill numbers also allows us to define several measures of similarity between soundscapes in the wider system. Let's take a look at how these are calculated:

$$(7) \quad C_{qN} = \frac{\left[\left(\frac{1}{qD_\beta} \right)^{(q-1)} - \left(\frac{1}{N} \right)^{(q-1)} \right]}{\left[1 - \left(\frac{1}{N} \right)^{(q-1)} \right]}$$

$$(8) \quad U_{qN} = \frac{\left[\left(\frac{1}{qD_\beta} \right)^{(1-q)} - \left(\frac{1}{N} \right)^{(1-q)} \right]}{\left[1 - \left(\frac{1}{N} \right)^{(1-q)} \right]}$$

$$(9) \quad V_{qN} = \frac{(N - qD_\beta)}{(N - 1)}$$

$$(10) S_{qN} = \frac{\left(\frac{1}{qD_{\beta}} - \frac{1}{N}\right)}{\left(1 - \frac{1}{N}\right)}$$

Equations (5) and (6) are measures of overlap between soundscapes. The local or **Sørensen-type overlap** (CqN) quantifies the effective average proportion of a soundscape's OSUs which are shared across all soundscapes. It captures the overlap between soundscapes from the sub-system's perspective. For N soundscapes each having S equally common OSUs and sharing A OSUs between them, this function reduces to $CqN=A/S$. The regional or **Jaccard-type overlap** (UqN) quantifies the effective proportion of shared OSUs in a pooled assemblage of soundscapes, and thus captures the overlap between soundscapes from a regional perspective. Assume N soundscapes in a region with S unique and equally abundant OSUs. Here, R OSUs are shared between all soundscapes and the remaining OSUs ($S-R$) are distributed evenly among N soundscapes. In this scenario, Eqn. 8 reduces to $UqN = R/S$.

Equations (7) and (8) are measures of turnover in OSUs between soundscapes. The local or **Sørensen-type turnover complement** (VqN) quantifies the normalised OSU turnover rate with respect to the average soundscape. It measures the proportion of a typical soundscape which changes as one goes from one soundscape to the next. The regional or **Jaccard-type turnover complement** (SqN) quantifies the proportion of the regional soundscape diversity contained in the average assemblage and is a measure of regional homogeneity.

For all of the aforementioned similarity indices, the `ss_pairdis` function transforms the values into metrics of dissimilarity by taking their one-complement (e.g. $1 - XqN$). Unlike the beta soundscape turnover, these dissimilarity indices range from 0-1, where 0 means the soundscapes are completely identical, and 1 indicates the soundscapes are completely unique.

If you want to learn more about the computation of similarity metrics using the framework of Hill numbers, have a look at the [hilldiv GitHub tutorial here](#) and [this paper](#).

To use the `ss_pairdis` function, we need to supply the same parameters as the `ss_divpart` function: `soundscape_list`, `qvalue` and `hier_table` (optional).

Let's have a look:

```
ss_pairdis(soundscape_list = soundscape_list,
           qvalue = 0)
```

```
## $L1_beta
##           Andre Mascote_A1 Mascote_A2 Mascote_B1 Mascote_B2
## Andre           NA           NA           NA           NA
## Mascote_A1 1.608346           NA           NA           NA
## Mascote_A2 1.606310  1.409356           NA           NA
## Mascote_B1 1.614435  1.312740  1.374302           NA
## Mascote_B2 1.623355  1.264852  1.367437  1.274029           NA
##
## $L1_CqN
##           Andre Mascote_A1 Mascote_A2 Mascote_B1 Mascote_B2
## Andre           NA           NA           NA           NA
## Mascote_A1 0.6083460           NA           NA           NA
## Mascote_A2 0.6063103  0.4093560           NA           NA
## Mascote_B1 0.6144346  0.3127399  0.3743021           NA
## Mascote_B2 0.6233550  0.2648524  0.3674368  0.2740286           NA
##
## $L1_UqN
##           Andre Mascote_A1 Mascote_A2 Mascote_B1 Mascote_B2
```

```

## Andre          NA          NA          NA          NA          NA
## Mascote_A1 0.7564865          NA          NA          NA          NA
## Mascote_A2 0.7549106 0.5809122          NA          NA          NA
## Mascote_B1 0.7611762 0.4764689 0.5447159          NA          NA
## Mascote_B2 0.7679836 0.4187878 0.5374095 0.4301766          NA
##
## $L1_VqN
##           Andre Mascote_A1 Mascote_A2 Mascote_B1 Mascote_B2
## Andre          NA          NA          NA          NA          NA
## Mascote_A1 0.6083460          NA          NA          NA          NA
## Mascote_A2 0.6063103 0.4093560          NA          NA          NA
## Mascote_B1 0.6144346 0.3127399 0.3743021          NA          NA
## Mascote_B2 0.6233550 0.2648524 0.3674368 0.2740286          NA
##
## $L1_SqN
##           Andre Mascote_A1 Mascote_A2 Mascote_B1 Mascote_B2
## Andre          NA          NA          NA          NA          NA
## Mascote_A1 0.7564865          NA          NA          NA          NA
## Mascote_A2 0.7549106 0.5809122          NA          NA          NA
## Mascote_B1 0.7611762 0.4764689 0.5447159          NA          NA
## Mascote_B2 0.7679836 0.4187878 0.5374095 0.4301766          NA

```

Indeed, based on this output, we can see that the pairwise dissimilarity between the plots in our case study is greatest between the soundscape of *Andre* island and all other plots. Furthermore, within Mascote island, we can see that plot Mascote_A2 is most dissimilar from the other plots on the island - a pattern which we previously observed used the `ss_pcoa` function.

Vignette by [Thomas Luypaert](#)

thomas.luypaert@nmbu.no / thomas.luypaert@outlook.com



ISBN: 978-82-575-2102-8

ISSN: 1894-6402



Norwegian University
of Life Sciences

Postboks 5003
NO-1432 Ås, Norway
+47 67 23 00 00
www.nmbu.no